高等教育（研究生）国家级教学成果奖申请书附件

教学成果应用及效果证明材料

成果名称：　　创新引领+内生协同+国际赋能：物理学科基础拔尖人才培养模式构建与实践

成果完成人：　田浩、张宇、赵纪军、马晶、任延宇、孙秀冬、钱冬、袁承勋、高峻峰、李立、李淑凤、李德友、谭鹏、蒋雪、王宇

成果完成单位：哈尔滨工业大学、大连理工大学、上海交通大学

附件目录：

(1) 教学成果获奖情况

(2) 自制科教仪器推广应用佐证材料

(3) 教材专著等成果佐证材料

(4) 高水平文章佐证材料

(5) 专利授权情况佐证材料

(6) 学术竞赛等奖项佐证材料

(7) 教学项目佐证材料

(8) 教学论文发表佐证材料

(9) 教师获奖佐证材料

（1）教学成果获奖情况

序号	成果名称/获奖名称	级别	获奖等级	教师姓名	年份
1.	黑龙江省高等教育教学成果奖	省级	一等奖	田浩	2022
2.	辽宁省教学成果奖	省级	一等奖	赵纪军	2018
3.	辽宁省教学成果奖	省级	一等奖	李淑凤	2018
4.	黑龙江省高等教育教学成果奖	省级	二等奖	张宇	2022
5.	辽宁省教学成果奖	省级	二等奖	李淑凤	2022
6.	辽宁省教学成果奖	省级	二等奖	赵纪军	2021
7.	工业和信息化部研究型教学创新团队	省部级		张宇	2017
8.	哈尔滨工业大学研究生教育成果奖	校级	一等奖	田浩	2022
9.	哈尔滨工业大学教学成果奖	校级	一等奖	张宇	2022

（1）黑龙江省高等教育教学成果奖一等奖获奖证明

（2）辽宁省教学成果奖一等奖获奖证明

（3）辽宁省教学成果奖一等奖获奖证明

（4）黑龙江省高等教育教学成果奖二等奖获奖证明

（5）辽宁省教学成果奖二等奖获奖证明

（6）辽宁省教学成果奖二等奖获奖证明

（7）工业和信息化部研究型教学创新团队

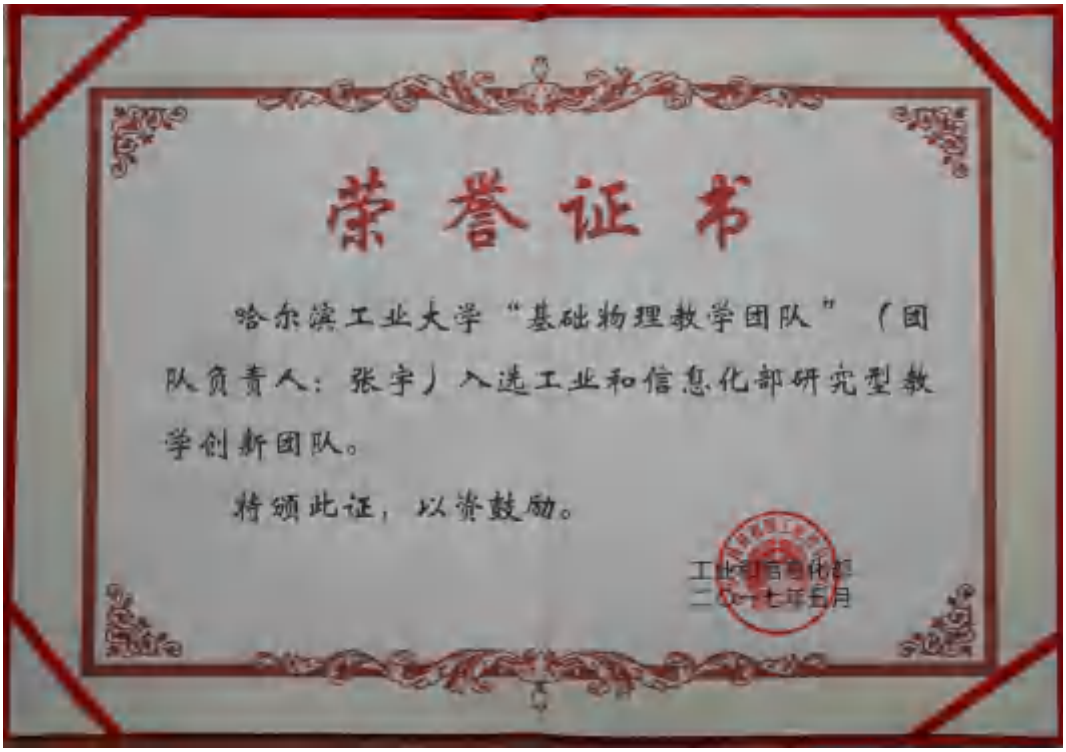

荣誉证书

哈尔滨工业大学“基础物理教学团队”（团队负责人：张宇）入选工业和信息化部研究型教学创新团队。

特颁此证，以资鼓励。

工业和信息化部
二〇一七年五月

（8）哈尔滨工业大学研究生教育成果奖

荣誉证书

创新引领+内生协同+国际赋能：物理学科基础拔尖人才培养模式构建与实践 成果

2022年被评为哈尔滨工业大学研究生教育成果 壹 等奖，特颁此证。

获奖者：田 浩 袁承勋 任延宇 李 均 李俊庆
姜秀涛 王 健 王 爱 李建友

证书号：HITYJS2022002

哈尔滨工业大学
2022年5月31日

（9）哈尔滨工业大学教学成果奖


哈爾濱工業大學
HARBIN INSTITUTE OF TECHNOLOGY

教学成果奖获奖证书

获奖成果：以研究性学习促进物理拔尖学生科学研究能力培养的探索与实践

获 奖 人：乖宇、吕喆、王玉晓、张学知、时红艳、周可雅、靳辰飞、王志红、应涛

获奖等级：一等奖

哈尔滨工业大学

2022年6月

（2）自制科教仪器推广应用佐证材料

推广类别	单位名称（总套数）
国外高校（1 所）	澳大利亚卧龙岗大学（1）
985 高校（17 所）	清华大学（9）、中国科技大学（1）、南京大学（1）、西安交通大学（4）、四川大学（8）、华中科技大学（1）、哈尔滨工业大学（8）、天津大学（1）、中南大学（1）、中山大学（22）、电子科技大学（2）、兰州大学（11）、吉林大学（14）、厦门大学（5）、大连理工大学（9）、重庆大学（3）、中国海洋大学（6）
211 高校（9 所）	南京航空航天大学（1）、南京理工大学（3）、西南大学（3）、陕西师范大学（5）、武汉理工大学（1）、东华大学（1）、东华理工大学（1）、西南交通大学（10）、北京工业大学（4）
其他高校（23 所）	东北大学秦皇岛分校（2）、陕西科技大学（2）、西安工业大学（3）、江苏大学（2）、河南大学（2）、河南师范大学（2）、合肥学院（2）、西安建筑科技大学（2）、桂林理工大学（4）、桂林电子科技大学（11）、西南民族学院（2）、沈阳工业大学（1）、盐城工学院（2）、重庆科技学院（2）、信阳师范学院（1）、太原科技大学（2）、成都大学（1）、齐鲁工业大学（4）、西安外事学院（5）、河北大学（1）、安阳工学院（1）、昆明理工大学（16）、南京工业大学（14）
研究院所（10 所）	中科院成都光电所（2）、中科院物理研究所（2）、山东科学院新材料研究所（1）、中电 46 所（1）、佛山新材料研究所（4）、中国船舶重工集团公司第 715 所（3）、中国散裂中子源研究中心（1）、北京中芯云科仪器有限公司（1）、乌镇实验室（1）、深圳先进电子材料国际创新研究院（2）

应用证明

项目名称：	高温介电温谱测量仪（型号 TZDM-200-300，1套）
应用单位：	江苏科技大学材料科学与工程学院
通讯地址：	江苏省镇江市[illegible]号
应用起止时间：	2014年至今

应用情况及社会效益：

[illegible]

特此证明！

[illegible]
江苏科技大学材料学院
2019年12月10日

应用证明

项目名称：	超高温介电温谱测量仪（型号 TZDM-RT-1200，1套） 高温介电温谱测量仪（型号 TZDM-RT-1000，1套） 低温介电温谱测量仪（型号 TZDM-200-300，1套）
应用单位：	清华大学新型陶瓷与精细工艺国家重点实验室
通讯地址：	北京市海淀区清华大学[illegible] B513 室
应用起止时间：	2015年至今

应用情况及社会效益：

[illegible]

特此证明！

[illegible]
清华大学新型陶瓷与精细工艺国家重点实验室
2019年12月17日

应用证明

项目名称：	高温介电温谱测量仪（型号 TZDM-RT-1000，1套） 低温介电温谱测量仪（型号 TZDM-200-300，1套）
应用单位：	电子科技大学电子科学与工程学院
通讯地址：	四川省成都市建设北路二段四号[illegible]
应用起止时间：	2017年至今

应用情况及社会效益：

[illegible]

特此证明！

[illegible] 副教授
电子科技大学电子科学与工程学院
2019年12月15日

应用证明

项目名称：	高温介电温谱测量仪（型号 TZDM-RT-1000，1套） 低温介电温谱测量仪（型号 TZDM-200-300，1套）
应用单位：	[illegible]
通讯地址：	四川成都[illegible]
应用起止时间：	[illegible]

应用情况及社会效益：

[illegible]

特此证明！

[illegible]
[illegible]
2019年12月[illegible]日

应用证明

仪器名称：	低温介电温谱测量仪（型号 TZDM-200-300，1套）
应用单位：	东华理工大学
通讯地址：	江西省南昌市经开区广兰大道418号
应用起止时间：	2016年至今

应用情况及社会效益：

[illegible]

特此证明！

仪器负责人：[illegible]

[illegible]

2018年12月15日

应用证明

仪器名称：	低温介电温谱测量仪（型号 TZDM-200-300，1套）
应用单位：	山东省科学院新材料研究所
通讯地址：	山东省济南市科院路19号
应用起止时间：	2017年至今

应用情况及社会效益：

[illegible]

特此证明！

仪器负责人：[illegible]

山东省科学院新材料研究所

2019年10月8日

应用证明

仪器名称：	高温介电温谱测量仪（型号 TZDM-RT-1000，1套） 低温介电温谱测量仪（型号 TZDM-200-300，1套）
应用单位：	陕西科技大学材料科学与工程学院
通讯地址：	陕西省西安市未央大学园区
应用起止时间：	2019年至今

应用情况及社会效益：

[illegible]

特此证明！

仪器负责人：[illegible]

陕西科技大学材料科学与工程学院

2019年12月11日

应用证明

仪器名称	低温介电温谱测量仪（型号 TZDM-200-300，1套）
应用单位	陕西师范大学物理学与信息技术学院
通讯地址	陕西省西安市长安区西长安街620号
应用起止时间	2018年至今

应用情况及社会效益：

[illegible]

特此证明！

仪器负责人：[illegible]

陕西师范大学物理学与信息技术学院

2019年12月16日

应用证明

项目名称：	高温介电温谱测量仪（型号 TZDM-RT-1000，1套）
应用单位：	西安交通大学前沿科学技术研究院
通讯地址：	陕西省西安市雁塔区[illegible]路 28 号
应用起止时间：	2018 年至今

应用情况及社会效益：

由哈尔滨工业大学物理学院[illegible]研究开发的高温介电温谱测量仪（型号 TZDM-RT-1000，1 套）在我单位使用，[illegible]

该系统测试精度高、效率高、稳定性好、扩展性强，技术优势明显，应用效果好。

特此证明！

[illegible]
西安交通大学[illegible]
2019 年 12 月 18 日

应用证明

项目名称：	高温介电温谱测量仪（型号 TZDM-RT-1000，1套）
应用单位：	华中科技大学材料科学与工程学院
通讯地址：	武汉市洪山区珞喻路 1037 号
应用起止时间：	2015 年至今

应用情况及社会效益：

由哈尔滨工业大学物理学院[illegible]研究开发的高温介电温谱测量仪（型号 TZDM-RT-1000，1 套）在我单位使用，[illegible]（U1732117）[illegible]（51672083）[illegible]

该系统测试精度高、效率高、稳定性好、扩展性强，技术优势明显，应用效果好。

特此证明！

[illegible]
华中科技大学材料科学与工程学院
2019 年 12 月 18 日

应用证明

项目名称：	高温介电温谱测量仪（型号 TZDM-RT-1000，1 套）
应用单位：	南京大学现代工程与应用科学学院
通讯地址：	南京市鼓楼区汉口路 22 号
应用起止时间：	2016 年至今

应用情况及社会效益：

由哈尔滨工业大学物理学院[illegible]研究开发的高温介电温谱测量仪（型号 TZDM-RT-1000，1 套）在我单位使用，[illegible]

该系统测试精度高、效率高、稳定性好、扩展性强，技术优势明显，应用效果好。

特此证明！

[illegible]
南京大学现代工程与应用科学学院
2019 年 12 月 18 日

应用证明

项目名称：	高温介电温谱测量仪（型号 TZDM-RT-1000，1 套）
应用单位：	[illegible]有限公司
通讯地址：	浙江省嘉兴市[illegible] 705 号[illegible]
应用起止时间：	2018 年至今

应用情况及社会效益：

由哈尔滨工业大学物理学院[illegible]研究开发的高温介电温谱测量仪（型号 TZDM-RT-1000，1 套）在我公司使用，[illegible]

该系统测试精度高、效率高、稳定性好、扩展性强，技术优势明显，应用效果好。

特此证明！

[illegible]

应用证明

项目名称：	高温介电温谱测量仪（型号TZDM-RT-1000，1套）
应用单位：	西安交通大学电子陶瓷与器件教育部重点实验室
通讯地址：	陕西省西安市碑林区西安交通大学兴庆校区[illegible]
应用起止时间：	2018年至今

应用情况及社会效益：

由哈尔滨工业大学[illegible]研究开发的高温介电温谱测量仪（型号TZDM-RT-1000，1套）在我单位使用，[illegible]得到了应用。[illegible]

该系统测试精度高、[illegible]、稳定性好、扩展性强，技术[illegible]，应用效果好。

特此证明！

[illegible]

西安交通大学电子陶瓷与器件教育部重点实验室

2019年[illegible]日

应用证明

项目名称：	高温介电温谱测量仪（型号TZDM-RT-1000，1套） [illegible]（型号TZDM-200-300，1套）
应用单位：	重庆大学材料与能源学院
通讯地址：	重庆市[illegible]号
应用起止时间：	2016年至今

应用情况及社会效益：

由哈尔滨工业大学[illegible]研究开发的高温介电温谱测量仪（型号TZDM-RT-1000，1套）、[illegible]（型号TZDM-200-300，1套）在我单位使用，[illegible]得到了应用，[illegible]，带来了可观的社会效益。

同时，[illegible]，受益本科生200余人，研究生[illegible]余人。

该系统测试精度高、[illegible]、稳定性好、扩展性强，技术[illegible]，应用效果好。

特此证明！

[illegible]

[illegible]

应用证明

项目名称：	高温介电温谱测量仪（型号TZDM-RT-600，1套）
应用单位：	浙江嘉康电子股份有限公司
通讯地址：	浙江省嘉兴市[illegible]号
应用起止时间	2017年至今

应用情况及社会效益：

由哈尔滨工业大学物理学院[illegible]研究开发的高温介电温谱测量仪（型号TZDM-RT-600，1套）在我公司使用，[illegible]中得到了应用。[illegible]，带来了可观的社会效益和经济效益。

该系统测试精度高、[illegible]、稳定性好、扩展性强，技术[illegible]，应用效果好。

特此证明！

浙江嘉康电子股份有限公司

2019年12月[illegible]日

应用证明

项目名称：	高温介电温谱测量仪（型号TZDM-RT-1000，1套）
应用单位：	中南大学[illegible]
通讯地址：	湖南省长沙市[illegible]号
应用起止时间：	2019年2月至今

应用情况及社会效益：

由哈尔滨工业大学物理学院[illegible]研究开发的高温介电温谱测量仪（型号TZDM-RT-1000，1套）在我单位使用，[illegible]得到了应用，[illegible]，带来了可观的社会效益。

同时，[illegible]，受益本科生100余人，研究生10余人。

该系统测试精度高、[illegible]、稳定性好、扩展性强，技术[illegible]，应用效果好。

特此证明！

[illegible]

中南大学[illegible]

2019年12月[illegible]日

应用证明

项目名称：	高温介电温谱测量仪（型号 TZDM-RT-1000，1套）
应用单位：	西安工业大学光电工程学院
通讯地址：	西安市未央区学府中路2号
应用起止时间：	2018年至今

应用情况及社会效益：

[illegible]

该高温测试精度高，效率高，稳定性好，扩展性强，技术优势明显，应用效果好。

特此证明！

仪器负责人：[illegible]

西安工业大学光电工程学院

[illegible]

应用证明

项目名称： 高温介电温谱测量仪（型号 TZDM-RT-[illegible]，1套）

低温介电温谱测量仪（型号 TZDM-200-[illegible]，1套）

应用单位： [illegible]

通讯地址： [illegible]

应用起止时间： [illegible]

应用情况及社会效益：

[illegible]

特此证明！

仪器负责人：[illegible]

[illegible]

2019年12月[illegible]日

应用证明

项目名称：	高温介电温谱测量仪(型号 TZDM-RT-1000，1套)
应用单位：	河南大学物理与电子学院
通讯地址：	开封市金明大道1号河南大学新校区13教[illegible]
应用起止时间：	2019年7月-至今

应用情况及社会效益：

由哈尔滨工业大学物理学院[illegible]研究开发的高温介电温谱测量仪(型号 TZDM-RT-1000，1套)在我单位使用，并在国家自然科学基金面上项目“[illegible]”等科研项目中得到了应用。[illegible]

该高温测试精度高，效率高，稳定性好，扩展性强，技术优势明显，应用效果好。

特此证明！

仪器负责人：[illegible]

河南大学物理与电子学院

2019年12月[illegible]日

应用证明

项目名称：	高温介电温谱测量仪（型号 TZDM-RT-1000，1套）
应用单位：	沈阳工业大学材料科学与工程学院
通讯地址：	辽宁省沈阳经济技术开发区沈辽西路111号
应用起止时间：	2016年至今

应用情况及社会效益：

[illegible]

该高温测试精度高，效率高，稳定性好，扩展性强，技术优势明显，应用效果好。

特此证明！

仪器负责人：王[illegible]教授

沈阳工业大学材料科学与工程学院

2019年12月15日

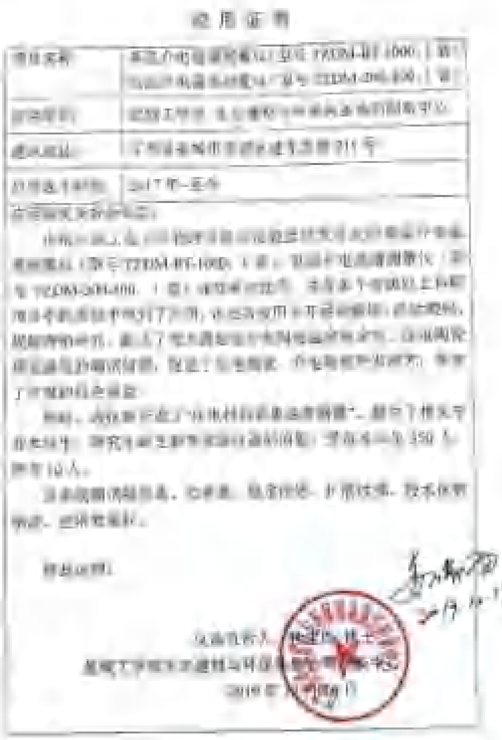

应用证明

特此证明！

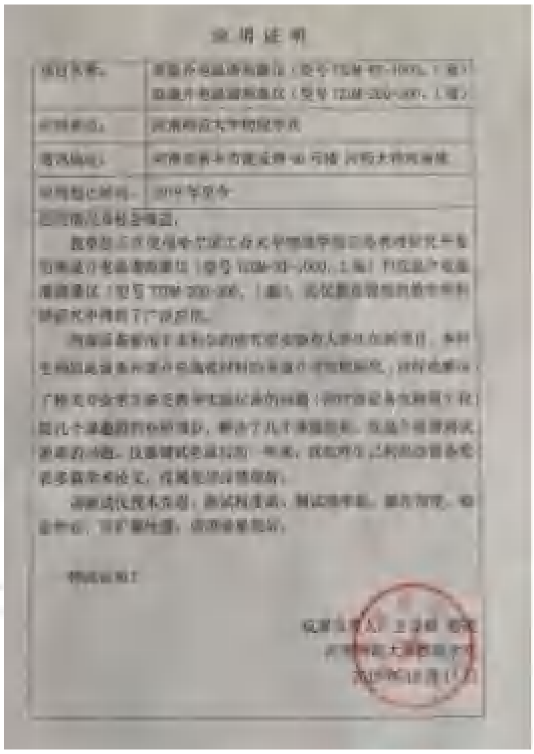

应用证明

特此证明！

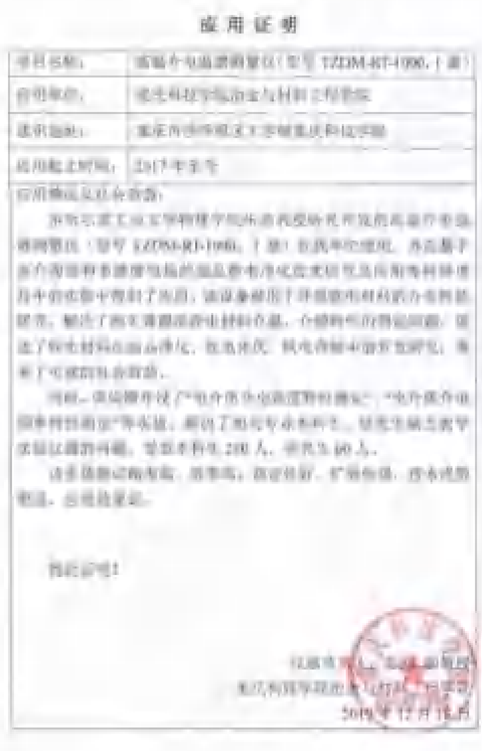

应用证明

特此证明！

应用证明

特此证明！

应用证明

项目名称：	[illegible]
应用单位：	[illegible]
通讯地址：	[illegible]
应用起止时间：	2019年前

应用情况及社会效益：

[illegible]

特此证明！

[illegible]

2019 年 12 月 15 日

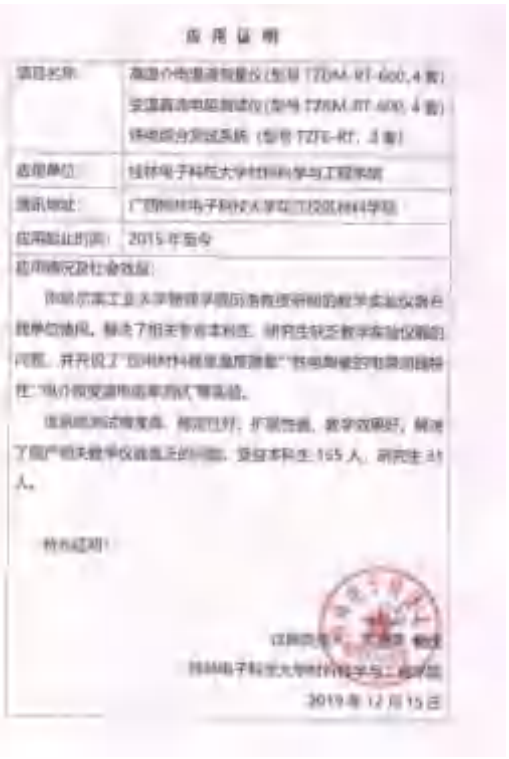

应 用 证 明

项目名称：	高温介电温谱测量仪（型号 TZDM-RT-600，4 套） 交流高温电阻测试仪（型号 TZRM-RT-600，4 套） 铁电综合测试系统（型号 TZFE-RT，3 套）
应用单位：	桂林电子科技大学材料科学与工程学院
通讯地址：	广西桂林电子科技大学花江校区材料学院
应用起止时间：	2015 年至今

应用情况及社会效益：

[illegible]

特此证明！

[illegible]

2019 年 12 月 15 日

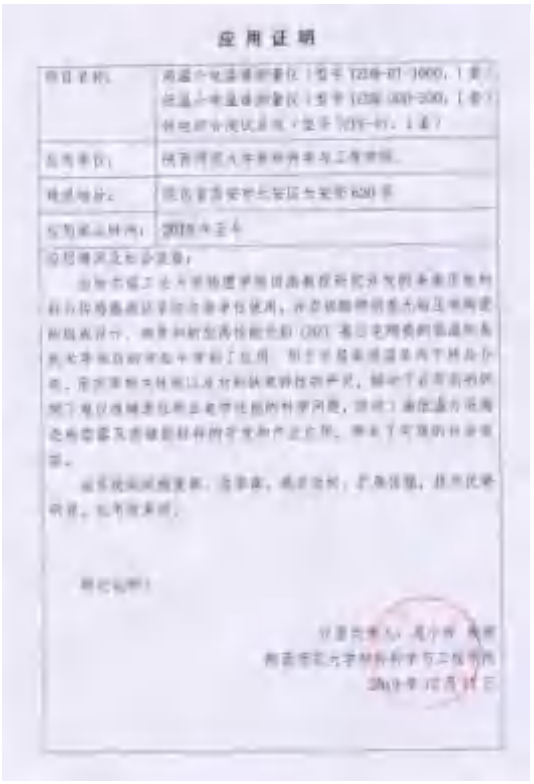

应 用 证 明

项目名称：	[illegible]
应用单位：	[illegible]
通讯地址：	[illegible]
应用起止时间：	2015年至今

应用情况及社会效益：

[illegible]

特此证明！

[illegible]

应 用 证 明

项目名称：	铁电综合测试仪（型号 TZFE，1 套）
应用单位：	桂林理工大学理学院
通讯地址：	广西桂林七星区雁子路 12 号桂林理工大学
应用起止时间：	2015 年至今

应用情况及社会效益：

[illegible]

特此证明！

[illegible]

2019 年 12 月 15 日

应用证明

项目名称：	
应用单位：	
通讯地址：	
应用起止时间：	2015 年至今

应用情况及社会效益：

证明单位：

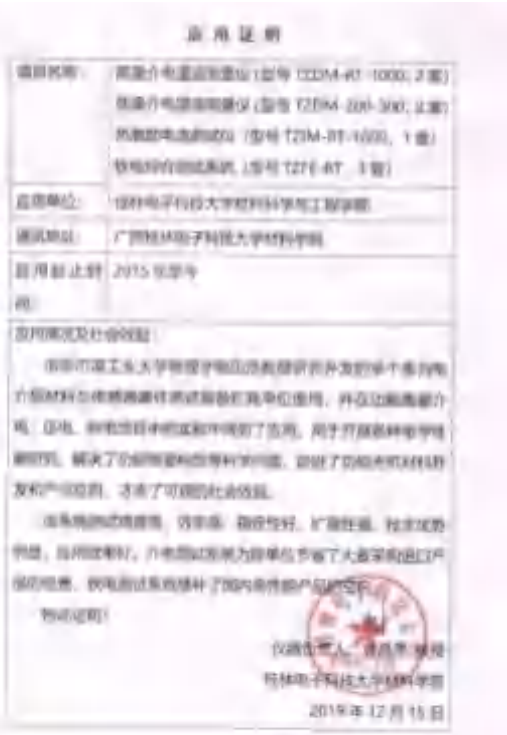

应 用 证 明

项目名称：	
应用单位：	
通讯地址：	
应用起止时间：	2015 年至今

应用情况及社会效益：

证明单位：

2015 年 12 月 15 日

推广应用证明

项目名称：	
推广单位：	四川世纪中科光电技术有限公司
通讯地址：	四川省成都经济技术开发区南二路 [illegible] 号
推广应用起止时间：	2015 年至今

推广应用情况及社会效益：

证明单位：

四川世纪中科光电技术有限公司

年 月 日

（3）教材专著等成果佐证材料

序号	教材名称	出版社	出版年份
1	核电子学基础	新华大学出版社	2021
2	中温固体氧化物燃料电池双钙钛矿结构阴极材料的性能研究与改进	哈尔滨工业大学出版社	2019
3	Introduction to Kinetics of Glow Discharges	Morgan&Claypool Publisher	2018
4	钽铌酸钾功能晶体	科学出版社	2018
5	In:Fe:Cu:$LiNbO_3$ 晶体蓝光光折变与非挥发全息存储	哈尔滨工业大学出版社	2018
6	分数阶变换与光学图像加密	科学出版社	2017
7	光电功能材料与器件	高等教育出版社	2017
8	光学非线性测量新技术—4f 相位成像技术	国防工业出版社	2016
9	宇宙中的生命	机械工业出版社	2016
10	《大学物理学》（第四版）	科学出版社	2017
11	光波导理论基础	电子工业出版社	2018
12	碳基和类碳超硬材料的第一性原理研究	大连理工大学出版社	2018
13	Graphene Oxide: Physics and Applications	Springer	2015

（1）核电子学基础

（2）中温固体氧化物燃料电池双钙钛矿结构阴极材料的性能研究与改进

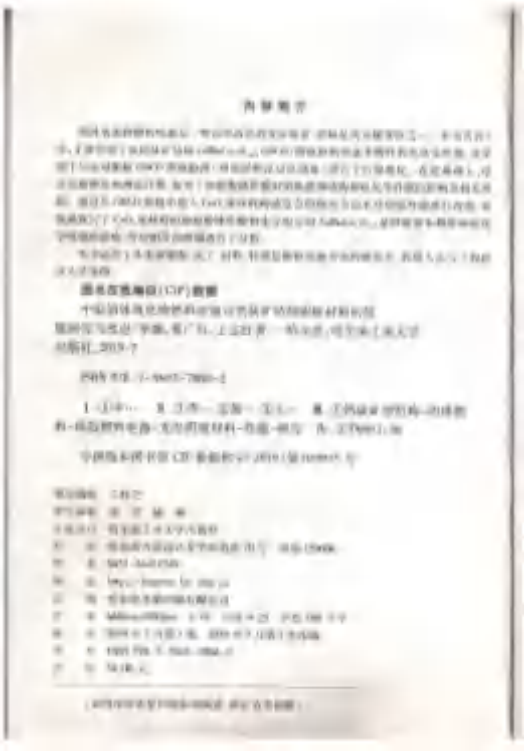

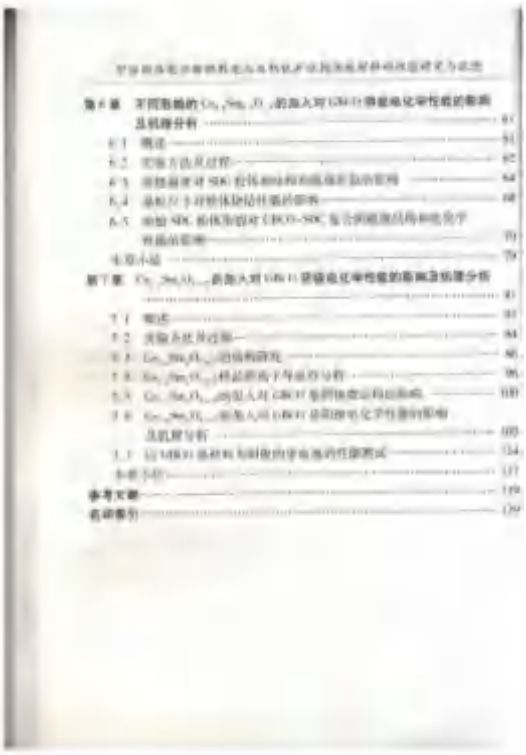

（3）Introduction to the Kinetics of Glow Discharges

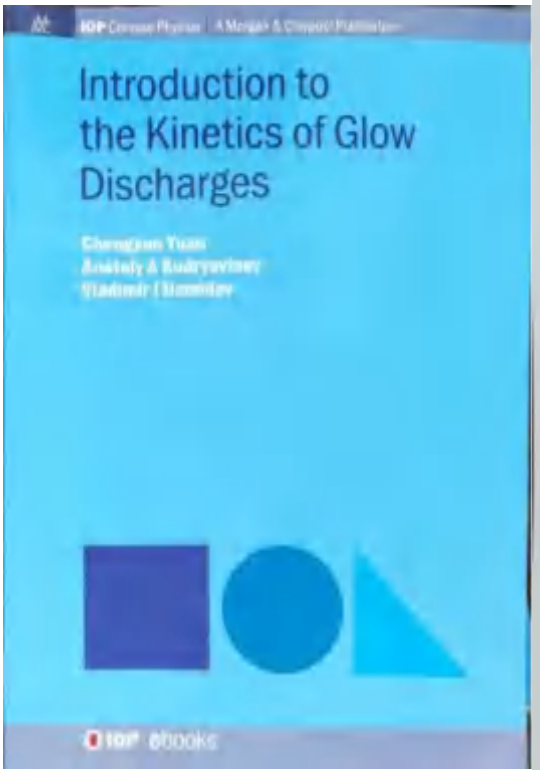

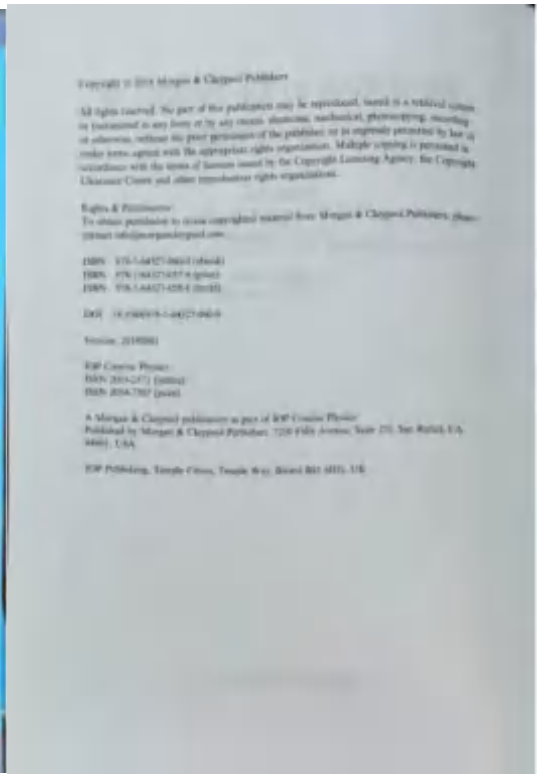

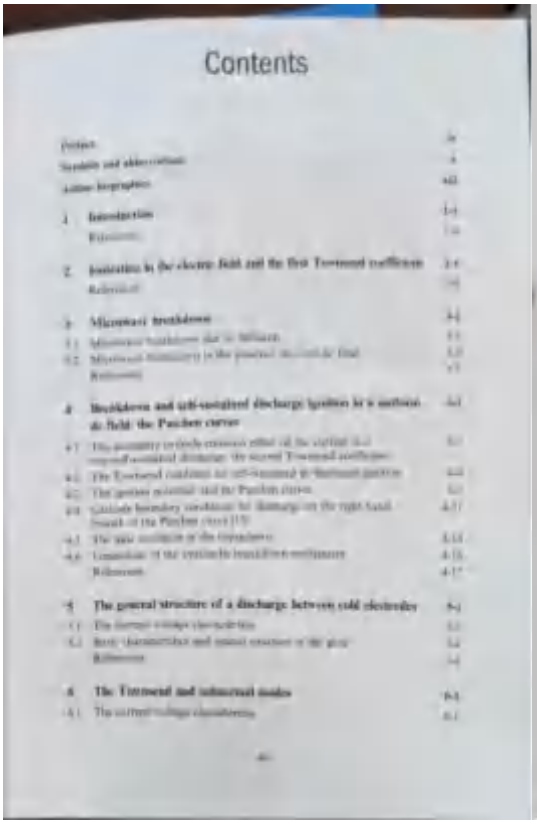

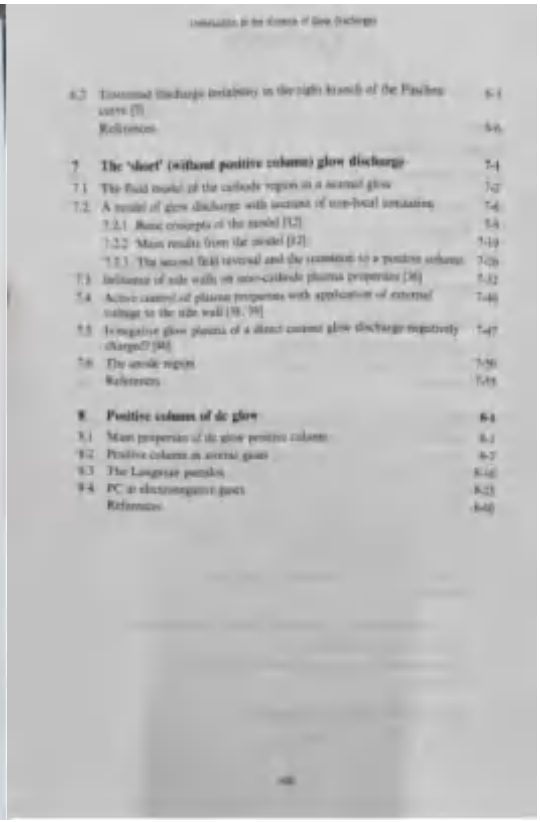

（4）钽铌酸钾功能晶体


内 容 简 介


目 录

（5）In:Fe:Cu:LiNbO3 晶体蓝光光折变与非挥发全息存储

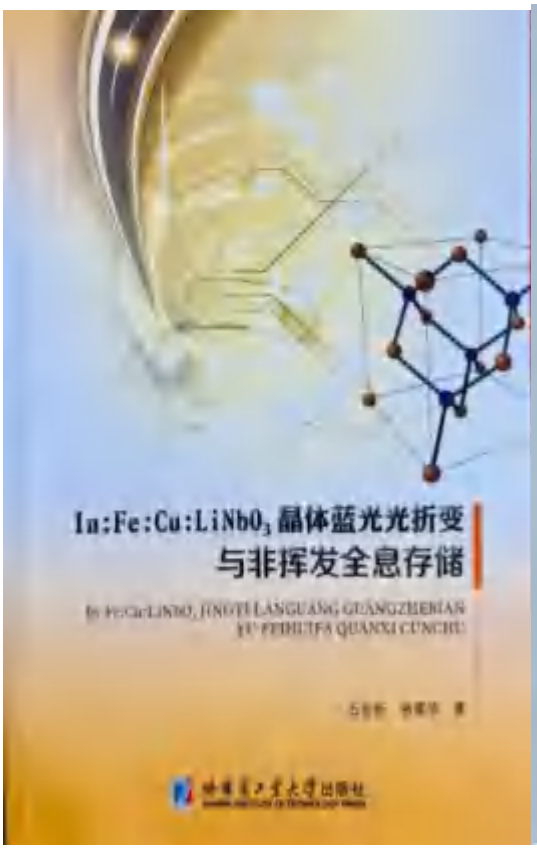

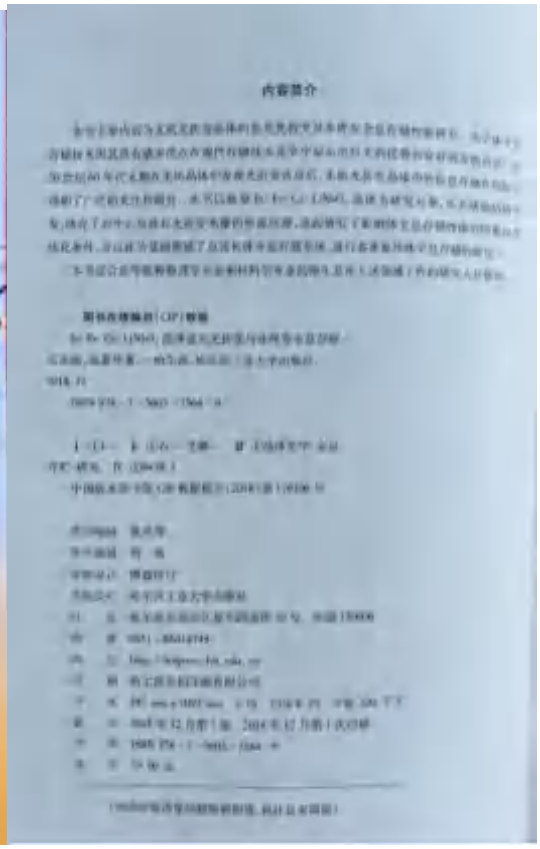
内容简介

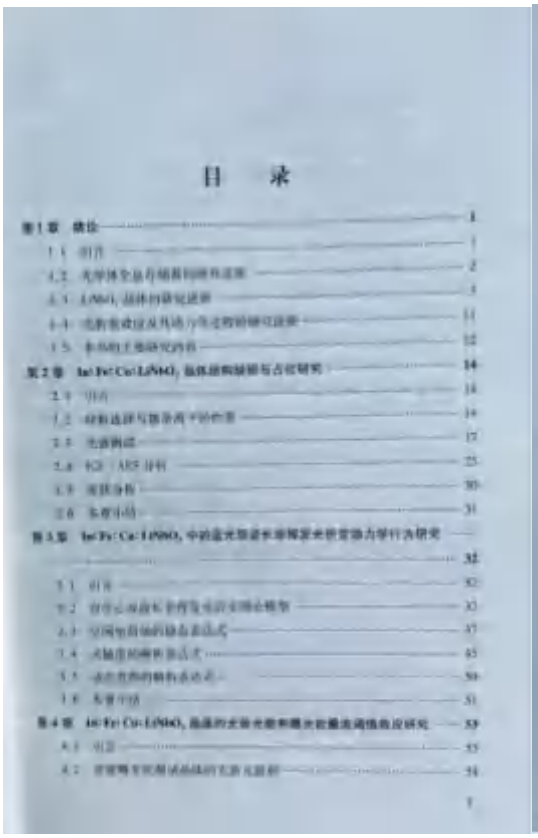
目　录

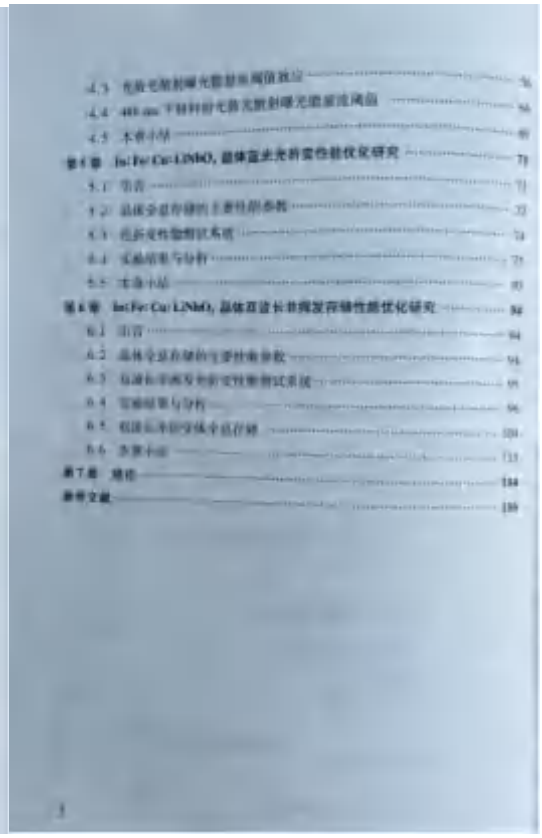

（6）分数阶变换与光学图像加密

（7）光电功能材料与器件

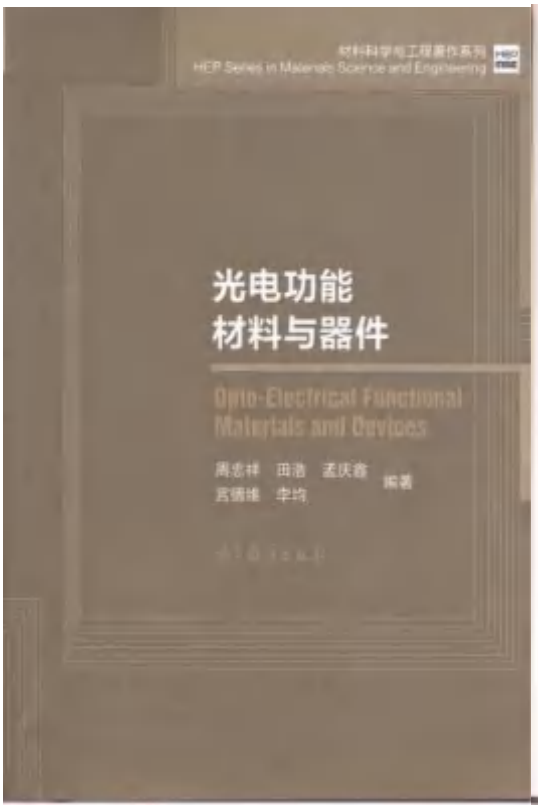
材料科学与工程著作系列
HEP Series in Materials Science and Engineering
光电功能
材料与器件
Opto-Electrical Functional
Materials and Devices
周志祥 田浩 孟庆森
宫骚维 李均 编著

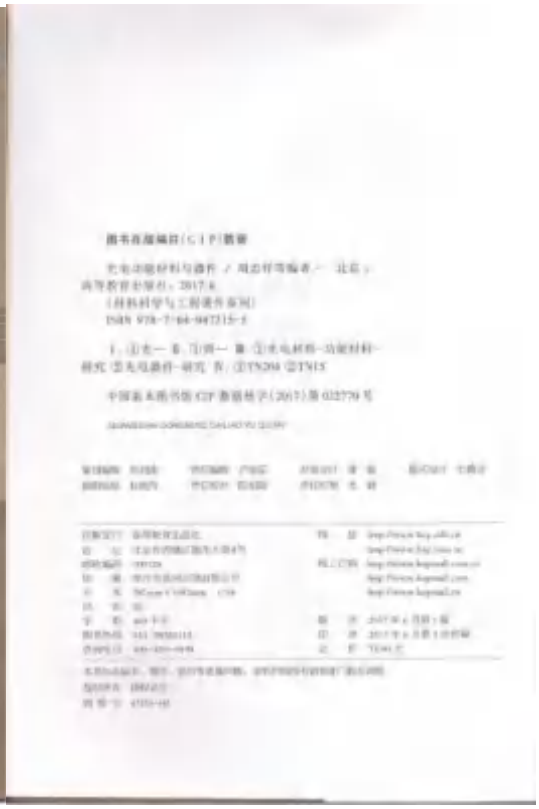


目 录

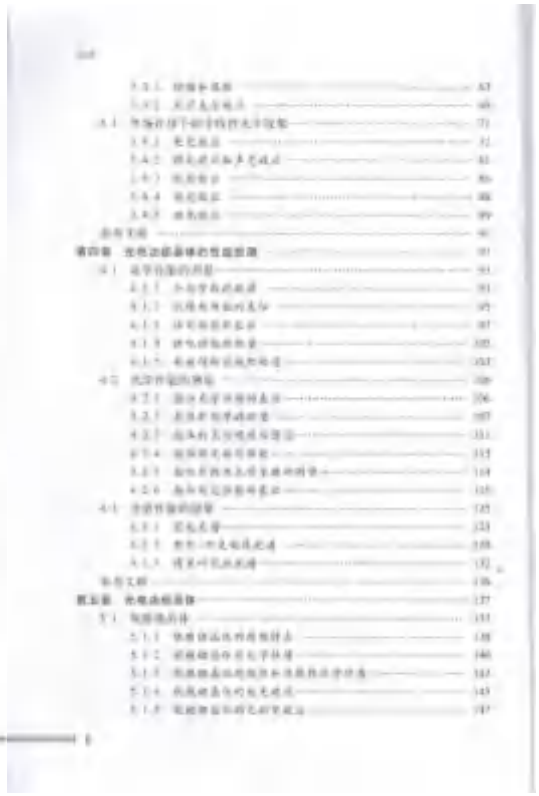

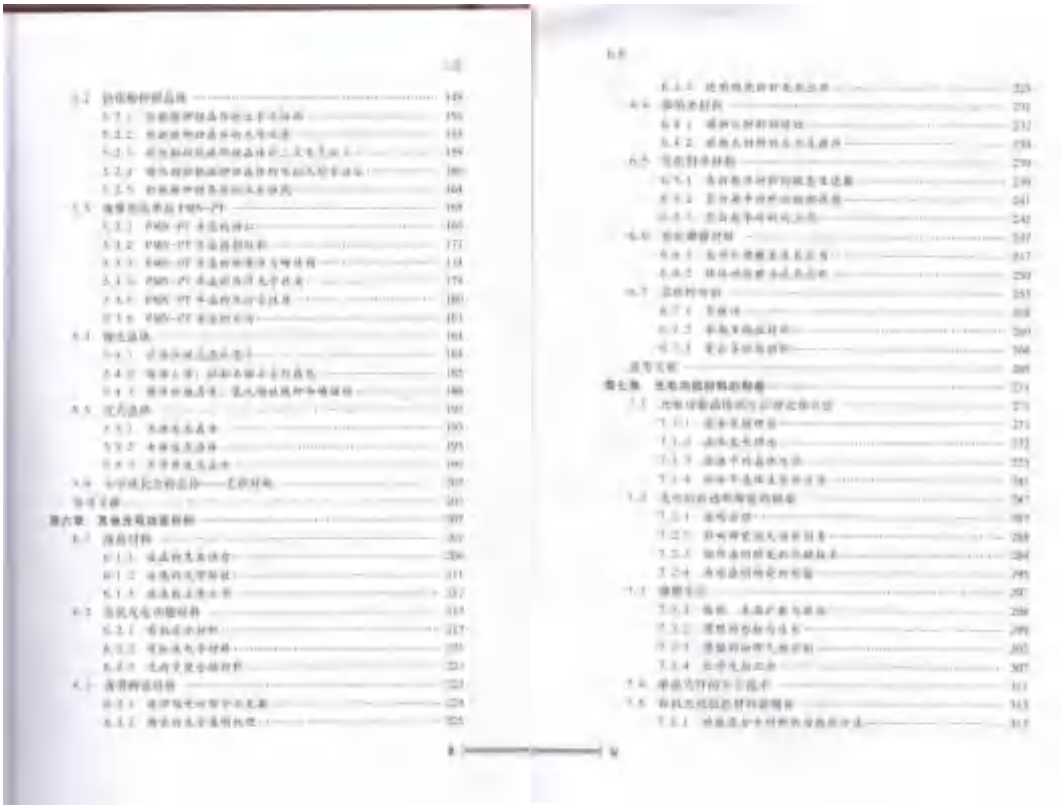

（8）光学非线性测量新技术—4f 相位成像技术

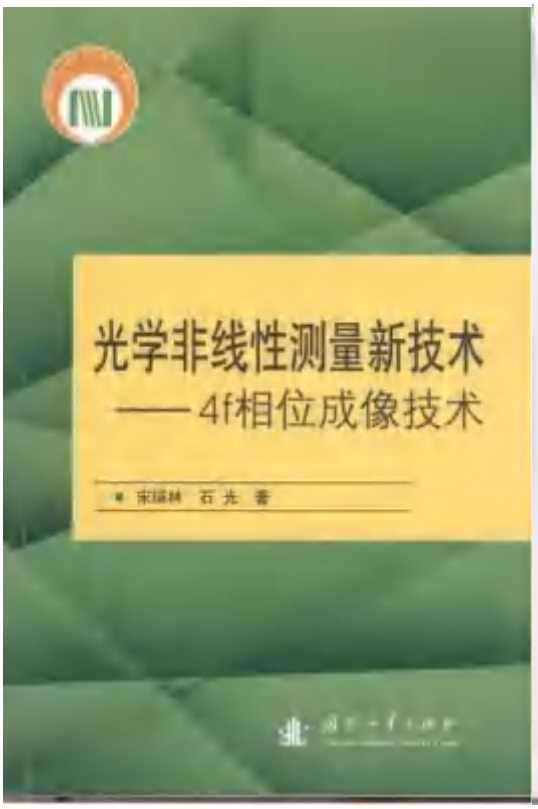

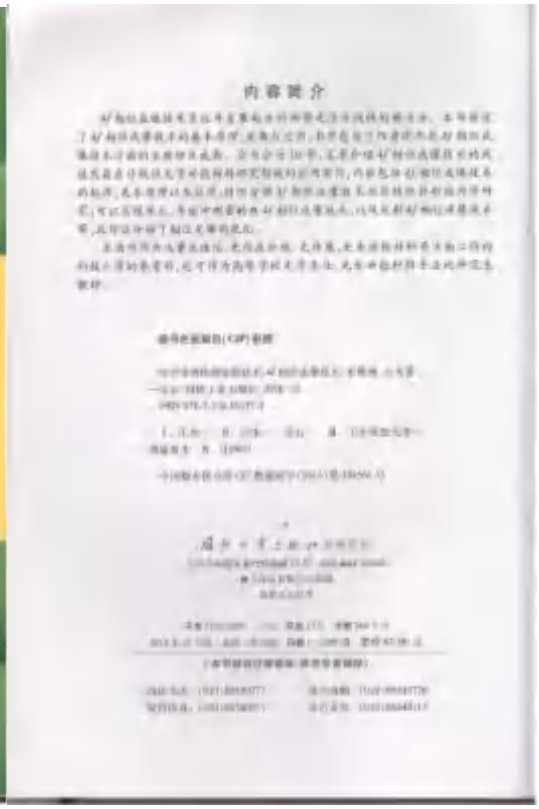
内容简介

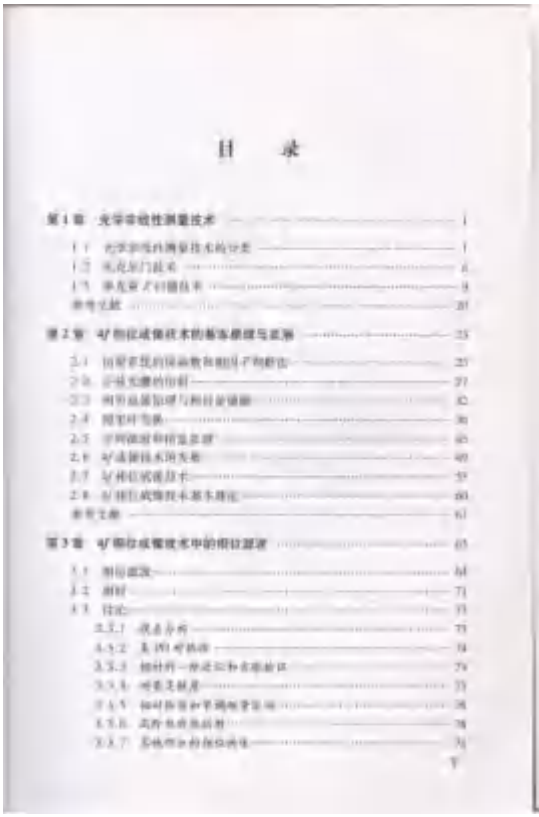
目 录

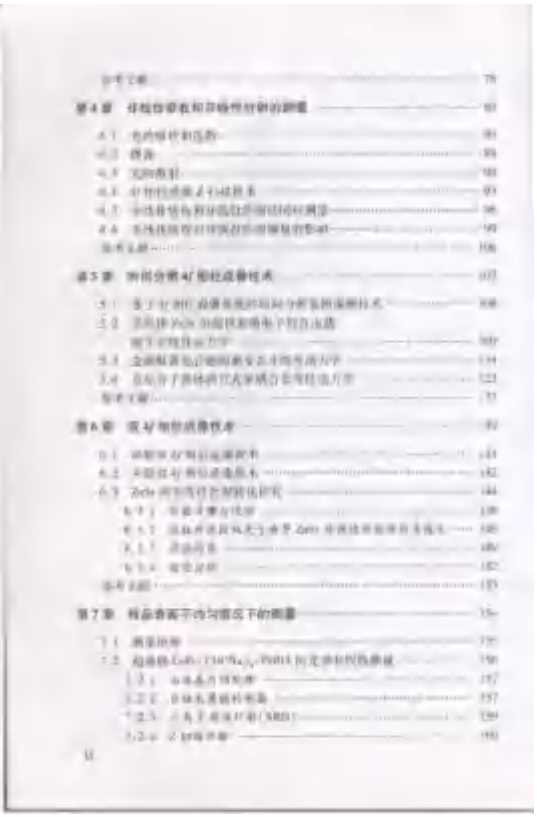

（9）宇宙中的生命

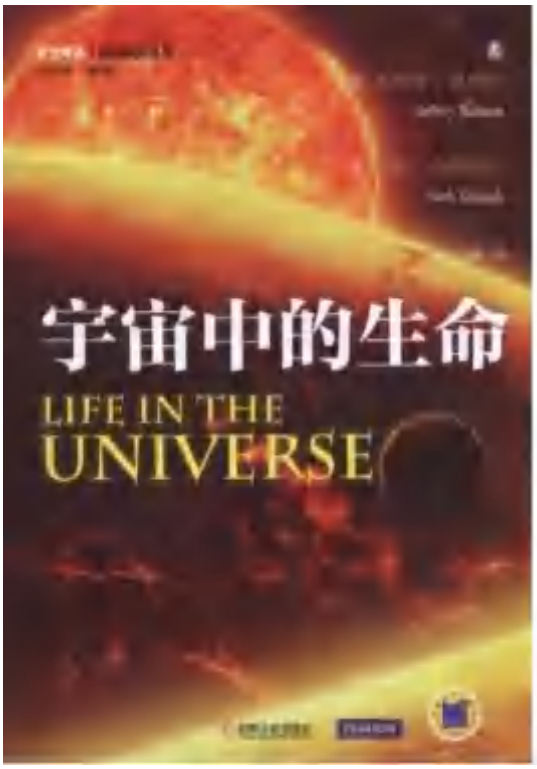

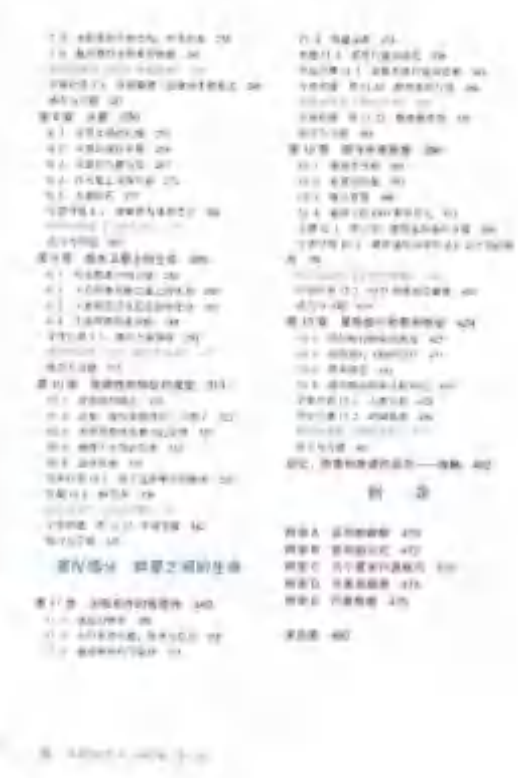

（10）《大学物理学》（第四版）

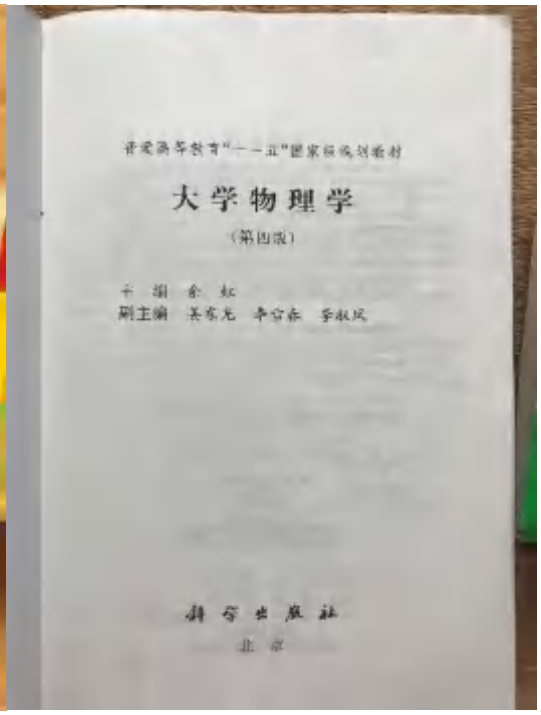

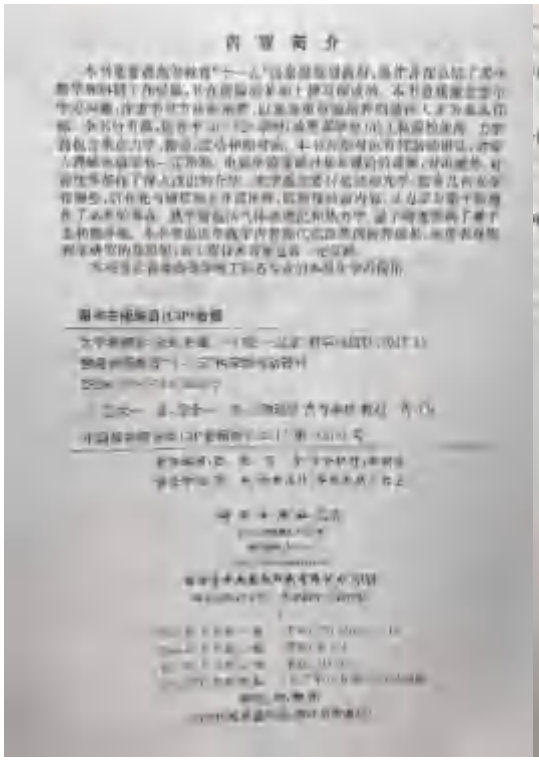

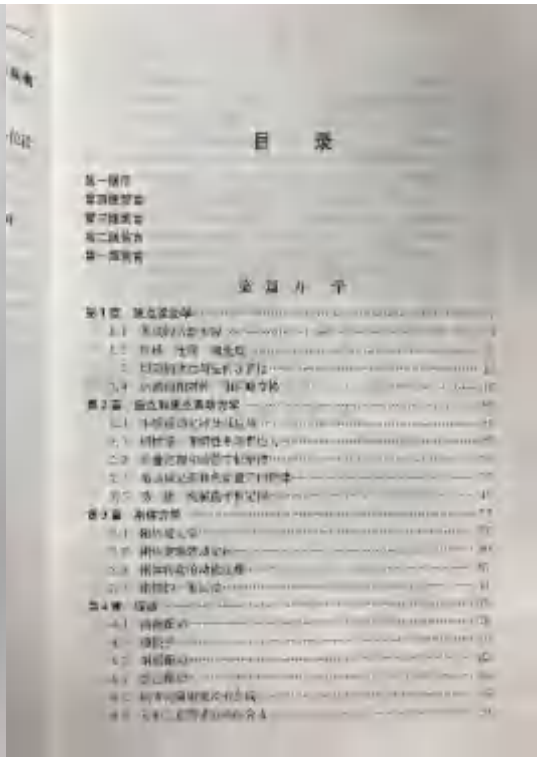

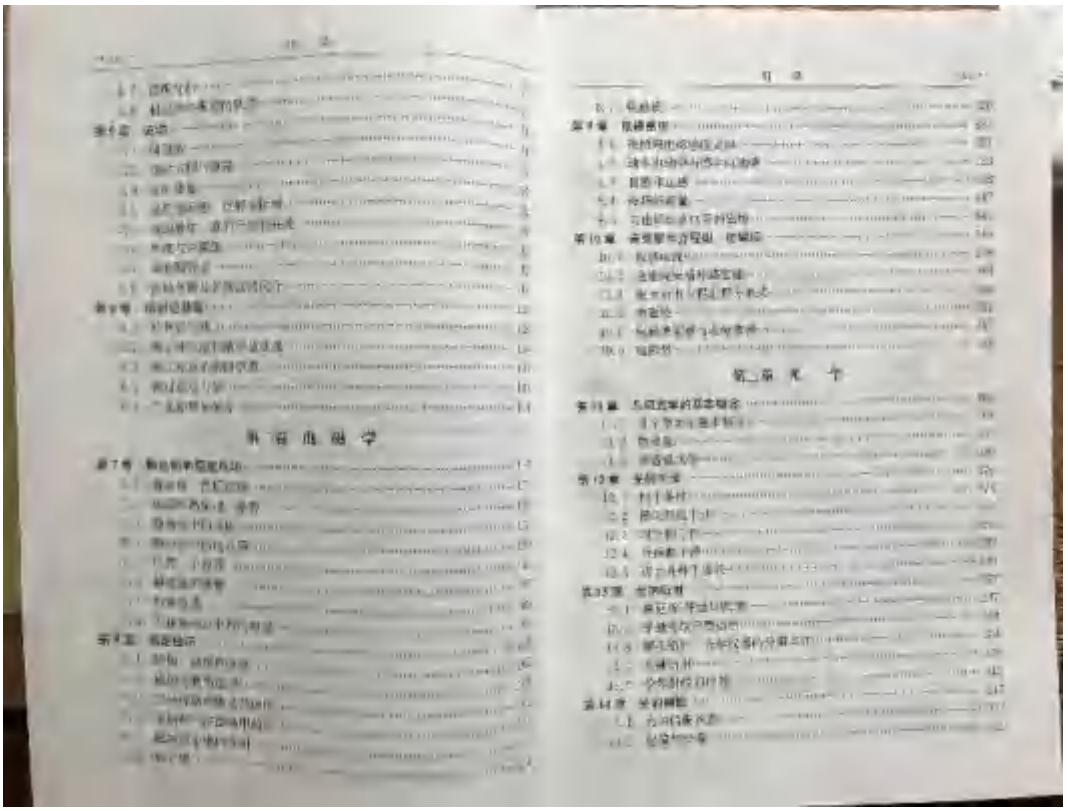

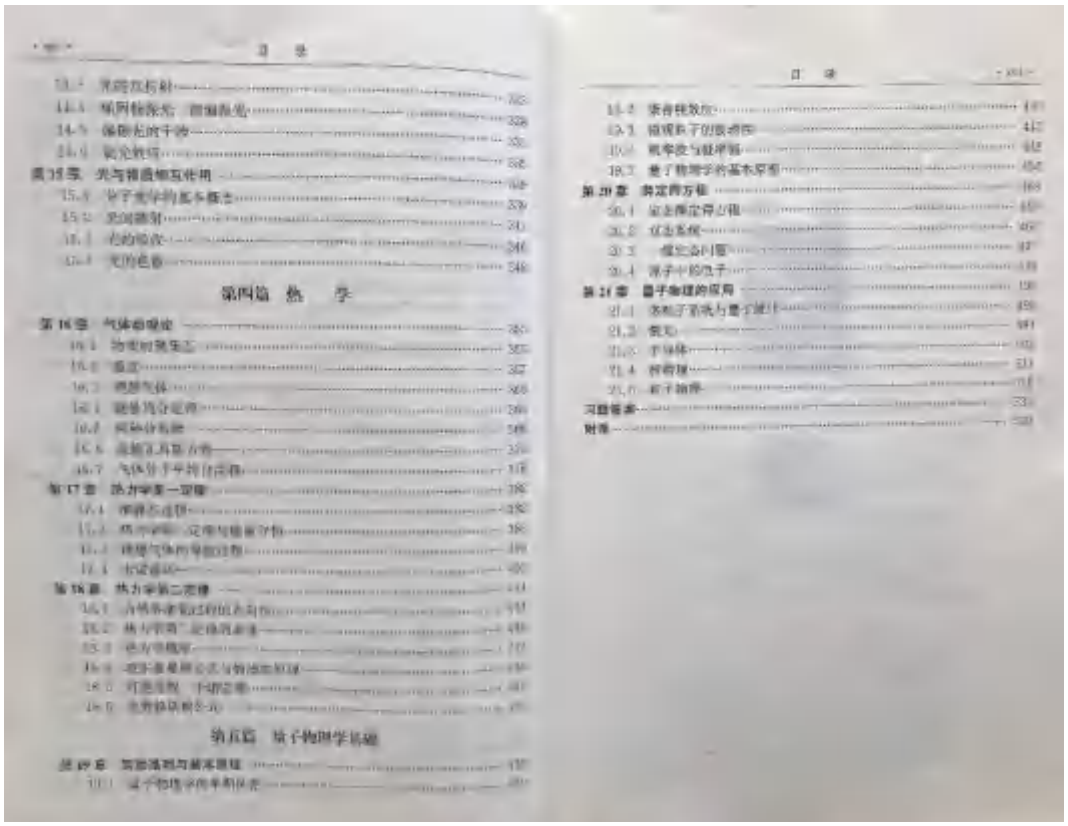

（11）光波导理论基础

目　录

（12）碳基和类碳超硬材料的第一性原理研究

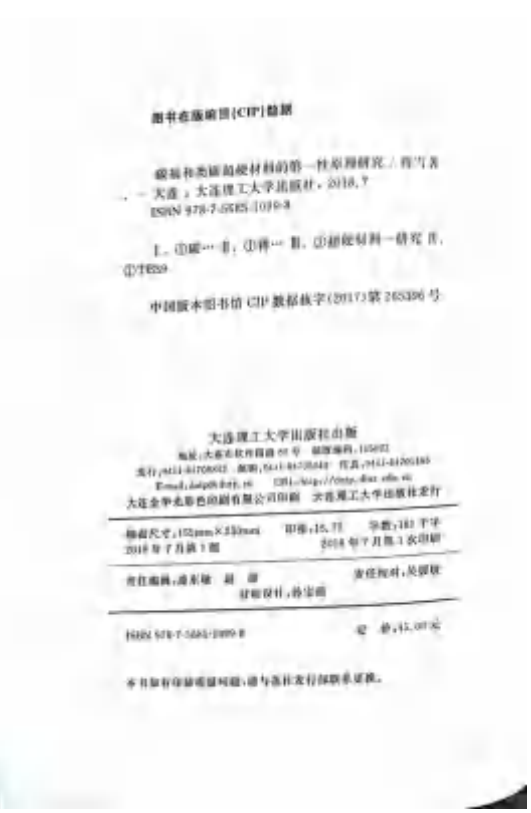


目　录

（13）Graphene Oxide: Physics and Application

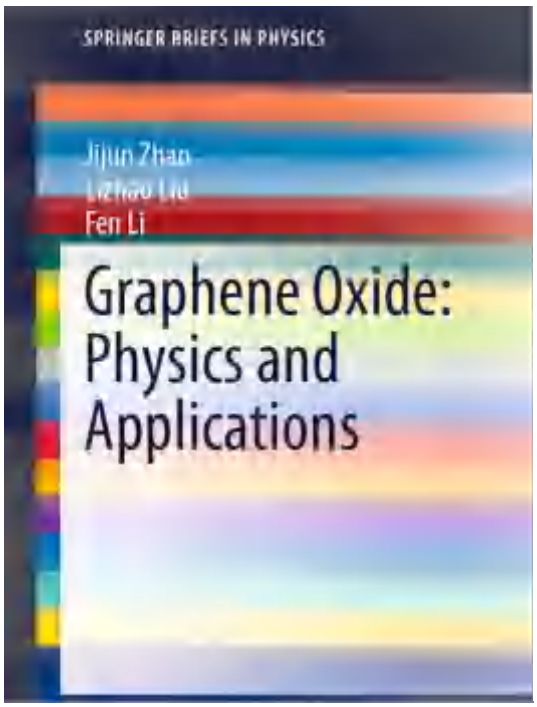

Contents

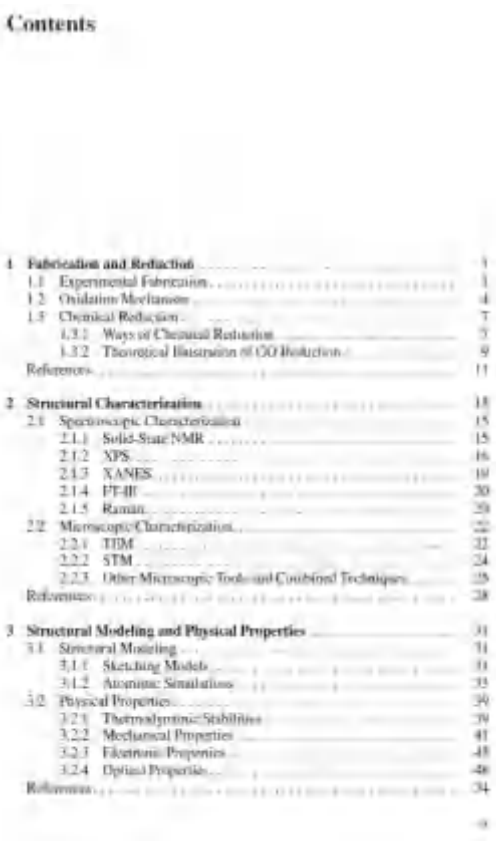

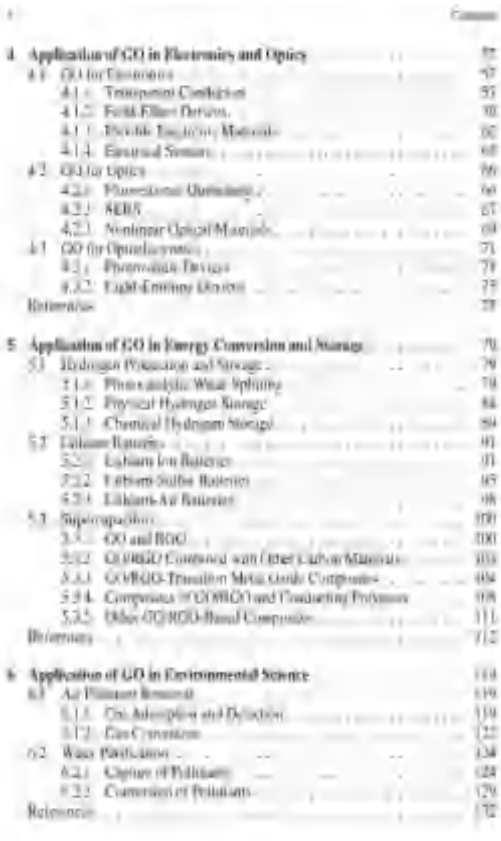

（4）高水平文章佐证材料

序号	文章名称	文章类型	刊载论文的刊物名称、期刊号、期刊来源及收录情况等	主要完成人
1	Ferroelectric crystals with giant electro-optic property enabling ultracompact Q-switches	SCI	Science 376, 6591, 2022	Xin Liu, Peng Tan, Xue Ma
2	Light-induced dimension crossover dictated by excitonic correlations	SCI	Nature Communications 13, 963, 2022	Yun Cheng, Alfred Zong, Jun Li
3	Multidimensional phase singularities in nanophotonics	SCI	Science 374(6555): eabj0039, 2021	Jincheng Ni, Can Huang, LeiMing Zhou
4	Photoluminescence mechanism of carbon dots: triggering high-color-purity red fluorescence emission through edge amino protonation	SCI	Nature Communications 12,6856,2021	Qing Zhang, Ruoyu Wang, Bowen Feng
5	High-efficiency broadband achromatic metalens for near-IR biological imaging window	SCI	Nature Communications 12, 5560, 2021	Yujie Wang, Qinmiao Chen, Wenhong Yang
6	Engineering single-atomic ruthenium catalytic sites on defective nickel-iron layered double hydroxide for overall water splitting	SCI	Nature Communications 12, 4587, 2021	Panlong Zhai, Mingyue Xia, Yunzhen Wu
7	Direct observation of chaotic resonances in optical microcavities	SCI	Light Science & Applications 10, 135, 2021	Shuai Wang, Shuai Liu, Yilin Liu
8	Suppressing meta-holographic artifacts by laser coherence tuning	SCI	Light Science & Applications 10, 104, 2021	Yaniv Eliezer, Geyang Qu, Wenhong Yang
9	Transparent ferroelectric crystals with ultrahigh piezoelectricity	SCI	Nature 577, 7790, 2020	Chaorui Qiu, Bo Wang, Nan Zhang
10	Breaking 50 Femtosecond Resolution Barrier in MeV Ultrafast Electron Diffraction with a Double Bend Achromat	SCI	Physical Review Letters 124, 134803, 2020	Fengfeng Qi, Zhuoran Ma, Lingrong Zhao

	Compressor			
11	Ultrafast control of vortex microlasers	SCI	Science 367(6481):1018-1021, 2020	Can Huang, Chen Zhang Shumin Xiao
12	Comprehensive defect suppression in perovskite nanocrystals for high-efficiency light-emitting diodes	SCI	Nature Photonics 15, 148-155, 2021	Young-Hoon Kim, Sungjin Kim, Arvin Kakekhani
13	Reprogrammable meta-hologram for optical encryption	SCI	Nature Communications 11, 5484, 2020	Geyang Qu, Wenhong Yang, Qinghai Song
14	Universal growth of ultra-thin III–V semiconductor single crystals	SCI	Nature Communications 11, 3979, 2020	Yunxu Chen, Jinxin Liu, Mengqi Zeng
15	Engineering active sites on hierarchical transition bimetal oxides/sulfides heterostructure array enabling robust overall water splitting	SCI	Nature Communications 11, 5462, 2020	Panlong Zhai, Yanxue Zhang, Yunzhen Wu, Junfeng Gao
16	Ultra-large electric field–induced strain in potassium sodium niobate crystals	SCI	Science Advances 13(6), eaay5979, 2020	Chengpeng Hu, Xiangda Meng, Mao-hua Zhang
17	High-performance position-sensitive detector based on the lateral photoelectrical effect of two-dimensional materials	SCI	Light Science & Applications 9, 88, 2020	Chang Hu, Xianjie Wang, Bo Song
18	Momentum-Topology-Induced Optical Pulling Force	SCI	Physical Review Letters 124, 143901, 2020	Hang Li, Yongyin Cao, Bojian Shi
19	Breakup and Recovery of Topological Zero Modes in Finite Non-Hermitian Optical Lattices	SCI	Physical Review Letters 123, 165701, 2019	Wange Song, Wenzhao Sun, Chen Chen
20	All-optical control of lead halide perovskite microlasers	SCI	Nature Communications 10, 1770, 2019	Nan Zhang, Yubin Fan, Kaiyang Wang

21	Arbitrarily routed mode-division multiplexed photonic circuits for dense integration	SCI	Nature Communications 10, 3263, 2019	Yingjie Liu, Ke Xu, Shuai Wang
22	Resonance-enhanced three-photon luminesce via lead halide perovskite metasurfaces for optical encoding	SCI	Nature Communications 10, 2085, 2019	Yubin Fan, Yuhan Wang, Nan Zhang
23	Room temperature electrofreezing of water yields a missing dense ice phase in the phase diagram	SCI	Nature Communications 10, 1925, 2019	Weiduo Zhu, Yingying Huang, Chongqin Zhu
24	Quasiparticle interference and nonsymmorphic effect on a floating band surface state of ZrSiSe	SCI	Nature Communications 9, 4153, 2018	Zhen Zhu, Tay-Rong Chang, Cheng-Yi Huang
25	Antiferromagnetic Order in Epitaxial FeSe Films on $SrTiO_3$	SCI	Physical Review Letters 120, 097001, 2018	Y. Zhou, L. Miao, P. Wang
26	Self-induced backaction optical pulling force	SCI	Physical Review Letters 120, 123901, 2018	Tongtong Zhu, Yongyin Cao, Lin Wang
27	Atomic-level insight into super-efficient electrocatalytic oxygen evolution on iron and vanadium co-doped nickel (oxy)hydroxide	SCI	Nature Communications 9, 2885, 2018	Jian Jiang, Fanfei Sun, Si Zhou
28	Stabilization of body-centred cubic iron under inner-core conditions	SCI	Nature Geoscience 10, 312, 2017	Anatoly B. Belonoshko, Timofei Lukinov, Jie Fu, Jijun Zhao

29	A new phase diagram of water under negative pressure: The rise of the lowest-density clathrate s-III	SCI	Science Advances 2, e1501010, 2016	Yingying Huang, Chongqin Zhu, Lu Wang
30	Quasi-freestanding epitaxial silicene on Ag(111) by oxygen intercalation	SCI	Science Advances 2, e1600067, 2016	Yi Du, Jincheng Zhuang, Jiaou Wang
31	Majorana Zero Mode Detected with Spin Selective Andreev Reflection in the Vortex of a Topological Superconductor	SCI	Physical Review Letters 116, 257003,2016	Hao-Hua Sun, Kai-Wen Zhang, Lun-Hui Hu
32	Epitaxial growth of two-dimensional stanene	SCI	Nature Materials 14, 1020-1025,2015	Feng-feng Zhu, Wei-jiong Chen, Yong Xu
33	The structural origin of the hard-sphere glass transition in granular packing	SCI	Nature Communications 6, 8409, 2015	Chengjie Xia, Jindong Li, Yixin Cao
34	Superconductivity above 100 K in single-layer FeSe films on doped $SrTiO_3$	SCI	Nature Materials 14, 285-289, 2015	Jian-Feng Ge, Zhi-Long Liu, Canhua Liu
35	Demonstration of Nonlinear-Energy-Spread Compensation in Relativistic Electron Bunches with Corrugated Structures	SCI	Physical Review Letters 114,114801,2015	Feichao Fu, Rui Wang, Pengfei Zhu
36	Multichromatic Narrow-Energy-Spread Electron Bunches from Laser-Wakefield Acceleration with Dual-Color Lasers	SCI	Physical Review Letters 114, 084801, 2015	M. Zeng, M. Chen, L.L. Yu
37	Experimental Detection of a Majorana Mode in the core of a Magnetic Vortex inside a Topological Insulator-Superconductor Bi2Te3/NbSe2 Heterostructure	SCI	Physical Review Letters 114, 017001, 2015	Jin-Peng Xu, Mei-Xiao Wang, Zhi Long Liu
38	Quantum teleportation with independent sources and prior entanglement distribution over a network	SCI	Nature Photonics 10, 671-675, 2016	Qi-Chao Sun, Ya-Li Mao, Si-Jing Chen

39	Bimetallic Microswimmers Speed Up in Confining Channels	SCI	Physical Review Letters 117, 198001, 2016	Chang Liu, Chao Zhou, Wei Wang
40	Controllable Terahertz Radiation from a Linear-Dipole Array Formed by a Two-Color Laser Filament in Air	SCI	Physical Review Letters 117, 243901, 2016	Zhelin Zhang, Yanping Chen, Min Chen
41	Carrier-Envelope-Phase Characterization for an Isolated Attosecond Pulse by Angular Streaking	SCI	Physical Review Letters 116, 203601, 2016	Pei-Lun He, Camilo Ruiz, Feng He
42	Extreme Mechanics of Probing the Ultimate Strength of Nanotwinned Diamond	SCI	Physical Review Letters 117, 116103, 2016	Bing Li, Hong Sun, Changfeng Chen
43	Granular materials flow like complex fluids	SCI	Nature 551, 360-363, 2017	Binquan Kou, Yixin Cao, Jindong Li
44	Experimental studies of vibrational modes in a two-dimensional amorphous solid	SCI	Nature Communications 8, 67, 2017	Ling Zhang, Jie Zheng, Yinqiao Wang
45	Origin of Noncubic Scaling Law in Disordered Granular Packing	SCI	Physical Review Letters 118, 238002, 2017	Chengjie Xia, Jindong Li, Binquan Kou
46	Dynamical Transition of Collective Motions in Dry Proteins	SCI	Physical Review Letters 119, 048101, 2017	Zhuo Liu, Juan Huang, Madhusudan Tyag
47	Strong Field Theories beyond Dipole Approximations in Nonrelativistic Regimes	SCI	Physical Review Letters 118, 163203, 2017	Pei-Lun He, Di Lao, Feng He
48	Structural and topological nature of plasticity in sheared granular materials	SCI	Nature Communications 9, 2911, 2018	Yixin Cao, Jindong Li, Binquan Kou

49	Manipulation of polarizations for broadband terahertz waves emitted from laser plasma filaments	SCI	Nature Photonics 12, 554-559, 2018	Zhelin Zhang, Yanping Chen, Sen Cui
50	Coulomb-Driven Relativistic Electron Beam Compression	SCI	Physical Review Letters 120, 044801, 2018	Chao Lu, Tao Jiang, Shengguang Liu
51	Experimental Machine Learning of Quantum States	SCI	Physical Review Letters 120, 240501, 2018	Jun Gao, Ku-Feng Qiao, Zhi-Qiang Jiao
52	Frozen Condition of Quantum Coherence for Atoms on a Stationary Trajectory	SCI	Physical Review Letters 121, 073602, 2018	Anwei Zhang, Keye Zhang, Lan Zhou
53	Gradual Crossover from Subdiffusion to Normal Diffusion: A Many-Body Effect in Protein Surface Water	SCI	Physical Review Letters 120, 248101,2018	Pan Tan, Yihao Liang, Qin Xu
54	Mapping Twisted Light into and out of a Photonic Chip	SCI	Physical Review Letters 121, 233602, 2018	Yuan Chen, Jun Gao, Zhi-Qiang Jiao
55	Multistage Coupling of Laser-Wakefield Accelerators with Curved Plasma Channels	SCI	Physical Review Letters 120, 154801, 2018	J. Luo, M. Chen, W. Y. Wu
56	Translational and Rotational Dynamical Heterogeneities in Granular Systems	SCI	Physical Review Letters 121, 018002, 2018	Binquan Kou, Yixin Cao, Jindong Li
57	Broadband THz to NIR up-converter for photon type THz imaging	SCI	Nature Communications 10, 3513, 2019	Peng Bai, Yueheng Zhang, Tianmeng Wang
58	Direct Observation of Topology from Single-Photon Dynamics	SCI	Physical Review Letters 122, 193903, 2019	Yao Wang, Yong-Heng Lu, Feng Mei

59	Parity-Induced Thermalization Gap in Disordered Ring Lattices	SCI	Physical Review Letters 122, 013903, 2019	Yao Wang, Jun Gao, Xiao-Ling Pang
60	Superhigh-Resolution Recognition of Optical Vortex Modes Assisted by a Deep-Learning Method	SCI	Physical Review Letters 123, 183902, 2019	Zhanwei Liu, Shuo Yan, Haigang Liu
61	Coupling of Edge States and Topological Bragg Solitons	SCI	Physical Review Letters 123,254103,2019	Weifeng Zhang, Xianfeng Chen, Yaroslav V. Kartashov
62	Terahertz Oscilloscope for Recording Time Information of Ultrashort Electron Beams	SCI	Physical Review Letters 122, 144801, 201	Lingrong Zhao, Zhe Wang, Heng Tang
63	Connecting shear localization with the long-range correlated polarized stress fields in granular materials	SCI	Nature Communications 11, 4349, 2020	Yinqiao Wang, Yujie Wang, Jie Zhang
64	Designer spin order in diradical nanographenes	SCI	Nature Communications 11, 6076, 2020	Yuqiang Zheng, Can Li, Chengyang Xu
65	Optical soliton formation controlled by angle twisting in photonic moiré lattices	SCI	Nature Photonics 14, 663-668, 2020	Qidong Fu, Peng Wang, Changming Huang
66	Localization and delocalization of light in photonic moiré lattices	SCI	Nature 577, 42-46, 2020	Peng Wang, Yuanlin Zheng, Xianfeng Chen
67	Direct Visualizing the Spin Hall Effect of Light via Ultrahigh-Order Modes	SCI	Physical Review Letters 124, 053902, 2020	Hailang Dai, Luqi Yuan, Cheng Yin
68	Integrated Quantum-Walk Structure and NAND Tree on a Photonic Chip	SCI	Physical Review Letters 125, 160502, 2020	Yao Wang, Zi-Wei Cui, Yong-Heng Lu
69	Subharmonic Entrainment Breather Solitons in Ultrafast Lasers	SCI	Physical Review Letters 125, 163901, 2020	Tianhao Xian, Li Zhan, Wenchao Wang

70	Vector Vortex Beam Emitter Embedded in a Photonic Chip	SCI	Physical Review Letters 124, 153601, 2020	Yuan Chen, Ke-Yu Xia, Wei-Guan Shen
71	Femtosecond Relativistic Electron Beam with Reduced Timing Jitter from THz Driven Beam Compression	SCI	Physical Review Letters 124, 054802, 2020	Lingrong Zhao, Heng Tang, Chao Lu
72	Young's Double-Slit Interference in a Hydrogen Atom	SCI	Physical Review Letters 124, 163201, 2020	Pei-Lun He, Zhao-Han Zhang, Feng He
73	Engineering of Magnetic Coupling in Nanographene	SCI	Physical Review Letters 124, 147206, 2020	Yuqiang Zheng, Can Li, Yan Zhao
74	Multiple In-Gap States Induced by Topological Surface States in the Superconducting Topological Crystalline Insulator Heterostructure Sn1−xPbxTe-Pb	SCI	Physical Review Letters 125, 136802, 2020	Hao Yang, Yao-Yi Li, Teng-Teng Liu
75	Strain Tunable Semimetal–Topological-Insulator Transition in Monolayer 1T0 -WTe2	SCI	Physical Review Letters 125, 046801, 2020	Chenxiao Zhao, Mengli Hu, Jin Qin
76	A hybrid quantum memory-enabled network at room temperature	SCI	Science Advances 6, eaax1425, 2020	Xiao-Ling Pang, Ai-Lin Yang, Jian-Peng Dou
77	A scalable photonic computer solving the subset sum problem	SCI	Science Advances 6, eaay5853, 2020	Xiao-Yun Xu, Xuan-Lun Huang, Zhan-Ming Li
78	Extremely brilliant GeV-rays from a two-stage laser-plasma accelerator	SCI	Science Advances 6, eaaz7240, 2020	Xing-Long Zhu, Min Chen, Su-Ming Weng
79	Multifunctional antiferromagnetic materials with giant piezomagnetism and noncollinear spin current	SCI	Nature Communications 12, 2846, 2021	Hai-Yang Ma, Mengli Hu, Nana Li

80	Sierpiński Structure and Electronic Topology in Bi Thin Films on InSb(111)B Surfaces	SCI	Physical Review Letters 126, 176102, 2021	Chen Liu, Yinong Zhou, Guanyong Wang
81	Controlling Cell Motion and Microscale Flow with Polarized Light Fields	SCI	Physical Review Letters 126, 058001, 2021	Siyuan Yang, Mingji Huang, Yongfeng Zhao
82	X-Ray Tomography Investigation of Cyclically Sheared Granular Materials	SCI	Physical Review Letters 126, 048002, 2021	Yi Xing, Jie Zheng, Jindong Li
83	Connecting Packing Efficiency of Binary Hard Sphere Systems to Their Intermediate Range Structure	SCI	Physical Review Letters 127,278001,2021	Houfei Yuan, Zhen Zhang, Walter Kob
84	Dynamical Transitions and Critical Behavior between Discrete Time Crystal Phases	SCI	Physical Review Letters 126, 020602, 2021	Xiaoqin Yang, Zi Cai
85	Experimentally Detecting Quantized Zak Phases without Chiral Symmetry in Photonic Lattices	SCI	Physical Review Letters 127, 147401, 2021	Zhi-Qiang Jiao, Stefano Longhi, Xiao-Wei Wang
86	Symmetry-Induced Error Filtering in a Photonic Lieb Lattice	SCI	Physical Review Letters 126, 110501, 2021	Yi-Jun Chang, Yong-Heng Lu, Yao Wang
87	Microscopic structure and dynamics study of granular segregation mechanism by cyclic shear	SCI	Science Advances 7, eabe8737, 2021	Zhifeng Li, Zhikun Zeng, Yi Xing
88	Anomalous Contribution to the Nematic Electronic States from the Structural Transition in FeSe Revealed by Time- and Angle-Resolved Photoemission Spectroscopy	SCI	Physical Review Letters 128, 246401, 2022	Yuanyuan Yang, Qisi Wang, Shaofeng Duan
89	Nonlinear Thouless Pumping: Solitons and Transport Breakdown	SCI	Physical Review Letters 128, 154101, 2022	Qidong Fu, Peng Wang, Yaroslav V. Kartashov

（1）Ferroelectric crystals with giant electro-optic property enabling ultracompact Q-switches, Science

RESEARCH ARTICLE

ELECTROOPTICS

Ferroelectric crystals with giant electro-optic property enabling ultracompact Q-switches

（2）Light-induced dimension crossover dictated by excitonic correlations, Nature Communications

nature COMMUNICATIONS

ARTICLE

OPEN

Light-induced dimension crossover dictated by excitonic correlations

Yun Cheng[1,2,15], Alfred Zong[3,4,15], Jun Li[5], Wei Xia[6,7], Shanfeng Duan[8], Wenxuan Zhao[9], Yalian Li[9], Fengfeng Qi[1,2], Jun Wu[1,2], Lingyang Zhao[1,2], Pengfei Zhu[1,2], Xiao Zou[1,2], Tao Jiang[1,2], Yanfeng Guo[6], Lexian Yang[9], Dong Qian[8], Wentao Zhang[8,9], Anshul Kogar[10,11], Michael W. Zuerch[3,4,12], Dao Xiang[1,2,13,14] & Jie Zhang[1,2,11,12]

In low-dimensional systems with strong electronic correlations, the application of an ultrashort laser pulse often yields novel phases that are otherwise inaccessible. The central challenge in understanding such phenomena is to determine how dimensionality and many-body correlations together govern the pathway of a non-adiabatic transition. To this end, we examine a layered compound, 1T-TiSe$_2$, whose three-dimensional charge-density-wave (3D CDW) state also features exciton condensation due to strong electron-hole interactions. We find that photoexcitation suppresses the equilibrium 3D CDW while creating a nonequilibrium 2D CDW. Remarkably, the dimension reduction does not occur unless bound electron-hole pairs are broken. This relation suggests that excitonic correlations maintain the out-of-plane CDW coherence, settling a long-standing debate over their role in the CDW transition. Our findings demonstrate how optical manipulation of electronic interaction enables one to control the dimensionality of a broken-symmetry order, paving the way for realizing other emergent states in strongly correlated systems.

（3）Multidimensional phase singularities in nanophotonics， Science

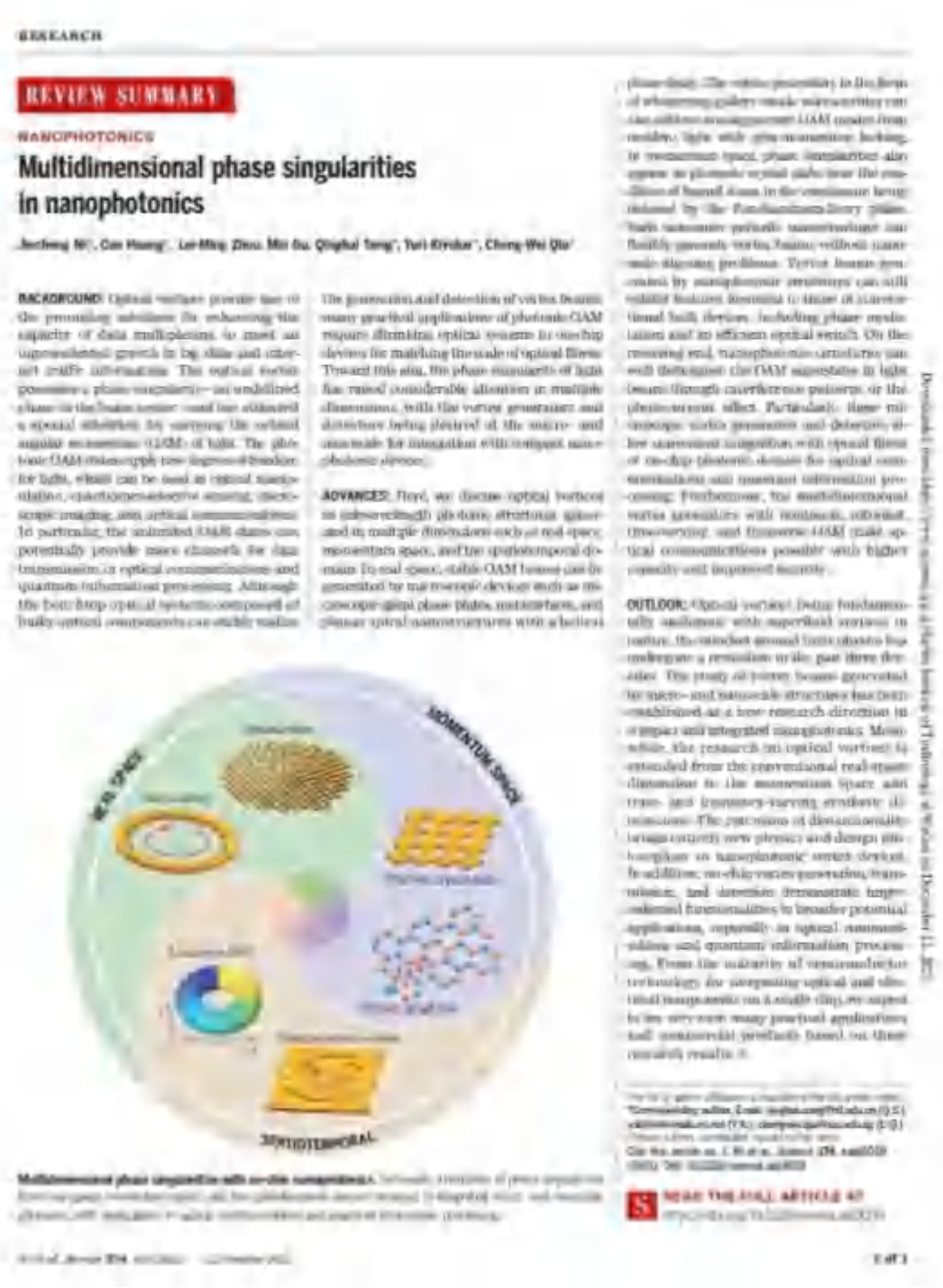

RESEARCH

REVIEW SUMMARY

NANOPHOTONICS

Multidimensional phase singularities in nanophotonics

Jincheng Ni, Cao Huang, Lei-Ming Zhou, Min Gu, Qinghai Song, Yuri Kivshar, Cheng-Wei Qiu

BACKGROUND: Optical vortices provide one of the promising solutions for enhancing the capacity of data multiplexing to meet an unprecedented growth in big data and other multi-dimensions. The optical vortex possesses a phase singularity—an undefined phase in the beam center—and has obtained a special attention by carrying the orbital angular momentum (OAM) of light. The photonic OAM eigenmodes form high-dimensional bases for light, which can be used in optical manipulation, quantum-enhanced sensing, electromagnetic imaging, and optical communications. In particular, the unlimited OAM states can potentially provide more channels for data transmission in optical communications and quantum information processing. Although the bulk-lens optical systems composed of bulky optical components can stably realize the generation and detection of vortex beams, many practical applications of photonic OAM require dimensions optical systems to on-chip devices for matching the scale of optical fibers. Toward this aim, the phase singularity of light has raised considerable attention in multiple dimensions, with the vortex generators and detectors being desired at the micro- and nanoscale for integration with compact nanophotonic devices.

ADVANCES: First, we discuss optical vortices in subwavelength photonic structures spanned in multiple dimensions such as real space, momentum space, and the spatiotemporal domain. In real space, stable OAM beams can be generated by metasurface devices such as microscope-spiral phase plates, metasurfaces, and planar optical nanoantennas with a helicoid phase front. The vortex generators in the form of whispering-gallery-mode microcavities can also address nanoscale OAM modes from incident light with zero orbital angular momentum. In momentum space, phase singularities also appear in photonic crystal slabs near the conditions of bound states in the continuum being induced by the Friedrich-Wintgen origin. Such nanoscale photonic nanostructures can flexibly generate vortex beams without many-body diffusion problems. Vortex beams generated by nanophotonic structures can still exhibit features identical to those of conventional bulk devices, including phase modulation and an efficient optical switch. On the receiving end, nanophotonic structures can also distinguish the OAM eigenstates in light beams through interference patterns or the photoluminescent effect. Particularly, these nanoscale vortex generators and detectors allow convenient integration with optical fibers or on-chip photonic devices for optical communications and quantum information processing. Furthermore, the multidimensional vortex generators with nontrivial, off-plane, time-varying, and frequency-OAM make optical communications possible with higher capacity and improved security.

OUTLOOK: Optical vortices have fundamentally significant with superficial resonance in nature. Its mischief around little objects has undergone a revolution in the past three decades. The study of vortex beams generated by micro- and nanoscale structures has been established as a new research direction in optics and integrated nanophotonics. Meanwhile, the research on optical vortices is extended from the conventional real-space dimensions to the momentum space and time- and frequency-varying synthetic dimensions. The processes of dimensionality engage currently new physics and design principles in nanophotonic vortex devices. In addition, on-chip vortex generation, transmission, and detection demonstrate high-order functionalities to broader potential applications, especially in optical communications and quantum information processing. From the maturity of semiconductor technology for integrating optical and electrical components on a single chip, we expect to see very soon many practical applications and commercial products based on these research results.

Corresponding author. E-mail: [illegible]

Cite this article as J. Ni et al., Science 374, eabj0039 (2021). DOI: [illegible]

READ THE FULL ARTICLE AT [illegible]

Multidimensional phase singularities with on-chip nanophotonics. [illegible]

（4）Photoluminescence mechanism of carbon dots: triggering high-color-purity red fluorescence emission through edge amino protonation, Nature Communications

nature COMMUNICATIONS

ARTICLE

OPEN

Photoluminescence mechanism of carbon dots: triggering high-color-purity red fluorescence emission through edge amino protonation

Qing Zhang[1,2✉], Ruoyu Wang[1], Bowen Feng[1], Xiaoxia Zhong[1✉] & Kostya (Ken) Ostrikov[3]

Due to complex structure and surface functionalities, photoluminescence mechanisms of Carbon Dots are unknown, and it is challenging to synthesize Carbon Dots to achieve the desired optical properties. Herein, Carbon Dots simultaneously exhibiting high-color-purity (FWHM-24 nm) long wavelength one-photon fluorescence emission at 620 nm and NIR induced two-photon fluorescence emission at 630 and 680 nm are prepared by edge amino protonation treatment. Systematic analysis reveals that the protonation of 2,3-diaminophenazine changes the molecular state of Carbon Dots, decreases the photon transition band gap, and triggers red fluorescence emission with the dramatically narrowed peak width. As the oxidation products of reactant o-phenylendiamine, the emergence of 2,3-diaminophenazine as a photoluminescence determiner suggests that fluorophore products of precursor conversion are viable determinants of the desired luminescence properties of Carbon Dots. This work shows a new way for predicting and controlling photoluminescence properties of Carbon Dots, and may guide the development of tunable Carbon Dots for a broad range of applications.

[illegible]

（5）High-efficiency broadband achromatic metalens for near-IR biological imaging window, Nature Communications

nature COMMUNICATIONS

ARTICLE

OPEN

High-efficiency broadband achromatic metalens for near-IR biological imaging window

Yujie Wang[1,5], Qinmiao Chen[1,5], Wenhong Yang[1,5], Ziheng Ji[1,5], Limin Jin[1], Xing Ma[1], Qinghai Song[1], Alexandra Boltasseva[2], Jiecai Han[3], Vladimir M. Shalaev[2] & Shumin Xiao[1,3,4]

Over the past years, broadband achromatic metalenses have been intensively studied due to their great potential for applications in consumer and industry products. Even though significant progress has been made, the efficiency of technologically relevant silicon metalenses is limited by the intrinsic material loss above the bandgap. In turn, the recently proposed achromatic metalens utilizing transparent, high-index materials such as titanium dioxide has been restricted by the small thickness and showed relatively low focusing efficiency at longer wavelengths. Consequently, metalens-based optical imaging in the biological transparency window has so far been severely limited. Herein, we experimentally demonstrate a polarization-insensitive, broadband titanium dioxide achromatic metalens for applications in the near-infrared biological imaging. A large-scale fabrication technology has been developed to produce titanium dioxide nanopillars with record-high aspect ratios featuring pillar heights of 1.5 μm and ~90° vertical sidewalls. The demonstrated metalens exhibits dramatically increased group delay range, and the spectral range of achromatism is substantially extended to the wavelength range of 650–1000 nm with an average efficiency of 77.1%–88.5% and a numerical aperture of 0.24–0.1. This research paves a solid step towards practical applications of flat photonics.

[1] State Key Laboratory on Tunable Laser Technology, Ministry of Industry and Information Technology Key Lab of Micro-Nano Optoelectronic Information System, Harbin Institute of Technology (Shenzhen), Shenzhen 518055, P. R. China. [2] School of Electrical and Computer Engineering and Birck Nanotechnology Center, Purdue University, West Lafayette, IN 47907, USA. [3] National Key Laboratory of Science and Technology on Advanced Composites in Special Environments, Harbin Institute of Technology, Harbin 150080, P. R. China. [4] Collaborative Innovation Center of Extreme Optics, Shanxi University, Taiyuan 030006, Shanxi, P. R. China. [5] These authors contributed equally: Yujie Wang, Qinmiao Chen, Wenhong Yang, Ziheng Ji.
✉email: ...

... | https://doi.org/10.1038/s41467-021-25797-9 | www.nature.com/naturecommunications 1

（6）Engineering single-atomic ruthenium catalytic sites on defective nickel-iron layered double hydroxide for overall water splitting, Nature Communications

nature COMMUNICATIONS

ARTICLE

OPEN

Engineering single-atomic ruthenium catalytic sites on defective nickel-iron layered double hydroxide for overall water splitting

Panlong Zhai[1,6], Mingyue Xia[2,6], Yunzhen Wu[1,6], Guanghui Zhang[1], Junfeng Gao[2], Bo Zhang[1], Shuyan Cao[1], Yanting Zhang[1], Zhuwei Li[1], Zhaozhong Fan[1], Chen Wang[1], Xiaomeng Zhang[1], Jeffrey T. Miller[3], Licheng Sun[1,4,5] & Jungang Hou[1✉]

Rational design of single atom catalyst is critical for efficient sustainable energy conversion. However, the atomic-level control of active sites is essential for electrocatalytic materials in alkaline electrolyte. Moreover, well-defined surface structures lead to in-depth understanding of catalytic mechanisms. Herein, we report a single-atomic-site ruthenium stabilized on defective nickel-iron layered double hydroxide nanosheets (Ru_1/D-NiFe LDH). Under precise regulation of local coordination environments of catalytically active sites and the existence of the defects, Ru_1/D-NiFe LDH delivers an ultralow overpotential of 18 mV at 10 mA cm^{-2} for hydrogen evolution reaction, surpassing the commercial Pt/C catalyst. Density functional theory calculations reveal that Ru_1/D-NiFe LDH optimizes the adsorption energies of intermediates for hydrogen evolution reaction and promotes the O–O coupling at a Ru–O active site for oxygen evolution reaction. The Ru_1/D-NiFe LDH as an ideal model reveals superior water splitting performance with potential for the development of promising water-alkali electrocatalysts.

State Key Laboratory of Fine Chemicals, School of Chemical Engineering, Dalian University of Technology, Dalian, China. [2] Laboratory of Materials Modification by Laser, Ion and Electron Beams (Dalian University of Technology), Ministry of Education, Dalian, China. [3] Davidson School of Chemical Engineering, Purdue University, West Lafayette, IN, USA. [4] Center of Artificial Photosynthesis for Solar Fuels, School of Science, Westlake University, Hangzhou, China. [5] Department of Chemistry, School of Engineering Sciences in Chemistry, Biotechnology and Health, KTH Royal Institute of Technology, Stockholm, Sweden. [6] These authors contributed equally: Panlong Zhai, Mingyue Xia, Yunzhen Wu. ✉email: [illegible]

[illegible] | (2020)2:4567 | https://doi.org/10.1038/s41467-020-18485-1 | www.nature.com/naturecommunications 1

（7）Direct observation of chaotic resonances in optical microcavities, Light Science & Applications

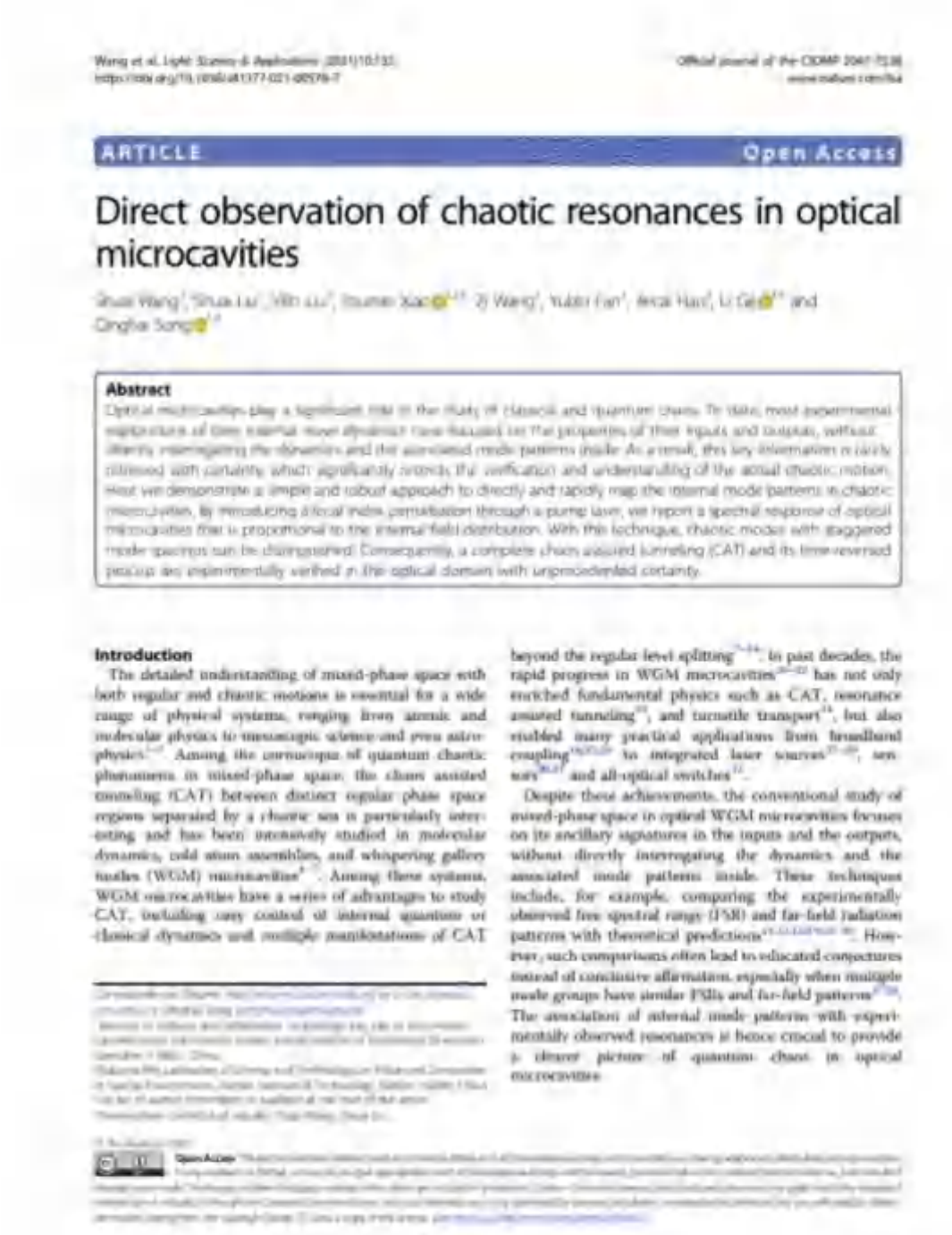

Wang et al. Light: Science & Applications (2021)10:132
https://doi.org/10.1038/s41377-021-00578-7

Official journal of the CIOMP 2047-7538
www.nature.com/lsa

ARTICLE Open Access

Direct observation of chaotic resonances in optical microcavities

Shuai Wang[1], Shiqia Liu[1], Wei Liu[1], Xiaomin Xiao[1,2], Zi Wang[1], Yubin Fan[1], Jiecai Han[1], Li Ge[3,4] and Dinghui Song[1,2]

Abstract

Optical microcavities play a significant role in the study of classical and quantum chaos. To date, most experimental explorations of their external wave dynamics have focused on the properties of their inputs and outputs, without directly interrogating the dynamics and their associated mode patterns inside. As a result, this key information is rarely obtained with certainty, which significantly restricts the verification and understanding of the actual chaotic motion. Here we demonstrate a simple and robust approach to directly and rapidly map the internal mode patterns in chaotic microcavities. By introducing a local index perturbation through a pump laser, we report a spectral response of optical microcavities that is proportional to the internal field distribution. With this technique, chaotic modes with staggered mode spacings can be distinguished. Consequently, a complete chaos-assisted tunneling (CAT) and its time-reversed process are experimentally verified in the optical domain with unprecedented certainty.

Introduction

The detailed understanding of mixed-phase space with both regular and chaotic motions is essential for a wide range of physical systems, ranging from atomic and molecular physics to mesoscopic science and even astrophysics[1–3]. Among the cornucopia of quantum chaotic phenomena in mixed-phase space, the chaos assisted tunneling (CAT) between distinct regular phase space regions separated by a chaotic sea is particularly interesting and has been intensively studied in molecular dynamics, cold atom assemblies, and whispering gallery nanlas (WGM) microcavities[4–7]. Among these systems, WGM microcavities have a series of advantages to study CAT, including easy control of internal quantum or classical dynamics and multiple manifestations of CAT beyond the regular level splitting[8–14]. In past decades, the rapid progress in WGM microcavities[15–22] has not only enriched fundamental physics such as CAT, resonance assisted tunneling[23], and turnstile transport[24], but also enabled many practical applications from broadband coupling[18,25,26] to integrated laser sources[27–29], sensors[30,31] and all-optical switches[32].

Despite these achievements, the conventional study of mixed-phase space in optical WGM microcavities focuses on its ancillary signatures in the inputs and the outputs, without directly interrogating the dynamics and the associated mode patterns inside. These techniques include, for example, comparing the experimentally observed free spectral range (FSR) and far-field radiation patterns with theoretical predictions[15,33,34]. However, such comparisons often lead to educated conjectures instead of conclusive affirmations, especially when multiple mode groups have similar FSRs and far-field patterns[35,36]. The association of internal mode patterns with experimentally observed resonances is hence crucial to provide a clearer picture of quantum chaos in optical microcavities.

（8）Suppressing meta-holographic artifacts by laser coherence tuning, Light Science & Applications

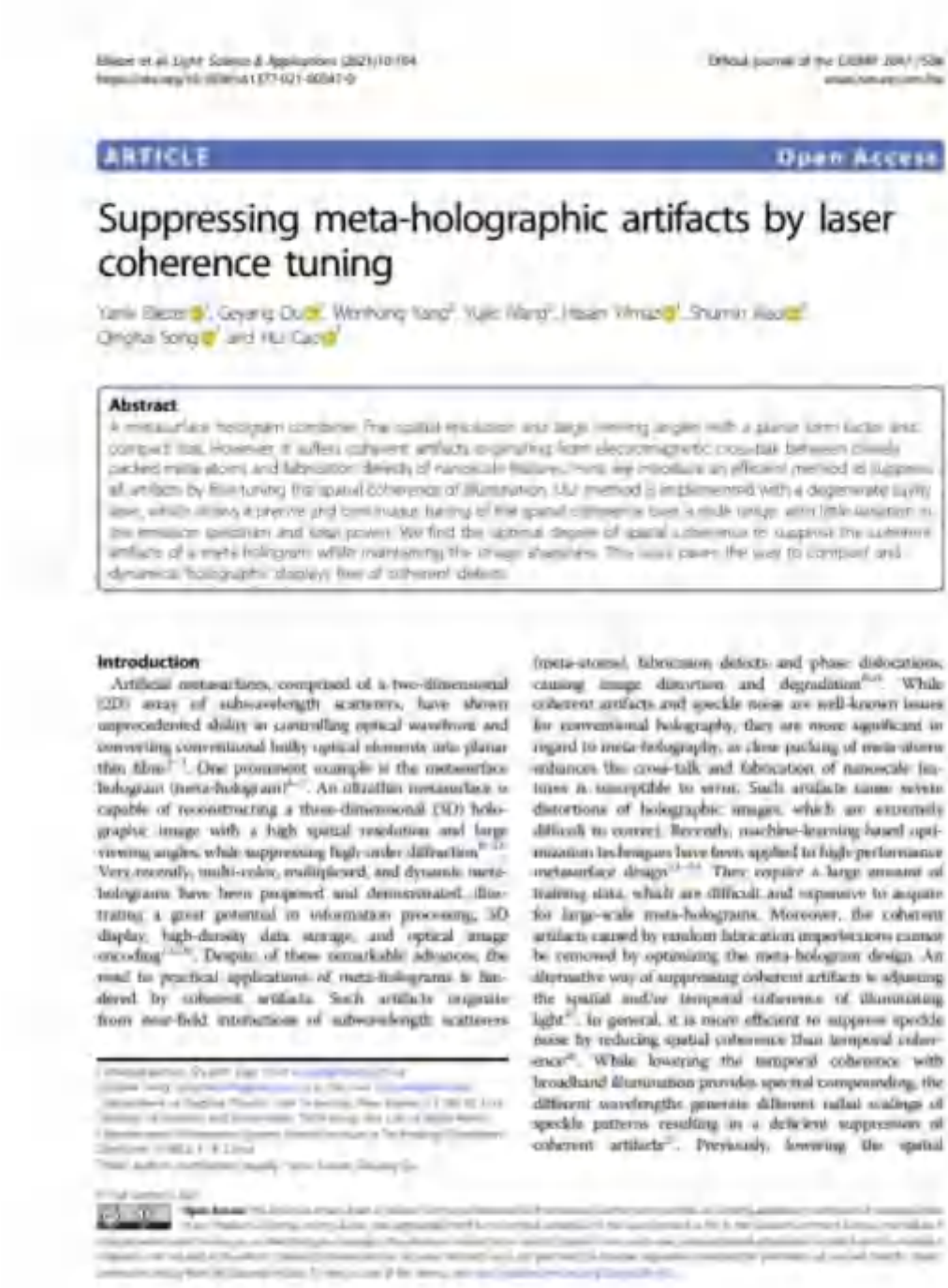

Official journal of the CIOMP 2047-7538

ARTICLE Open Access

Suppressing meta-holographic artifacts by laser coherence tuning

Yanlei Baozhi, Geyang Du, Wenhong Yang, Yujie Wang, Hsuan Ming, Shumin Xiao, Qinghai Song and Hui Cao

Abstract

A metasurface hologram combines the spatial resolution and large viewing angles with a planar form factor and compact size. However, it suffers coherent artifacts originating from electromagnetic cross-talk between closely packed meta-atoms and fabrication defects of nanoscale features. Here, we introduce an efficient method to suppress all artifacts by their tuning the spatial coherence of illumination. Our method is implemented with a degenerate cavity laser, which allows preserving and continuous tuning of the spatial coherence over a wide range, with little variation in the emission spectrum and total power. We find the optimal degree of spatial coherence to suppress the coherent artifacts of a meta-hologram while maintaining the image sharpness. This work paves the way to compact and dynamic holographic displays free of coherent defects.

Introduction

Artificial metasurfaces, comprised of a two-dimensional (2D) array of subwavelength scatterers, have shown unprecedented ability in controlling optical wavefront and converting conventional bulky optical elements into planar thin films[1–3]. One prominent example is the metasurface hologram (meta-hologram)[4–6]. An ultrathin metasurface is capable of reconstructing a three-dimensional (3D) holographic image with a high spatial resolution and large viewing angles, while suppressing high-order diffraction[6–12]. Very recently, multi-color, multiplexed, and dynamic meta-holograms have been proposed and demonstrated, illustrating a great potential in information processing, 3D display, high-density data storage, and optical image encoding[13–19]. Despite of these remarkable advances, the road to practical applications of meta-holograms is hindered by coherent artifacts. Such artifacts originate from near-field interactions of subwavelength scatterers (meta-atoms), fabrication defects and phase dislocations, causing image distortion and degradation[20,21]. While coherent artifacts and speckle noise are well-known issues for conventional holography, they are more significant in regard to meta-holography, as close packing of meta-atoms enhances the cross-talk and fabrication of nanoscale features is susceptible to error. Such artifacts cause severe distortions of holographic images, which are extremely difficult to correct. Recently, machine-learning based optimization techniques have been applied to high-performance metasurface design[13,14]. They require a large amount of training data, which are difficult and expensive to acquire for large-scale meta-holograms. Moreover, the coherent artifacts caused by random fabrication imperfections cannot be removed by optimizing the meta-hologram design. An alternative way of suppressing coherent artifacts is adjusting the spatial and/or temporal coherence of illuminating light[22]. In general, it is more efficient to suppress speckle noise by reducing spatial coherence than temporal coherence[23]. While lowering the temporal coherence with broadband illumination provides spectral compounding, the different wavelengths generate different radial scalings of speckle patterns resulting in a deficient suppression of coherent artifacts[22]. Previously, lowering the spatial

（9）Transparent ferroelectric crystals with ultrahigh piezoelectricity, Nature

Article

Transparent ferroelectric crystals with ultrahigh piezoelectricity

https://doi.org/10.1038/s41586-019-1901-y

Received: 20 May 2019

Accepted: 16 November 2019

Published online: 15 January 2020

Chaoxu Qi[1,3], Bin Wang[1,3], Nan Zhang[1,3], Shujun Zhang[2]✉, Jinfeng Liu[1], David Wallen[2], Yu Wang[1], Hao Tian[1], Thomas R. Shrout[2], Zhuo Xu[1], Long-Qing Chen[1,4]✉ & Fei Li[1]✉

Transparent piezoelectrics are highly desirable for numerous hybrid ultrasound–optical devices ranging from photoacoustic imaging transducers to transparent actuators for haptic applications[1–3]. However, it is challenging to achieve high piezoelectricity and perfect transparency simultaneously because most high-performance piezoelectrics are ferroelectrics (functional on high-density light-scattering domain walls). Here, through a combination of phase-field simulations and experiments, we demonstrate a relatively simple method of using an alternating current electric field to engineer the domain structures of originally opaque rhombohedral $Pb(Mg_{1/3}Nb_{2/3})O_3$–$PbTiO_3$ (PMN–PT) crystals to simultaneously generate near-perfect transparency, an ultrahigh piezoelectric coefficient d_{33} (greater than 2,300 picocoulombs per newton), an excellent electromechanical coupling factor k_{33} (about 94 per cent) and a large electro-optical coefficient r_{13} (approximately 220 picometres per volt), which is far beyond the performance of the commonly used transparent ferroelectric crystal $LiNbO_3$. We find that increasing the domain size leads to a higher d_{33} value for the [001]-oriented rhombohedral PMN–PT crystals, challenging the conventional wisdom that decreasing the domain size always results in higher piezoelectricity[4–6]. This work presents a paradigm for achieving high transparency and piezoelectricity by ferroelectric domain engineering, and we expect the transparent ferroelectric crystals reported here to provide a route to a wide range of hybrid device applications, such as medical imaging, self-energy-harvesting touch screens and invisible robotic devices.

Achieving simultaneously high piezoelectricity and perfect transparency in a piezoelectric material has long been a challenge. For example, traditional high-performance polycrystalline piezoelectrics are typically made from perovskite ferroelectric ceramics, single crystals with chemical compositions that are close to their morphotropic phase boundaries (MPBs), such as $Pb(Zr,Ti)O_3$ (PZT) ceramics and domain-engineered PMN–PT crystals. These materials possess very high d_{33} and k_{33} values[4–6], but they are usually opaque in the visible-light spectrum. On the other hand, the commonly used transparent piezoelectric $LiNbO_3$ crystals and polyvinylidene fluoride (PVDF) polymers[7–9] have good transparency but much lower d_{33} and k_{33} values ($LiNbO_3$: d_{33} ≈ 40 pC N^{-1}, k_{33} ≈ 47%; PVDF: d_{33} ≈ 20 pC N^{-1}, k_{33} ≈ 16%) that severely limit the actuation/sensing level, bandwidth and sensitivity of the transducers.

In addition to the extrinsic effects, such as proximity and grain boundaries, which are ubiquitous in ceramics, the poor transparency in PZT ceramics and domain-engineered PMN–PT crystals is closely associated with light scattering and reflection from their ferroelectric domain walls. There are two possible approaches to reducing the light-scattering domain walls. The first is to pole a ferroelectric crystal along the polar-direction to achieve a single-domain state. However, the d_{33} value of such single-domain PMN–PT crystals is generally low[10–14]—much lower than that of [001]-poled multi-domain rhombohedral PMN–PT crystals (~1,500 pC N^{-1}). In principle, one could first pole a rhombohedral PMN–PT crystal along the [411] direction to achieve a single-domain state with good transparency, then rotate the crystal to the [001] direction to guarantee high longitudinal piezoelectricity. However, this approach is not feasible in practice (see Methods for a detailed explanation). The second approach is to dramatically reduce the domain sizes by breaking the domains into polar nanoregions with spatial sizes far below that of nanometres[15], much smaller than the wavelength of visible light, thus greatly improving their light transparency—as observed in relaxor-PT[16–18]. However, improving the transparency using polar nanoregions is achieved at the expense of a markedly reduced remanent polarization and thus very low d_{33} values. Therefore, despite more than 30 years of effort, optical functionality in high-performance piezoelectrics have not been realized.

[1] Electronic Materials Research Laboratory, Key Laboratory of the Ministry of Education & International Center for Dielectric Research, Xi'an Jiaotong University, Xi'an, China. [2] Materials Research Institute, The Pennsylvania State University, University Park, PA, USA. [3] These authors contributed equally: Chaoxu Qi, Bin Wang. [4] Deceased: Long-Qing Chen. ✉e-mail: sjz12@psu.edu; lfeli@mail.xjtu.edu.cn

（10）Breaking 50 Femtosecond Resolution Barrier in MeV Ultrafast Electron Diffraction with a Double Bend Achromat Compressor, Physical Review Letters


PHYSICAL REVIEW LETTERS 124, 134803 (2020)

Breaking 50 Femtosecond Resolution Barrier in MeV Ultrafast Electron Diffraction with a Double Bend Achromat Compressor

© 2020 American Physical Society

（11）Ultrafast control of vortex microlasers, Science

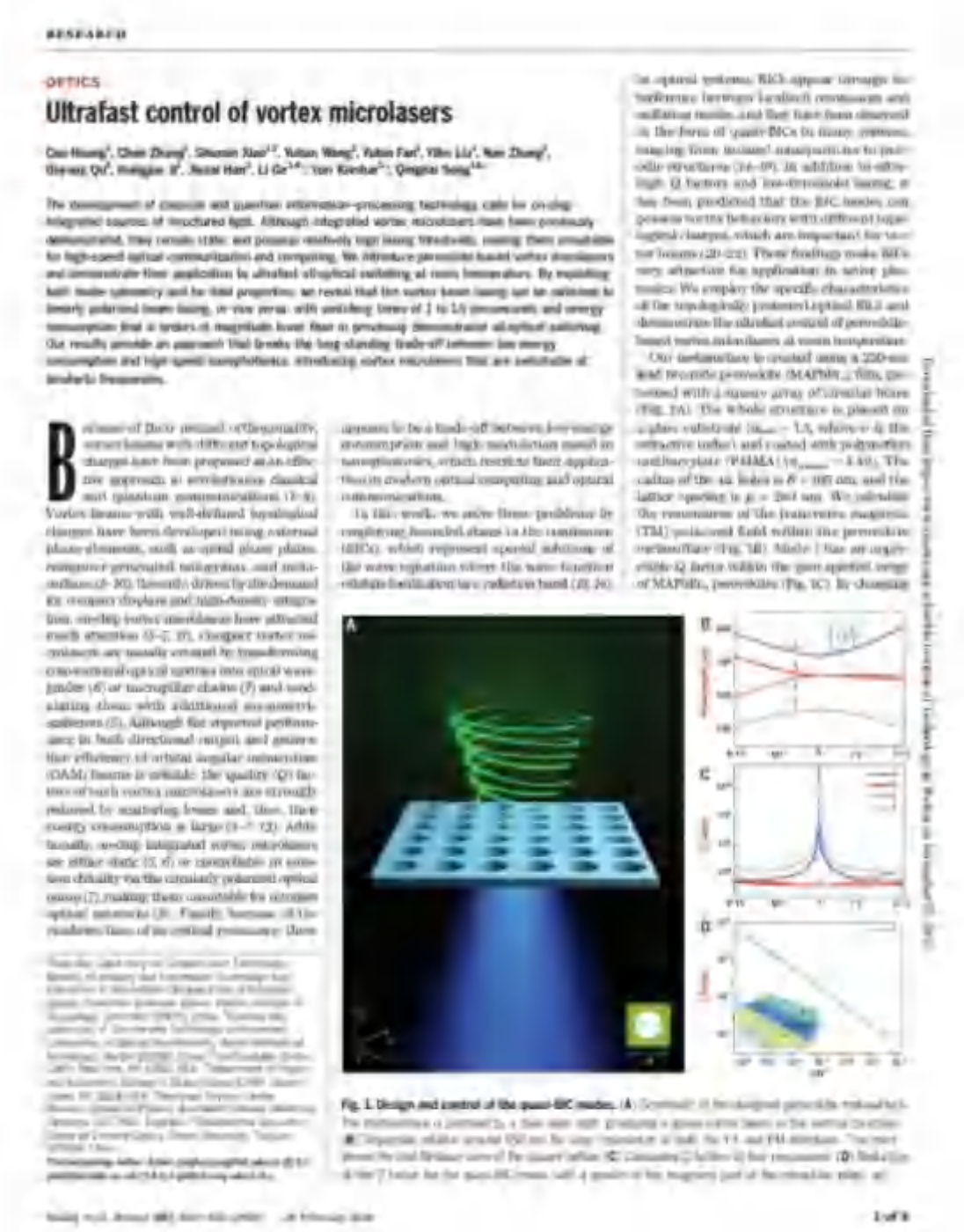

RESEARCH

OPTICS

Ultrafast control of vortex microlasers

Can Huang[1], Chen Zhang[2], Shuxin Xiao[1,2], Yutao Wang[2], Yufan Fan[2], Yilin Liu[2], Nan Zhang[2], Guowei Qu[2], Hongjian Ji[2], Jiecai Han[2], Li Ge[3,4]*, Yan Kivshar[5]*, Qinghai Song[1,6]*

The development of classical and quantum information-processing technology calls for on-chip integrated sources of structured light. Although integrated vortex microlasers have been previously demonstrated, they remain rather inefficient and possess relatively high lasing thresholds, making them unsuitable for high-speed optical communications and computing. We introduce perovskite-based vortex microlasers and demonstrate their application to ultrafast all-optical switching at room temperature. By exploiting both mode symmetry and bound properties, we reveal that the vortex beam lasing can be switched to linearly polarized beam lasing, in real time, with switching times of 2 to 10 picoseconds and energy consumption that is orders of magnitude lower than in previously demonstrated all-optical switching. Our results provide an approach that breaks the long-standing trade-off between low energy consumption and high-speed nanophotonics, introducing vortex microlasers that are switchable at terahertz frequencies.

Because of their unique orthogonality, vortex beams with different topological charges have been proposed as an effective approach to accommodate classical and quantum communications (1–6). Vortex beams with well-defined topological charges have been developed using external phase elements, such as spiral phase plates, computer-generated holograms, and metasurfaces (7–10). Recently, driven by the demand for compact chip-scale and high-density integration, on-chip vortex microlasers have attracted much attention (3–5, 11). Compact vortex microlasers are usually created by transforming conventional optical systems into optical waveguides (4) or waveguide chains (3) and modulating them with additional microstructured scatterers (5). Although the reported performance in both directional output and guaranteed efficiency of orbital angular momentum (OAM) beams is notable, the quality (Q) factors of such vortex microlasers are strongly reduced by scattering losses and, thus, their energy consumption is large (3–5, 12). Additionally, on-chip integrated vortex microlasers are either static (3, 4) or susceptible to unwanted chirality via the circularly polarized optical pump (5), making them unsuitable for ultrafast optical networks (3). Finally, because of the randomness of the critical resonances, there appears to be a trade-off between low-energy consumption and high-resolution mode in nanophotonics, which restricts their applications in modern optical computing and optical communications.

In this work, we solve these problems by employing bound states in the continuum (BICs), which represent special solutions of the wave equation where the wave function exhibits finite amplitude and zero radiation loss (13, 14). In optical systems, BICs appear through the interference between localized resonances and radiation modes and they have been observed in the form of quasi-BICs in many systems, ranging from photonic nanostructures to periodic structures (14–19). In addition to ultrahigh Q factors and low-threshold lasing, it has been predicted that the BIC modes can possess vortex behaviors with different topological charges, which are important for vortex beams (20–22). These findings make BICs very attractive for application in vortex photonics. We employ the specific characteristics of the topologically protected optical BICs and demonstrate the ultrafast control of perovskite-based vortex microlasers at room temperature.

Our metasurface is created using a 220-nm-thick organic-inorganic perovskite ($MAPbBr_3$) film, patterned with a square array of circular holes (Fig. 1A). The whole structure is placed on a glass substrate ($n_{sub} = 1.5$, where n is the refractive index) and coated with polymethyl methacrylate (PMMA) ($n_{cover} = 1.49$). The radius of the air holes is $R = 105$ nm, and the lattice spacing is $a = 260$ nm. We calculate the resonances of the transverse magnetic (TM) polarized field within this perovskite metasurface (Fig. 1B). Mode 1 has an experimentally accessible Q factor within the gain spectral range of $MAPbBr_3$ perovskites (Fig. 1C). By changing

Fig. 1. Design and control of the quasi-BIC modes. (A) [illegible] (B) [illegible] (C) [illegible] (D) [illegible]

Downloaded from https://www.science.org at Peking University on [illegible]

[illegible]

（12）Comprehensive defect suppression in perovskite nanocrystals for high-efficiency light-emitting diodes, Nature Photonics

ARTICLES

nature photonics

Comprehensive defect suppression in perovskite nanocrystals for high-efficiency light-emitting diodes

Young-Hoon Kim, Sungjin Kim, Arvin Kakekhani, Jinwoo Park, Jaehyeok Park, Yong-Hee Lee, Hengxing Xu, Satyawan Nagane, Robert B. Wexler, Dong-Hyeok Kim, Seung Hyeon Jo, Laura Martinez-Sarti, Peng Tan, Aditya Sadhanala, Gyeong-Su Park, Young-Woon Kim, Bin Hu, Henk J. Bolink, Seunghyup Yoo, Richard H. Friend, Andrew M. Rappe and Tae-Woo Lee

Electroluminescence efficiencies of metal halide perovskite nanocrystals (PNCs) are limited by a lack of material strategies that can both suppress the formation of defects and enhance the charge carrier confinement. Here we report a size-dependent alloying strategy that generates smaller, monodisperse colloidal particles (confining electrons and holes, and boosting radiative recombination) with fewer surface defects (reducing non-radiative recombination). Doping of guanidinium into formamidinium lead bromide PNCs yields limited bulk solubility while creating an entropy-stabilized phase in the PNCs and leading to smaller PNCs with more carrier confinement. The extra guanidinium segregates to the surface and stabilizes the undercoordinated sites. Furthermore, a surface-stabilizing 1,3,5-tris(bromomethyl)-2,4,6-trimethylbenzene was applied as a bromide vacancy healing agent. The result is highly efficient PNC-based light-emitting diodes that have current efficiency of 100 cd A^{-1} (external quantum efficiency of 23.4%), which rises to 205 cd A^{-1} (external quantum efficiency of 45.5%) with a hemispherical lens.

（13）Reprogrammable meta-hologram for optical encryption, Nature Communications

nature COMMUNICATIONS

ARTICLE

OPEN

Reprogrammable meta-hologram for optical encryption

Geyang Qu[1], Wenhong Yang[1], Qinghai Song[1,2], Yilin Liu[1], Cheng-Wei Qiu[3], Jiecai Han[4], Din-Ping Tsai[5,6✉] & Shumin Xiao[1,2,4,6✉]

Meta-holographic encryption is a potentially important technique for information security. Despite rapid progresses in multi-tasked meta-holograms, the number of information channels available in metasurfaces is limited, making meta-holographic encryption vulnerable to some attacking algorithms. Herein, we demonstrate a re-programmable metasurface that can produce arbitrary holographic images for optical encryption. The encrypted information is divided into two matrices. These two matrices are imposed to the incident light and the metasurface, respectively. While the all-dielectric metasurface is static, the phase matrix of incident light provides additional degrees of freedom to precisely control the eventual functions at will. With a single Si metasurface, arbitrary holographic images and videos have been transported and decrypted. We hope that this work paves a more promising way to optical information encryption and authentication.

[1] Ministry of Industry and Information Technology Key Lab of Micro-Nano Optoelectronic Information System, Shenzhen Graduate School, Harbin Institute of Technology, 518055 Shenzhen, China. [2] Collaborative Innovation Center of Extreme Optics, Shanxi University, 030006 Taiyuan, China. [3] Department of Electrical and Computer Engineering, National University of Singapore, 4 Engineering Drive 3, Singapore 117583, Singapore. [4] National Key Laboratory of Science and Technology on Advanced Composites in Special Environments, Harbin Institute of Technology, 150080 Harbin, China. [5] Department of Electronic and Information Engineering, The Hong Kong Polytechnic University, Hong Kong, China. [6] These authors jointly supervised this work: Din-Ping Tsai, Shumin Xiao. ✉email: [illegible]

| (2020)11:5484 | https://doi.org/10.1038/s41467-020-19512-9 | www.nature.com/naturecommunications 1

（14）Universal growth of ultra-thin III–V semiconductor single crystals, Nature Communications

nature COMMUNICATIONS

ARTICLE

https://doi.org/10.1038/s41467-020-17699-5 OPEN

Universal growth of ultra-thin III–V semiconductor single crystals

Yunxu Chen[1,4], Jinxin Liu[1,4], Mengqi Zeng[1,4], Fangyun Lu[1], Tianrui Lv[1], Yuan Chang[2], Haihui Lan[1], Bin Wei[3], Rong Sun[3], Junfeng Gao[2], Zhongchang Wang[3] & Lei Fu[1✉]

Ultra-thin III-V semiconductors, which exhibit intriguing characteristics, such as two-dimensional (2D) electron gas, enhanced electron-hole interaction strength, and strongly polarized light emission, have always been anticipated in future electronics. However, their inherent strong covalent bonding in three dimensions hinders the layer-by-layer exfoliation, and even worse, impedes the 2D anisotropic growth. The synthesis of desirable ultra-thin III-V semiconductors is hence still in its infancy. Here we report the growth of a majority of ultra-thin III-V single crystals, ranging from ultra-narrow to wide bandgap semiconductors, through enhancing the interfacial interaction between the III-V crystals and the growth substrates to proceed the 2D layer-by-layer growth mode. The resultant ultra-thin single crystals exhibit fascinating properties of phonon frequency variation, bandgap shift, and giant second harmonic generation. Our strategy can provide an inspiration for synthesizing unexpected ultra-thin non-layered systems and also drive exploration of III-V semiconductor-based electronics.

[1] College of Chemistry and Molecular Sciences, Wuhan University, Wuhan 430072, China. [2] Laboratory of Materials Modification by Laser, Ion and Electron Beams, Dalian University of Technology, Ministry of Education, Dalian 116024, China. [3] International Iberian Nanotechnology Laboratory (INL), Av. Mestre Jose Veiga s/n, 4715-330 Braga, Portugal. [4] These authors contributed equally: Yunxu Chen, Jinxin Liu, Mengqi Zeng. ✉email: ...

（15）Engineering active sites on hierarchical transition bimetal oxides/sulfides heterostructure array enabling robust overall water splitting, Nature Communications

nature COMMUNICATIONS

ARTICLE

OPEN

Engineering active sites on hierarchical transition bimetal oxides/sulfides heterostructure array enabling robust overall water splitting

Panlong Zhai[1,5], Yanxue Zhang[2,5], Yunzhen Wu[1,5], Junfeng Gao[2], Bo Zhang[1], Shuyan Cao[1], Yanting Zhang[1], Zhuwei Li[1], Licheng Sun[1,3,4] & Jungang Hou[1✉]

Rational design of the catalysts is impressive for sustainable energy conversion. However, there is a grand challenge to engineer active sites at the interface. Herein, hierarchical transition bimetal oxides/sulfides heterostructure arrays interacting two-dimensional MoO_x/MoS_2 nanosheets attached to one-dimensional NiO_x/Ni_3S_2 nanorods were fabricated by oxidation/hydrogenation-induced surface reconfiguration strategy. The $NiMoO_x$/NiMoS heterostructure array exhibits the overpotentials of 38 mV for hydrogen evolution and 186 mV for oxygen evolution at 10 mA cm^{-2}, even surviving at a large current density of 500 mA cm^{-2} with long-term stability. Due to optimized adsorption energies and accelerated water splitting kinetics by theory calculations, the assembled two-electrode cell delivers the industrially relevant current densities of 500 and 1000 mA cm^{-2} at record low cell voltages of 1.60 and 1.66 V with excellent durability. This research provides a promising avenue to enhance the electrocatalytic performance of the catalysts by engineering interfacial active sites toward large-scale water splitting.

[1] State Key Laboratory of Fine Chemicals, School of Chemical Engineering, Dalian University of Technology, 116024 Dalian, P. R. China. [2] Laboratory of Materials Modification by Laser, Ion and Electron Beams, Dalian University of Technology, Ministry of Education, 116024 Dalian, P. R. China. [3] College of Science, Westlake University, 310024 Hangzhou, P. R. China. [4] Department of Chemistry, School of Engineering Sciences in Chemistry, Biotechnology and Health, KTH Royal Institute of Technology, 10044 Stockholm, Sweden. [5] These authors contributed equally: Panlong Zhai, Yanxue Zhang, Yunzhen Wu. ✉email: [redacted]

(2020)11:5462 | https://doi.org/10.1038/s41467-020-19214-w | www.nature.com/naturecommunications

（16）Ultra-large electric field–induced strain in potassium sodium niobate crystals, Science Advances

SCIENCE ADVANCES | RESEARCH ARTICLE

MATERIALS SCIENCE

Ultra-large electric field–induced strain in potassium sodium niobate crystals

Chengpeng Hu[1†], Xiangda Meng[1†], Mao-Hua Zhang[2†], Hao Tian[1†], John E. Daniels[3], Peng Tan[1], Fei Huang[1], Li Li[4], Ke Wang[2†], Jing-Feng Li[2], Qieni Lu[2], Wenwu Cao[5–7], Zhongxiang Zhou[1]

Electromechanical coupling in piezoelectric materials allows direct conversion of electrical energy into mechanical energy and vice versa. Here, we demonstrate lead-free $(K,Na)_{1-x}NbO_3$ single crystals with an ultrahigh large-signal piezoelectric coefficient d_{33}^* of 9000 pm V^{-1}, which is superior to the highest value reported in state-of-the-art lead-based single crystals (~2500 pm V^{-1}). The enhanced electromechanical properties in our crystals are realized by an engineered compositional gradient in the as-grown crystal, allowing notable reversible non-180° domain switching. Moreover, our crystals exhibit temperature-insensitive strain performance within the temperature range of 25°C to 125°C. The enhanced temperature stability of the response also allows the materials to be used in a wider range of applications that exceed the temperature limits of current lead-based piezoelectric crystals.

INTRODUCTION

RESULTS AND DISCUSSION

The ultra-large piezoelectric properties

（17）High-performance position-sensitive detector based on the lateral photoelectrical effect of two-dimensional materials, Light Science & Applications

Wu et al. Light: Science & Applications (2020)9:88
https://doi.org/10.1038/s41377-020-0327-y

Official journal of the CIOMP 2047-7538
www.nature.com/lsa

REVIEW ARTICLE Open Access

High-performance position-sensitive detector based on the lateral photoelectrical effect of two-dimensional materials

Chang Hu[1], Kanglei Wang[1] and Bo Song[1]

Abstract

Two-dimensional (2D) materials such as graphene and transition-metal chalcogenides have been extensively studied because of their superior electronic and optical properties. Recently, 2D materials have shown great practical application in position-sensitive detectors (PSDs) originating from the lateral photoelectrical effect of the materials or junctions. The high position sensitivity and ultrafast photoresponse of PSDs based on 2D materials, especially compatibility with Si technology, may enable diverse optoelectronic applications. In this review, recent studies of PSDs based on 2D materials are summarized, providing a promising route for high-performance PSDs.

Introduction

Since Schottky and Wallmark discovered and pioneered the lateral photovoltaic effect (LPE) in *p*–*n* junctions[1,2], intensive research has been conducted on the LPE in diverse applications, including space exploration, environmental monitoring, and optical engineering. In the LPE, when one side of a *p*–*n* junction is illuminated by a light spot, the optically excited electron-hole pairs will be separated up and down by the built-in electric field. Notably, the formation mechanisms of the built-in field in position-sensitive detectors (PSDs) with different architectures is different. As shown in Fig. 1a, the PSD based on a *p*–*n* junction uses the built-in field formed at the interface due to different band structures to separate the photogenerated carriers. The built-in field in the PSD based on the insulator-coated substrate (such as a graphene transistor on a SiO_2/Si substrate) is formed by band energy bending induced by the localized interface states, and the photogenerated carriers accumulate at the SiO_2/Si interface and then diffuse laterally, as shown in Fig. 1b.

The mechanism of carrier lateral diffusion can be explained by the model shown in Fig. 1c. The photogenerated electrons enter the *n*-type semiconductor, while the photogenerated holes enter the *p*-type semiconductor. Then, these generated carriers diffuse laterally from the light spot to balance the electric field along the layer[3–5]. In general, the relationship between the total number of photogenerated electrons n_0 and that of photogenerated electrons transmitted into *n*-type semiconductor N_0 can be described as follows:

$$N_0 = n_0\left[1 - P^{\gamma(-\alpha)}\right] \tag{1}$$

where P is the probability of photogenerated electrons entering the *n*-type semiconductor, ρ is the laser power, and γ is a time-dependent coefficient.

The electron diffusion equation at position r is

$$D_n\frac{d^2N(r)}{dr^2} = \frac{N(r)}{\tau_n} \tag{2}$$

（18）Momentum-Topology-Induced Optical Pulling Force, Physical Review Letters

PHYSICAL REVIEW LETTERS 124, 143901 (2020)

Momentum-Topology-Induced Optical Pulling Force

Hanze Li,[1] Yingyan Cao,[1] Boyan Shi,[1] Tongtong Zhang,[2] Yong Gong,[1] Rui Feng,[1] Lei Wang,[1] Fanglei Sun,[1] Yufei Shi,[1] Mohammad Ali Miri,[3] Mansel Nieto-Vesperinas,[4] Cheng-Wei Qiu,[5] and Wenqiang Ding[6,7]
[1]Institute of Advanced Photonics, School of Physics, Harbin Institute of Technology, Harbin 150001, China
[2]School of Optoelectronic Engineering and Instrumentation Science, Dalian University of Technology, Dalian 116024, China
[3]Center of Ultra-Precision Optoelectronic Instrument Engineering, Harbin Institute of Technology, Harbin 150001, China
[4]School of Electrical and Electronic Engineering, Nanyang Technological University, Singapore 639798, Singapore
[5]Department of physics, Queens College of the City University of New York, Queens, New York 11367, USA
[6]Instituto de Ciencia de Materiales de Madrid, Consejo Superior de Investigaciones Científicas, Campus de Cantoblanco, Madrid 28049, Spain
[7]Department of Electrical and Computer Engineering, National University of Singapore, Singapore 117583, Singapore
[8]Collaborative Innovation Center of Extreme Optics, Shanxi University, Taiyuan 030006, Shanxi, China

(Received 4 August 2019; accepted 31 March 2020; published 10 April 2020)

We report an ingenious mechanism to obtain robust optical pulling force by a single plane wave via engineering the topology of light momentum in the background. The underlying physics is found to be the topological transition of the light momentum from a usual convex shape to a saddlelike concave shape in the carefully designed background such as a photonic crystal structure. The principle and results reported here shed insightful concepts concerning optical pulling, and pave the way for a new class of advanced optical manipulation technique, with potential applications of drug delivery and cell sorting.

DOI: 10.1103/PhysRevLett.124.143901

Optical manipulations using various forms of optical forces have been widely used in diverse disciplines, including biology [1–6], atom physics [7–10], quantum physics [11–15], and nanotechnology [16–19]. Recently, the counterintuitive optical pulling force (OPF) has attracted broad interest due to its intriguing physics underlying and potential applications [20–26]. An OPF can transport objects towards the source over a long range, rather than pushing them away, which provides a new freedom of optical manipulation beyond trapping and pushing. According to the conservation of linear momentum, the realization of OPF requires the increase of forward momentum of the incident light when scattered by the object, which is the common challenge to be solved in all the mechanisms of OPF generation.

Except for exotic media, such as optically active medium [27–30], chiral medium [31–33], PT symmetry objects [34,35], nonreciprocal objects [36,37], and negative refractive-index objects [38–40], various structured optical beams are always needed in order to get an OPF, including nondiffracted Bessel beams [20,22,41–43], chiral beams [21,44–46], interference fields of multiple beams [47–49], the eigenmodes in a waveguide [50,51], or near an interface [52–54]. The common feature of these engineered fields is their off-axial alignment (relative to the average Poynting vector) of the incident momentum, as shown in Fig. 1(a). When the beam is scattered by an object, the off-axial momentum may be redirected partially or even totally to the incident direction. In this case, the light momentum projection on z direction increases obviously due to the convex shape of the isofrequency contour, as illustrated in Fig. 1(b), and the OPF is generated according to the linear momentum conservation. Actually, this has been the standard mechanism to get an optical pulling force, which was first proposed by Marston in acoustics more than ten years ago [55,56]. Certainly, we can get an effective OPF using the thermal effect of light on an absorptive object or background [57,58], which is, however, not due to the transfer of light momentum, but due to the Brownian motion.

From Figs. 1(a) and 1(b) and the above discussion, we find that the key factor that prevents the generation of an OPF by a plane wave is the convex-shaped isofrequency contour, which forbids the forward light momentum increase of the plane wave. This is also the reason of structured beams being indispensable in most previous OPF investigations. In order to surmount this constraint, we propose to engineer the intrinsic feature of light momentum in an artificial background, where the isofrequency contour is concave, rather than convex, as shown in Figs. 1(c) and 1(d).

The change of isofrequency contours in k space from one shape to another is called topological transition in the research of optical metamaterials [59–61]. Since k is proportional to the light momentum: $p = \hbar k$ [62–65], the shape of isofrequency contour can be named as the topology of light momentum (TLM). In Fig. 1(c), when the incident plane wave is scattered by the object

（19）Breakup and Recovery of Topological Zero Modes in Finite Non-Hermitian Optical Lattices, Physical Review Letters

PHYSICAL REVIEW LETTERS 123, 165701 (2019)

Breakup and Recovery of Topological Zero Modes in Finite Non-Hermitian Optical Lattices

Wange Song,[1,*] Wenzhao Sun,[2] Chen Chen,[1,*] Qinghai Song,[2] Shumin Xiao,[2] Shining Zhu,[1] and Tao Li[1,†]
[1]National Laboratory of Solid State Microstructures, Key Laboratory of Intelligent Optical Sensing and Manipulation, Jiangsu Key Laboratory of Artificial Functional Materials, College of Engineering and Applied Sciences, Nanjing University, Nanjing 210093, China
[2]Joint Key Laboratory for Quantum Laser Technologies, Ministry of Industry and Information Technology, Key Lab of Micro-Nano Optoelectronic Information System, Shenzhen Graduate School, Harbin Institute of Technology, Shenzhen 518055, China
[3]Collaborative Innovation Center of Advanced Microstructures, Nanjing 210093, China

(Received 2 February 2019; published 16 October 2019)

The topological edge state (TES) in a one-dimensional optical lattice has exhibited robust field localization or immunizing against the structural perturbations that would give rise to finite-volume geometric integrations. However, the zero mode at a kind of TES usually deviates from the exact zero-energy state in a finite Hermitian lattice due to the coupling between these edge states, which inevitably weakens the topological protection. Here, we have found a breakup of zero modes in finite Su-Schrieffer-Heeger optical lattices and then reveal their recovery by introducing non-Hermitian degeneracies with parity-time (PT) symmetry. We carry out experiments on a three-circle waveguide lattice, where a passive-PT symmetry was implemented with carefully controlled lossy silicon waveguides. The experimental results are fully compatible with the theoretical predictions. Our results show that the topological property of an open system can be tuned by non-Hermitian lattice engineering, which offers a route to enhance the topological protection of a finite system.

DOI: 10.1103/PhysRevLett.123.165701

Parity-time (PT) symmetric systems with non-Hermitian Hamiltonians have received increasing attention over the past decade [1–12]. On crossing the transition point (i.e., the exceptional point (EP) [2,3]), the spectrum is no longer purely real due to spontaneous PT-symmetry breaking. Among various PT symmetric systems, PT photonics with intentionally modulated gain and loss has become an attractive topic [4,5], which has witnessed a series of novel optical phenomena and functionalities [6–12]. On the other hand, topological photonics has sparked a great deal of interest with intriguing phenomena associated with the topological edge states (TESs) [13–15]. The dimensionless edge state with its eigenenergy pinned at the middle of a gapped band structure is referred to as the zero mode [16], which is expected to work in fault-tolerant waveguiding and quantum computation [17,18]. In fact, topological systems are usually of finite system size, which will weaken the topological protection. For example, zero modes may deviate from the exact-zero energy in a finite Hermitian lattice due to the coupling effect [16], which inevitably leads to weakness of the intriguing topologically protected characteristics. It is necessary to strengthen these zero modes in a finite topological system. Recently, the topological properties of non-Hermitian systems have been studied [19–24] and TESs in non-Hermitian systems are demonstrated [25–36]. Non-Hermitian properties have been proven to give rise to a lot of useful aspects in topological phenomena, such as selective enhancement of topological states [27], non-Hermitian-induced topological protection [28–30], topological insulator lasers [30–33], etc. They provide us with the foundation to investigate a variety of topological phenomena in open systems and a possible route for the recovery of zero modes by non-Hermiticity in finite systems.

In the Letter, we clearly demonstrate both the breakup and recovery of zero modes in a finite 1D topological optical system, where the recovery of zero modes was realized by introducing the loss to form a non-Hermitian topological configuration. We systematically investigated the interplay of PT phases and edge states in the non-Hermitian Su-Schrieffer-Heeger (SSH) model [34]. On crossing the EPs, the edge states are driven to undergo a transition from a trivial PT-symmetric edge state to a topological broken-PT one. The experimental results on silicon waveguide lattices with controlled losses are in good agreement with theoretical results. Our study reveals that the topological property of an open system can be tuned by non-Hermitian parameters and implies some interesting physics and photonic applications in PT and topological systems.

We would like to start from a general 1D non-Hermitian SSH model defined by a finite coupled optical waveguide

（20）All-optical control of lead halide perovskite microlasers, Nature Communications

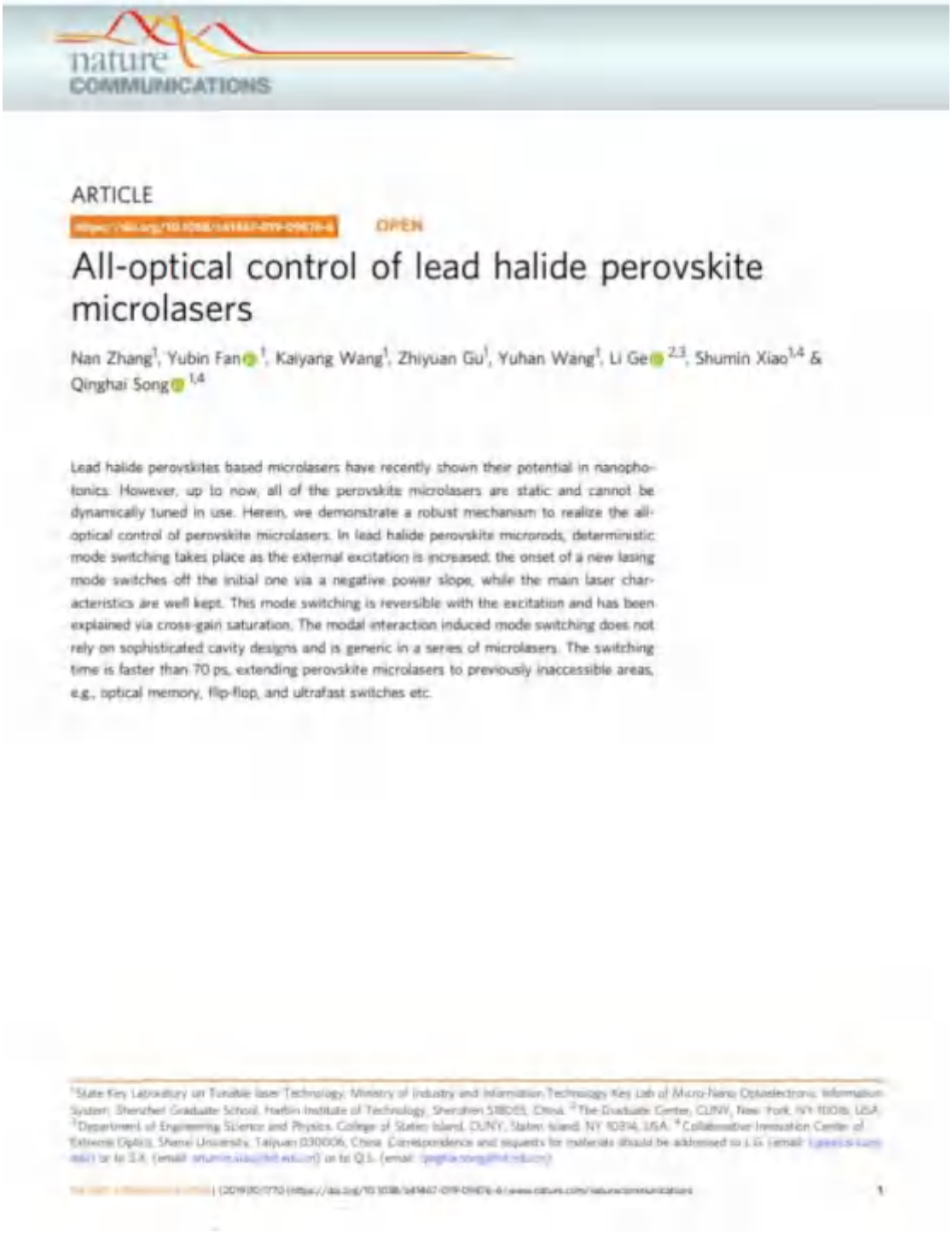

nature COMMUNICATIONS

ARTICLE

OPEN

All-optical control of lead halide perovskite microlasers

Nan Zhang[1], Yubin Fan[1], Kaiyang Wang[1], Zhiyuan Gu[1], Yuhan Wang[1], Li Ge[2,3], Shumin Xiao[1,4] & Qinghai Song[1,4]

Lead halide perovskites based microlasers have recently shown their potential in nanophotonics. However, up to now, all of the perovskite microlasers are static and cannot be dynamically tuned in use. Herein, we demonstrate a robust mechanism to realize the all-optical control of perovskite microlasers. In lead halide perovskite microrods, deterministic mode switching takes place as the external excitation is increased: the onset of a new lasing mode switches off the initial one via a negative power slope, while the main laser characteristics are well kept. This mode switching is reversible with the excitation and has been explained via cross-gain saturation. The modal interaction induced mode switching does not rely on sophisticated cavity designs and is generic in a series of microlasers. The switching time is faster than 70 ps, extending perovskite microlasers to previously inaccessible areas, e.g., optical memory, flip-flop, and ultrafast switches etc.

[1] State Key Laboratory on Tunable Laser Technology, Ministry of Industry and Information Technology Key Lab of Micro-Nano Optoelectronic Information System, Shenzhen Graduate School, Harbin Institute of Technology, Shenzhen 518055, China. [2] The Graduate Center, CUNY, New York, NY 10016, USA. [3] Department of Engineering Science and Physics, College of Staten Island, CUNY, Staten Island, NY 10314, USA. [4] Collaborative Innovation Center of Extreme Optics, Shanxi University, Taiyuan 030006, China. Correspondence and requests for materials should be addressed to L.G. (email: [illegible]) or to S.X. (email: [illegible]) or to Q.S. (email: [illegible])

| (2019)10:1770 | https://doi.org/10.1038/s41467-019-09678-6 | www.nature.com/naturecommunications

（21）Arbitrarily routed mode-division multiplexed photonic circuits for dense integration, Nature Communications

ARTICLE

https://doi.org/10.1038/s41467-019-11996-8 OPEN

Arbitrarily routed mode-division multiplexed photonic circuits for dense integration

Yingjie Liu[1], Ke Xu[1], Shuai Wang[1], Weihong Shen[2], Hucheng Xie[1], Yujie Wang[1], Shumin Xiao[1,3], Yong Yao[1], Jiangbing Du[2], Zuyuan He[2] & Qinghai Song[1,3]

On-chip integrated mode-division multiplexing (MDM) is an emerging technique for large-capacity data communications. In the past few years, while several configurations have been developed to realize on-chip MDM circuits, their practical applications are significantly hindered by the large footprint and inter-mode cross talk. Most importantly, the high-speed MDM signal transmission in an arbitrarily routed circuit is still absent. Herein, we demonstrate the MDM circuits based on digitized meta-structures which have extremely compact footprints. 112 Gbit/s signals encoded on each mode are arbitrarily routed through the circuits consisting of many sharp bends and compact crossings with a bit error rate under forward error correction limit. This will significantly improve the integration density and benefit various on-chip multimode optical systems.

[1] State Key Laboratory on Tunable Laser Technology, Ministry of Industry and Information Technology Key Lab of Micro-Nano Optoelectronic Information System, Harbin Institute of Technology (Shenzhen), 518055 Shenzhen, P. R. China. [2] State Key Laboratory of Advanced Optical Communication Systems and Networks, Shanghai Jiao Tong University, 200240 Shanghai, P. R. China. [3] Collaborative Innovation Center of Extreme Optics, Shanxi University, 030006 Taiyuan, P. R. China. Correspondence and requests for materials should be addressed to K.X. (email: kxu@hit.edu.cn) or to Y.Y. (email: yaoyong@hit.edu.cn) or to J.D. (email: dujiangbing@hit.edu.cn) or to Q.S. (email: qinghai.song@hit.edu.cn)

（22）Resonance-enhanced three-photon luminesce via lead halide perovskite metasurfaces for optical encoding, Nature Communications

ARTICLE

OPEN

Resonance-enhanced three-photon luminesce via lead halide perovskite metasurfaces for optical encoding

Yubin Fan[1,4], Yuhan Wang[1,4], Nan Zhang[1], Wenzhao Sun[1], Yisheng Gao[1], Cheng-Wei Qiu[2], Qinghai Song[1,3] & Shumin Xiao[1,3]

Lead halide perovskites have emerged as promising materials for photovoltaic and optoelectronic devices. However, their exceptional nonlinear properties have not been fully exploited in nanophotonics yet. Herein we fabricate methyl ammonium lead tri-bromide perovskite metasurfaces and explore their internal nonlinear processes. While both of third-order harmonic generation and three-photon luminescence are generated, the latter one is less affected by the material loss and has been significantly enhanced by a factor of 60. The corresponding simulation reveals that the improvement is caused by the resonant enhancement of incident laser. Interestingly, such kind of resonance-enhanced three-photon luminescence holds true for metasurfaces with a small period number of 4, enabling promising applications of perovskite metasurface in high-resolution nonlinear color nanoprinting and optical encoding. The encoded information 'NANO' is visible only when the incident laser is on-resonance. The off-resonance pumping and the single-photon excitation just produce a uniform dark or photoluminescence background.

[1] State Key Laboratory on Tunable Laser Technology, Ministry of Industry and Information Technology Key Lab of Micro-Nano Optoelectronic Information System, Shenzhen Graduate School, Harbin Institute of Technology, Shenzhen 518055, China. [2] Department of Electrical and Computer Engineering, National University of Singapore, 4 Engineering Drive 3, Singapore 117583, Singapore. [3] Collaborative Innovation Center of Extreme Optics, Shanxi University, Taiyuan 030006, China. [4] These authors contributed equally: Yubin Fan, Yuhan Wang. Correspondence and requests for materials should be addressed to C.-W.Q. (email: [redacted]) or to Q.S. (email: [redacted]) or to S.X. (email: [redacted])

（23）Room temperature electrofreezing of water yields a missing dense ice phase in the phase diagram, Nature Communications

ARTICLE

https://doi.org/10.1038/s41467-019-09950-z OPEN

Room temperature electrofreezing of water yields a missing dense ice phase in the phase diagram

Weiduo Zhu[1,2,6], Yingying Huang[2,3,4,6], Chongqin Zhu[2,6], Hong-Hui Wu[2], Lu Wang[1], Jaeil Bai[2], Jinlong Yang[1], Joseph S. Francisco[2], Jijun Zhao[3], Lan-Feng Yuan[1] & Xiao Cheng Zeng[1,2,5]

Water can freeze into diverse ice polymorphs depending on the external conditions such as temperature (*T*) and pressure (*P*). Herein, molecular dynamics simulations show evidence of a high-density orthorhombic phase, termed ice χ, forming spontaneously from liquid water at room temperature under high-pressure and high external electric field. Using free-energy computations based on the Einstein molecule approach, we show that ice χ is an additional phase introduced to the state-of-the-art *T*–*P* phase diagram. The χ phase is the most stable structure in the high-pressure/low-temperature region, located between ice II and ice VI, and next to ice V exhibiting two triple points at 6.06 kbar/131.23 K and 9.45 kbar/144.24 K, respectively. A possible explanation for the missing ice phase in the *T*–*P* phase diagram is that ice χ is a rare polarized ferroelectric phase, whose nucleation/growth occurs only under very high electric fields.

[1] Hefei National Laboratory for Physical Sciences at Microscale, Department of Chemical Physics, University of Science and Technology of China, Hefei, Anhui 230026, China. [2] Department of Chemistry, University of Nebraska, Lincoln, NE 68588, USA. [3] Key Laboratory of Materials Modification by Laser, Ion and Electron Beams, Ministry of Education, Dalian University of Technology, Dalian 116024, China. [4] Shanghai Advanced Research Institute, Chinese Academy of Sciences, Shanghai 201210, China. [5] Department of Chemical & Biomolecular Engineering and Department of Mechanical and Materials Engineering, University of Nebraska, Lincoln, NE 68588, USA. [6] These authors contributed equally: Weiduo Zhu, Yingying Huang, Chongqin Zhu. Correspondence and requests for materials should be addressed to J.Z. (email: zhaojijun@dlut.edu.cn) or to L.-F.Y. (email: wuhf@ustc.edu.cn) or to X.C.Z. (email: xzeng1@unl.edu)

（24）Quasiparticle interference and nonsymmorphic effect on a floating band surface state of ZrSiSe, Nature Communications

ARTICLE

DOI: 10.1038/s41467-018-06661-6 OPEN

Quasiparticle interference and nonsymmorphic effect on a floating band surface state of ZrSiSe

Zhen Zhu[1], Tay-Rong Chang[2], Cheng-Yi Huang[3], Haiyang Pan[4], Xiao-Ang Nie[1], Xin-Zhe Wang[1], Zhe-Ting Jin[1], Su-Yang Xu[5], Shin-Ming Huang[6], Dan-Dan Guan[1,7], Shiyong Wang[1,7], Yao-Yi Li[1,7], Canhua Liu[1,7], Dong Qian[1,7], Wei Ku[1,7], Fengqi Song[4,7], Hsin Lin[3], Hao Zheng[1,7] & Jin-Feng Jia[1,7]

Non-symmorphic crystals are generating great interest as they are commonly found in quantum materials, like iron-based superconductors, heavy-fermion compounds, and topological semimetals. A new type of surface state, a floating band, was recently discovered in the nodal-line semimetal ZrSiSe but also exists in many non-symmorphic crystals. Little is known about its physical properties. Here, we employ scanning tunneling microscopy to measure the quasiparticle interference of the floating band state on ZrSiSe (001) surface and discover rotational symmetry breaking interference, healing effect and half-missing-type anomalous Umklapp scattering. Using simulation and theoretical analysis we establish that the phenomena are characteristic properties of a floating band surface state. Moreover, we uncover that the half-missing Umklapp process is derived from the glide mirror symmetry, thus identify a non-symmorphic effect on quasiparticle interferences. Our results may pave a way towards potential new applications of nanoelectronics.

[1] School of Physics and Astronomy, Shanghai Jiao Tong University, Shanghai 200240, China. [2] Department of Physics, National Cheng Kung University, Tainan 701, Taiwan. [3] Institute of Physics, Academia Sinica, Taipei City 11529, Taiwan. [4] College of Physics, Nanjing University, Nanjing 210093, China. [5] Department of Physics, Massachusetts Institute of Technology, Cambridge, MA 02139, USA. [6] Department of Physics, National Sun Yat-Sen University, Kaohsiung 80424, Taiwan. [7] Collaborative Innovation Center of Advanced Microstructures, Nanjing University, Nanjing 210093, China. These authors contributed equally: Zhen Zhu, Tay-Rong Chang, Cheng-Yi Huang. Correspondence and requests for materials should be addressed to H.Z. (email: haozheng@sjtu.edu.cn) or to J.-F.J. (email: jfjia@sjtu.edu.cn)

(25) Antiferromagnetic Order in Epitaxial FeSe Films on $SrTiO_3$, Physical Review Letters


PHYSICAL REVIEW LETTERS 120, 097001 (2018)

Antiferromagnetic Order in Epitaxial FeSe Films on $SrTiO_3$

（26）Self-induced backaction optical pulling force, Physical Review Letters

Self-Induced Backaction Optical Pulling Force

Tongtong Zhu,[1] Yongyin Cao,[1] Lin Wang,[1] Zhongquan Nie,[1] Yun Lu,[2] Fangkui Sun,[1] Zehui Jiang,[1] Manuel Nieto-Vesperinas,[3] Yongmin Liu,[4] Cheng Wei Qiu,[2,*] and Weiqiang Ding[1,†]
[1]Department of Physics, Harbin Institute of Technology, Harbin 150001, China
[2]Department of Electrical and Computer Engineering, National University of Singapore, 4 Engineering Drive 3, Singapore 117583, Singapore
[3]Key Lab of Advanced Transducers and Intelligent Control System, Ministry of Education and Shanxi Province, College of Physics and Optoelectronics, Taiyuan University of Technology, Taiyuan 030024, China
[4]Department of Biomedical Engineering, Dalian University of Technology, Dalian 116024, China
[5]Instituto de Ciencia de Materiales de Madrid, Consejo Superior de Investigaciones Científicas, Campus de Cantoblanco, Madrid 28049, Spain
[6]Department of Mechanical and Industrial Engineering and Electrical and Computer Engineering, Northeastern University, Boston, Massachusetts 02115, USA

(Received 11 September 2017; published 21 March 2018; corrected 23 March 2018)

We achieve long-range and continuous optical pulling in a periodic photonic crystal background, which supports a unique Bloch mode with the self-collimation effect. More interestingly, the pulling force reported here is mainly contributed by the intensity gradient force originating from the self-induced backaction of the object to the self-collimation mode. This force is sharply distinguished from the widely held conception that optical matter forces based on the scattering force. Also, the pulling force is insensitive to the angle of incidence and can pull multiple objects simultaneously.

DOI: 10.1103/PhysRevLett.120.123903

Since the pioneering work of Ashkin [1–4], the concepts and techniques of matter trapping and manipulation by an optical force have experienced impressive progress in the past decades [5–9]. Optical tweezers have become an indispensable tool in various disciplines, including biology [6–10], optics [11–13], and condensed matter [14], as well as quantum physics [15]. In traditional optical trapping, however, it is extremely challenging to scale down below 100 nm due to both the diffraction-limited resolving of light and the r^{-3} decaying law of the optical force with the radius r of small particles. Under these circumstances, by setting the trapping operation inside a nanocavity, the self-induced backaction optical trapping was proposed in nanocavities [16–22], which can trap objects of tens of nanometers or even smaller, thanks to the active feedback of the trapping objects to the trapping system.

Despite its power in nanometer trapping, the self-induced backaction method has not been explored in long-range optical pulling (or in optical tractor beams), because it influences the intensity gradient component of the scattering force in a nanocavity, while a tractor beam relies on the scattering component in a translation-invariant structure. A tractor beam, initially proposed in acoustics by Marston *et al.* [23–25], is an intensity gradient-free beam along the propagation direction, which can transport objects towards the source over a long distance rather than push them away. The counterintuitive optical pulling [26–28] raises increasing attention due to its sophisticated underlying physics and potential applications [29–48].

In the extensive studies up to now, except for the photophoretic forces [49,50], all optical pulling forces have been regarded as optical scattering forces, like in the schemes of structured light beams [26–33,40], plasmonic media [34–42], [52], inhomogeneous background media [36,51], and guiding mode scattering [34,43,54].

In this Letter, we propose a novel approach based on the self-induced backaction-generated gradient force that achieves long-range optical pulling in a periodic photonic structure, namely, in a photonic crystal (PC) [55–57]. Interestingly, the pulling force arising in the PC is not predominantly contributed by the scattering force as reported before, but induced by the intensity gradient force generated by the dynamic interaction of the object with the self-collimation (SC) mode of the PC [57–59]. The SC mode is a unique kind of Bloch mode with a finite transversal size that can propagate infinitely long without diffraction. Hence, our results are sharply distinct to the widely held conception that the optical pulling force should be a scattering force, and shed new insightful concepts concerning the optical force and momentum physics and technologies.

To illustrate the underlining physics, we address a two-dimensional PC structure with a square lattice as illustrated in Fig. 1. Figure 1(a) shows the outline of the entire configuration. The SC mode is excited by a Gaussian beam at an angle of incidence θ_{in} and propagates along the $+x$

（27）Atomic-level insight into super-efficient electrocatalytic oxygen evolution on iron and vanadium co-doped nickel (oxy)hydroxide, Nature Communications

nature COMMUNICATIONS

ARTICLE

[illegible] OPEN

Atomic-level insight into super-efficient electrocatalytic oxygen evolution on iron and vanadium co-doped nickel (oxy)hydroxide

Jian Jiang[1], Fanfei Sun[2], Si Zhou[3], Wei Hu[4], Hao Zhang[2], Jinchao Dong[5], Zheng Jiang[2], Jijun Zhao[3], Jianfeng Li[5], Wensheng Yan[4] & Mei Wang[1]

It is of great importance to understand the origin of high oxygen-evolving activity of state-of-the-art multimetal oxides/(oxy)hydroxides at atomic level. Herein we report an evident improvement of oxygen evolution reaction activity via incorporating iron and vanadium into nickel hydroxide lattices. X-ray photoelectron/absorption spectroscopies reveal the synergistic interaction between iron/vanadium dopants and nickel in the host matrix, which subtly modulates local coordination environments and electronic structures of the iron/vanadium/nickel cations. Further, in-situ X-ray absorption spectroscopic analyses manifest contraction of metal-oxygen bond lengths in the activated catalyst, with a short vanadium-oxygen bond distance. Density functional theory calculations indicate that the vanadium site of the iron/vanadium co-doped nickel (oxy)hydroxide gives near-optimal binding energies of oxygen evolution reaction intermediates and has lower overpotential compared with nickel and iron sites. These findings suggest that the doped vanadium with distorted geometric and disturbed electronic structures makes crucial contribution to high activity of the trimetallic catalyst.

[1] State Key Laboratory of Fine Chemicals, DUT-KTH Joint Education and Research Centre on Molecular Devices, Dalian University of Technology, Dalian 116024, China. [2] Shanghai Institute of Applied Physics, Chinese Academy of Sciences, Shanghai 201204, China. [3] MOE Key Laboratory of Materials Modification by Laser, Ion and Electron Beams, Dalian University of Technology, Dalian 116024, China. [4] National Synchrotron Radiation Laboratory, University of Science and Technology of China, Hefei 230029, China. [5] State Key Laboratory of Physical Chemistry of Solid Surfaces, College of Chemistry and Chemical Engineering, Xiamen University, Xiamen 361005, China. These authors contributed equally: Jian Jiang, Fanfei Sun. Correspondence and requests for materials should be addressed to W.Y. (email: [illegible]) or to M.W. (email: [illegible])

（28）Stabilization of body-centred cubic iron under inner-core conditions, Nature Geoscience

ARTICLES

nature geoscience

Stabilization of body-centred cubic iron under inner-core conditions

Anatoly B. Belonoshko[1*], Timofei Lukinov[1], Jie Fu[1,2], Jijun Zhao[2], Sergio Davis[3] and Sergei I. Simak[4]

The Earth's solid core is mostly composed of iron. However, despite being central to our understanding of core properties, the stable phase of iron under inner-core conditions remains uncertain. The two leading candidates are hexagonal close-packed and body-centred cubic (bcc) crystal structures, but the dynamic and thermodynamic stability of bcc iron under inner-core conditions has been challenged. Here we demonstrate the stability of the bcc phase of iron under conditions consistent with the centre of the core using *ab initio* molecular dynamics simulations. We find that the bcc phase is stabilized at high temperatures by a diffusion mechanism that arises due to the dynamical instability of the phase at lower temperatures. On the basis of our simulations, we reinterpret experimental data as support for the stability of bcc iron under inner-core conditions. We suggest that the diffusion of iron atoms in solid state may explain both the anisotropy and the low shear modulus of the inner core.

Stability–instability relation

（29）A new phase diagram of water under negative pressure: The rise of the lowest-density clathrate s-III, Science Advances


RESEARCH ARTICLE

WATER CHEMISTRY

A new phase diagram of water under negative pressure: The rise of the lowest-density clathrate s-III

Yingying Huang, Chongqin Zhu, Lu Wang, Xiaoxiao Cao, Yan Su, Xue Jiang, Sheng Meng, Jijun Zhao, Xiao Cheng Zeng

INTRODUCTION

（30）Quasi-freestanding epitaxial silicene on Ag(111) by oxygen intercalation, Science Advances

RESEARCH ARTICLE

MATERIALS ENGINEERING

Quasi-freestanding epitaxial silicene on Ag(111) by oxygen intercalation

Yi Du,[1]* Jincheng Zhuang,[1] Jiaou Wang,[2] Zhi Li,[1] Hongsheng Liu,[1] Jijun Zhao,[3]* Xun Xu,[1] Haifeng Feng,[1] Lan Chen,[4] Kehui Wu,[4] Xiaolin Wang,[1] Shi Xue Dou[1]

Silicene is a monolayer allotrope of silicon atoms arranged in a honeycomb structure with massless Dirac fermion characteristics, similar to graphene. It meets development of silicon-based multifunctional nanoelectronic and spintronic devices operated at room temperature because of strong spin-orbit coupling. Nevertheless, unfortunately, silicene could only be epitaxially grown on conductive substrates. The strong silicene-substrate interaction may depress its superior electronic properties. We report a quasi-freestanding silicene layer that has been successfully obtained through oxidization of bilayer silicene on the Ag(111) surface. The oxygen atoms intercalate into the underlayer of silicene, resulting in isolation of the top layer of silicene from the substrate. In consequence, the top layer of silicene exhibits the signature of a (1 × 1) honeycomb lattice and hosts massless Dirac fermions because of much less interaction with the substrate. Furthermore, the oxidized silicon buffer layer is expected to serve as an ideal dielectric layer for electric gating in electronic devices. These findings are relevant for the future design and application of silicene-based nanoelectronic and spintronic devices.

INTRODUCTION

RESULTS

（31）Majorana Zero Mode Detected with Spin Selective Andreev Reflection in the Vortex of a Topological Superconductor, Physical Review Letters

Majorana Zero Mode Detected with Spin Selective Andreev Reflection in the Vortex of a Topological Superconductor

（32）Epitaxial growth of two-dimensional stanine, Nature Materials

ARTICLES

nature materials

Epitaxial growth of two-dimensional stanene

Feng-feng Zhu[1†], Wei-jiong Chen[1†], Yong Xu[2,3,4*], Chun-lei Gao[1,5], Dan-dan Guan[1,5], Can-hua Liu[1,5], Dong Qian[1,2*], Shou-Cheng Zhang[2,3,4] and Jin-feng Jia[1,5*]

Following the first experimental realization of graphene, other ultrathin materials with unprecedented electronic properties have been explored, with particular attention given to the heavy group-IV elements Si, Ge and Sn. Two-dimensional buckled Si-based silicene has been recently realized by molecular beam epitaxy growth, whereas Ge-based germanene was obtained by molecular beam epitaxy and mechanical exfoliation. However, the synthesis of Sn-based stanene has proved challenging so far. Here, we report the successful fabrication of 2D stanene by molecular beam epitaxy, confirmed by atomic and electronic characterization using scanning tunnelling microscopy and angle-resolved photoemission spectroscopy, in combination with first-principles calculations. The synthesis of stanene and its derivatives will stimulate further experimental investigation of their theoretically predicted properties, such as a 2D topological insulating behaviour with a very large bandgap, and the capability to support enhanced thermoelectric performance, topological superconductivity and the near-room-temperature quantum anomalous Hall effect.

（33）The structural origin of the hard-sphere glass transition in granular packing, Nature Communications

nature COMMUNICATIONS

ARTICLE

Received 11 Feb 2015 | Accepted 14 Aug 2015 | Published 28 Sep 2015

OPEN

The structural origin of the hard-sphere glass transition in granular packing

Chengjie Xia[1], Jindong Li[1], Yixin Cao[1], Binquan Kou[1], Xianghui Xiao[2], Kamel Fezzaa[2], Tiqiao Xiao[3] & Yujie Wang[1,4]

Glass transition is accompanied by a rapid growth of the structural relaxation time and a concomitant decrease of configurational entropy. It remains unclear whether the transition has a thermodynamic origin, and whether the dynamic arrest is associated with the growth of a certain static order. Using granular packing as a model hard-sphere glass, we show the glass transition as a thermodynamic phase transition with a 'hidden' polytetrahedral order. This polytetrahedral order is spatially correlated with the slow dynamics. It is geometrically frustrated and has a peculiar fractal dimension. Additionally, as the packing fraction increases, its growth follows an entropy-driven nucleation process, similar to that of the random first-order transition theory. Our study essentially identifies a long-sought-after structural glass order in hard-sphere glasses.

[1] Department of Physics and Astronomy, Shanghai Jiao Tong University, 800 Dong Chuan Road, Shanghai 200240, China. [2] Advanced Photon Source, Argonne National Laboratory, 9700 South Cass Avenue, Argonne, Illinois 60439, USA. [3] Shanghai Institute of Applied Physics, Chinese Academy of Sciences, Shanghai 201800, China. [4] Collaborative Innovation Center of Advanced Microstructures, Nanjing University, Nanjing 210093, China. Correspondence and requests for materials should be addressed to Y.W. (email: yujiewang@sjtu.edu.cn).

（34）Superconductivity above 100 K in single-layer FeSe films on doped SrTiO3, Nature Materials

nature materials

LETTERS

Superconductivity above 100 K in single-layer FeSe films on doped $SrTiO_3$

Jian-Feng Ge[1], Zhi-Long Liu[2], Canhua Liu[1,2*], Chun-Lei Gao[1,2], Dong Qian[1,2], Qi-Kun Xue[3*], Ying Liu[1,2*] and Jin-Feng Jia[1,2*]

Recent experiments on FeSe films grown on $SrTiO_3$ (STO) suggest that interface effects can be used as a means to reach superconducting critical temperatures (T_c) of up to 80 K (ref. 1). This is nearly ten times the T_c of bulk FeSe and higher than the record value of 56 K for known bulk Fe-based superconductors[2]. Together with recent studies of superconductivity at oxide heterostructure interfaces[3–5], these results rekindle the long-standing idea that electron pairing at interfaces between two different materials can be tailored to achieve high-temperature superconductivity[6–12]. Subsequent angle-resolved photoemission spectroscopy measurements of the FeSe/STO system revealed an electronic structure distinct from bulk FeSe (refs 13,14), with an energy gap vanishing at around 65 K. However, ex situ electrical transport measurements[1,15] have so far detected zero resistance—the key experimental signature of superconductivity—only below 30 K. Here, we report the observation of superconductivity with T_c above 100 K in the FeSe/STO system by means of in situ four-point probe electrical transport measurements. This finding confirms FeSe/STO as an ideal material for studying high-T_c superconductivity.

（35）Demonstration of Nonlinear-Energy-Spread Compensation in Relativistic Electron Bunches with Corrugated Structures, Physical Review Letters

Demonstration of Nonlinear-Energy-Spread Compensation in Relativistic Electron Bunches with Corrugated Structures

Feichao Fu,[1,2] Rui Wang,[1,2] Pengfei Zhu,[1,2] Lingrong Zhao,[1,2] Tao Jiang,[1,2] Chao Lu,[1,2] Shengguang Liu,[1,2] Lanfa Shi,[1,2] Lixin Yan,[1] Haixiao Deng,[3] Chao Feng,[3] Qiang Gu,[3] Dazhang Huang,[4] Bo Liu,[4] Dong Wang,[4] Xingtao Wang,[4] Meng Zhang,[4] Zhentang Zhao,[4] Gennady Stupakov,[5] Dao Xiang,[1,2,*] and Jie Zhang[1,2,†]

[1]Key Laboratory for Laser Plasmas (Ministry of Education), Department of Physics and Astronomy, Shanghai Jiao Tong University, Shanghai 200240, China

[2]IFSA Collaborative Innovation Center, Shanghai Jiao Tong University, Shanghai 200240, China

[3]Department of Engineering Physics, Tsinghua University, Beijing 100084, China

[4]Shanghai Institute of Applied Physics, Chinese Academy of Sciences, Shanghai 201800, China

[5]SLAC National Accelerator Laboratory, Menlo Park, California 94025, USA

(Received 7 February 2015; published 20 March 2015)

High quality electron beams with flat distributions in both energy and current are critical for many accelerator based scientific facilities such as free-electron lasers and MeV ultrafast electron diffraction and microscopes. In this Letter, we report on using corrugated structures to compensate for the beam nonlinear energy chirp imprinted by the curvature of the radio-frequency field, leading to a significant reduction in beam energy spread. By using a pair of corrugated structures with tailored orientations, we show that the quadrupole wakefields, which, otherwise, can cause beam emittance, can be effectively canceled. This work also extends the applications of corrugated structures to the low beam charge (a few pC) and low beam energy (a few MeV) regime and may have a strong impact in many accelerator based facilities.

DOI: 10.1103/PhysRevLett.114.114801 PACS numbers: 41.60.Cr, 41.75.Ht, 41.85.Ct

"Flat-flat" electron beams, i.e., flat in both beam energy and current [1], are critical for achieving high performance in many accelerator based facilities such as seeded free-electron lasers (FELs) [2–6] and MeV ultrafast electron microscopes (UEMs) [7,8]. By either sending the relativistic electron beams through undulators to produce coherent intense x rays or directly using the electrons as probes, these facilities are enabling new opportunities in an extraordinarily wide array of sciences. With the beam produced in a photocathode radio-frequency (rf) gun and accelerated to high energy in rf structures, the electron beam longitudinal phase space, however, typically consists of nonlinear chirps (energy-time correlations) from the varying rf phase along the bunch. In seeded FELs, this nonlinear energy chirp deteriorates the performance of bunch compressors and broadens the FEL spectrum. In UEMs, the nonlinear energy chirp increases the beam global energy spread and, thus, leads to serious chromatic aberrations that reduce the microscope resolution. A similar detrimental effect also holds for ultrafast electron diffraction facilities where the nonlinear energy chirp sets the lower limit of the electron bunch length that can be achieved with velocity bunching [9].

The standard method for compensating for the nonlinear energy chirp is to use a harmonic cavity (HC), for example, [10]. The idea is rather simple. Consider a beam passing through two rf structures with wave numbers at $k_{1,2}$, peak energy gains at $E_{1,2}$, and phases at $\phi_{1,2}$; the energy of a particle at longitudinal position z with respect to the reference particle can be written as

$$E(z) = E_1 \cos(\phi_1 - k_1 z) + E_2 \cos(\phi_2 + k_2 z). \quad (1)$$

Assuming the first rf structure is mainly used for beam acceleration and the second structure for cancellation of the nonlinear chirp, then the phase of the main acceleration structure should be correspondingly set at $\phi_1 = 0$ to provide maximal energy gain, and the phase of the harmonic cavity should be set at the decelerating phase ($\phi_2 = \pi$). Under this condition, the energy chirp is canceled up to the second order if $E_2 k_2^2 = E_1 k_1^2$, i.e., the required voltage for the harmonic cavity scales as $1/n^2$, where $n = k_2/k_1$ is the harmonic number.

Cancellation of the nonlinear chirp with series rf structures not only requires dedicated expensive rf stations, the relative phase of the rf structures needs to be accurately controlled as well. Another unwanted outcome is that the beam energy will also be reduced by $1/n^2$ (e.g., if a C-band structure with frequency at 5712 MHz is used to cancel the nonlinear chirp from an S-band structure with frequency at 2856 MHz, the beam energy will drop by 1/4). While reduction of beam energy by a fraction for FELs is typically not a big concern, it may result in stronger space charge effect in UEMs since the beam energy is only a few MeV [7,8]. Furthermore, it may add considerable complexity and cost to such compact facilities.

（36）Multichromatic Narrow-Energy-Spread Electron Bunches from Laser-Wakefield Acceleration with Dual-Color Lasers, Physical Review Letters

PRL 114, 084801 (2015) PHYSICAL REVIEW LETTERS week ending 27 FEBRUARY 2015

Multichromatic Narrow-Energy-Spread Electron Bunches from Laser-Wakefield Acceleration with Dual-Color Lasers

M. Zeng,[1,2] M. Chen,[1,2,*] L. L. Yu,[1,3] W. B. Mori,[3] Z. M. Sheng,[1,2,4] B. Hidding,[5] D. A. Jaroszynski,[5] and J. Zhang[1,2]
[1]Key Laboratory for Laser Plasmas (Ministry of Education), Department of Physics and Astronomy, Shanghai Jiao Tong University, Shanghai 200240, China
[2]IFSA Collaborative Innovation Center, Shanghai Jiao Tong University, Shanghai 200240, China
[3]University of California, Los Angeles, California 90095, USA
[4]SUPA, Department of Physics, University of Strathclyde, Glasgow G4 0NG, United Kingdom
[5]SUPA, Department of Physics, University of Strathclyde, Glasgow G4 0NG, United Kingdom

(Received 30 June 2014; published 24 February 2015)

A method based on laser wakefield acceleration with controlled ionization injection triggered by another frequency-tripled laser is proposed, which can produce electron bunches with low energy spread. As two colorful pulses copropagate in the background plasma, the peak amplitude of the combined laser field is modulated in time and space during the laser propagation due to the plasma dispersion. Ionization injection occurs when the peak amplitude exceeds a certain threshold. The threshold is exceeded for limited duration periodically at different propagation distances, leading to multiple, localized, and separated electron bunches. The method is demonstrated through multidimensional particle-in-cell simulations. Such electron bunches may be used to generate multicolor x-ray sources for a variety of applications.

PACS numbers: 29.25.Bx, 41.75.Jv, 41.85.Ja, 52.38.Hb

Versatile x-ray sources with tunable brightness, spectrum range, pulse duration, and temporal-spatial coherence could be used for scientific discoveries as well as medical and industrial applications. Continuous efforts are being made to push x-ray sources towards new limits such as coherent x rays over 10 keV [1,2], attosecond pulses [3], two-color hard x-ray lasers [4], etc. However, currently most of these sources are based on conventional accelerators. More compact and low cost x-ray devices with comparable quality are highly desired. Recently, laser wakefield acceleration (LWFA) offers the possibility for a new generation of compact particle accelerators [5]. Single or multiple bunches can be generated for different applications [6–8]. LWFA-based compact and low cost x- and γ-ray sources also have attracted much interest [9–12].

In spite of the significant progress made in LWFA research in the past decade [13–18], it is widely recognized that the beam quality and stability still need to be improved considerably before its wide applications. The injection process is a key issue of high quality beam production. There are a few interesting schemes proposed. A cold optical injection scheme is proposed to produce ultralow energy spread beams as shown by two-dimensional (2D) simulations [19]. Besides, ionization-induced injection in mixed gaseous targets has been proposed and demonstrated as an attractive scheme [20–30] due to the relatively easier experiment. In this scheme a minority of gases is chosen. In the mixture, at least one of the gas elements has a relatively low ionization threshold such that it is effectively preionized and acts as background plasma, while at least another has inner shells with higher ionization thresholds (such as nitrogen and oxygen). The laser releases these inner shell electrons at a location within the wake such that they can be easily trapped and accelerated. Generally the final electron beam energy spread is related to the effective injection length [31–33], which often leads to energy spread much larger than 1% unless some techniques, such as laser self-focusing, is used [34].

In this Letter, we propose a new electron injection scheme to produce ultralow energy spread and single or multiple electron bunches with equally spaced energy peaks. We use a bichromatic laser to trigger sequential ionization injections. In our one-dimensional (1D) and multidimensional particle-in-cell (PIC) simulations using the code OSIRIS [35], low energy spread beams are generated because the effective injection length is suppressed to a few hundred micrometers. A multipeak energy spectrum can also be observed if a specific condition is satisfied.

This scheme is illustrated in Fig. 1. A manipulator with the fundamental frequency is responsible for driving an accelerating wakefield in the blowout regime [36–38]. A second copropagating harmonic pulse with a smaller amplitude modulates the peak laser field strength and acts as a trigger of the high-Z gas K-shell ionization. Because of the laser dispersion in the plasma, the phase speed of the two frequency components are different. By tuning the amplitude of the two components, one can limit the K-shell ionization only occurring when the peaks of the two lasers overlap.

To understand this process, we first study the propagation of a bichromatic laser in plasmas. Consider two plane waves ($i = 1, 2$) with the normalized vector potential

$$a_i(z,t) = a_{0i}\sin(\omega_i t - k_i z + \phi_i), \quad (1)$$

0031-9007/15/114(8)/084801(5) 084801-1

（37）Experimental Detection of a Majorana Mode in the core of a Magnetic Vortex inside a Topological Insulator-Superconductor Bi2Te3/NbSe2 Heterostructure, Physical Review Letters

PRL 114, 017001 (2015) PHYSICAL REVIEW LETTERS week ending 9 JANUARY 2015

Experimental Detection of a Majorana Mode in the core of a Magnetic Vortex inside a Topological Insulator-Superconductor $Bi_2Te_3/NbSe_2$ Heterostructure

Jin-Peng Xu,[1] Mei-Xiao Wang,[1] Zhi Long Liu,[1] Jian-Feng Ge,[1] Xiaojun Yang,[2] Canhua Liu,[1,3] Zhu An Xu,[2,4] Dandan Guan,[1] Chun Lei Gao,[1] Deng Qian,[1] Ying Liu,[1,5,6] Qiang-Hua Wang,[1,5] Fu-Chun Zhang,[1,5] Qi-Kun Xue,[6] and Jin-Feng Jia[1,5,*]

[1]Key Laboratory of Artificial Structures and Quantum Control (Ministry of Education), Department of Physics and Astronomy, Shanghai Jiao Tong University, Shanghai 200240, China
[2]State Key Laboratory of Silicon Materials and Department of Physics, Zhejiang University, Hangzhou 310027, China
[3]Department of Physics, Pennsylvania State University, University Park, Pennsylvania 16802, USA
[4]National Laboratory of Solid State Microstructures and School of Physics, Nanjing University, Nanjing 210093, China
[5]Collaborative Innovation Center of Advanced Microstructures, Nanjing University, Nanjing 210093, China
[6]State Key Laboratory for Low-Dimensional Quantum Physics, Department of Physics, Tsinghua University, Beijing 100084, China

(Received 29 August 2014; revised manuscript received 20 November 2014; published 5 January 2015)

Majorana fermions have been intensively studied in recent years for their importance to both fundamental science and potential applications in topological quantum computing. They are predicted to exist in a vortex core of superconducting topological insulators. However, it is extremely difficult to distinguish them experimentally from other quasiparticle states for the tiny energy difference between Majorana fermions and those states, which is beyond the energy resolution of most available techniques. Here, we circumvent the problem by systematically investigating the spatial profile of the Majorana mode and the bound quasiparticle states within a vortex in Bi_2Te_3 films grown on a superconductor $NbSe_2$. While the zero-bias peak in local conductance splits right off the vortex center in conventional superconductors, it persists over a finite distance ~20 nm away from the vortex center in Bi_2Te_3. This unusual splitting behavior has never been observed before and could be possibly due to the Majorana fermion zero mode. While the Majorana mode is described by the interaction between vortices, the zero-bias peak splits as a conventional superconductor again. This work provides self-consistent evidence of Majorana fermions and also suggests a possible route to manipulating them.

DOI: 10.1103/PhysRevLett.114.017001 PACS numbers: 73.20.-r, 68.37.Ef, 74.25.Ha, 71.55.-i

Identical to their antiparticles, Majorana fermions (MF) were proposed in 1937 as an alternative to Dirac theory of ordinary fermions that carry opposite charge from their antiparticles [1]. Neutrinos are the first candidate for MF in particle physics, but their Majorana nature remains to be confirmed [2]. There are also proposals that quasiparticles in certain quantum condensed matter systems may be MFs. Examples include 5/2 fractional quantum Hall state, cold atoms, and chiral p-wave superconductors [3,4]. Experimental realization of MFs is of great significance in fundamental physics. MFs obey non-Abelian statistics, and thus can be used to develop topological quantum computation. The recent work by Fu and Kane predicted that MFs should be present as zero-energy bound states at vortex cores of an engineered heterostructure consisting of a normal s-wave superconductor (SC) and a topological insulator (TI) [5]. Cooper pairs are introduced via the proximity effect to the TI surface where spin and momentum are locked in the topological surface state (TSS) band [6,7]. This leads to an unusual p-wave-like paired state that is time-reversal invariant and robust against disorder [8]. Theoretical studies have shown that the MFs may also reside at two ends of a semiconductor nanowire (NW) with strong spin-orbit coupling when it is contacted to an s-wave SC in a proper external magnetic field [9]. Several transport measurements revealed a signature of MFs, i.e., a sharp zero-bias peak in differential conductance spectrum in various NW-SC junctions [10–14]. In InSb/Nb junctions, an unconventional fractional ac Josephson effect was observed and attributed to the existence of MFs [15]. However, alternative explanations of these transport results based on disorder and/or band bending in the NWs have been proposed [16–19]. Very recently, S. Nadj-Perge *et al.* have reported first observation of MF on Fe atomic chains [20], as yet, no conclusive evidence has been established for the existence of MF [21].

In contrast, the disorder alone is unlikely to induce a zero-bias peak in a superconducting TI, which can be used to detect MFs without the complications mentioned above. Proximity effect induced superconductivity in a TI surface has been demonstrated in several TI/SC heterostructures [22–25]. To obtain the evidence for the existence of MFs, a promising route is to detect the zero-bias bound state at vortex cores of a TI/SC heterostructure with scanning

（38）Quantum teleportation with independent sources and prior entanglement distribution over a network, Nature Photonics

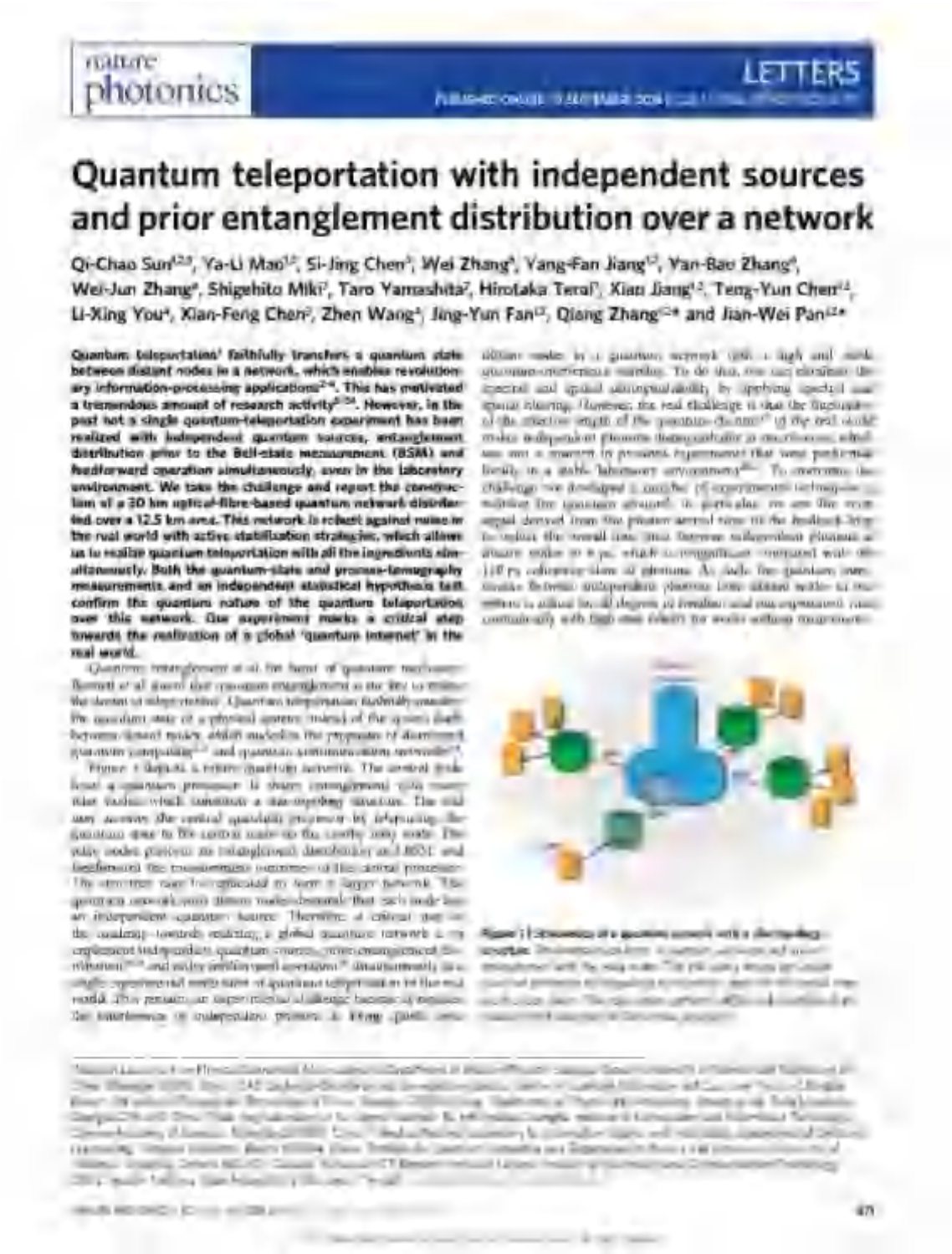

nature photonics

LETTERS

Quantum teleportation with independent sources and prior entanglement distribution over a network

Qi-Chao Sun[1,2,3], Ya-Li Mao[1,2], Si-Jing Chen[1], Wei Zhang[4], Yang-Fan Jiang[1,2], Yan-Bao Zhang[4], Wei-Jun Zhang[4], Shigehito Miki[5], Taro Yamashita[5], Hirotaka Terai[5], Xiao Jiang[1,2], Teng-Yun Chen[1,2], Li-Xing You[4], Xian-Feng Chen[2], Zhen Wang[1], Jing-Yun Fan[1,2], Qiang Zhang[1,2]* and Jian-Wei Pan[1,2]*

Quantum teleportation[1] faithfully transfers a quantum state between distant nodes in a network, which enables revolutionary information-processing applications[2–6]. This has motivated a tremendous amount of research activity[6–20]. However, in the past not a single quantum-teleportation experiment has been realized with independent quantum sources, entanglement distribution prior to the Bell-state measurement (BSM) and feedforward operation simultaneously, even in the laboratory environment. We take the challenge and report the construction of a 30 km optical-fibre-based quantum network distributed over a 12.5 km area. This network is robust against noise in the real world with active stabilization strategies, which allows us to realize quantum teleportation with all the ingredients simultaneously. Both the quantum-state and process-tomography measurements and an independent statistical hypothesis test confirm the quantum nature of the quantum teleportation over this network. Our experiment marks a critical step towards the realization of a global 'quantum internet' in the real world.

（39）Bimetallic Microswimmers Speed Up in Confining Channels, Physical Review Letters

Bimetallic Microswimmers Speed Up in Confining Channels

Chang Liu,[1] Chao Zhou,[2] Wei Wang,[2,*] and H. P. Zhang[1,†]
[1]Department of Physics and Astronomy, and Institute of Natural Sciences, Shanghai Jiao Tong University, Shanghai 200240, China
[2]School of Material Science and Engineering, Harbin Institute of Technology, Shenzhen Graduate School, Shenzhen 518055, China
[3]Center for Soft and Living Matter, Institute for Basic Science (IBS), Ulsan 44919, Republic of Korea
[4]Collaborative Innovation Center of Advanced Microstructures, Nanjing 210093, China
(Received 15 June 2016; revised manuscript received 22 September 2016; published 1 November 2016)

Synthetic microswimmers are envisioned to be useful in numerous applications, many of which occur in tightly confined spaces. It is therefore important to understand how confinement influences swimmer dynamics. Here we study the motility of bimetallic microswimmers in linear and curved channels. Our experiments show swimmer velocities increase, up to 5 times, with the degree of confinement and the relative velocity increase depends weakly on the fuel concentration and ionic strength in solution. Experimental results are reproduced in a numerical model which attributes the swimmer velocity increase to electrostatic and electrohydrodynamic boundary effects. Our work not only helps to elucidate the confinement effect on phoretic swimmers, but also suggests that spatial confinement may be used as an effective control method for them.

DOI: 10.1103/PhysRevLett.117.198001

Material transport at micro- or nanometer scales is conventionally driven by externally imposed fields, such as pressure or temperature [1,2]. In contrast, microswimmers move autonomously without external driving: they self-propel by converting local sources of energy into mechanical work [3–8]. Many synthetic microswimmers can mimic their biological counterparts in achieving autonomous motion [3–10]. For example, Janus particles generate local gradients of temperature [11], chemical concentration [12–14], or electric potential [15–19] and self-propel through respective phoretic mechanisms [20–22]. These phoretic microswimmers have demonstrated preliminary applications, such as cargo delivery [23,24], chemical sensing [25,26], and water purification [27,28]. They have also been recently used to explore the nonequilibrium physics of active matter [13,14,29].

Microswimmers are often required to move through narrow channel-like passages [30]. Hydrodynamic swimmers in such strong confinement have been investigated. Experiments showed that *Paramecium* [31] and *E. coli* bacteria [32] slow down in narrow channels; these results were later reproduced numerically [33,34]. Wu *et al.* showed numerically that amoeboid shows slows in strong confinement [35]. Other numerical studies predicted that swimmer velocity may increase with confinement for a squirmer driven by normal deformations [33], a Taylor-like swimmer [36], and a rotating helix [37]. Ledesma *et al.* [38] reported that elasticity of confining boundary may speed up a dipolar swimmer. These studies show hydrodynamic interaction with confinement can lead to rich swimmer dynamics.

In contrast with the numerous studies of hydrodynamic swimmers [31–38], the subject of synthetic microswimmers in confinement has remained largely unexplored until quite recently. Synthetic swimmers are found to strongly interact with boundaries, such as a flat plane [39–44], a corner [42,43,45], a colloid crystal [46], or a spherical confinement [47]. We are therefore motivated to investigate how strongly confining channels affect synthetic swimmers, particularly their motility. Our experiments show bimetallic swimmers significantly increase their velocity in channels. A numerical model reproduces our experimental results and reveals that the channels influence swimmers through electrostatic and electrohydrodynamic boundary effects. This knowledge not only helps us better understand the complex interplay between phoretic microswimmers and their environment, but also suggests control strategies for their practical applications in confined situations.

We fabricate two kinds of bimetallic microswimmers. One contains Au and Ru segments of equal length, the other Au and Rh segments. Both swimmers are rodlike and have a diameter $d_s = 0.3$ μm and different length, denoted as L (1.8 to 3.7 μm). A two-photon direct laser writing system fabricates microchannels with a submicron accuracy; the system's efficiency and flexibility allow us to systematically vary channel size and topology. Scanning electron images and detailed fabrication procedures can be found in the Supplemental Material [48]. After fabrication, we immerse swimmers and channels in a solution containing hydrogen peroxide (H_2O_2, 5% to 30% by weight). Swimmer motion in the sample is recorded through a 60× objective at a rate of 30 frames per sec with a camera (Basler acA2040-90um) and analyzed with standard particle tracking algorithms.

A bimetallic microswimmer propels through a self-electrophoretic mechanism. As sketched in Fig. S1a

0031-9007/16/117(19)/198001(6)

（40）Controllable Terahertz Radiation from a Linear-Dipole Array Formed by a Two-Color Laser Filament in Air, Physical Review Letters

PRL 117, 243901 (2016) PHYSICAL REVIEW LETTERS 9 DECEMBER 2016

Controllable Terahertz Radiation from a Linear-Dipole Array Formed by a Two-Color Laser Filament in Air

Zhelin Zhang,[1,2] Yanping Chen,[1,2] Min Chen,[1,2] Zhen Zhang,[1,2] Jun Yu,[1] Zhengming Sheng,[1,3]* and Jie Zhang[1,2]†
[1]Key Laboratory for Laser Plasmas (Ministry of Education), Department of Physics and Astronomy, Shanghai Jiao Tong University, Shanghai 200240, China
[2]Collaborative Innovation Center of IFSA, Shanghai Jiao Tong University, Shanghai 200240, China
[3]Department of Physics, SUPA, University of Strathclyde, Glasgow G4 0NG, United Kingdom
(Received 11 August 2016; published 9 December 2016)

We demonstrate effective control on the carrier-envelope phase and angular distribution as well as the peak intensity of a nearly single-cycle terahertz pulse emitted from a laser filament formed by two-color, the fundamental and the corresponding second harmonic, femtosecond laser pulses propagating in air. Experimentally, such control has been performed by varying the filament length and the initial phase difference between the two-color laser components. A linear-dipole-array model, including the descriptions of both the generation (via laser field ionization) and propagation of the emitted terahertz pulse, is proposed to present a quantitative interpretation of the observations. Our results contribute to the understanding of terahertz generation in a femtosecond laser filament and suggest a practical way to control the electric field of a terahertz pulse for potential applications.

DOI: 10.1103/PhysRevLett.117.243901

Terahertz (THz) radiation is of enormous interest for a variety of promising applications such as remote THz sensing and imaging, THz spectroscopy, THz nonlinear high field physics, and the diagnostics of a high-power laser-matter interaction [1–5]. High peak-power broadband THz radiations can be generated by two-color laser-induced air plasmas which can be moreover delivered to remote targets by laser self-guiding, avoiding thus the strong absorption of THz radiation by water vapor in the atmosphere [6–9]. THz radiation generation in air plasmas can be mainly described using four-wave rectification [10–12] and transient photocurrent [13–21] models. In particular, it is well known from previous studies that the electric field of a THz pulse emitted from a two-color laser plasma is usually with a single cycle waveform. Thus, a precise control of the carrier-envelope phase (CEP) is crucial for applications, e.g., THz nonlinear optics and spectroscopy on various systems [22–24].

In this Letter, we have performed an effective control of the spatiotemporal structure of a THz pulse emitted from a two-color laser-induced air-plasma channel (filament), including its electric field waveform (or CEP) and angular distribution as well as its peak intensity. Such control was realized through a change of the filament length as well as the initial phase difference between the two-color laser components. A theoretical model has been developed to describe both the generation and the propagation of the THz wave emitted from a filament, where the THz radiation is considered as a coherent superposition of THz waves emitted from a linear-dipole array (LDA) along the filament. A good agreement has been obtained between the experimental observations and the predictions from the theoretical model.

A laser pulse of 40 fs pulse duration and 3.5 mJ energy at 800 nm was focused by a plano-convex lens of 30 cm focal length to form a filament in air. Before the laser pulse underwent filamentation [25,26], it was intercepted by a β-barium borate (β-BaB_2O_4) crystal of 0.4 mm thickness, leading to second harmonic (SH) generation as shown in Fig. 1(a). The initial phase difference ($\Delta\phi_0$) between the fundamental wave (FW) and its SH could be controlled by translating the BBO along the propagation axis of the laser.

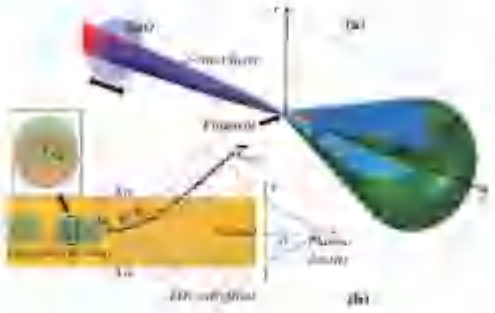

FIG. 1. (a) Schematic presentation of the experimental setup in a polar coordinate (z, θ), where the origin O corresponds to the geometric focus of the lens. The z axis corresponds to the propagation axis of the laser beam as well as the THz radiation. θ and r are used to describe the transverse propagation direction of the THz radiation. (b) Evolution of a THz wave front (red dashed curves) while a THz wave passes through different layers of a plasma channel. W_0, W_1, W_2, ... are typical points on the trace of a THz wave. The inset shows a dipole formed by charge separation inside a laser-plasma filament.

（41）Carrier-Envelope-Phase Characterization for an Isolated Attosecond Pulse by Angular Streaking, Physical Review Letters

PRL 116, 203601 (2016) PHYSICAL REVIEW LETTERS

Carrier-Envelope-Phase Characterization for an Isolated Attosecond Pulse by Angular Streaking

Fei-Lin He,[1] Cheng Ruiz,[1] and Feng He[1,*]
[1]Key Laboratory for Laser Plasmas (Ministry of Education) and Department of Physics and Astronomy, Collaborative Innovation Center of IFSA (CICIFSA), Shanghai Jiao Tong University, Shanghai 200240, China
[2]Departamento de Física de Partículas, Universidad de Santiago de Compostela, E-15782 Santiago de Compostela, Spain
(Received 26 August 2015; published 19 May 2016)

The carrier-envelope phase (CEP) is a crucial parameter for a few-cycle laser pulse since it substantially determines the laser waveform. Stepping forward from infrared to extreme ultraviolet (XUV) pulses, we propose a strategy to directly characterize the CEP of an isolated attosecond pulse (IAP) by numerically simulating the tunneling ionization of a hydrogen atom in a combined IAP and phase-stabilized few-cycle polarized IR laser pulse. The field modulations of the combined laser fields, due to the variation of the CEP of the IAP, are experimentally enlarged and the intrinsic time-dependent ionization probabilities of electrons with different momenta are angularly streaked at different directions. By measuring the resulting photoelectron momentum distributions, the CEP of the IAP can be retrieved. The characterization of the CEP of an IAP will open the possibility of exploring attosecond dynamics.

DOI:

The CEP of a few-cycle laser pulse determines the electric field, which in turn governs many strong field processes observed in ultrafast physics [1]. The availability of few-cycle CEP-stabilized IR laser pulses [2,3] opens the possibility of exploring the subcycle dynamics in atoms and molecules. Over the last few decades, a series of interesting phenomena have been explored using few-cycle CEP-locked IR pulses. For example, Lindner *et al.* controlled the electron ejection from an atom at one of two possible instants, producing a Young's double-slit type interference in the photoelectron energy spectra [4]. Kling *et al.* steered the electron movement in a subcycle time scale and controlled the path of molecular breakup [5]. Kubodera *et al.* generated supercontinuum high harmonics [6], which could be synthesized into an IAP [7]. The IAP provides accesses to unprecedented high time resolution and has pushed ultrafast science into attosecond time scales [1]. By combining an IAP and CEP-locked IR pulse, people have successfully observed many ultrafast processes with attosecond resolutions, such as Auger decay [8], direct measurement of a few-cycle light wave [9], time delay in photoionization [10], tunneling processes [11], charge directional steering [12–14], control of absorption line shapes [15], and many others.

The CEP of a few-cycle strong IR pulse has been characterized with several methods [16–20]. All these methods fundamentally depend on the tunneling ionization of atoms in strong laser fields. When the CEP of the IR laser pulse is varied, the symmetry of the laser waveform is modified. The slight and subcycle modification of the laser waveform is magnified into the photoelectron since the tunneling ionization is highly nonlinear. By diagnosing the asymmetric photoelectron energy spectra one may retrieve the CEP information [17] in a single shot. The tunneled electron may recollide with its parent ion and emit high harmonics, where the CEP information is also imprinted [21].

The successful characterization of the CEP of a few-cycle strong IR pulse motivates us to undertake the ambitious task of characterizing the CEP of an IAP. Compared to a few-cycle CEP-stabilized IR field, a few-cycle CEP-stabilized IAP will make it possible to access dynamics in the sub-fs/XUV period. Few-cycle IAPs have already been produced in many labs with different strategies [7,22–25]. Unfortunately, the concepts which work well for strong IR pulses cannot be directly applied to characterize the CEP of an IAP because the IAP in most labs is currently far too weak to initiate highly nonlinear processes. The characterization of attosecond pulses is normally performed using the reconstruction of attosecond beating by interference of two-photon transitions (RABBIT) [26] or frequency-resolved optical gating for complete reconstruction of attosecond burst (FROCRAB) [27] methods. Both methods are accurate but are limited to characterize the temporal envelope and the spectral phase of a pulse. The characterization of the CEP of an IAP is still a big challenge.

In this Letter, we propose to use the angular streaking technique to characterize the CEP of an IAP. Note that angular streaking cameras have been used to unveil several interesting phenomena [28–31]. In our strategy, the prototypical hydrogen atom is tunneling ionized by the

0031-9007/16/116(20)/203601(6)

（42）Extreme Mechanics of Probing the Ultimate Strength of Nanotwinned Diamond, Physical Review Letters

PRL 117, 116103 (2016) PHYSICAL REVIEW LETTERS

Extreme Mechanics of Probing the Ultimate Strength of Nanotwinned Diamond

Bing Li, Huiling Sun, and Changfeng Chen

Recently synthesized nanotwinned diamond (NTD) exhibits unprecedented Vickers hardness exceeding 200 GPa [Q. Huang *et al.*, Nature (London) **510**, 250 (2014)]. This extraordinary finding challenges the existing understanding of material deformation and stress response under extreme loading conditions. Here we unveil by first-principles calculations a novel indenter-determined pressure-confinement mechanism that suppresses the graphitization to bond collapse failure modes commonly known in strong covalent solids, leading to greatly enhanced peak stress and strain range in the tolerant diamond nanotwin. Moreover, the twin boundaries in NTD promote a strong stress concentration that drives preferential local rearrangements, producing a giant indentation strain softening. These results explain the experimental indentation strength of NTD and offer insights into the extreme mechanics of the intricate interplay of the indenter and nanotwin crystal in probing ultrahard materials.

(Received 2 June 2016; published 8 September 2016)

Searching for materials harder and more stable than diamond has been an endeavor quest driven by both practical needs and the fundamental desire to probe the ultimate limits of material strength. There have been extensive efforts exploring materials with different (ionic and/or covalent) chemical compositions that exhibit high hardness and superior thermal stability. Notable examples include carbon nitrides, boron nitrides, and transition metal borides [1–4], but these materials fall short of reaching, let alone exceeding, the strength and hardness of diamond. Another approach achieves strength enhancement in materials by controlling their microstructural size, known as the Hall-Petch effect [5,6], based on the idea that reducing grain (or twin-lamellae) size would suppress the nucleation and motion of dislocations by grain (or twin) boundaries. This approach has produced remarkable results in nanostructured metals [7] and strong covalent solids like boron nitride [8] and diamond [9], turning them harder than their bulk counterparts. As further reduced grain (twin) sizes, however, an opposite phenomenon, known as the inverse Hall-Petch effect [10,11], takes place when the weakly strain interactions at the grain (twin) boundaries dominate the plastic deformation process.

It was recently reported [12] that a nanotwinned diamond (NTD) structure exhibits unprecedented high Vickers indentation hardness exceeding 200 GPa, which is twice the commonly quoted hardness value of about 100 GPa for single-crystal cubic diamond. This result surpasses by a surprising large margin the hardness of all previously reported materials. More intriguing, this colossal hardness enhancement in NTD cannot be explained by the Hall-Petch effect since the typical twin boundary (TB) separation (~3–6 nm) in the synthesized NTD are well inside the inverse Hall-Petch region (below about 10 nm), where the TB interactions are expected to dominate. To elucidate the unexpected strengthening of NTD, it is essential to examine the structural and stress response to indentation loading.

In this work, we explore the extreme resistance of probing the ultimate strength of NTD. We employ first-principles calculations to examine the deformation and stress response of both the indenter and indented material under a variety of loading conditions. From calculated compressive stress-strain we set up a compressible Vickers indenter model to account for the large but finite normal stress beneath the indenter, which has been assumed to be unlimited (i.e., incompressible indenter) in past studies. This new indenter-deformation generated stress confinement prevents the graphitization or bond collapse failure modes commonly known for strong covalent solids, leading to greatly enhanced peak stress and strain range compared to those obtained from the incompressible indenter model. Moreover, we have identified a unique mechanism for bond rearrangement stemming from a TB-induced stress concentration, which produces a giant indentation strain softening in NTD. These results explain the unprecedented high strength and hardness of NTD and offer insights into the novel structural deformation and strengthening mechanisms to advance the fundamental understanding of material behaviors under extreme indentation loading conditions.

Stress-strain relations from first-principles calculations provide an accurate description of material deformation and strength [13–23], and the results can be directly compared to well-controlled nanoindentation measurements [24–26]. Under indentation, shear instability usually precedes the initiation of cracks and dislocations [27], initiating the onset of incipient plasticity [28,29] and bond collapse and

（43）Granular materials flow like complex fluids, Nature

LETTER

Granular materials flow like complex fluids

（44）Experimental studies of vibrational modes in a two-dimensional amorphous solid, Nature Communications

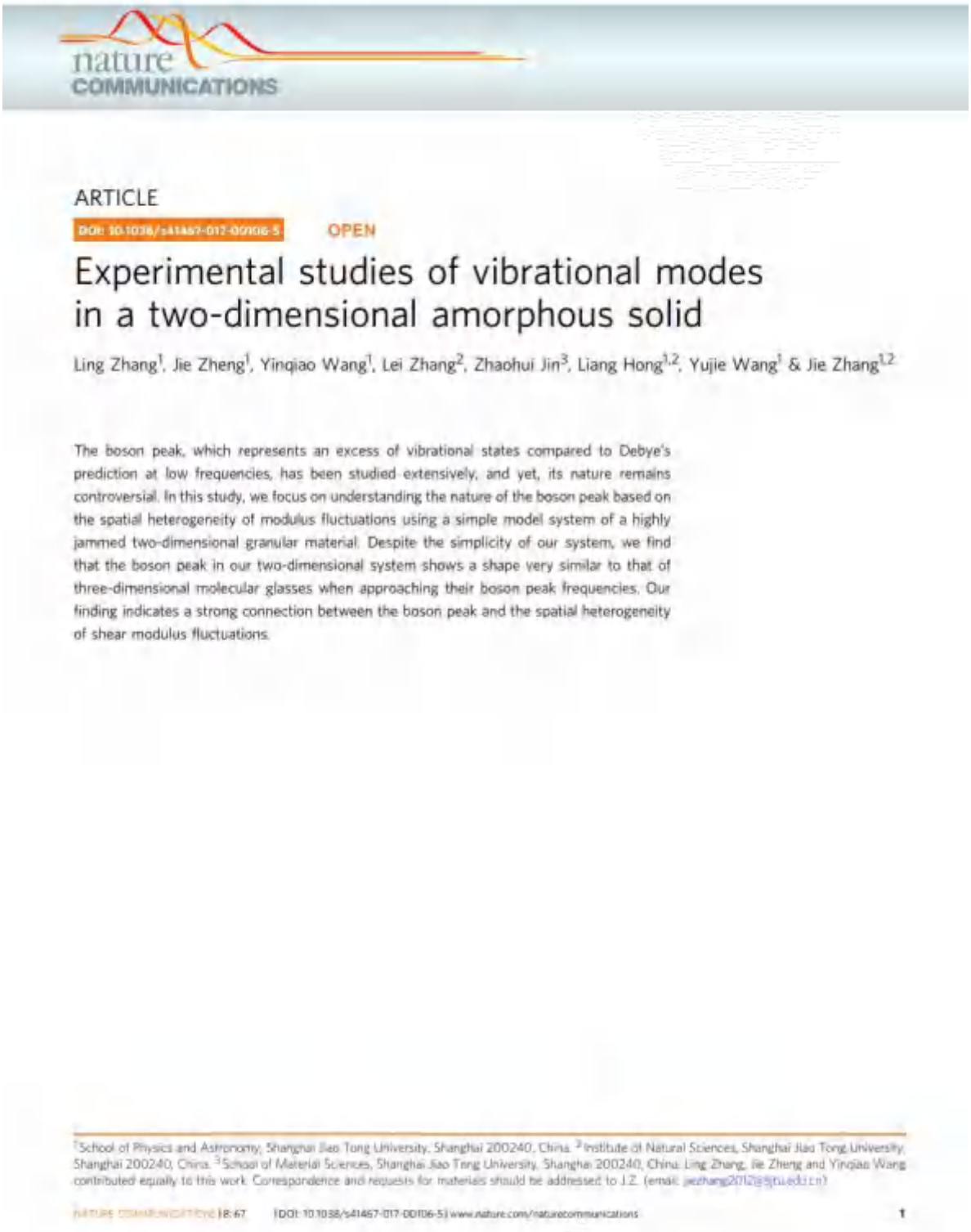

nature COMMUNICATIONS

ARTICLE

DOI: 10.1038/s41467-017-00106-5 OPEN

Experimental studies of vibrational modes in a two-dimensional amorphous solid

Ling Zhang[1], Jie Zheng[1], Yinqiao Wang[1], Lei Zhang[2], Zhaohui Jin[3], Liang Hong[1,2], Yujie Wang[1] & Jie Zhang[1,2]

The boson peak, which represents an excess of vibrational states compared to Debye's prediction at low frequencies, has been studied extensively, and yet, its nature remains controversial. In this study, we focus on understanding the nature of the boson peak based on the spatial heterogeneity of modulus fluctuations using a simple model system of a highly jammed two-dimensional granular material. Despite the simplicity of our system, we find that the boson peak in our two-dimensional system shows a shape very similar to that of three-dimensional molecular glasses when approaching their boson peak frequencies. Our finding indicates a strong connection between the boson peak and the spatial heterogeneity of shear modulus fluctuations.

[1] School of Physics and Astronomy, Shanghai Jiao Tong University, Shanghai 200240, China. [2] Institute of Natural Sciences, Shanghai Jiao Tong University, Shanghai 200240, China. [3] School of Material Sciences, Shanghai Jiao Tong University, Shanghai 200240, China. Ling Zhang, Jie Zheng and Yinqiao Wang contributed equally to this work. Correspondence and requests for materials should be addressed to J.Z. (email: jiezhang2012@sjtu.edu.cn)

（45）Origin of Noncubic Scaling Law in Disordered Granular Packing, Physical Review Letters

Origin of Noncubic Scaling Law in Disordered Granular Packing

（46）Dynamical Transition of Collective Motions in Dry Proteins, Physical Review Letters

Dynamical Transition of Collective Motions in Dry Proteins

Zhen Liu,[1] Juan Huang,[2] Madhusudan Tyagi,[3] Hugh O'Neill,[4] Qiu Zhang,[5] Eugene Mamontov,[3] Nitin Jain,[6] Yufei Wang,[1] Jie Zhang,[2,7] Jeremy C. Smith,[6,8] and Liang Hong[1,7,*]

[1]School of Physics and Astronomy, Shanghai Jiao Tong University, Shanghai 200240, China
[2]School of Life Sciences and Biotechnology, Shanghai Jiao Tong University, Shanghai 200240, China
[3]NIST Center for Neutron Research, National Institute of Standards and Technology (NIST), Gaithersburg, Maryland 20899, USA and Department of Materials Science and Engineering, University of Maryland, College Park, Maryland 20742, USA
[4]Biology and Soft Matter Division, Oak Ridge National Laboratory, Oak Ridge, Tennessee 37831, USA
[5]Spallation Neutron Source, Oak Ridge National Laboratory, Oak Ridge, Tennessee 37831, USA
[6]Department of Biochemistry and Cellular and Molecular Biology, University of Tennessee, Knoxville, Tennessee 37996, USA
[7]Institute of Natural Sciences, Shanghai Jiao Tong University, Shanghai 200240, China
[8]Center for Molecular Biophysics, Oak Ridge National Laboratory, Oak Ridge, Tennessee 37831, USA

(Received 28 December 2016; revised manuscript received 19 April 2017; published 25 July 2017)

Water is widely assumed to be essential for protein dynamics and function. To percolate the well-documented "dynamical" transition at ~200 K, at which the protein changes from a rigid, nonfunctional form to a flexible, functional state, as detected in hydrogenated proteins by incoherent neutron scattering, requires hydration. Here, we report on coherent neutron scattering experiments on perdeuterated proteins and reveal that a transition occurs in dry proteins at the same temperature, resulting primarily from the collective heavy-atom motions. The dynamical transition discovered is intrinsic to the energy landscape of dry proteins.

DOI: 10.1103/PhysRevLett.119.048101

Water is intimately involved in protein function [1–7]. In enzymes, for example, hydration enhances enzymatic rates, and noncatalytic water molecules can aid in transporting substrates and protons into the catalytic sites [1,8,9]. Numerous experiments have suggested that a minimum hydration level of $h = 0.2$ (g water/g protein) is required for enzymes to function [1,10–12]. Hydration may also enhance the internal motions required for the functional chemical steps [1,7,8,10]. Indeed, $h \sim 0.2$ has also been reported to be the minimum hydration level required for the widely studied dynamical transition in proteins at ~200 K, also named as the "glass" transition in analogy to the glass transition process in glass-forming systems, at which internal protein motions change from nonfunctional, glasslike, rigid, harmonic vibrations to incorporating liquidlike, flexible, anharmonic dynamics required for function [1,5,13–18]. A large body of experimental and simulation work has suggested that this transition is coupled to the activation of the translational motion of the hydration water on the protein surface [3,5,7,9,13,17–22]. However, the energy landscape of a globular protein is intrinsically complex and highly anharmonic, leading to the question as to whether the protein dynamical transition may be an intrinsic property of dry proteins.

Deuteration is key to the present observations. For simplicity, in what follows hydrogenated and perdeuterated samples are denoted using the prefixes of H and D. The neutron data collected on H proteins are mostly incoherent scattering signals (~90%, see Fig. S4(a) in the Supplemental Material [23]), resulting from self-correlations of the motions of hydrogen atoms. In contrast, the scattering from D proteins is primarily coherent (~90%, Fig. S1(b) in Ref. [24]), arising mainly from cross-correlations in motions between protein atoms [50–52], and is dominated by scattering signals from the heavy (non-H) atoms (~70%), especially those on the backbone (Fig. S1(c) in Ref. [25]).

Here, by performing neutron scattering and molecular dynamics (MD) simulation on lyophilized hydration level, $h \sim 0.02$, Fig. S2 in Ref. [25]) perdeuterated cytochrome P450 (CYP) and green fluorescent protein (GFP) (Figs. 1(a) and 1(b)), we show that the motions of heavy atoms in an essentially dry protein themselves present a dynamical transition at ~200 K.

On the high-flux backscattering spectrometer HFBS at NIST, we measured $S(q, \Delta t)$, the intensity of the elastic peak of the dynamic structure factor, which is an estimate of the average amplitude of the atomic motions up to the temporal resolution time of the instrument, Δt, which is ~1 ns [53]. Figure 1 presents the temperature dependence of $S(q, \Delta t)$ for both dry ($h \sim 0.02$) H and D samples. The presence of a downward change in gradient in the temperature dependence of $S(q, \Delta t)$ indicates that an anharmonic dynamic process is activated at the corresponding temperature [54]. Figures 1(c) and 1(d) show that both H-CYP and H-GFP present a kink at ~125 K. This transition has been observed several times previously in various hydrogenated

（47）Strong Field Theories beyond Dipole Approximations in Nonrelativistic Regimes, Physical Review Letters

PRL 118, 163203 (2017) PHYSICAL REVIEW LETTERS week ending 21 APRIL 2017

Strong Field Theories beyond Dipole Approximations in Nonrelativistic Regimes

Pei-Lun He, Di Lao, and Feng He*

Key Laboratory for Laser Plasmas (Ministry of Education) and School of Physics and Astronomy, Collaborative Innovation Center of IFSA (CICIFSA), Shanghai Jiao Tong University, Shanghai 200240, China

(Received 31 October 2016; revised manuscript received 9 February 2017; published 21 April 2017)

The exact nondipole Volkov solutions to the Schrödinger equation and Pauli equation are found, based on which a strong field theory beyond the dipole approximation is built for describing the nondipole effects in nonrelativistic electron dynamics. The theory is applied to investigate momentum partition laws for multiphoton and tunneling ionization and especially shows that the compact interplay of a laser field and Coulomb action may increase the expected photoelectron momentum along the laser propagation direction. The magnetic-spin coupling does not bring considerable effect on the photoelectron momentum distribution and can be neglected. Compared to the strong field approximation within the dipole approximation, this theory works in a much wider range of laser parameters and lays a solid foundation for describing nonrelativistic electron dynamics in both short wavelength and unconfined regimes where nondipole effects are unavoidable.

DOI: 10.1103/PhysRevLett.118.163203

Two kinds of processes are very fundamental in ultrafast laser-atom and laser-molecule interactions, i.e., the deposition of photon energies into atoms and molecules and the transfer of photon linear momentum into targets. Plenty of studies focused on the energy deposition and a series of intriguing ultrafast phenomena were explored, such as tunneling ionization [1], high harmonic generation and its synthesization of attosecond light pulses [2], nonsequential double ionization [3], coherent control of electron localization [4–7], and energy sharing between electrons and nuclei [8]. For the second one, the transfer of photon linear momentum attracts much less attention due to the fact that a photon is not an effective momentum courier as compared to a nonrelativistic electron.

Thanks to the detection techniques with high resolutions developed recently, Smeenk *et al.* [9] and Ludwig *et al.* [10] reported that photoelectrons acquire a momentum shift along the direction of laser propagation (termed as longitudinal momentum shift in the rest of the Letter) during tunneling ionization, and this photon momentum transfer is also reported in the time-dependent Dirac equation simulation [11], time-dependent Schrödinger equation (TDSE) simulations [12,13], and classical trajectory Monte Carlo calculations [14]. Some characters of the longitudinal momentum shift [15–20] were explored by calculations of strong field approximation (SFA). Though it is well recognized that the longitudinal momentum shift must be due to the nondipole laser-atom coupling, the exact nondipole Volkov solution was not built into these studies. To circumvent this obstacle, some attempts have been made. Chelkowski *et al.* adopted the Volkov solution of the Klein-Gordon equation in their SFA calculations [19]. Krajewska *et al.* made an analogy with quantum electrodynamics in obtaining the transition amplitude [21]. Cricchio and others rewrote the space-time dependent laser vector potential as $\mathbf{A}(\mathbf{x},t) \approx \mathbf{A}(t) + (z/c)\dot{\mathbf{E}}(t)$ [15,22–24]. Here, $\mathbf{A}(t)$ and $\mathbf{E}(t)$ are the dipole approximated laser vector potential and laser electric field, and c is the light speed. To build a self-consistent strong field theory beyond the dipole approximation is still difficult because there is no exact nondipole Volkov wave function to the Schrödinger equation until today, though the Volkov solution to the Schrödinger equation within the dipole approximation had been obtained around eighty years ago.

In the Letter, we analytically solved the TDSE for a free electron in a monochromatic laser field and achieved the exact nondipole Volkov solution. Based on this, we built the nondipole SFA theory, which is then applied to describing how the electron acquires the momentum along the laser propagation direction, and how rescattering alters the photon momentum partition between electrons and nuclei. For very wide ranges of laser parameters, this theory is self-consistent and is able to grasp the main dynamics and offer intuitive physical explanations with easy computations.

We used the light cone coordinate $\eta = t - (z/c)$ to describe the laser pulse by assuming it propagates along the z axis. The components of the laser vector potential are $\mathbf{A}(\mathbf{r},t) = \mathbf{A}(\eta) = (A_x(\eta), A_y(\eta), 0)$. The behavior of a free electron embedded in such a laser field is described by the TDSE in (atomic units used unless stated otherwise)

$$i\frac{\partial}{\partial t}\psi_V(\mathbf{r},t) = \frac{1}{2}[\mathbf{p}_\perp + \mathbf{A}_\perp(\eta)]^2 + p_z^2]\psi_V(\mathbf{r},t), \quad (1)$$

with $\mathbf{p}$ being the electron momentum operator. We postulated that the Volkov solution of Eq. (1) has the form

（48）Structural and topological nature of plasticity in sheared granular materials, Nature Communications

nature COMMUNICATIONS

ARTICLE

DOI: 10.1038/s41467-018-05329-8 OPEN

Structural and topological nature of plasticity in sheared granular materials

Yixin Cao[1], Jindong Li[1], Binquan Kou[1], Chengjie Xia[1], Zhifeng Li[1], Rongchang Chen[2], Honglan Xie[2], Tiqiao Xiao[2], Walter Kob[3], Liang Hong[1,4], Jie Zhang[1,4] & Yujie Wang[1,5,6]

Upon mechanical loading, granular materials yield and undergo plastic deformation. The nature of plastic deformation is essential for the development of the macroscopic constitutive models and the understanding of shear band formation. However, we still do not fully understand the microscopic nature of plastic deformation in disordered granular materials. Here we used synchrotron X-ray tomography technique to track the structural evolutions of three-dimensional granular materials under shear. We establish that highly distorted coplanar tetrahedra are the structural defects responsible for microscopic plasticity in disordered granular packings. The elementary plastic events occur through flip events which correspond to a neighbor switching process among these coplanar tetrahedra (or equivalently as the rotation motion of 4-ring disclinations). These events are discrete in space and possess specific orientations with the principal stress direction.

[1] School of Physics and Astronomy, Shanghai Jiao Tong University, 800 Dong Chuan Road, Shanghai 200240, China. [2] Shanghai Institute of Applied Physics, Chinese Academy of Sciences, Shanghai 201800, China. [3] Laboratoire Charles Coulomb, UMR 5521, University of Montpellier and CNRS, 34095 Montpellier, France. [4] Institute of Natural Sciences, Shanghai Jiao Tong University, Shanghai 200240, China. [5] Materials Genome Initiative Center, Shanghai Jiao Tong University, 800 Dong Chuan Road, Shanghai 200240, China. [6] Collaborative Innovation Center of Advanced Microstructures, Nanjing University, Nanjing 210093, China. Correspondence and requests for materials should be addressed to Y.W. (email: [redacted])

（49）Manipulation of polarizations for broadband terahertz waves emitted from laser plasma filaments, Nature Photonics

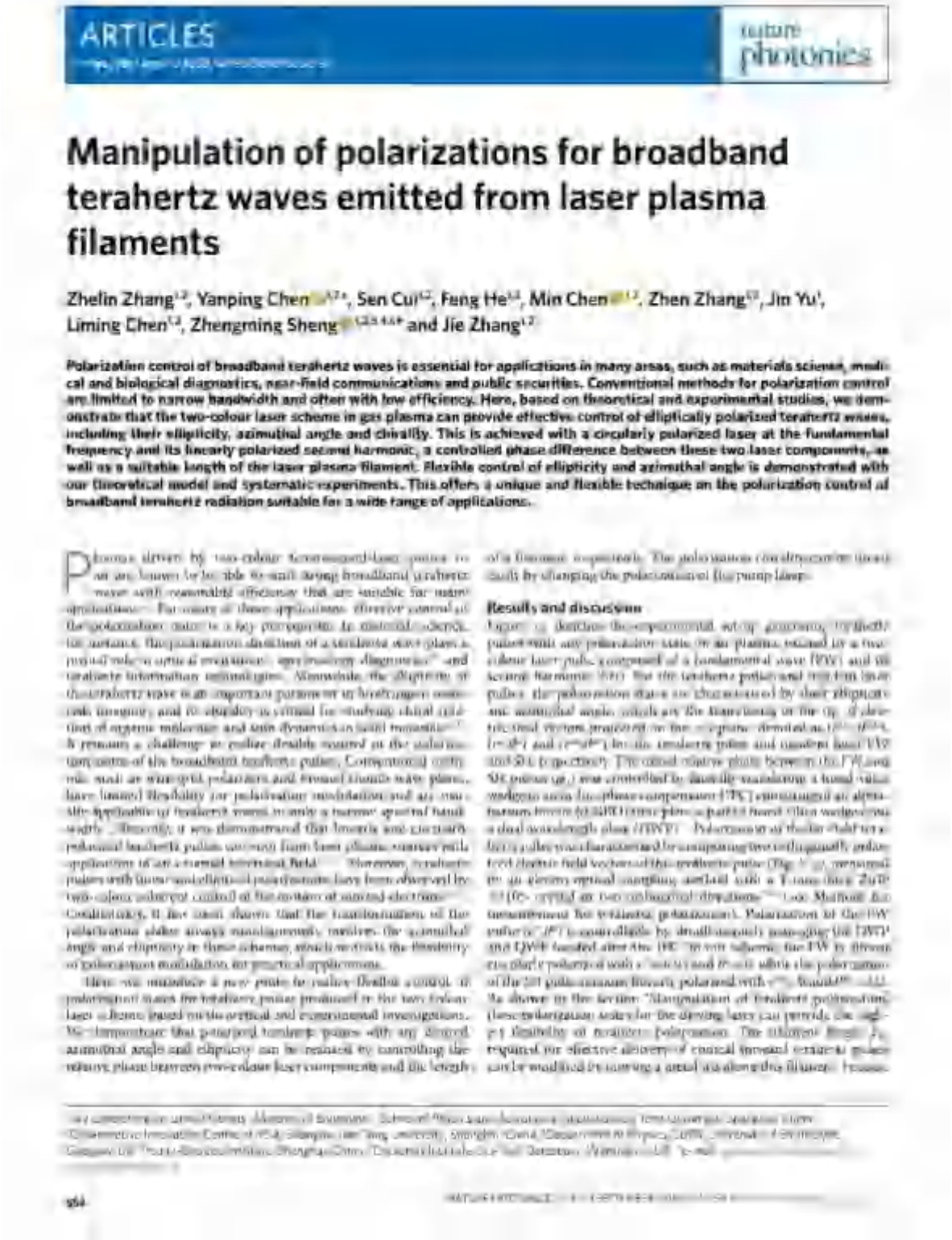

ARTICLES

nature photonics

Manipulation of polarizations for broadband terahertz waves emitted from laser plasma filaments

Zhelin Zhang[1,2], Yanping Chen[1,2,7]*, Sen Cui[1,2], Feng He[1,2], Min Chen[1,2], Zhen Zhang[1,2], Jin Yu[1], Liming Chen[1,2], Zhengming Sheng[1,2,3,4,5,6]* and Jie Zhang[1,2]

Polarization control of broadband terahertz waves is essential for applications in many areas, such as materials science, medical and biological diagnostics, near-field communications and public securities. Conventional methods for polarization control are limited to narrow bandwidth and often with low efficiency. Here, based on theoretical and experimental studies, we demonstrate that the two-colour laser scheme in gas plasma can provide effective control of elliptically polarized terahertz waves, including their ellipticity, azimuthal angle and chirality. This is achieved with a circularly polarized laser at the fundamental frequency and its linearly polarized second harmonic, a controlled phase difference between these two laser components, as well as a suitable length of the laser plasma filament. Flexible control of ellipticity and azimuthal angle is demonstrated with our theoretical model and systematic experiments. This offers a unique and flexible technique on the polarization control of broadband terahertz radiation suitable for a wide range of applications.

（50）Coulomb-Driven Relativistic Electron Beam Compression, Physical Review Letters

PHYSICAL REVIEW LETTERS 120, 044801 (2018)

Coulomb-Driven Relativistic Electron Beam Compression

Chao Lu,[1,2] Tao Tang,[1,2] Shengguang Liu,[1,2] Rui Wang,[1,2] Lingrong Zhao,[1,2] Pengfei Zhu,[1,2] Dao Xiang,[1,2,3,*] and Jie Zhang[1,2,†]

[1]Key Laboratory for Laser Plasmas (Ministry of Education), School of Physics and Astronomy, Shanghai Jiao Tong University, Shanghai 200240, China

[2]Collaborative Innovation Center of IFSA (CICIFSA), Shanghai Jiao Tong University, Shanghai 200240, China

[3]Tsung-Dao Lee Institute, Shanghai Jiao Tong University, Shanghai 200240, China

(Received 25 October 2017; published 25 January 2018)

Coulomb interaction between charged particles is a well-known phenomenon in many areas of research. In general, the Coulomb repulsion force broadens the pulse width of an electron bunch and limits the temporal resolution of many scientific facilities such as ultrafast electron diffraction and x-ray free-electron lasers. Here we demonstrate a scheme that actually makes use of the Coulomb force to compress a relativistic electron beam. Furthermore, we show that the Coulomb-driven bunch compression process does not introduce additional timing jitter, which is in sharp contrast to the conventional radio-frequency bunching technique. Our work not only leads to enhanced temporal resolution in electron-beam-based ultrafast instruments that may provide new opportunities in probing material systems far from equilibrium, but also opens a promising direction for advanced beam manipulation through self-field interactions.

DOI: 10.1103/PhysRevLett.120.044801

Ultrafast electron diffraction (UED) in which a fast-evolving process is excited by a pump laser and then probed by a delayed electron pulse has been widely used for watching atoms in motion during structural changes of which the characteristic time scale extends from a few femtoseconds to a few picoseconds [1,2]. With the advent of ultrashort lasers, the temporal resolution in UED applications now depends primarily on the pulse width and timing jitter of the electron beam. In x-ray free-electron lasers (FELs) [3–7], because the x rays are produced by sending a high-brightness relativistic electron beam through a series of magnetic undulators [8–10], the temporal resolution in laser-pump x-ray-probe experiments is also largely dependent on the electron beam pulse width and timing jitter. Therefore, one of the long-standing goals in both the FEL and UED communities is to generate a high-brightness electron beam with a short pulse width and small timing jitter.

According to Coulomb's law, the magnitude of the electric force is directly proportional to the charge and inversely proportional to the square of the distance. So when millions of electrons are produced with a femtosecond laser pulse through photoemission, they tend to repel each other. The Coulomb force, in general, accelerates the electrons in the front part of the bunch while it decelerates them in the back, leading to pulse broadening [11]. Fortunately, the elongated electron beam can be compressed with an radio-frequency (rf) buncher [12,13]. In this method, the electron beam is first sent through an rf buncher cavity, where the bunch head is decelerated to a lower energy while the bunch tail is accelerated to higher energy; after passing through a dispersive element (typically, a drift for keV and MeV electrons, or a magnetic chicane for ultrarelativistic electrons, e.g., [14]), the bunch tail may catch up with the bunch head, leading to bunch compression. While this method has been widely used in the UED and FEL community, it is also realized that the phase jitter in the rf cavity leads to considerable timing jitter, which limits the temporal resolution achievable [15,16]. The physics behind this effect is rather simple: e.g., in practical cases, the bunch centroid does not always pass through the cavity at a constant phase, and the variation of beam energy from this phase jitter is translated to the variation of the time of flight after passing through the dispersive element.

It should be noted that the Coulomb force is not always detrimental. The Coulomb force has been used before to suppress beam shot noise in an optical wavelength [17,18], as well as to enhance the electron beam density modulation at a terahertz wavelength [19,20]. In this Letter, we demonstrate a scheme that makes use of the Coulomb force to compress a relativistic electron beam without introducing additional timing jitter. The setup is shown in Fig. 1. The laser is first split into two pulses with a beam splitter (BS1) so that the energy, pulse width, transverse size, and timing of each pulse can be independently adjusted. The main pulse (containing of 96% of the energy) is used to produce the drive beam, and the remaining part is used to produce the target beam in the third (261.6 MHz) photocathode rf gun. After BS1, the main pulse is sent through four a barium borate birefringent crystals with the first one (7.5 mm thick) used to produce a double pulse separated by 6.4 ps and the remaining three of them

（51）Experimental Machine Learning of Quantum States, Physical Review Letters

Experimental Machine Learning of Quantum States

Jun Gao,[1,2] Lu-Feng Qiao,[1,2] Zhi-Qiang Jiao,[1,2] Yue-Chi Ma,[3,4] Cheng-Qiu Hu,[1,2] Ruo-Jing Ren,[1,2] An-Lin Yang,[1,2] Hao Tang,[1,2] Man-Hong Yung,[3,5,*] and Xian-Min Jin[1,2,†]

[1]State Key Laboratory of Advanced Optical Communication Systems and Networks, Department of Physics and Astronomy, Shanghai Jiao Tong University, Shanghai 200240, China
[2]Synergetic Innovation Center of Quantum Information and Quantum Physics, University of Science and Technology of China, Hefei, Anhui 230026, China
[3]Center for Quantum Information, Institute for Interdisciplinary Information Sciences, Tsinghua University, Beijing 100084, China
[4]Institute for Quantum Science and Engineering and Department of Physics, Southern University of Science and Technology, Shenzhen 518055, China
[5]Shenzhen Key Laboratory of Quantum Science and Engineering, Shenzhen 518055, China

(Received 26 January 2018; revised manuscript received 28 March 2018; published 11 June 2018)

Quantum information technologies provide promising applications in communication and computation, while machine learning has become a powerful technique for extracting meaningful structures in "big data." A crossover between quantum information and machine learning represents a new interdisciplinary area stimulating progress in both fields. Traditionally, a quantum state is characterized by quantum-state tomography, which is a resource-consuming process when scaled up. Here we experimentally demonstrate a machine-learning approach to construct a quantum-state classifier for identifying the separability of quantum states. We show that it is possible to experimentally train an artificial neural network to efficiently learn and classify quantum states, without the need of obtaining the full information of the states. We also show how adding a hidden layer of neurons to the neural network can significantly boost the performance of the state classifier. These results shed new light on how classification of quantum states can be achieved with limited resources, and represent a step towards machine-learning based applications in quantum information processing.

DOI: 10.1103/PhysRevLett.120.240501

Over the past few years, there has been a significant advancement in an emerging field of quantum machine learning [1,2], where quantum information meets the modern information-processing technologies. On one hand, various modern quantum technologies, such as quantum communication [3–5], quantum computation [6,7], and quantum metrology have been experimentally demonstrated by exploiting quantum entanglement as a resource [8,9]. On the other hand, machine learning, a modern technique for making predictions by mining information from "big data" [10], has been proven as one of the most successful achievements in artificial intelligence. Notable examples include self-driving cars and the famous AlphaGo, which surpasses the top human players at the game "Go" [11,12].

The key question in quantum machine learning is how to develop new ideas for applying technologies in machine learning to quantum information, or, vice versa, to gain advancements in both fields. In fact, several promising steps along both directions have already been taken in the community. In particular, machine learning can in principle exploit quantum superposition to enhance its performance. For example, quantum versions of the principal component analysis [13] and support vector machine [14] have been proposed. Other quantum algorithms along with their experimental implementations [15–19] have also been demonstrated in recent years to broaden the versatility of machine learning.

Additionally, machine learning can also be applied to certain quantum tasks, from classifying separability of quantum states [20,21] to classifying phases in condensed matter physics [22,23], and even the development of new classical algorithms for solving many-body systems [24]. These results suggest that machine learning of quantum states represents a new platform for solving problems in quantum information science.

Here we report an experimental machine learning of quantum states where an artificial neural network (ANN) is trained for classifying the separability of some quantum states, given that only *partial information* about the quantum states is available. More specifically, based on the experimental data, we have constructed a quantum-state classifier [20], which generalizes the pattern recognition in learning theory for quantum data. In the classical setting, a set $\{x_j, y_j\}$ of data x_j and label y_j are supplied as the training set for the machine-learning program, and the

（52）Frozen Condition of Quantum Coherence for Atoms on a Stationary Trajectory, Physical Review Letters

PHYSICAL REVIEW LETTERS 121, 073602 (2018)

Frozen Condition of Quantum Coherence for Atoms on a Stationary Trajectory

Jiawei Zhang,[1,*] Keye Zhang,[2,*] Lan Zhou,[3] and Weiping Zhang[2,†]
[1]School of Physics and Astronomy, Shanghai Jiao Tong University, Shanghai 200240, China
[2]Quantum Institute for Light and Atoms, School of Physics and Material Science, East China Normal University, Shanghai 200241, China
[3]Key Laboratory of Low-Dimensional Quantum Structures and Quantum Control of Ministry of Education, Department of Physics and Synergetic Innovation Center for Quantum Effects and Applications, Hunan Normal University, Changsha 410081, China
[4]Department of Physics and Astronomy, Shanghai Jiao Tong University, and Zhiyuan College, Shanghai Jiao Tong University, Shanghai 200240, China
[5]Collaborative Innovation Center of Extreme Optics, Shanxi University, Taiyuan 030006, China

(Received 23 September 2017; published 16 August 2018)

The quantum coherence (QC) of two comoving atoms on a stationary trajectory is investigated. We develop a formalism to characterize the properties of atoms on a stationary trajectory. We give a criterion under which QC is frozen to a nonzero value. The frozen condition that vanishing super- or subradiant decay rate is not so sensitive to the initial condition of state. We show that enhanced QC and a subradiant state can be gained from the initial state.

DOI: 10.1103/PhysRevLett.121.073602

Introduction.—QC as a consequence of the quantum state superposition principle is one of the key features that results in nonclassical phenomena. It is a powerful resource in quantum information theory as well as entanglement and discord type quantum correlation. Though it is important in fundamental physics, only recently have relevant experiments attempted to develop a rigorous framework to quantify QC for general states, such as the relative entropy of QC and the l_1 norm [1].

A long-standing and significant issue concerning QC is the decoherence induced by the inevitable interaction between the system and environment. In the past few years, several proposals have been suggested for fighting against the deterioration of QC, for instance, decoherence-free subspaces [2,3], quantum error correction codes [4], dynamical decoupling [5], or quantum Zeno dynamics [6,7]. Recently, the conditions of sustaining long-lived QC were investigated [8]. It was shown that QC can remain unchanged with time (freezing coherence) and the frozen condition (FC) for two qubits undergoing local identical bit-flip channels with Bell-diagonal initial states was only dependent on the initial condition of the states [9].

In a realistic physical system, atoms usually cannot be handled simply as noninteracting individual qubits when atomic spacing is small. Besides, for an ensemble of atoms, motion and temperature are also important factors which should be taken into account. Then, searching for a general FC for interacting atoms under normal conditions is necessary in practice.

In this Letter, we investigate the FC of QC for two identical two-level atoms on a stationary trajectory which has a characterization that the geodesic distance between two points on the trajectory depends only on the proper time interval [10,11]. Thus, for a stationary trajectory, field correlation function is invariance under translations in time. Besides, the stationary trajectory guarantees that the atoms have stationary states. The inertial atom in a Minkowski vacuum or thermal bath and a uniformly or circularly accelerated atom viewed by an instantaneous inertial observer are all stationary. We find that the QC for interacting atoms on a stationary trajectory can also be long lived; however, the FC is not so sensitive to the initial condition of the single excitation state but to the super- or subradiant decay rate of atoms. We develop a formalism to describe atoms on a stationary trajectory and give the general relationship between the quantum characterizing properties of atoms. Besides, we show that enhanced QC and the subradiant state can be obtained from the initial state.

Formulation.—We consider two identical two-level atoms moving on stationary trajectories $x_j(\tau) = (t(\tau), \vec{x}_j(\tau))$ in a fluctuating vacuum electromagnetic field, where $(t, \vec{x}_j)$ are the Minkowski coordinates of atom j referring to an inertial reference frame and τ denotes proper time of these two comoving atoms (see Fig. 1). The total Hamiltonian of the coupled system can be described by $H = H_f + H_A + H_I$. Here, H_A is the free Hamiltonian of atoms, and its explicit expression in the Schrödinger picture is $H_A = \sum_{j=1}^{2} \omega_j \sigma_j^+ \sigma_j^-$, where ω_j is the level spacing of the two-level atoms, $\sigma_j^+ = |e_j\rangle\langle g_j|$ and $\sigma_j^- = |g_j\rangle\langle e_j|$ are, respectively, the raising and lowering operators of the atom j. The free Hamiltonian H_f with respect to t takes the form $H_f = \sum_{\vec{k}} \omega_{\vec{k}} a_{\vec{k}\lambda}^\dagger a_{\vec{k}\lambda} [d(t)/dt]$ [12]. Here $a_{\vec{k}\lambda}^\dagger$, $a_{\vec{k}\lambda}$ are the creation and annihilation operators for a photon with momentum $\vec{k}$, frequency $\omega_{\vec{k}}$, and polarization λ. The Hamiltonian H_I that

（53）Gradual Crossover from Subdiffusion to Normal Diffusion: A Many-Body Effect in Protein Surface Water, Physical Review Letters

PHYSICAL REVIEW LETTERS 120, 248101 (2018)

Gradual Crossover from Subdiffusion to Normal Diffusion: A Many-Body Effect in Protein Surface Water

Pan Tan,[1,*] Yihui Liang,[2,*] Qin Xu,[1] Eugene Mamontov,[3] Jinglai Li,[4,5] Xiangjun Xing,[4,6,†] and Liang Hong[1,‡]
[1]School of Physics and Astronomy, Shanghai Jiao Tong University, Shanghai 200240, China
[2]Institute of Natural Sciences, Shanghai Jiao Tong University, Shanghai 200240, China
[3]Neutron Scattering Laboratory at Materials Physics Division and School of Life Sciences and Biotechnology, Shanghai Jiao Tong University, Shanghai 200240, China
[4]Spallation Neutron Source, Oak Ridge National Laboratory, Oak Ridge, Tennessee 37831, USA
[5]School of Mathematical Sciences, Shanghai Jiao Tong University, Shanghai 200240, China
[6]Shanghai Innovation Center of Advanced Microstructures, Nanjing 210000, China

(Received 24 November 2017; revised manuscript received 12 March 2018; published 11 June 2018)

Dynamics of hydration water is essential for the function of biomacromolecules. Previous studies have demonstrated that water molecules exhibit subdiffusion on the surface of biomacromolecules, yet the microscopic mechanism remains vague. Here, by performing neutron scattering, molecular dynamics simulations, and analytic modeling on hydrated perdeuterated protein powders, we found water molecules jump randomly between trapping sites on protein surfaces, whose waiting times obey a broad distribution, resulting in subdiffusion. Moreover, the subdiffusive exponent gradually increases with observation time towards normal diffusion due to a many-body volume-exclusion effect.

DOI: 10.1103/PhysRevLett.120.248101

Introduction.—Water is the solvent of life, playing a crucial role in determining the native structure, dynamics, and function of biological macromolecules [1–3]. The diffusive motions of water molecules not only aid the transportation of the function-required essential ingredients, e.g., protons, ions, and substrates across membranes and into the catalytic site of enzymes [4–6,7], but also render internal flexibility to the biomacromolecules. This flexibility is likely to be crucial for the biofunction, as it is absent when the biomacromolecules are dehydrated [1–3,8]. On the other hand, as an active solute, the biomacromolecule will significantly alter the structure and dynamics of the hydration water molecules surrounding it [9–13]. Both experiments and simulations showed that the diffusive motions of the hydration water on the surface of various biomacromolecules: DNA [10], RNA [14], proteins [11], and lipid membranes [12], are significantly retarded as compared to bulk water, and present an anomalous subdiffusion [11,12,15,16]. This subdiffusive motion is characterized by a fractional power-law dependence on time of the mean square atomic displacement (MSD), i.e., $\langle N^2(\Delta t)\rangle \sim t^{\beta}$ with $\beta < 1$ [11,12,15,16]. Two plausible physical pictures have been proposed to explain subdiffusion of hydration water [17–19]: spatial disorder, i.e., the rough surface of the biomacromolecules forms a fractal, percolated network to hinder the diffusion of water molecules, or temporal disorder, i.e., water molecules jump between traps on the surface of the biomacromolecules with a broad distribution of trapping times. Because of a lack of microscopic evidence, however, the precise physical mechanism remains largely unclear [17,19].

In this work, we studied the diffusive dynamics of surface water on hydrated perdeuterated green fluorescent protein (GFP) and cytochrome P450 (CYP) at physiological conditions by combining neutron scattering experiments with molecular dynamics (MD) simulations and analytic modeling. We showed that the dynamics of hydration water is subdiffusive and the subdiffusion exponent gradually increases with observation time. By analyzing the MD trajectories of individual water molecules, we directly observed the discrete trapping events of the water molecules on the protein surface and found that the associated trapping times obey a broad distribution, leading to the subdiffusion. Moreover, the deep trapping sites are mostly occupied, and thus water molecules prefer to jump among shallow traps, rendering a gradual increase of subdiffusive power law with the observation time. Finally, a lattice toy model, many-body continuous time random walk, is developed to provide a complete, quantitative description of all the relevant features of diffusive dynamics of the hydration water.

Results and discussions.—Neutron scattering directly probes the fluctuation of the nuclear position and is highly sensitive to hydrogen atoms. Hence, it is a powerful tool for studies of diffusion of water in a variety of environments, from porous silica to carbon nanotube or the surface of biomacromolecules [11,16,20,21]. Here, the neutron scattering experiments were performed at 280 K on both perdeuterated GFP and CYP [see Figs. 1(a) and 1(b)] at a hydration level of 0.4 g water/g protein, using the high-flux backscattering spectrometer (BASIS) at Oak Ridge National

（54）Mapping Twisted Light into and out of a Photonic Chip, Physical Review Letters

PHYSICAL REVIEW LETTERS 121, 233602 (2018)

Mapping Twisted Light into and out of a Photonic Chip

Yuan Chen,[1,2] Jun Gao,[1,2] Zhi-Qiang Jiao,[1,2] Ke Sun,[1] Wei-Guan Shen,[1,2] Lu-Feng Qiao,[1,2] Hao Tang,[1,2,3] Xiao-Feng Lin,[1,2] and Xian-Min Jin[1,2,3,4,*]
[1]State Key Laboratory of Advanced Optical Communication Systems and Networks, School of Physics and Astronomy, Shanghai Jiao Tong University, Shanghai 200240, China
[2]Institute for Quantum Science and Engineering and Department of Physics, Southern University of Science and Technology, Shenzhen 518055, China
[3]Synergetic Innovation Center of Quantum Information and Quantum Physics, University of Science and Technology of China, Hefei, Anhui 230026, China
[4]Institute of Natural Sciences, Shanghai Jiao Tong University, Shanghai 200240, China

(Received 4 May 2018; published 7 December 2018)

Twisted light carrying orbital angular momentum (OAM) provides an additional degree of freedom for modern optics and an emerging resource for both classical and quantum information technologies. Its inherently infinite dimensions can potentially be exploited by using mode multiplexing to enhance data capacity for sustaining the unprecedented growth in big data and internet traffic and can be encoded to build large-scale quantum computing machines in high-dimensional Hilbert space. While the emission of twisted light from the surface of integrated devices to free space has been widely investigated, the transmission and processing inside a photonic chip remain to be addressed. Here, we present the first laser-direct-written waveguide being capable of supporting OAM modes and experimentally demonstrate a faithful mapping of twisted light into and out of a photonic chip. The states OAM_0, OAM_{+1}, OAM_{-1}, and their superpositions can transmit through the photonic chip with a total efficiency up to 80% with minimal crosstalk. In addition, we present the transmission of quantum twisted light, state of single photons and measure the output states with single-photon imaging. Our results may add OAM as a new degree of freedom to be encoded and manipulated in a photonic chip for high-capacity communication and high-dimensional quantum information processing.

DOI: 10.1103/PhysRevLett.121.233602

The phase of an optical beam with a spatial degree of freedom of orbital angular momentum (OAM) is twisted like a corkscrew around its axis of travel and the cancellative of light waves at the axis itself results in a "doughnut" intensity profile. The twisted light has a helical wave front with an azimuthal phase term $e^{il\phi}$ [1], with which every photon can carry an OAM of $l\hbar$ [2], l is topological charge, ϕ is azimuthal angle, and $\hbar$ is the Planck constant h divided by 2π. Having the special features of mutually orthogonal inherently phase structure (spiral phase front), and dynamic characteristic (carrying OAM), the twisted light has been widely applied into the field of optical manipulation [2], optical trapping [3,4], and optical tweezers [5].

In recent years, OAM has shown great potential in communication systems for overcoming the channel capacity crunch [6,7]. The unlimited topological charges and the inherent orthogonality may provide tremendous resources for mode multiplexing. The inherently infinite dimensions can also potentially be exploited to deliver high-dimensional quantum states with larger alphabets and to build quantum computing machines in high-dimensional Hilbert space [8–12].

Large-scale applications of OAM beyond proof-of-principle demonstrations require developing integrated devices to enable the generation, transmission, and processing of such a new degree of freedom. Previous works have demonstrated on-chip generation twisted light with integrated star couplers [13], microring resonators [14], and unidirectional phase arrays [15]. While the emission of twisted light from the surface of integrated devices to free space has been widely investigated, the transmission and processing inside a photonic chip remain to be solved.

In this Letter, we demonstrate a faithful mapping of twisted light into and out of a photonic chip by prototyping doughnut waveguides with femtosecond laser direct writing [16,17]. We couple the states OAM_0, OAM_{+1}, OAM_{-1}, and their superpositions into and out of the photonic chip with overall efficiency up to 80% and verify the output states by interfering with the Gaussian reference beam and making projection measurements, which clearly demonstrate that the output state basically keeps the OAM of the input state. In addition, we present the transmission of single-photon quantum twisted light and measure the output states with single-photon imaging.

（55）Multistage Coupling of Laser-Wakefield Accelerators with Curved Plasma Channels, Physical Review Letters

Multistage Coupling of Laser-Wakefield Accelerators with Curved Plasma Channels

J. Luo,[1] M. Chen,[1,*] W. Y. Wu,[1] S. M. Weng,[1,†] Z. M. Sheng,[2,3,‡] C. B. Schroeder,[4] D. A. Jaroszynski,[5] J. Easter,[6] W. P. Leemans,[7] W. B. Mori,[8] and J. Zhang[1,†]

[1]Key Laboratory for Laser Plasmas (MOE), School of Physics and Astronomy, Shanghai Jiao Tong University, Shanghai 200240, China
[2]SUPA, Department of Physics, University of Strathclyde, Glasgow G4 0NG, United Kingdom
[3]Tsinghua University, Beijing 100084, China
[4]Lawrence Berkeley National Laboratory, Berkeley, California 94720, USA
[5]University of California, Los Angeles, California 90095, USA
[6]Tsung-Dao Lee Institute, Shanghai Jiao Tong University, Shanghai 200240, China
[7]Cockcroft Institute, Sci-Tech Daresbury, Cheshire WA4 4AD, United Kingdom
[8]Collaborative Innovation Center of IFSA (CICIFSA), Shanghai Jiao Tong University, Shanghai 200240, China

(Received 5 November 2017; published 10 April 2018)

Multistage coupling of laser wakefield accelerators is essential to overcome laser energy depletion for high-energy applications, such as TeV-level electron-positron colliders. Current staging schemes have subsequent laser pulses into stages using plasma mirrors while controlling electron beam focusing with plasma lenses. Here a more compact and efficient scheme is proposed to realize the simultaneous coupling of the electron beam and the laser pulse into a second stage. A partly curved channel, integrating a straight acceleration stage with a curved transition segment, is used to guide a fresh laser pulse into a subsequent straight channel, while the electron continue straight. This scheme benefits from a shorter coupling distance and continuous guiding of the electrons in plasma while suppressing transverse beam dispersion. Particle-in-cell simulations demonstrate that the electron beam from a previous stage can be efficiently injected into a subsequent stage for further acceleration while maintaining high capture efficiency, stability, and beam quality.

DOI: 10.1103/PhysRevLett.120.154801

Laser-wakefield accelerators (LWFAs) have recently attracted considerable attention as a promising new accelerator technology [1–4]. They are capable of supporting extremely high acceleration gradients, as high as hundreds of GeV/m. This makes it possible to build compact accelerators in university-scale laboratories for many applications, such as compact electron diffraction devices [5], high-energy particle accelerators [6–9], and tabletop radiation sources [10–13].

Among the many applications, perhaps the most interesting and challenging application is a LWFA-based TeV-level electron-positron linear collider [14,15]. However, the energy gained by electrons in a single-stage LWFA is limited by several effects, including electron dephasing, laser diffraction, and laser energy depletion. Although a few schemes have been proposed to increase the single-stage energy gain by mitigating dephasing and diffraction, a single-stage LWFA is still limited by pump depletion. Currently, single-stage acceleration up to 10 GeV energy is thought to be a reasonable value, given present laser technology and plasma density scaling, and a worldwide effort is pursuing this goal [9,16–21]. For future TeV colliders, the multistage coupling of LWFAs is inevitable. Electron beams accelerated in a first stage should be injected into a second wakefield stage that is driven by a fresh laser pulse. Because of the micrometer-size electron beams and wake structures, the synchronization precision at the femtosecond scale, and the limited coupling distance, multistage coupling is considered to be very challenging. Recently, staged acceleration has been demonstrated by Steinke *et al.* [22]. By using a plasma mirror [23] to reflect a fresh laser pulse and a plasma lens [24] to refocus electrons, about 3.5% of the electron beam charge was coupled into a second stage, which produced 100 MeV energy gain. In this staging scheme, the dedicated plasma mirror and the lens had to be installed between the LWFA stages. Besides its complexity, the matching of the electron beam between stages is still very challenging, particularly in achieving efficient coupling. The coupling efficiency must be near 100%, if one considers the requirements for up to a hundred stages. Thus, a simple and efficient multistage coupling scheme is highly desirable.

Besides plasma mirrors, including plasma channels may be considered to guide lasers [25–28]. Reitsma [26] theoretically studied laser propagation in curved plasma channels and found an equilibrium laser centroid trajectory. Chen [27] and Palastro [28] discussed applications of synchrotron radiation based on curved plasma channels, and one patent was published on compact undulators and a radiation source based on curved channels [29]. In this

（56）Translational and Rotational Dynamical Heterogeneities in Granular Systems, Physical Review Letters

Translational and Rotational Dynamical Heterogeneities in Granular Systems

Binquan Kou,[1] Yitao Cao,[1] Jindong Li,[1] Chengjie Xia,[1] Zhifeng Li,[1] Haiyang Dong,[2] Anyang Zhang,[3] Jie Zhang,[1,*] Walter Kob,[4,†] and Yujie Wang[1,5,‡]

[1]School of Physics and Astronomy, Shanghai Jiao Tong University, 800 Dong Chuan Road, Shanghai 200240, China
[2]Department of Radiology, Ruijin Hospital, Shanghai Jiao Tong University School of Medicine, Shanghai 200025, China
[3]Institute of Natural Sciences, Shanghai Jiao Tong University, Shanghai 200240, China
[4]Laboratoire Charles Coulomb, University of Montpellier and CNRS, Montpellier 34095, France
[5]Materials Genome Initiative Center, Shanghai Jiao Tong University, 800 Dong Chuan Road, Shanghai 200240, China
[6]Collaborative Innovation Center of Advanced Microstructures, Nanjing University, Nanjing 210093, China

(Received 6 March 2018; published 6 July 2018)

We use x-ray tomography to investigate the translational and rotational dynamical heterogeneities in a three-dimensional bead-packing granular packing driven by oscillatory shear. We find that particles which translate quickly form clusters with a size distribution given by a power law with an exponent that is independent of the strain amplitude. Identical behavior is found for particles that are translationally slowly, rotating quickly, or rotating slowly. The geometrical properties of these four different types of clusters are the same as those of random clusters. Different cluster types are considerably correlated or anticorrelated, indicating a significant coupling between translational and rotational degrees of freedom. Surprisingly, these clusters are formed already at time scales that are much shorter than the α-relaxation time, in stark contrast to the behavior found in glass-forming systems.

DOI: 10.1103/PhysRevLett.121.018002

The relaxation dynamics of most disordered materials, such as glass-forming liquids, polymers, foams, and granular materials, differs significantly from the Debye behavior found in simple liquids in that it shows a marked non-exponential time dependence [1,2]. Although several mechanisms can give rise to this type of time dependence, it is often the local disorder of the particle arrangement that is the origin for this behavior [3–5], i.e., each particle has a different local environment, and as a result the relaxation dynamics depends strongly on the particle considered. Previous studies have shown that the slowly (or quickly) relaxing particles are not distributed uniformly in space but instead form clusters. This effect, named "dynamical heterogeneity" (DH) is believed to be a key ingredient to understanding the α-process of glass-forming systems and hence the phenomenon of the glass transition. As a consequence, many studies have been carried out to study the nature of the DHs [3–12].

Usually DH are associated with the translational degrees of freedom (TDOF) of the particles. The particles in molecular systems and granular materials have, however, also rotational degrees of freedom (RDOF). Since these are coupled with the TDOF in a system that they will be important for the relaxation dynamics of the system as well [13–17]. However, in practice it is difficult to probe the RDOF in molecular systems since experiments do not allow us to track directly the orientation of individual particles. As a consequence, only indirect experimental probing of the RDOF has been possible so far [7,13] and most of our current knowledge of them comes from computer simulations [18–20]. (Plastic crystals are an exception since they have no disorder in the TDOF [21].) The situation is not much better for the case of granular materials since these are usually opaque and hence it is very challenging to probe in three dimensions (3D) the displacement and reorientation of the particles [22–28]. Because of the non-spherical shape of the particles and the presence of friction, there is often a strong coupling between the TDOF and RDOF, making the experimental study of the DH for both TDOF and RDOF indispensable for understanding of the relaxation dynamics [29]. In the present work we thus use x-ray tomography to investigate these DH in a *three dimensional* granular packing driven by oscillatory shear, making it, to the best of our knowledge, the first experimental investigation to probe the DH of the TDOF *as well as* the ones for the RDOF.

Our system consists of 4100 hard prolate ellipsoids made of polyvinyl chloride with an aspect ratio of 1.5 (polydispersity 0.9%), i.e., a shape that makes the crystallization of the system difficult [30] and allows for a rather strong F-R coupling. The dimension of the minor axis of the particles is $2b = 12.7$ mm, and in the following we will use b as the unit of length. The particles are in a rectangular box of dimension $40.2b \times 45.6 \times 22.6b$ that can be sheared in the y direction. More details of the setup are given in [31]. We drive the system to a steady state by cycling it many times at all strain amplitude γ investigated ($\gamma = 0.26, 0.38, 0.48$, and 0.87; see Supplemental Material [32] for details)

（57）Broadband THz to NIR up-converter for photon type THz imaging, Nature Communications

ARTICLE

OPEN

Broadband THz to NIR up-converter for photon-type THz imaging

Peng Bai[1,2], Yueheng Zhang[1,2], Tianmeng Wang[1,3], Zhanglong Fu[4], Dixiang Shao[4], Ziping Li[4], Wenjian Wan[4], Hua Li[4], Juncheng Cao[4], Xuguang Guo[5] & Wenzhong Shen[1,2]

High performance terahertz imaging devices have drawn wide attention due to their significant application in healthcare, security of food and medicine, and nondestructive inspection, as well as national security applications. Here we demonstrate a broadband terahertz photon-type up-conversion imaging device, operating around the liquid helium temperature, based on the gallium arsenide homojunction interfacial workfunction internal photoemission (HIWIP)-detector-LED up-converter and silicon CCD. Such an imaging device achieves broadband response in 4.2–20 THz and can absorb the normal incident light. The peak responsivity is 0.5 AW^{-1}. The light emitting diode leads to a 72.5% external quantum efficiency improvement compared with the one widely used in conventional up-conversion devices. A peak up-conversion efficiency of 1.14×10^{-2} is realized and the optimal noise equivalent power is 29.1 $pWHz^{-1/2}$. The up-conversion imaging for a 1000 K blackbody pinhole is demonstrated. This work provides a different imaging scheme in the terahertz band.

[1] Key Laboratory of Artificial Structures and Quantum Control (School of Physics and Astronomy, Shanghai Jiao Tong University, 200240 Shanghai, China. [2] Collaborative Innovation Center of Advanced Microstructures, 210093 Nanjing, China. [3] Department of Chemical and Biological Engineering, Rensselaer Polytechnic Institute, Troy, NY 12180, USA. [4] Key Laboratory of Terahertz Solid-State Technology, Shanghai Institute of Microsystem and Information Technology, Chinese Academy of Sciences, 200050 Shanghai, China. [5] School of Optical-Electrical and Computer Engineering, University of Shanghai for Science and Technology, 200093 Shanghai, China. Correspondence and requests for materials should be addressed to Y.H.Z. (email: wshen@sjtu.edu.cn)

（58）Direct Observation of Topology from Single-Photon Dynamics, Physical Review Letters

Direct Observation of Topology from Single-Photon Dynamics

Yao Wang,[1,2] Yong-Heng Lu,[1,3] Feng Mei,[4,2,*] Jun Gao,[1,2] Zhan-Ming Li,[1,4] Hao Tang,[1,2] Shi-Liang Zhu,[5,2] Suotang Jia,[4,2] and Xian-Min Jin[1,2,†]

[1]School of Physics and Astronomy, Shanghai Jiao Tong University, Shanghai 200240, China
[2]Institute for Quantum Science and Engineering and Department of Physics, Southern University of Science and Technology, Shenzhen 518055, China
[3]Synergetic Innovation Center of Quantum Information and Quantum Physics, University of Science and Technology of China, Hefei, Anhui 230026, China
[4]State Key Laboratory of Quantum Optics and Quantum Optics Devices, Institute of Laser Spectroscopy, Shanxi University, Taiyuan, Shanxi 030006, China
[5]Collaborative Innovation Center of Extreme Optics, Shanxi University, Taiyuan, Shanxi 030006, China
[6]National Laboratory of Solid State Microstructures and School of Physics, Nanjing University, Nanjing 210093, China

(Received 11 December 2018; published 16 May 2019)

Topology manifesting in many branches of physics deepens our understanding on state of matter. Topological photonics has recently become a rapidly growing field since artificial photonic structures can be well designed and constructed to support topological states, especially a promising large-scale implementation of these states using photonic chips. Meanwhile, due to the inapplicability of Hall conductance to photons, it is still an elusive problem to directly measure the integer topological invariants and topological phase transitions in photonic system. Here, we present a direct observation of topological winding numbers by using bulk-state photon dynamics on a chip. Furthermore, we for the first time experimentally observe the topological phase transition points via single-photon dynamics. The integrated topological invariants, direct measurement in the single-photon regime and strong robustness against disorder add the key elements into the toolbox of "quantum topological photonics" and may enable topologically protected quantum information processing in large scale.

DOI: 10.1103/PhysRevLett.122.193903

The introduction of topology into condensed-matter and material sciences originates from the connection of integer quantum Hall conductances with topological Chern invariants [1], which greatly expands our knowledge on state of matters. With the birth of topological insulators, searching topological state of matters in solid state materials [2,3] and photonic systems [4,5] has recently become a leading research field. In contrast to the challenging experimental requirements for realizing topological states in solid state materials, photonic systems provide a convenient and versatile platform to design various topological lattice models and study different topological states including topological insulator states [6–10] and topological Weyl points [11,12]. The found topological edge states and phase transition potentially can be utilized for developing inherently robust and efficient artificial photonic devices [13–20].

Although photonic topological edge states have been extensively studied, the photonic topological invariant defined on the bulk states, which is the essential observable for characterizing topological states, is still less explored. In fermion systems, the topological invariant can be revealed by conductance measurements, while the concept of Hall conductance is inapplicable in photonic systems. Several methods recently have been proposed for indirectly detecting topological invariants, based on probing Berry curvature [21,22], non-Hermitian photon loss [23,24], bulk-edge correspondence [25,26], and phase spectroscopy [27]. Nevertheless, direct measuring photonic topological invariants remains elusive.

Waveguide lattice provides a natural platform for studying photon dynamics. The reason is that the propagation of photons in a photonic waveguide lattice is naturally equivalent to a time evolution. However, direct measuring topological invariants based on photon dynamics has never been reported before in topological waveguide lattices. Here, for the first time, we experimentally demonstrate that both the topological invariants and the topological phase transitions can be directly measured based on the propagation of photons in the bulk of a topological waveguide lattice. Our work generalizes the method proposed in linear optics–based quantum walks [28,29] to the continuous-time dynamics to directly measure topology. This dynamical method is very *generic* for observing topology, which recently also has been experimentally demonstrated in ultracold atoms [30].

To extend protected topological protection into the quantum regime, we have to find an appropriate system that is physically scalable and has inherently low loss when

（59）Parity-Induced Thermalization Gap in Disordered Ring Lattices, Physical Review Letters

Parity-Induced Thermalization Gap in Disordered Ring Lattices

Yao Wang,[1,2] Jun Gao,[1,2,*] Xiao-Ling Pang,[1,3] Zhi-Qiang Jiao,[1] Hao Tang,[1,2] Yuan Chen,[1,2] Lu-Feng Qiao,[1] Zhen-Wei Gao,[1,2] Jian-Peng Dou,[1,2] Ai-Lin Yang,[2,3] and Xiao-Min Jin[1,2,†]
[1]School of Physics and Astronomy, Shanghai Jiao Tong University, Shanghai 200240, China
[2]Institute for Quantum Science and Engineering and Department of Physics, Southern University of Science and Technology, Shenzhen 518055, China
[3]Synergetic Innovation Center of Quantum Information and Quantum Physics, University of Science and Technology of China, Hefei, Anhui 230026, China
[4]Institute of Natural Sciences, Shanghai Jiao Tong University, Shanghai 200240, China

(Received 17 May 2018; published 8 January 2019)

The gaps separating two different states widely exist in various physical systems: from the electrons in periodic lattices to the analogs in photonic, phononic, plasmonic systems, and even quasicrystals. Recently, a thermalization gap, an inaccessible range of photon statistics, was reported for light in disordered structures [Nat. Phys. 11, 930 (2015)], which is universally induced by the disorder-immune chiral symmetry and can be reflected by the photon statistics. The lattice topology was further identified as a decisive role in determining the photon statistics when the chiral symmetry is satisfied. Being very distinct from one-dimensional lattices, the photon statistics in ring lattices are dictated by its parity, i.e., odd or even sited. Here, we for the first time experimentally observe a parity-induced thermalization gap in strongly disordered ring photonic structures. In a limited scale, though the light tends to be localized, we are still able to find clear evidence of the parity-dependent disorder-immune chiral symmetry and the resulting thermalization gap by measuring photon statistics, while strong disorder-induced Anderson localization overwhelms such a phenomenon in larger-scale structures. Our results shed new light on the relation among symmetry, disorder, and localization, and may inspire new resources and artificial devices for information processing and quantum control on a photonic chip.

DOI: 10.1103/PhysRevLett.122.013903

Symmetry is crucial for establishing energy gaps for electrons in lattices and analogs [1–5]. Disorder often decreases such effects [1], but not for all cases. Certain disorder-immune chiral symmetries [6–9] would emerge in random matrix theory [10], such as chiral [8] and particle-hole symmetric ensembles [11], and play a key role in fields ranging from superconductivity [12] to quantum chromodynamics [13]. A distinctive characteristic of disorder-immune chiral symmetry is that the system Hamiltonian can be transformed into a block off-diagonal matrix form, a separate bipartite sublattice [10,14,15], and is disorder-immune behaving as holding for each realization from a disordered ensemble [16].

The tight-binding lattices have been suggested to study disorder-immune chiral symmetry [16]. The resulting thermalization gap, not by parity, is unambiguously confirmed in one-dimensional disordered lattices [17,18]. Inspired by the works on photonic thermalization gap [16] and the effect of lattice topology [19], we investigate the scenario of parity-dependent disorder-immune chiral symmetry in ring lattices: chiral symmetry for even-sited ring lattices, and chiral-symmetry breaking for odd-sited ones. The resulting thermalization gap can be revealed by observing the photon statistics in even-parity disordered ring lattices.

In this Letter, we demonstrate experimental observation of the parity-induced thermalization (PIT) gap on a photonic chip. By using femtosecond laser direct writing, we are able to freely prototype waveguides as sites of lattices and introduce disorder by precise coupling control in three dimensions. We measure the evolved light distribution out of 120 lattices with randomly picked coupling parameters in a fixed disorder level to obtain photon statistics. We observe a thermalization gap in an even-parity disordered ring lattice where the cross-correlation cannot go below a certain limit due to disorder-immune symmetries. As a way to demonstrate such a parity-induced thermalization gap, we observe that the cross-correlation in even-sited lattices is significantly larger than the one in odd-sited lattices. This work may deepen the understanding of the relation among symmetry, disorder, and localization, and inspire applications for quantum integrated photonics.

The dynamics of light in photonic lattices can be described by a set of coupled discrete Schrödinger equations [20], which are derived from the Schrödinger-type paraxial

（60）Superhigh-Resolution Recognition of Optical Vortex Modes Assisted by a Deep-Learning Method, Physical Review Letters

PHYSICAL REVIEW LETTERS 123, 183902 (2019)

Superhigh-Resolution Recognition of Optical Vortex Modes Assisted by a Deep-Learning Method

Zhaowei Liu, Shitao Yan, Hongeng Liu, and Xianfeng Chen*
State Key Laboratory of Advanced Optical Communication Systems and Networks, School of Physics and Astronomy, Shanghai Jiao Tong University, Shanghai 200240, China

(Received 27 June 2019; published 29 October 2019)

Orbital angular momentum (OAM) has demonstrated great success in the optical communication field, which theoretically allows an infinite increase of the transmitted capacity. The availability of a receiver to precisely recognize OAM modes is crucial to expand the communication capacity. Here, we propose a deep-learning (DL) method to precisely recognize OAM modes with fractional topological charges. The minimum interval step gauged between adjacent modes decreases to 0.01, which as far as we know is the first time the superhigh resolution has been realized. To exhibit its efficiency in the optical communication process, we transfer an illustrious portrait by a superhigh-resolution OAM multiplexing system. As the convolutional neuron networks can be trained by data up to an infinitely large volume in theory, this work exhibits a huge potential of generalized suitability for next generation DL-based ultralow OAM optical communications, which might even be applied to microwave, millimeter wave, and terahertz OAM communication systems.

DOI: 10.1103/PhysRevLett.123.183902

Vortex beams carrying orbital angular momentum (OAM) have been extensively investigated in optical manipulation [1], imaging [2], interaction between light and matter [3,4], and optical communication [5] since it was recognized in 1992 [6]. The helical wave front of such a vortex beam is described by a phase factor $\exp(il\phi)$, where ϕ is the azimuthal angle and the topological charge l is an unlimited integer or fractional value. Owing to the unbounded dimensional space, it provides high degrees of freedom for multiplexing information, which infinitely boosts the transmitted capacity in optical communication processes [7,8].

Because of its significant application, the generation of OAM states has aroused tremendous enthusiasm ranging from spiral phase plate [9], q plate [10–13], and metasurface [14] to integrated devices [15]. One of the most accomplished types of technology is to use spatial light modulator (SLM) uploading spiral holograms [16], which can simply create vortex beams and flexibly manipulate the phase information of light. Besides, the recognizable ability of the receiver is also crucial for both OAM shift keying (OAM-SK) [15] and OAM division multiplexing (OAM-DM) [16] in terms of OAM-based optical communication. Therefore, much work has been conducted focusing on efficiently developing an OAM sorter recently. Some techniques utilize traditional optics theories that transform the azimuthal position into transverse position [17] based on interferometers [18–20] and vortex diffractive gratings [21]. One currently efficient sorting method is to implement coordinate transformation that separates states with different topological charges by a distinct focal spot on the detect plane [22,23]. And a computational method to measure the transmission matrix (TM) provides an anti-interference approach to retrieve the propagation of vortex beams [24]. In addition, the OAM to-polarization coupling effect is also proposed to sort different OAM states of light [25]. All those methods pave the way for effective OAM-based optical communication.

However, owing to the limitation of the resolution, only eigenmodes where topological charges are integers are considered in all methods mentioned above. With the increase of an integer topological charge value, the growing phase singularity and the diffraction effect enormously affects the intensity distributions of vortex beams, which extremely adds the difficulties of being focused in free-space and being coupled in fibers. This problem limits the development of the OAM-based optical communication. Consequently, it is of fundamental importance to expand communication capacity adequately with more OAM states but smaller phase singularity.

Our goal here is to develop a superhigh-resolution technique to precisely separate modes into subdivisible space between adjacent eigenmodes. That is, the minimum interval Δl among recognized modes is a fractional value and can be as small as possible. The pioneering techniques of generating fractional OAM modes were proposed in 2004 [26,27]. However, the tiny variety of fractional OAM modes is further complicated to be discriminated compared to that of integer changes [28–30]. Recently, the deep learning (DL) method has been developed to possess the ability of extracting intrinsic features and dividing decision boundary according to data [31]. The original assignment

（61）Coupling of Edge States and Topological Bragg Solitons, Physical Review Letters

Coupling of Edge States and Topological Bragg Solitons

Weidong Zhang,[1] Xiaoteng Chen,[1] Yaroslav V. Kartashov,[2] Vladimir V. Konotop,[3] and Fangwei Ye[1]
[1]State Key Laboratory of Advanced Optical Communication Systems and Networks, School of Physics and Astronomy, Shanghai Jiao Tong University, Shanghai 200240, China
[2]Institute of Spectroscopy, Russian Academy of Sciences, Troitsk, Moscow Region, 108840, Russia
[3]Departamento de Física and Centro de Física Teórica e Computacional, Faculdade de Ciências, Universidade de Lisboa, Campo Grande, Edifício C8, Lisboa 1749-016, Portugal

(Received 18 May 2019; published 19 December 2019)

The existence of the edge states at the interface between two media with different topological properties is protected by symmetry, which makes such states robust against structural defects or disorder. We show that if a system supports more than one topological edge state at the interface, even a weak periodic deformation may scatter one edge state into another without coupling to bulk modes. This is the Bragg scattering of the edge modes, which in a topological system is highly selective, with closed bulk and backward scattering channels, even when conditions for resonant scattering are not satisfied. When such a system bears nonlinearity, Bragg scattering enables the formation of a new type of soliton—topological Bragg solitons. We report them in a spin-orbit coupled (SOC) Bose-Einstein condensate in a honeycomb optical lattice and Zeeman lattice. An interface supporting two edge states is created by two different SOCs, with the x components of the synthetic magnetic field having opposite directions at different sides of the interface. The created Bragg solitons are found to be stable.

DOI: 10.1103/PhysRevLett.123.254103

Topological edge states are fundamental for understanding the physics of many phenomena including quantum [1,2], anomalous [3], and quantum spin [4,5] Hall effects, topological insulators [6], Majorana fermions [7], just to mention a few. Introduced in solid state physics, topological edge states were shown to be a universal wave phenomenon. In particular, they enable protected edge currents in photonic crystals as predicted in [8] and observed in [9–14] (see review [12]), in surface plasmon-polariton systems [15], in systems of cold atoms in optical lattices [16–18], in spin-orbit coupled Bose-Einstein condensates (SOC BECs) [17], and in optoelectronic systems, such as exciton-polariton condensates [18,19].

Topological edge states are robust against disorder [6], which distinguishes them from bulk states that can be manipulated by perturbations [20]. This makes such states promising for a variety of applications. Meanwhile, when it is necessary to selectively excite or remove edge states, or transform them in any other way, this robustness becomes a drawback. Topological edge states can be coupled by nonlinearity that gives rise to a rich set of phenomena, such as modulation instability [19] or envelope soliton propagating along the edge [17]. However, by enabling *linear* coupling one qualitatively enriches the physics of respective systems. New nonlinear interactions, requiring simultaneous energy and momentum conservation laws, can be made resonant. That leads to a plethora of novel phenomena, which so far were not considered for edge states. In particular, linear mode coupling resulting from periodic modulation of the system, i.e., from Bragg scattering, in the presence of nonlinearity can lead to the formation of Bragg solitons [21,22], which are relevant for many applications [23], and whose properties qualitatively differ from those of the envelope solitons mentioned above.

In this Letter, we introduce an efficient mechanism of coupling and conversion of topological edge states based on Bragg scattering by periodic undulations of an interface between topologically different media. This mechanism works when a system supports more than one topological edge state per interface. We show that even a *very* weak periodic perturbation of such an interface may result in periodic transitions between two edge states moving with different group velocities. Such a coupling is highly selective, with closed bulk and backward scattering channels. Furthermore, we construct Bragg solitons propagating along the interface and representing a spatially localized envelope of two coupled edge states.

As a case example, we address an atomic SOC BEC [24,25], characterized by a spinor order parameter $\Psi = (\psi^{(1)}, \psi^{(2)})^T$ (T stands for the transpose). The condensate is placed in a honeycomb lattice, which can be created experimentally by applying at least three laser beams [26,27]. Allows arbitrary 2D field distributions, and thus optical potentials can be produced by the interference of quasinondiffracting laser beams [28]. The lattice is characterized by inverted potential profiles for the spinor components and can be created by periodically varying Zeeman splitting (see [29] for a possibility of experimental

（62）Terahertz Oscilloscope for Recording Time Information of Ultrashort Electron Beams, Physical Review Letters

PHYSICAL REVIEW LETTERS 122, 144801 (2019)

Terahertz Oscilloscope for Recording Time Information of Ultrashort Electron Beams

Lingrong Zhao,[1,2] Zhe Wang,[1,2] Heng Tang,[1,2] Rui Wang,[1,2] Yun Cheng,[1,2] Chao Lu,[1,2] Tao Jiang,[1,2] Pengfei Zhu,[1,2] Long Hu,[1] Wei Song,[1] Huida Wang,[3] Jiaqi Qiu,[3] Ramani Kosim,[3] Chunguang Jing,[3] Sergey Antipov,[3] Peng Wang,[4] Jia Qi,[4] Ya Cheng,[4,5] Dao Xiang,[4,5,6,*] and Jie Zhang[1,2,†]

[1]Key Laboratory for Laser Plasmas (Ministry of Education), School of Physics and Astronomy, Shanghai Jiao Tong University, Shanghai 200240, China
[2]Collaborative Innovation Center of IFSA (CICIFSA), Shanghai Jiao Tong University, Shanghai 200240, China
[3]Science and Technology on High Power Microwave Laboratory, Northwest Institute of Nuclear Technology, Xi'an, Shaanxi 710024, China
[4]Nanjch Company Limited, Beijing 100084, China
[5]Euclid Techlabs LLC, Bolingbrook, Illinois 60440, USA
[6]State Key Laboratory of High Field Laser Physics, Shanghai Institute of Optics and Fine Mechanics, Chinese Academy of Sciences, Shanghai 201800, China
[7]State Key Laboratory of Precision Spectroscopy, East China Normal University, Shanghai 200062, China
[8]Tsung-Dao Lee Institute, Shanghai 200240, China

(Received 25 December 2018; published 9 April 2019)

We propose and demonstrate a terahertz (THz) oscilloscope for recording time information of an ultrashort electron beam. By injecting a laser-driven THz pulse with circular polarization into a dielectric tube, the electron beam is swept helically such that the time information is uniformly encoded into the angular distribution that allows one to characterize both the temporal profile and timing jitter of an electron beam. The dynamic range of the measurement in such a configuration is significantly increased compared to deflection with a linearly polarized THz pulse. With this THz oscilloscope, nearly 50-fold longitudinal compression of a relativistic electron beam to about 15 fs (rms) is directly visualized with its arrival time determined with 3 fs accuracy. This technique bridges the gap between streaking of photoelectrons with optical lasers and deflection of relativistic electron beams with radio-frequency deflectors and should have wide applications in many ultrashort electron-beam-based facilities.

DOI: 10.1103/PhysRevLett.122.144801

The ability to characterize the time information of an ultrashort electron beam including both the temporal profile and arrival time is crucial for optimizing and enhancing the performance of many electron-beam-based scientific facilities such as free-electron lasers (FELs [1–3]), ultrafast electron diffraction (UED [4,5]) and microscopy (UEM [6–9]), laser-driven and beam-driven advanced accelerators [10–15], etc. In the accelerator community, rf deflecting cavities have been widely used to measure the temporal profile of relativistic electron beams with energy ranging from MeV to GeV (see, e.g., Refs. [16–18]). However, the information of beam arrival time with respect to an external laser as required in a pump-probe experiment cannot be directly measured with a rf deflector. In the attosecond science community, streaking of photoelectrons with optical lasers has become a standard technique for characterizing the complete information of attosecond pulses [19]. Recently, this technique has been adapted to characterize femtosecond x-ray pulses in FELs with the streaking imprinted by far-infrared and THz pulses [20–23]. However, this technique does not apply to a relativistic electron beam as dictated by the Lawson-Woodward theorem [24]. Very recently, THz streaking of keV and MeV electrons [25–27] in a subwavelength metallic structure has been used to measure both the temporal profile and the arrival time of electron beams. However, the small aperture used to enhance the THz field may significantly limit the number of useful electrons. Furthermore, with the streaking imprinted by a linearly polarized THz pulse, the beam receives sinusoidal angular streaking and thus the measurement has a rather limited dynamic range (time window where the measurement is accurate) comparable to about one-quarter of the wavelength.

In this Letter, we demonstrate a laser-driven THz oscilloscope that allows one to record the complete time information of an ultrashort electron beams with both large dynamic range and high temporal resolution. This scheme exploits the sustained interaction between the THz pulse and the electron beam in a dielectric tube, allowing sufficient deflection to be generated without enhancing the THz field with a narrow slit. With accurate control of the THz polarization, the electron

（63）Connecting shear localization with the long-range correlated polarized stress fields in granular materials, Nature Communications

nature COMMUNICATIONS

ARTICLE

OPEN

Connecting shear localization with the long-range correlated polarized stress fields in granular materials

Yinqiao Wang[1], Yujie Wang[1] & Jie Zhang[1,2,3]

One long-lasting puzzle in amorphous solids is shear localization, where local plastic deformation involves cooperative particle rearrangements in small regions of a few inter-particle distances, self-organizing into shear bands and eventually leading to the material failure. Understanding the connection between the structure and dynamics of amorphous solids is essential in physics, material sciences, geotechnical and civil engineering, and geophysics. Here we show a deep connection between shear localization and the intrinsic structures of internal stresses in an isotropically jammed granular material subject to shear. Specifically, we find strong (anti)correlations between the micro shear bands and two polarized stress fields along two directions of maximal shear. By exploring the tensorial characteristics and the rotational symmetry of force network, we reveal that such profound connection is a result of symmetry breaking by shear. Finally, we provide the solid experimental evidence of long-range correlated inherent shear stress in an isotropically jammed granular system.

[1] School of Physics and Astronomy, Shanghai Jiao Tong University, 800 Dong Chuan Road, 200240 Shanghai, China. [2] Institute of Natural Sciences, Shanghai Jiao Tong University, 200240 Shanghai, China. [3] Collaborative Innovation Center of Advanced Microstructures, 210093 Nanjing, China.

（64）Designer spin order in diradical nanographenes, Nature Communications

ARTICLE

https://doi.org/10.1038/s41467-020-19834-2 OPEN

Designer spin order in diradical nanographenes

Yuqiang Zheng[1,6], Can Li[1,6], Chengyang Xu[1], Doreen Beyer[2], Xinlei Yue[1], Yan Zhao[1], Guanyong Wang[1], Dandan Guan[1,3], Yaoyi Li[1,3], Hao Zheng[1,3], Canhua Liu[1,3], Junzhi Liu[4], Xiaoqun Wang[1,3], Weidong Luo[1,5], Xinliang Feng[2✉], Shiyong Wang[1,3✉] & Jinfeng Jia[1,3✉]

The magnetic properties of carbon materials are at present the focus of intense research effort in physics, chemistry and materials science due to their potential applications in spintronics and quantum computing. Although the presence of spins in open-shell nanographenes has recently been confirmed, the ability to control magnetic coupling sign has remained elusive but highly desirable. Here, we demonstrate an effective approach of engineering magnetic ground states in atomically precise open-shell bipartite/nonbipartite nanographenes using combined scanning probe techniques and mean-field Hubbard model calculations. The magnetic coupling sign between two spins was controlled via breaking bipartite lattice symmetry of nanographenes. In addition, the exchange-interaction strength between two spins has been widely tuned by finely tailoring their spin density overlap, realizing a large exchange-interaction strength of 42 meV. Our demonstrated method provides ample opportunities for designer above-room-temperature magnetic phases and functionalities in graphene nanomaterials.

[1] Key Laboratory of Artificial Structures and Quantum Control (Ministry of Education), Shanghai National Laboratory for Materials Science, School of Physics and Astronomy, Shanghai Jiao Tong University, 200240 Shanghai, China. [2] Center for Advancing Electronics Dresden and Department of Chemistry and Food Chemistry, Technische Universität Dresden, 01062 Dresden, Germany. [3] Tsung-Dao Lee Institute, Shanghai Jiao Tong University, 200240 Shanghai, China. [4] Department of Chemistry and State Key Laboratory of Synthetic Chemistry, The University of Hong Kong, Pokfulam Road, Hong Kong, China. [5] Institute of Natural Sciences, Shanghai Jiao Tong University, 200240 Shanghai, China. [6] These authors contributed equally: Yuqiang Zheng, Can Li. ✉email: xinliang.feng@tu-dresden.de; shiyong.wang@sjtu.edu.cn; jfjia@sjtu.edu.cn

（65）Optical soliton formation controlled by angle twisting in photonic moiré lattices, Nature Photonics

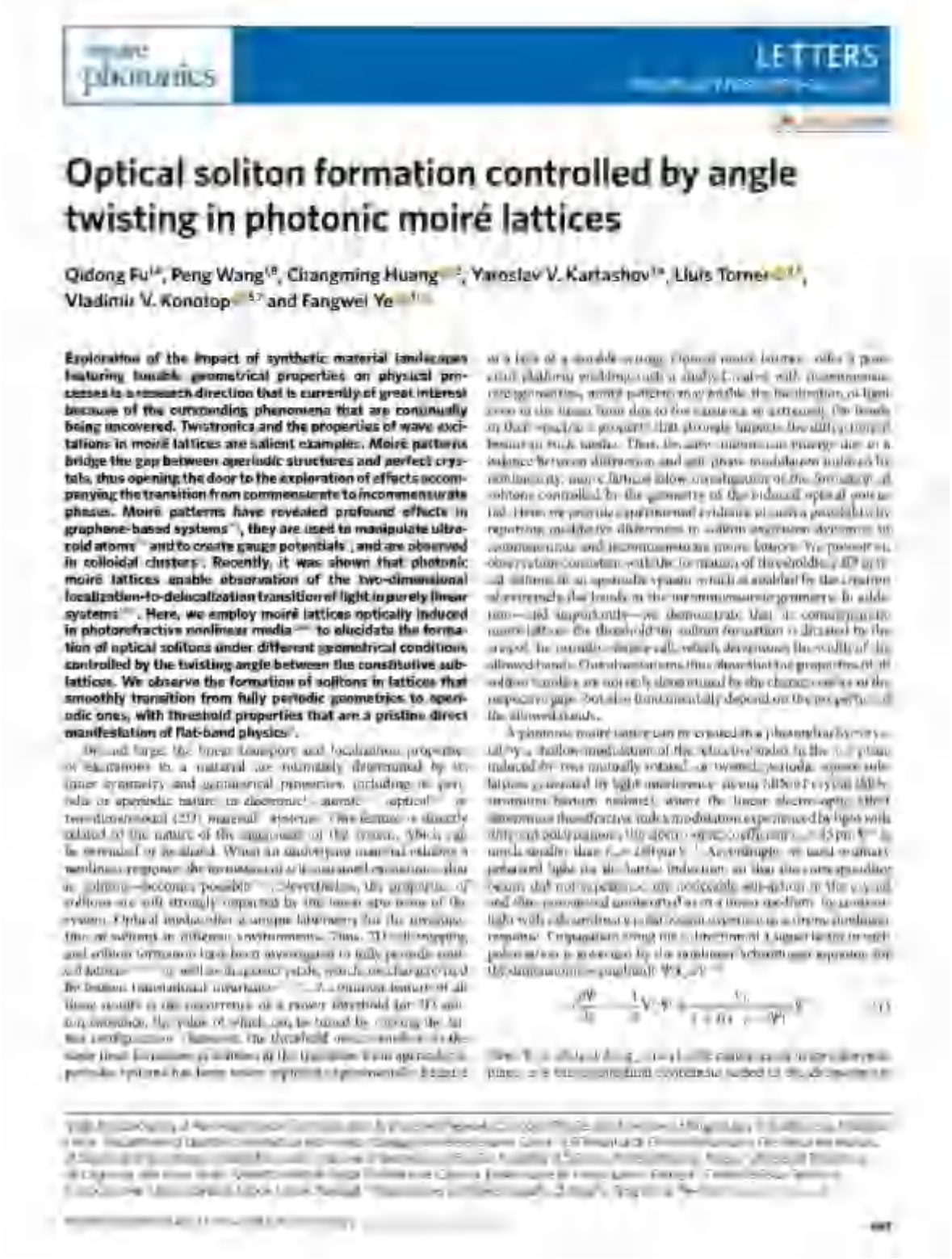

nature photonics LETTERS

Optical soliton formation controlled by angle twisting in photonic moiré lattices

Qidong Fu[1,2], Peng Wang[1,2], Changming Huang[1,2], Yaroslav V. Kartashov[1,3], Lluis Torner[1,2], Vladimir V. Konotop[4,5] and Fangwei Ye[1,2]

Exploration of the impact of synthetic material landscapes featuring tunable geometrical properties on physical processes is a research direction that is currently of great interest because of the outstanding phenomena that are continually being uncovered. Twistronics and the properties of wave excitations in moiré lattices are salient examples. Moiré patterns bridge the gap between aperiodic structures and perfect crystals, thus opening the door to the exploration of effects accompanying the transition from commensurate to incommensurate phases. Moiré patterns have revealed profound effects in graphene-based systems[1–3], they are used to manipulate ultracold atoms[4,5] and to create gauge potentials[6], and are observed in colloidal clusters[7]. Recently, it was shown that photonic moiré lattices enable observation of the two-dimensional localization-to-delocalization transition of light in purely linear systems[8,9]. Here, we employ moiré lattices optically induced in photorefractive nonlinear media[10–12] to elucidate the formation of optical solitons under different geometrical conditions controlled by the twisting angle between the constitutive sublattices. We observe the formation of solitons in lattices that smoothly transition from fully periodic geometries to aperiodic ones, with threshold properties that are a pristine direct manifestation of flat-band physics[13].

（66）Localization and delocalization of light in photonic moiré lattices, Nature

Article

Localization and delocalization of light in photonic moiré lattices

https://doi.org/10.1038/s41586-019-1861-6

Received: 8 January 2019

Accepted: 12 September 2019

Published online: 16 December 2019

Peng Wang[1,2], Yuanlin Zheng[1,2], Xianfeng Chen[1,2], Changming Huang[3], Yaroslav V. Kartashov[4,5], Lluis Torner[4,5], Vladimir V. Konotop[6] & Fangwei Ye[1,2]

Moiré lattices consist of two superimposed identical periodic structures with a relative rotation angle. Moiré lattices have several applications in everyday life, including artistic design, the textile industry, architecture, image processing, metrology and interferometry. For scientific studies, they have been produced using coupled graphene–hexagonal boron nitride monolayers[1,2], graphene–graphene layers[3,4] and graphene quasicrystals on a silicon carbide surface[5]. The recent surge of interest in moiré lattices arises from the possibility of exploring many salient physical phenomena in such systems: examples include commensurable–incommensurable transitions and topological defects[3], the emergence of insulating states owing to band flattening[1,2], unconventional superconductivity[6] controlled by the rotation angle[7], the quantum Hall effect[8], the realization of non-Abelian gauge potentials[9] and the appearance of quasicrystals at special rotation angles[10]. A fundamental question that remains unexplored concerns the evolution of waves in the potentials defined by moiré lattices. Here we experimentally create two-dimensional photonic moiré lattices, which—unlike their material counterparts—have readily controllable parameters and symmetry, allowing us to explore transitions between structures with fundamentally different geometries (periodic, general aperiodic and quasicrystal). We observe localization of light in deterministic linear lattices that is based on flat-band physics[9], in contrast to previous schemes based on light diffusion in optical quasicrystals[11], where disorder is required[12] for the onset of Anderson localization[13–15] (that is, wave localization in random media). Using commensurable and incommensurable moiré patterns, we experimentally demonstrate the two-dimensional localization–delocalization transition of light. Moiré lattices may feature an almost arbitrary geometry that is consistent with the crystallographic symmetry groups of two-dimensional superlattices, and therefore afford a powerful tool for controlling the properties of light patterns and exploring the physics of periodic–aperiodic photonic transitions and two-dimensional wavepacket phenomena relevant to several areas of science, including optics, acoustics, condensed matter and atomic physics.

One of the most salient properties of an engineered optical system is its capability to affect a light beam in a prescribed manner, such as to control its diffraction pattern or to localize it. The importance of wavepacket localization extends far beyond optics and impacts all branches of science dealing with wave phenomena. Homogeneous or strictly periodic linear systems cannot result in wave localization, and the latter require the presence of structure defects or randomness. Anderson localization[13–15] is a hallmark discovery in condensed matter physics. All electronic states in one- and two-dimensional potentials with uncorrelated disorder are localized. Three-dimensional systems with disordered potentials are known to have both localized and delocalized eigenstates[13–15], separated by an energy known as the mobility edge[16]. Coexistence of localized and delocalized eigenstates has been predicted also in regular quasiperiodic one-dimensional systems, first in the discrete Aubry–André[17] model and later in continuous optical and matter wave systems[18–21]. Quasiperiodic (or aperiodic) structures, even those that possess long-range order, fundamentally differ both from periodic systems, where all eigenmodes are delocalized Bloch waves, and from disordered media, where all states are localized (in one or two dimensions). Upon variation of the parameters of a quasiperiodic system, it is possible to observe the transition between localized and delocalized states. Such a localization–delocalization transition (LDT)

[illegible]

（67）Direct Visualizing the Spin Hall Effect of Light via Ultrahigh-Order Modes, Physical Review Letters

Direct Visualizing the Spin Hall Effect of Light via Ultrahigh-Order Modes

Haitang Dai,[1] Luqi Yuan,[2,*] Cheng Yin,[1] Zhuangqi Cao,[3] and Xianfeng Chen[1,2,†]
[1]The State Key Laboratory on Fiber Optic Local Area Communication Networks and Advanced Optical Communication Systems, School of Physics and Astronomy, Shanghai Jiao Tong University, Shanghai 200240, China
[2]Collaborative Innovation Center of Light Manipulations and Applications, Shandong Normal University, Jinan 250358, China
[3]Hunan Key Laboratory of Power Transmission and Distribution Equipment Technology, Hunan University of Technology, Zhuzhou 412007, China

(Received 5 September 2019; accepted 16 January 2020; published 4 February 2020)

We report an experiment showing the ultrahigher Imbert-Fedorov shift from the ultrastrong spin-orbital angular momentum coupling, which is a photonic version of the spin Hall effect, by measuring the reflection of light from the surface of a birefringent symmetrical metal cladding planar waveguide. The light incidents at a near-normal incident angle and excites resonant ultrahigh-order modes inside the waveguide. A lateral displacement of separated reflected light spots corresponding to two polarization states is distinguishable by human eyes. In our experiment, we demonstrate the control of polarizations of light and the direct observation of the spin Hall effect of light, which opens an important avenue towards potential applications for optical sensing and quantum information processing, where the spin nature of photons exhibits key features.

DOI: 10.1103/PhysRevLett.124.053902

The spin-orbit interaction of photons at the interface with the refractive index inhomogeneity corresponds to the interplay between the spin degree of freedom of light and the extrinsic orbital angular momentum, which is a photonic version of the spin Hall effect [1–3]. It leads to a perpendicular spin-dependent displacement of light, i.e., the so-called Imbert-Fedorov (IF) shift [4,5]. For many measurements of the spin Hall effect of light (SHEL), the displacement between two opposite spins is at the order of the wavelength of light, which cannot be distinguishable by human eyes. The quantum weak measurement technology [6–14] therefore has been utilized, which causes a complex experimental setup and hence limits potential practical applications [9,11]. On the other hand, the general concept of SHEL associated with the polarization nature of light occurs universally in many optical systems [1,6]. It leads to the longitudinal Goos-Hanchen shift from the spatial dispersion of light and also the transverse IF shift [7,9], which originates from the geometric Berry phase and the conservation of normal components of the total angular momentum of light [10]. Because of the unique physical nature [5–9] as well as possible implications in the metrology and the spin-based nano-optics [10,11], the research of SHEL is of important interest [12–14]. In particular, a large number of experimental works with the quantum weak measurement have been performed to observe the IF shift at a variety of optical platforms including the air-dielectric interface [15–20], metamaterial with the photon tunneling process [12], metasurfaces [17,21–24], Weyl semimetals [25], heavy-electron semiconductor [26], and thin films supporting leaky guided modes [27], where the quantum nature of light limits the efficiency of the measurement [11]. Recently, methods associated with the surface plasmon resonance (SPR) have been applied to enhance the SHEL [27–30]. For example, an enhancement with a factor of 50 is revealed for the light incident on the metal surface near the Brewster angle, which gives the IF shift ~3.2 μm [30]. Moreover, a small incident angle for the enhancement of SHEL in hyperbolic metamaterials has been explored and the transverse beam shift is ~9 μm [31]. A natural question arises, is there a system supporting an IF shift associated with the SHEL that is large enough to be distinguished by human eyes?

In this Letter, we show an ultrastrong spin-orbital angular momentum coupling of light in the experiment by using the resonance of resonant ultrahigh-order modes (UOMs). A linear-polarized light is incident into the birefringent symmetrical metal cladding planar waveguide at the near-normal incident angle θ_i and excites a high density of UOMs inside the waveguide [32–35]. The experiment shows a transverse spatial deviation at a subwavelength scale in the reflected light corresponding to two opposite spins, which can be visibly seen on the CCD. Our work points out a unique platform for studying the fundamental physics of the ultrastrong spin-orbital angular momentum coupling of light without applying the quantum weak measurement, leading towards broad potential implications including quantum information, optical communications, and biosensing.

We start with a brief description on the physical picture of the spin-orbital angular momentum coupling of light by considering a plane wave incident on a surface. Under the

（68）Integrated Quantum-Walk Structure and NAND Tree on a Photonic Chip, Physical Review Letters

Integrated Quantum-Walk Structure and NAND Tree on a Photonic Chip

Yao Wang,[1,2] Zi-Wei Cao,[3,4] Yong-Heng Lu,[1,2] Xiao-Ming Zhang,[5] Jun Gao,[1,2]
Yi-Jun Chang,[1,2] Man-Hong Yung,[3,4,6,7] and Xian-Min Jin[1,2,8,*]
[1]Center for Integrated Quantum Information Technologies (IQIT), School of Physics and Astronomy and State Key Laboratory of Advanced Optical Communication Systems and Networks, Shanghai Jiao Tong University, Shanghai 200240, China
[2]CAS Center for Excellence and Synergetic Innovation Center in Quantum Information and Quantum Physics, University of Science and Technology of China, Hefei, Anhui 230026, China
[3]Department of Physics, Southern University of Science and Technology, Shenzhen 518055, China
[4]Shenzhen Institute for Quantum Science and Engineering, Southern University of Science and Technology, Shenzhen 518055, China
[5]Department of Physics, City University of Hong Kong, Tat Chee Avenue, Kowloon, Hong Kong SAR, China
[6]Guangdong Provincial Key Laboratory of Quantum Science and Engineering, Southern University of Science and Technology, Shenzhen 518055, China
[7]Shenzhen Key Laboratory of Quantum Science and Engineering, Southern University of Science and Technology, Shenzhen 518055, China

(Received 19 June 2020; accepted 4 September 2020; published 14 October 2020)

In the age of the post-Moore era, the next-generation computing model would be a hybrid architecture consisting of different physical components, such as photonic chips. In 2008, it was proposed that the solving of the NAND-tree problem can be speeded up by quantum walk. This scheme is groundbreaking due to the universality of the NAND gate. However, experimental demonstration has not been achieved so far, mainly due to the challenge in preparing the propagating initial state. Here we propose an alternative solution by including a structure called a "quantum slide," where a propagating Gaussian wave packet can be generated deterministically along a properly engineered chain. In our experimental demonstration, the optical NAND tree is capable of solving computational problems with a total of four input bits, based on the femtosecond laser 3D direct-writing technique on a photonic chip. These results remove one main roadblock to photonic NAND-tree computations, and the construction of a quantum slide may find other interesting applications in quantum information and quantum optics.

DOI: 10.1103/PhysRevLett.125.160502

Quantum walk, the quantum generalization of the classical random walk, is a natural platform for discovering exotic quantum phenomena and developing quantum algorithms [1–8]. Quantum-walk-based schemes have provided speed-up for various problems of particular interests, including Boson sampling [9–12], black-box problem [13], element distinctness [14], binary addition [15], factoring integers [16], and machine learning [17]. It has also been shown that quantum walk is powerful enough to perform universal quantum computation [18–20].

A NAND tree is a binary tree of NAND gates containing a total of N inputs but only one output, enabling the computation of arbitrary Boolean function of the form $F:\{0,1\}^N \to \{0,1\}$. While there are many classical algorithms for the NAND-tree problem [21–24], this task can be mapped to the quantum walk to speed up the computation. In 2008, Farhi *et al.* proposed a continuous quantum-walk-based protocol for balanced NAND tree for the first time [22]. Inspired by it, several discrete quantum-walk schemes have been developed [25,26]. The schemes have also been generalized to the unbalanced NAND formula [25–27], which can, in principle, represent arbitrary Boolean functions [28].

The original scheme of the NAND tree in Ref. [22] is based on a continuous quantum walk on a graph. As shown in Fig. 1, the graph contains a chain of uniformly coupled sites, called "runway," the quantum NAND tree whose sites are connected in the structure as a binary tree, and a set of input nodes. Suppose the graph is represented by the adjacent matrix G, the time-independent Hamiltonian of the entire system is just $H = \lambda G$, where λ is the coupling constant. The input x is encoded by the on-off coupling of the input nodes (leaves) and the nodes on the top layer of the tree. For an incident wave packet with zero energy in the runway [22], if the computation outcome is $F(x) = 1$, the wave packet will pass through the quantum NAND tree; otherwise, the wave packet will be reflected when $F(x) = 0$. Therefore, by measuring whether the wave packet has passed through or been reflected, the binary computation outcome can be obtained.

The original protocol [22] of the quantum NAND tree is elegant and simple, and there is also proposal of realizing it on the molecular platform [29] being developed recently. However, its experimental realization remains challenging and, to our best knowledge, has not been

（69）Subharmonic Entrainment Breather Solitons in Ultrafast Lasers, Physical Review Letters

PHYSICAL REVIEW LETTERS 125, 163901 (2020)

Subharmonic Entrainment Breather Solitons in Ultrafast Lasers

Tianhao Xiao, Le Zhan, Wenchao Wang, and Wenyan Zhang
State Key Laboratory of Advanced Optical Communication Systems and Networks, School of Physics and Astronomy, Shanghai Jiao Tong University, Shanghai 200240, China

(Received 27 May 2020; revised 3 August 2020; accepted 14 September 2020; published 12 October 2020)

We study theoretically and experimentally the subharmonic entrainment (SHE) breather solitons in mode-locked lasers for the first time, in which the ratio of the breather period to the round-trip time is an integer. We build a non-Hermitian degeneracy map of breather solitons and illustrate that SHE arises between the two exceptional points (EPs). We observe SHE as the result of the evolution of breather solitons when tuning the pump and/or cavity loss, and prove that this phenomenon can improve the stability of breather solitons. Our research brings insight into the EP physics of ultrafast lasers and makes the mode-locked laser a powerful test bed for non-Hermitian degeneracy, which may open a new avenue in ultrafast laser research.

DOI: 10.1103/PhysRevLett.125.163901

Solitons, self-localized coherent structures, are ubiquitous in nature and have been observed in many branches of nonlinear science [1–5]. Mode-locked lasers constitute an ideal test bed for investigating solitons [6], where solitons arise from the balance among dispersion, nonlinearity, and environmental energy exchange. Once given the medium parameters, solitons generally display a fixed profile over propagation [7,8], which enables the application in designing pulse sources [9]. In many systems, the amplitude and duration of solitons can oscillate or breathe periodically. Breather solitons were first demonstrated in fiber cavities [10] and then observed in optical microresonators [11,12] and mode-locked lasers [13]. Because of strong connection with the Fermi-Pasta-Ulam recurrence [14], turbulence [15], modulation instability [16], and rogue wave formation [17], breather solitons have attracted considerable attention. Furthermore, the ability of breather soliton to increase the resolution of dual-comb source (composed of two frequency combs with slightly different repetition rates) implies that the breather soliton is attractive in practical applications [18].

Recently, the breather soliton generated in Kerr-nonlinear optical resonators was predicted to exhibit subharmonic entrainment (SHE): an integer ratio $T_b/T_r = n$ of the breather period T_b to the round-trip time T_r [19]. It is a special frequency locking that occurs between the two exceptional points (EPs) [20]. The EP is a branch point singularity in the parameter space [21–23] that arises when two or more eigenvalues of the non-Hermitian Hamiltonian and their corresponding eigenvectors become degenerate. Such degeneracies are distinct features of non-Hermitian systems which do not obey conservation laws because the systems exchange energy with environment. The breather soliton laser, which has two frequencies (the repetition frequency f_r and the breather frequency f_b), can be deemed as a non-Hermitian system. The eigenvalues of the non-Hermitian Hamiltonian between the EPs are complex with the same real part [22], resulting in frequency locking in the breather soliton system, from which the SHE breather soliton arises. Although it was predicted in Kerr-nonlinear resonators [19], the SHE breather soliton has not been examined experimentally.

In this Letter, we present the first experimental observation of the SHE breather soliton. We find that the breather soliton laser exhibits non-Hermitian degeneracy in certain condition and that the SHE arises between the two EPs. Experimentally, we fabricate a mode-locked fiber laser, which is easily driven into the breather soliton regime by tuning the pump power and/or cavity loss. We record the change of breather soliton with the pump power and characterize SHE using dispersive Fourier transform (DFT) technique [24–26] and dispersive temporal interferometer (DTI) [27]. We prove that SHE can enhance the stability of breather soliton. Simulations also prove that SHE arises between the EPs.

In principle, a stable mode-locked laser only sustains the modes at the free-running cavity frequency f_{cw} (corresponding to the cavity round-trip time T_{cw}) together with its harmonic (at the repetition frequency of mf_{cw}, m is an integer). Nevertheless, the breather soliton mode-locked laser source has is an unstable system, in which another mode, the free-running breather frequency f_{sw}, arises. Typically, $f_{sw} \ll f_{cw}$ [19]. Figure 1(a) depicts the free propagation of f_{sw}, which shows slight difference between nT_{cw} and the free-running breather period T_{sw} by $\Delta = T_{sw} - nT_{cw}$ with $|\Delta| \leq T_{cw}/2$. In Fig. 1(b), the evolution is treated as repeating in a period nT_{cw} with uniformly distributed n solitons in each period. Each soliton appears in the free-running subharmonic frequency $f_{sw} = f_{cw}/n$.

（70）Vector Vortex Beam Emitter Embedded in a Photonic Chip, Physical Review Letters

Vector Vortex Beam Emitter Embedded in a Photonic Chip

Yuan Chen,[1,2] Ke-Yu Xia,[1,2,3,*] Wei-Guan Shen,[1,2] Jun Gao,[1,2] Zeng-Quan Yan,[1,2] Zhi-Qiang Jiao,[3] Jian-Peng Dou,[1,2] Hao Tang,[1,2] Yun-Qing Lu,[1,4,5,6,†] and Xian-Min Jin[1,2,‡]

[1]Center for Integrated Quantum Information Technologies (IQIT), School of Physics and Astronomy and State Key Laboratory of Advanced Optical Communication Systems and Networks, Shanghai Jiao Tong University, Shanghai 200240, China

[2]Institute for Quantum Science and Engineering and Department of Physics, Southern University of Science and Technology, Shenzhen 518055, China

[3]College of Engineering and Applied Sciences, Nanjing University, Nanjing 210093, China

[4]National Laboratory of Solid State Microstructures, Collaborative Innovation Center of Advanced Microstructures, Nanjing University, Nanjing 210093, China

[5]Jiangsu Key Laboratory of Artificial Functional Materials, Nanjing University, Nanjing 210093, China

[6]Key Laboratory of Intelligent Optical Sensing and Manipulation (Nanjing University), Ministry of Education, Nanjing 210093, China

[7]CAS Center for Excellence and Synergetic Innovation Center in Quantum Information and Quantum Physics, University of Science and Technology of China, Hefei, Anhui 230026, China

(Received 26 February 2019; accepted 23 March 2020; published 16 April 2020)

Vector vortex beams simultaneously carrying spin and orbital angular momentum of light promise additional degrees of freedom for modern optics and emerging scenarios for both classical and quantum information technologies. The inherently infinite dimensions can be exploited to enhance data capacity for sustaining the unprecedented growth in big data and internet traffic and can be encoded to build quantum computing machines in high-dimensional Hilbert space. So far, much progress has been made in the emission of vector vortex beams from a chip surface into free space; however, the generation of vector vortex beams inside a photonic chip has not been realized yet. Here, we demonstrate the first vector vortex beam emitter embedded in a photonic chip by using femtosecond laser direct writing. We achieve a conversion of vector vortex beams with an efficiency up to 50% and scalar vortex beams with an efficiency up to 74% from Gaussian beams. We also present an expanded coupled-mode model for understanding the mode conversion and the influence of the imperfection in fabrication. The fusion of embedded generation makes vector vortex beams directly ready for further nanoscopic manipulation and emission without any additional interconnection. Together with the ability to be integrated as an array, our results may enable vector vortex beams to become accessible inside a photonic chip for high-capacity communication and high-dimensional quantum information processing.

DOI: [illegible]

Light can carry both spin and orbital angular momentum (OAM). Spin angular momentum is associated with optical polarization, which is one of the most prominent and well-known properties of light. OAM is an emerging degree of freedom, which has helical wavefronts described by an azimuthal phase term $e^{il\varphi}$ [1] (φ is the azimuthal angle in a cylindrical coordinate system). The topological charge l can take any integer value represented by the number of crossed spiral wavefronts when rotating around the axis once. Because of the unlimited topological charges and the inherent orthogonality, OAM can provide larger alphabets for classical information [2–4] and quantum information processing (QIP) [5–11].

Recently, there has been an increasing interest in vector vortex light beams, with a polarization varying along the azimuthal coordinate and a central optical singularity. Such beams exhibit some unique characteristics such as field structure, phase singularity, and rotation invariance [12]. Vector vortex beams have been applied in wide areas including microscopy [13], optical trapping [14], precision measurement [15], quantum communication [12,16], and QIP [17–21].

Large-scale applications beyond proof-of-principle demonstrations require developing integrated techniques to enable the generation [22–26], transmission [27], and even processing of vector vortex beams on a photonic chip. Several pioneering works have demonstrated on-chip generation of vector vortex beams with integrated microring resonators [22,23,25,26]. While the emission of vector vortex beams from the surface of integrated devices to free space has been widely investigated, generation and transmission inside a photonic chip remain to be realized and very challenging.

In this Letter, we demonstrate a direct generation of vector vortex beams inside a photonic chip based on mode

（71）Femtosecond Relativistic Electron Beam with Reduced Timing Jitter from THz Driven Beam Compression

PHYSICAL REVIEW LETTERS 124, 054802 (2020)

Femtosecond Relativistic Electron Beam with Reduced Timing Jitter from THz Driven Beam Compression

Lingrong Zhao,[1,2] Heng Tang,[1,2] Chao Lu,[1,2] Tao Jiang,[1,2] Pengfei Zhu,[1,2] Long Hu,[1,2] Wei Song,[1] Huida Wang,[1] Jiaqi Qiu,[1] Chunguang Jing,[3] Sergey Antipov,[3] Dao Xiang,[1,2,*] and Jie Zhang[1,2,4,†]
[1]Key Laboratory for Laser Plasmas (Ministry of Education), School of Physics and Astronomy, Shanghai Jiao Tong University, Shanghai 200240, China
[2]Collaborative Innovation Center of IFSA (CICIFSA), Shanghai Jiao Tong University, Shanghai 200240, China
[3]Science and Technology on High Power Microwave Laboratory, Northwest Institute of Nuclear Technology, Xi'an, Shaanxi 710024, China
[4]Nascent Computer Limited, Beijing 100084, China
[5]Euclid Techlabs, LLC, Bolingbrook, Illinois 60440, USA
[6]Tsung-Dao Lee Institute, Shanghai 200240, China

(Received 17 June 2019; revised manuscript received 12 December 2019; accepted 19 December 2019; published 4 February 2020)

We propose and demonstrate a method to reduce the pulse width and timing jitter of a relativistic electron beam through THz driven beam compression. In this method the longitudinal phase space of a relativistic electron beam is manipulated by ultrashort picosecond THz pulses propagating in a dielectric tube such that the bunch tail has a higher velocity than the bunch head, which allows simultaneous reduction of both pulse width and timing jitter after passing through a drift. In the experiment, the beam is compressed by more than a factor of 4 from 1.50 fs to 28.46 fs with the arrival time jitter also reduced from 97 fs to 16 fs, opening up new opportunities in using pulsed electron beams for studies of ultrafast dynamics. This technique provides an effective way to manipulate beam longitudinal phase space with a THz pulse and may have a strong impact in accelerator and ultrafast science facilities that require femtosecond electron beams with tight synchronization to external lasers.

DOI: 10.1103/PhysRevLett.124.054802

Ultrashort electron beams with small timing jitter with respect to external lasers are of fundamental interest in accelerator and ultrafast science communities. For instance, such beams are essential for laser and THz driven accelerators with an externally injected electron beam [1–4] where the beam energy spread and beam energy stability largely depend on the electron bunch length and injection timing jitter, respectively. For MeV ultrafast electron diffraction (UED) [5–12] where electrons with a few MeV energy are used to probe the atomic structure changes following the excitation of a pump laser, the temporal resolution is primarily limited by the electron bunch length and timing jitter. Similar limitations exist for x-ray free-electron lasers (FELs) [13–15] too, since the properties of the x-ray pulses depend primarily on that of the electron beams. Therefore, one of the long-standing goals in accelerator and ultrafast science communities is to generate ultrashort electron beams with small timing jitter.

A photocathode rf gun is the leading option for producing a high brightness ultrashort electron beam for FELs and MeV UED (see, e.g., Refs. [16,17]). Because of the space charge effect, the beam pulse width is broadened and therefore bunch compression is needed to reduce the pulse width. Bunch compression requires first a mechanism to imprint an energy chirp (correlation between an electron's energy and its longitudinal position) and then sending the beam through a dispersive element such that the longitudinal displacement of the electrons is changed in a controlled way for reducing the pulse width. For a MeV beam, this is typically achieved by first sending it through a rf buncher cavity at zero-crossing phase where the bunch head ($t < 0$) is decelerated while the bunch tail ($t > 0$) is accelerated. This imprints a positive chirp $h = d\delta/cdt > 0$ in the beam longitudinal phase space, where δ is the relative energy difference of an electron with respect to the reference electron and c is the speed of light. Then the electron beam is sent through a drift after which the electrons at the bunch tail catch up with those at the bunch head, leading to compression in the pulse width. Full compression is achieved when $hR_{56} = 1$, where $R_{56} = L/\gamma^2$ is the momentum compaction of the drift with length L and γ is the Lorentz factor of the electron.

Recently, sub-10 (fs) fs beams have been produced with this technique [18,19]. However, the rf phase jitter results in increased timing jitter after compression. While THz pulse-based time-stamping techniques have been developed to measure and correct the electron beam arrival time jitter [19,20] for UED, the detector response time limited this shot-to-shot correction technique to low repetition rate. It is highly desired (in particular for those

（72）Young's Double-Slit Interference in a Hydrogen Atom

PHYSICAL REVIEW LETTERS 124, 163201 (2020)

Young's Double-Slit Interference in a Hydrogen Atom

Pei-Lun He,[1,*] Zhao-Han Zhang,[1] and Feng He[1,2,†]
[1]Key Laboratory for Laser Plasmas (Ministry of Education) and School of Physics and Astronomy, Collaborative Innovation Center for IFSA (CICIFSA), Shanghai Jiao Tong University, Shanghai 200240, China
[2]CAS Center for Excellence in Ultra-intense Laser Science, Shanghai, 201800, China

(Received 30 September 2019; revised manuscript received 20 February 2020; accepted 7 April 2020; published 21 April 2020)

We demonstrate the possibility of realizing Young's double-slit interference in a hydrogen atom with an ultrashort pulse. By exposing the hydrogen atom to a high-frequency intense laser pulse, the bound state distorts into a dichotomic Kramers-Henneberger state whose photoelectron momentum distribution imprints a double-slit interference structure. The dichotomic hydrogen atom presents molecular peculiarities, such as charge-resonance enhanced ionization, electron spin flipping due to the non-Abelian Berry phase, etc. In return, the photoelectron momentum distribution carrying the double-slit interference structure provides unambiguous evidence on the existence of Kramers-Henneberger states, and thus the dichotomic stabilization.

DOI: 10.1103/PhysRevLett.124.163201

Double-slit interference, with which Young explicated light as waves in 1801, is one of the most vital experiments in history. Though more than two hundred years had passed, double-slit experiments continue to provide insights into both fundamental research and practical applications nowadays. For example, which-way information experiments provide testimony for the basic principle of quantum mechanics [1–3], a matterless double-slit experiment explored the fluctuation of vacuum [4], and the interference in the electron pair demonstrates the universal nonlocality of quantum entanglement [5]. As practical applications, double-slit interference can measure light coherence [6], detect molecular structures [7], and retrieve the motion of nuclei [8].

The double-slit experiment can be performed in diatomic molecules, in which the two Coulomb centers work as the double slits, and the valence electron plays the role of light in the original Young's experiment. The theoretical prediction made by Cohen and Fano [9] had been observed in molecules such as H_2 [10,11], N_2 [12], neon dimer [13], etc. It sounds counterintuitive to have such kind of double-slit interference in an atom since one atom is impossible to offer two Coulomb centers. However, there existed nontrivial analogies in the time domain. Lindner *et al.* [14] designed such kind of double slits, in which the ionization bursts produced by two successive wave packets of a few-cycle phase-stabilized pulse interfere with each other. These time-domain double slits were further studied by adding another orthogonally polarized assisting pulse [15,16]. Recently, Pursehouse *et al.* [17] considered a two-path ionization of a rubidium atom via intermediate 5P and 6P states, in which the excitation path is undetermined and the interference in wave-vector space is analogous to double-slit interference.

The existence of metastable Kramers-Henneberger states (KHSs) [18–20], which are the eigenstates of the time-averaged Hamiltonian in a high-frequency laser field [21], provides a possibility of realizing the double-slit interference in an atom. The KHS is known to be relevant for ionization stabilization [22], low-energy photoelectron generated by the nonadiabatic coupling [23,24], and dynamic interference [25–27]. The KHS plays an important role as long as the systems have exact or approximate Floquet symmetry [28]. However, while the acceleration of neutral atoms [29,30] and the amplifying of an lasing [31,32] provide tantalizing hints [30], there is still no "smoking gun" evidence for a direct experimental confirmation of the KHS up to now. The ionization stabilization of Rydberg atoms [33] does not provide convincible evidence since the nonadiabatic coupling [23,24] in intensive fields always populates a superposition of Rydberg states, as their energy gaps are small. Interference stabilization [34] might be responsible for the observed phenomena. The unavoidable focal intensity volume average effect in practice implies that the ionization signals are always from a mixture of KHSs and laser-free bound states. Thus, shifts of the photoelectron kinetic energy [35] and fine structures of the photoelectron momentum distribution (PMD) from the KH atom [36] are blurred after the focal intensity volume average.

In the Letter, we demonstrate the possibility of realizing molecular Young's double-slit interference using a single hydrogen atom. By exposing the atom to a high-frequency intensive laser field, the distorted bound state forms a dichotomic KHS [37,38]. When the atom gets ionized by a probe pulse, the PMD carries its structural information. The distinct angularly distributed PMD is robust against the focal intensity volume average, which provides

（73）Engineering of Magnetic Coupling in Nanographene

PHYSICAL REVIEW LETTERS 124, 147206 (2020)

Engineering of Magnetic Coupling in Nanographene

Yuqiang Zheng,[1] Cao Li,[1] Yan Zhao,[1] Deneke Beyer,[2] Guangyong Wang,[1] Chencheng Xu,[1] Xinlei Yue,[1] Yupeng Chen,[1] Han-Dan Guan,[1] Yan-Yi Li,[1,3] Hao Zheng,[1,3] Canhua Liu,[1,3] Wending Luo,[1,3] Xinliang Feng,[2,4] Shiyong Wang,[1,3,*] and Jinlong Hu[1,3,†]

[1]Key Laboratory of Advanced Structures and Quantum Control (Ministry of Education), Shiyanjiang National Laboratory for Materials Science, School of Physics and Astronomy, Shanghai Jiao Tong University, Shanghai 200240, China

[2]Center for Advancing Electronics Dresden & Department of Chemistry and Food Chemistry, Technische Universität Dresden, 01062 Dresden, Germany

[3]Zhangjiang Institute for Advanced Study, Shanghai Jiao Tong University, Shanghai 200240, China

[4]Max Planck Institute of Microstructure Physics, Weinberg 2, 06120 Halle, Germany

(Received 22 September 2019; revised manuscript received 17 January 2020; accepted 13 March 2020; published 10 April 2020)

Nanographenes with sublattice imbalance host a net spin according to Lieb's theorem for bipartite lattices. Here, we report the on-surface synthesis of atomically precise nanographenes and their atomic-scale characterization on a gold substrate by using low-temperature noncontact atomic force microscopy and scanning tunneling spectroscopy. Our results clearly confirm individual nanographenes host a single spin of $S = 1/2$ via the Kondo effect. In covalently linked nanographene dimers, two spins are uniformly magnetically coupled with each other as revealed by inelastic spin-flip excitation spectroscopy. The magnetic exchange interaction in dimers can be well engineered by tuning the local spin density distribution near the connecting region, consistent with mean-field Hubbard model calculations. Our work closely reveals the emergence of magnetism in nanographenes and provides an efficient way to further explore the carbon-based magnetism.

DOI: 10.1103/PhysRevLett.124.147206

Magnetism is usually associated with the 3*d* or the 4*f* elements and very rare materials (e.g., Fe, Co and Ni) are ferromagnets at room temperature. In the past decade, many works reported the emergence of magnetism in carbon-based materials [1–27], and some systems even show Curie temperatures above the room temperature [19,20,24]. Magnetic carbon-based nanostructures are particularly promising for applications in spintronics [1,28], due to the versatility of organic chemical synthesis offering flexible ways to control the structure and tune the magnetic properties, which is hard to achieve from inorganic materials. In addition, carbon-based nanomaterials are expected to have high magnitudes of spin-wave stiffness [29], weak spin-orbit coupling [30], and hyperfine couplings [31], which promise for high temperature magnets, transport of spin-polarized currents [32], and spin-based quantum information processing [1,17,28].

Intuitively, carbon atoms are unlikely to form magnetic order since *sp* electrons prefer to pair up to form covalent bonds. Theoretical calculations addressing carbon-based magnetism have mainly focused on impurities, point defects, or reduced dimensionality, such as the ferromagnetic order at graphene zigzag edges [32–34], the large net spin in graphene nanostructures with sublattice imbalance [20,34–38], and magnetic order in topological frustrated graphene nanostructures [39,40]. Magnetism of graphene-based materials depends crucially on their atomic structure and surrounding environments. Because of the difficulties encountered in fabricating and characterizing atomically precise graphene nanostructures, the direct comparison between experimental results and theory calculations is impeded, leaving many questions unclear. Thus, it is of great demanding to study the magnetic properties of graphene nanostructures at the atomic level.

In this Letter, we report the engineering of magnetism in atomically precise nanographenes monomers and covalently linked dimers. Scanning tunneling microscopy or spectroscopy (STM/STS), noncontact atomic force microscopy (nc-AFM), together with single particle mean-field Hubbard model and spin-polarized density functional theory (DFT) calculations are combined to determine the magnetic properties of the achieved nanographenes with atomic precision. Our studied nanographenes are fabricated by using the on-surface synthesis approach, which has been widely adopted to prepare atomically precise graphene nanostructures [5,6,11–26,41–44] (see detailed synthesis steps in Supplemental Material [45], Figs. (S1) and (S2)). Molecular precursors of 9,10-bis(4-bromo-2,6-dimethylphenyl)anthracene were thermally deposited on clean Au(111), and the sample was rapidly annealed to ~400 °C to induce C-C addition reactions and cyclodehydrogenation reactions, forming atomically precise magnetic

（74）Multiple In-Gap States Induced by Topological Surface States in the Superconducting Topological Crystalline Insulator Heterostructure Sn1−xPbxTe-Pb

PHYSICAL REVIEW LETTERS 125, 136802 (2020)

Multiple In-Gap States Induced by Topological Surface States in the Superconducting Topological Crystalline Insulator Heterostructure $Sn_{1-x}Pb_xTe$-Pb

Hao Yang,[1] Yan-Yu Liu,[1,*] Teng-Peng Liu,[1] Dan-Dan Guan,[1,3] Shi-Yong Wang,[1,3] Hao Zheng,[1,3] Canhua Liu,[2,3] Liang Fu,[2] and Jin-Feng Jia[1,3,4]

[1]Key Laboratory of Artificial Structures and Quantum Control (Ministry of Education), Shenyang National Laboratory for Materials Science, School of Physics and Astronomy, Shanghai Jiao Tong University, Shanghai 200240, China
[2]Department of Physics, Massachusetts Institute of Technology, Cambridge, Massachusetts 02139, USA
[3]CAS Center for Excellence in Topological Quantum Computation, University of Chinese Academy of Sciences, Beijing 100190, China
[4]Tsung-Dao Lee Institute, Shanghai Jiao Tong University, Shanghai 200240, China

(Received 14 April 2020; accepted 4 August 2020; published 22 September 2020)

Superconducting topological crystalline insulators (TCIs) have been proposed to be a new type of topological superconductor where multiple Majorana zero modes may coexist under the protection of mirror symmetries. The bulk superconductivity of TCIs has been realized, but it is quite challenging to detect the superconductivity of topological surface states inside their bulk superconducting gaps. Here, we report high-resolution scanning tunneling spectroscopy measurements on lateral $Sn_{1-x}Pb_xTe$-Pb heterostructures using superconducting tips. Both the bulk superconducting gap and the multiple in-gap states with energy differences of ~0.3 meV can be clearly resolved in TCI $Sn_{1-x}Pb_xTe$ at 0.38 K. Quasiparticle interference measurements further confirm the in-gap states are gapless. Our work demonstrates that the unique topological superconductivity of a TCI can be directly distinguished in the density of states, which helps to further investigate the realistic Dirac and Majorana fermions inside the superconducting gap.

DOI: 10.1103/PhysRevLett.125.136802

Research on topological superconductors (TSCs) is rapidly developing due to their significance in the quantum science and technology involving Majorana zero modes (MZMs) and topological qubits [1–3]. Evidence for unconventional superconductivity including MZMs has been found in superconducting topological insulators (TIs) such as Bi_2Te_3-type TIs/NbSe$_2$ heterostructures [4–9], some iron-based superconductors (SCs) [10–14], transition metal dichalcogenide 2M WS_2 [14,15]. In contrast to the TI protected by time-reversal symmetry, a topological crystalline insulator (TCI) possesses the topological surface states protected by crystalline symmetry [16,17]. The multiple surface Dirac cones are observed in the SnTe-type IV-VI semiconductors with a rock-salt crystal structure [18–20]. Recently, superconducting topological crystalline insulators (TCIs) have been predicted to be a new type of TSC containing MZMs [21,22]. The hybridization between MZMs is forbidden by lattice symmetry, so multiple MZMs are expected to coexist at a single vortex. The bulk superconductivity of TCIs can be induced through chemical doping [23,24] and superconducting proximity effect [25–27]. Tight-binding models predict that a superconducting TCI with topological superconductivity has multiple surface Andreev bound states inside its superconducting gap [28], which is topologically distinct from a conventional SC and a superconducting TI [29]. However, these unique properties have not been observed due to the challenges in the preparation of good samples with proper doping levels and the characterization of topological surface states inside such a small superconducting gap of only ~1 meV.

In this Letter, we report high-resolution scanning tunneling microscopy (STM) and scanning tunneling spectroscopy (STS) measurements on $Sn_{1-x}Pb_xTe$-Pb heterostructures. Atomically flat lateral $Sn_{1-x}Pb_xTe$-Pb heterostructures are prepared by molecular beam epitaxy. The intrinsic superconductivity of both TCI $Sn_{1-x}Pb_xTe$ and conventional SC Pb can be effectively detected. In order to increase the resolution, superconducting tips and low temperature down to 0.38 K are used. The STS spectra are simulated with the standard superconductor-insulator-superconductor (S-I-S) tunneling model. The in-gap resonances have energy differences of ~0.3 meV. Quasiparticle interference measurements taken inside the superconducting gap of $Sn_{1-x}Pb_xTe$ further confirm the in-gap states are gapless. The *in situ* low-temperature STS study provides the first direct experimental evidence of multiple in-gap states induced by topological surface states in a superconducting TCI.

Our experiments were performed in a commercial STM system (Unisoku) with a ^{3}He cryostat. Details about the growth of $Sn_{1-x}Pb_xTe$-Pb heterostructures ($x \sim 30\%$) are described elsewhere [30]. Figures 1(a) and 1(b) are STM topography and schematic diagram of a lateral $Sn_{1-x}Pb_xTe$-Pb heterostructure respectively. The temperature dependence of the superconducting gaps taken on Pb and

（75）Strain Tunable Semimetal–Topological-Insulator Transition in Monolayer 1T0 -WTe2

PHYSICAL REVIEW LETTERS 125, 046801 (2020)

Strain Tunable Semimetal–Topological-Insulator Transition in Monolayer 1T′-WTe_2

Chenhao Zhao,[1] Mengli Hu,[1] Jin Qin,[1] Bing Xia,[1] Caihua Liu,[1,2] Shiyong Wang,[1,3] DanDan Guan,[1] Yaoyi Li,[1,3] Hao Zheng,[1,3] Jinwei Liu,[1,3] and Jiafeng Jia[1,2,3]

[1]Key Laboratory of Artificial Structures and Quantum Control (Ministry of Education), Shanghai Jiao Tong University, Shanghai 200240, China
[2]Department of Physics, Hong Kong University of Science and Technology, Hong Kong, China
[3]Tsung-Dao Lee Institute, Shanghai Jiao Tong University, Shanghai 200240, China
[4]CAS Center for Excellence in Topological Quantum Computation, University of Chinese Academy of Sciences, Beijing 100190, China

(Received 3 January 2020; accepted 25 June 2020; published 24 July 2020)

A quantum spin Hall insulator is manifested by its conducting edge channels that originate from the nontrivial topology of the insulating bulk states. Monolayer 1T′-WTe_2 possesses the quantized edge conductance in transport measurements, but because of its semimetallic nature, the coherence length is restricted to around 1 μm. To overcome the restriction, we propose a strain engineering technique to tune the electronic structure, where either a compressive strain along the a axis or a tensile strain along the b axis can drive 1T′-WTe_2 into an full gap insulating phase. A combined study of molecular beam epitaxy and in situ scanning tunneling microscopy or spectroscopy then confirmed such a phase transition. Meanwhile, the topological edge states were found to be very robust in the presence of strain.

Monolayer transition metal dichalcogenides (TMDs) in 1T′ structure are predicted to be quantum spin Hall insulators (QSHIs) [1]. Within this family, WTe_2 and WSe_2 have been verified experimentally using angle-resolved photoemission spectroscopy (ARPES) [2–4] and scanning tunneling microscopy or spectroscopy (STM/STS) [2–5]. Moreover, monolayer 1T′-WTe_2 has already been confirmed to be topological nontrivial by various nonlocal transport measurements [6] and to exhibit a fully quantized conductance up to 100 K [7]. However, the coherent edge channel length is found to be around 100 nm because of the semimetallic nature of the bulk states [7], hindering both further fundamental research and potential applications. To overcome this hindrance, it is necessary to manipulate the electronic structure of monolayer WTe_2 to realize a full gap insulator. In principle, the electronic structure of a material can be engineered using various external fields such as electric or mechanical strain fields. Recently, electrical tuning has been applied extensively to TMD materials for many structures [8], superconductivity [9,10], and Berry curvature dipole [11]. For low-dimensional systems, strain engineering is a very general and effective approach and is technologically feasible. Examples include strain-induced topological phase transitions [12], strain engineering Dirac states [13–15], strain-induced flat band [15,16], strain tunable magnetism in domain walls [17], strain-induced surface-dominated conduction [18], and strain-enhanced superconductivity [19]. However, related studies in the TMD family are relatively limited and unproved [1,2,20]. So far, no method has been found to tune the band structures of monolayer 1T′-WTe_2 effectively.

In this work, based on orbital analysis and the first-principles calculations, we proposed to use strain to optimize the band structure of monolayer 1T′-WTe_2, and we found that a compressive strain along the a axis or a tensile strain along the b axis can convert monolayer WTe_2 from a semimetal to an insulator. This was further confirmed by a systematic study using molecular beam epitaxy (MBE) and STM, where strains were introduced by the distorted substrate. The strain status of WTe_2 films was measured by STM, and the corresponding band structures were characterized by differential conductance (dI/dV) spectra. Based on experimental data, we find that a moderate in-plane strain can open a full insulating gap in WTe_2, and the gap size is positively related with lattice constant b and negatively related with a (a and b are marked in Fig. 1(a)), consistently with the theoretical results. Moreover, the topological edge states are obtained on both semimetallic and insulating WTe_2 islands, indicating that the nontrivial topology is robust in the presence of external strains. Our results unambiguously demonstrate the feasibility of strain engineering to realize the fully gapped QSHI in monolayer 1T′-WTe_2, making 1T′-WTe_2 a suitable material platform for developing controllable topological electronic devices with a long coherence length.

Monolayer 1T′-WTe_2 has a rectangular unit cell as shown in Fig. 1(a), where one W-atom layer is sandwiched between two Te-atom layers. Moreover, there is a Peierls distortion along the a axis, inducing a large band inversion at the Γ point and driving monolayer 1T′-WTe_2 into a Z_2-topological phase [1]. However, a finite overlap between the valence

（76）A hybrid quantum memory-enabled network at room temperature

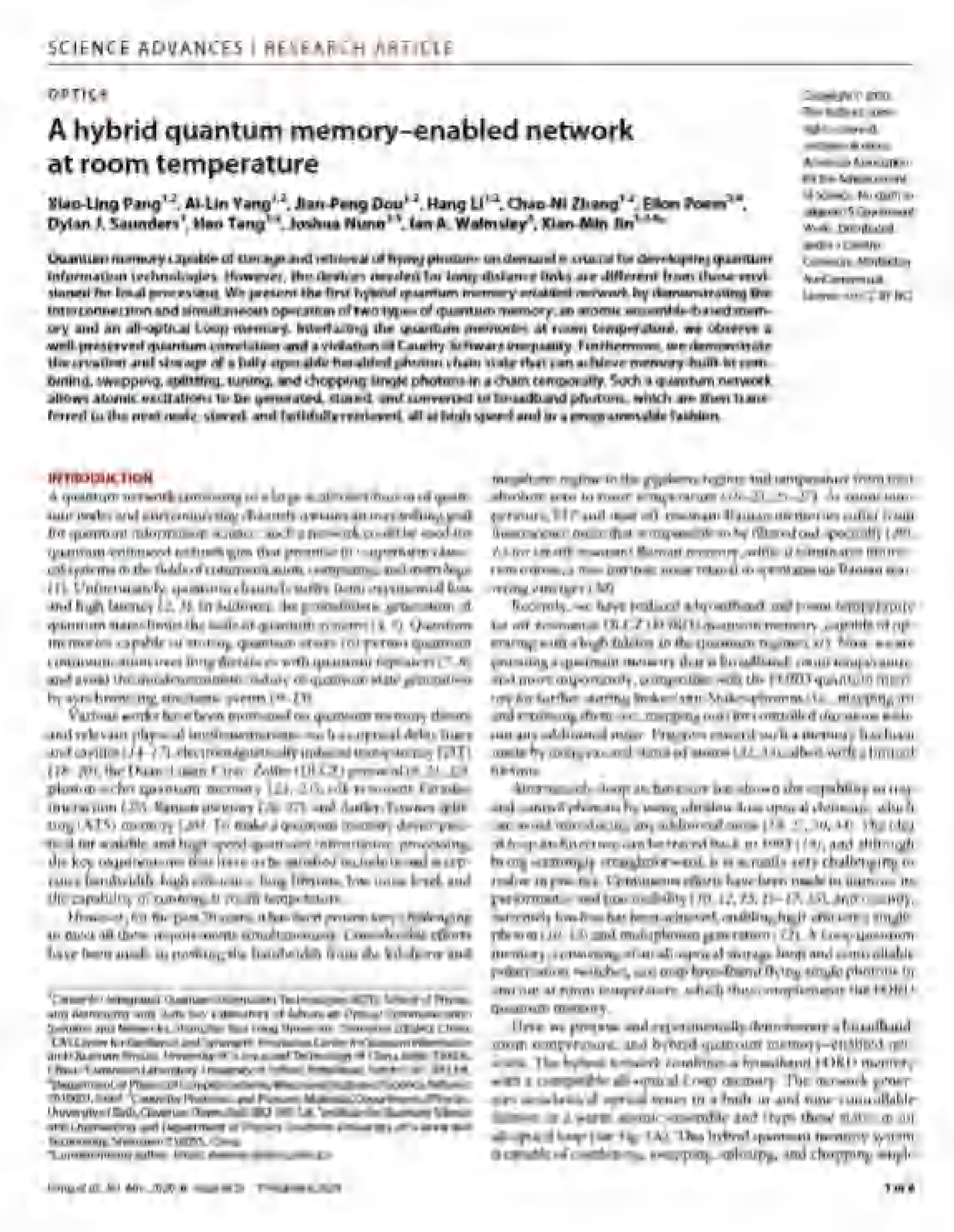

OPTICS

A hybrid quantum memory–enabled network at room temperature

Xiao-Ling Pang[1,2], Ai-Lin Yang[1,2], Jian-Peng Dou[1,2], Hang Li[1,2], Chao-Ni Zhang[1,2], Eilon Poem[3,4], Dylan J. Saunders[3], Hao Tang[1,2], Joshua Nunn[3,5], Ian A. Walmsley[3], Xian-Min Jin[1,2,6]*

Quantum memory capable of storage and retrieval of flying photons on demand is crucial for developing quantum information technologies. However, the devices needed for long-distance links are different from those envisioned for local processing. We present the first hybrid quantum memory–enabled network by demonstrating the interconnection and simultaneous operation of two types of quantum memory: an atomic ensemble–based memory and an all-optical Loop memory. Interfacing the quantum memories at room temperature, we observe a well-preserved quantum correlation and a violation of Cauchy-Schwarz inequality. Furthermore, we demonstrate the creation and storage of a fully operable heralded photon chain state that can achieve memory-built-in combining, swapping, splitting, tuning, and chopping single photons in a chain temporally. Such a quantum network allows atomic excitations to be generated, stored, and converted to broadband photons, which are then transferred to the next node, stored, and faithfully retrieved, all at high speed and in a programmable fashion.

INTRODUCTION

（77）A scalable photonic computer solving the subset sum problem

OPTICS

A scalable photonic computer solving the subset sum problem

Xiao-Yun Xu[1,2], Xuan-Lun Huang[1,2], Zhan-Ming Li[1,2], Jun Gao[1,2], Zhi-Qiang Jiao[1,2], Yao Wang[1,2], Ruo-Jing Ren[1,2], H. P. Zhang[3], Xian-Min Jin[1,2,4]*

The subset sum problem (SSP) is a typical nondeterministic-polynomial-time (NP)–complete problem that is hard to solve efficiently in time with conventional computers. Photons have the unique features of high propagation speed, strong robustness, and low detectable energy level and therefore can be promising candidates to meet the challenge. Here, we present a scalable chip built-in photonic computer to efficiently solve the SSP. We map the problem into a three-dimensional waveguide network through a femtosecond laser direct writing technique. We show that the photons sufficiently dissipate into the networks and search for solutions in parallel. In the case of successive primes, our approach exhibits a dominant superiority in time consumption even compared with supercomputers. Our results confirm the ability of light to realize computations intractable for conventional computers, and suggest the SSP as a good benchmarking platform for the race between photonic and conventional computers on the way toward "photonic supremacy."

INTRODUCTION

RESULTS

Configuration of the photonic computer for the SSP

（78）Extremely brilliant GeV -rays from a two-stage laser-plasma accelerator

（79）Multifunctional antiferromagnetic materials with giant piezomagnetism and noncollinear spin current

nature COMMUNICATIONS

ARTICLE

OPEN

Multifunctional antiferromagnetic materials with giant piezomagnetism and noncollinear spin current

Hai-Yang Ma[1,5], Mengli Hu[2,5], Nana Li[2,5], Jianpeng Liu[2], Wang Yao[3], Jin-Feng Jia[1,4✉] & Junwei Liu[2✉]

We propose a new type of spin-valley locking (SVL), named C-paired SVL, in antiferromagnetic systems, which directly connects the spin/valley space with the real space, and hence enables both static and dynamical controls of spin and valley to realize a multifunctional antiferromagnetic material. The new emergent quantum degree of freedom in the C-paired SVL is comprised of spin-polarized valleys related by a crystal symmetry instead of the time-reversal symmetry. Thus, both spin and valley can be accessed by simply breaking the corresponding crystal symmetry. Typically, one can use a strain field to induce a large net valley polarization/magnetization and use a charge current to generate a large noncollinear spin current. We predict the realization of the C-paired SVL in monolayer V_2Se_2O, which indeed exhibits giant piezomagnetism and can generate a large transverse spin current. Our findings provide unprecedented opportunities to integrate various controls of spin and valley with nonvolatile information storage in a single material, which is highly desirable for versatile fundamental research and device applications.

[1] Key Laboratory of Artificial Structures and Quantum Control (Ministry of Education), Shanghai National Laboratory for Materials Science, School of Physics and Astronomy, Shanghai Jiao Tong University, Shanghai, China. [2] Department of Physics, The Hong Kong University of Science and Technology, Hong Kong, China. [3] Department of Physics and Center of Theoretical and Computational Physics, University of Hong Kong, Hong Kong, China. [4] Tsung-Dao Lee Institute, Shanghai, China. [5] These authors contributed equally: Hai-Yang Ma, Mengli Hu, Nana Li. ✉email: jiafeng@sjtu.edu.cn; liuuw@ust.hk

（80）Sierpiński Structure and Electronic Topology in Bi Thin Films on InSb(111)B Surfaces

Sierpiński Structure and Electronic Topology in Bi Thin Films on InSb(111)B Surfaces

Chen Liu,[1] Yiming Zhou,[2] Chunyong Wang,[1] Yin Yin,[2] Can Li,[1] Haili Huang,[1] Dandan Guan,[1,3] Yaoyi Li,[1,3] Shiyong Wang,[1,3] Hao Zheng,[1,3] Canhua Liu,[1,3] Yong Han,[2,*] James W. Evans,[2,4] Feng Liu,[2] and Jinfeng Jia[1,3]
[1]Key Laboratory of Artificial Structures and Quantum Control (Ministry of Education), Shanyuan Natural Laboratory for Materials Science, School of Physics and Astronomy, Shanghai Jiao Tong University, Shanghai 200240, China
[2]Department of Materials Science and Engineering, University of Utah, Salt Lake City, Utah 84112, USA
[3]Shenzhen Institute for Quantum Science and Engineering, Southern University of Science and Technology, Shenzhen 518055, China
[4]Ames Laboratory, U.S. Department of Energy, Ames, Iowa 50011, USA

(Received 23 November 2020; revised 11 February 2021; accepted 19 March 2021; published 30 April 2021)

Deposition of Bi on InSb(111)B reveals a striking Sierpiński triangle (ST) like structure in Bi thin films. Such a fractal geometric topology is further shown to host the nontrivial electronic topology in a thin film. Relaxation of a huge misfit strain of about 30% to 40% for our Bi adlayer and substrate is revealed to drive the ST-like island formation. A Frenkel-Kontorova model is developed to illustrate the enhanced strain relief in the ST islands, offsetting the additional step energy cost. Besides a unique and large tensile strain, forming ST-like structure also requires large adlayer-substrate and intra-adlayer elastic stiffnesses, and weaker intra-adlayer interatomic interactions.

DOI: 10.1103/PhysRevLett.126.176102

The Sierpiński triangle (ST) [1] is a self-similar fractal with a fractional Hausdorff dimension $d_H = \log 3 / \log 2 = 1.584\,96\ldots$ and with fascinating mathematical properties [2]. Historically, such beautiful patterns were often utilized for aesthetic reasons, especially in architecture, e.g., on the medieval floors in Rome [3]. Many fundamental and intriguing phenomena in ancient and modern mathematics and physics, as well as everyday science, are related to the STs, such as Pascal triangles [4], towers of Hanoi [5], chaos games [6], cellular automata [7], DNA computing [8,9], etc.

Theory and experiments have shown that fractal materials can exhibit plentiful and unusual thermal, mechanical, electric, electronic, electromagnetic, and optical properties which are often desirable for prospective nanoskyscale applications [10–16]. Fractal quasicrystals have even been predicted to possess nontrivial electronic topology usually presumed to cry stals [17,18]. Recently, there has been also considerable interest in fabricating ST-like fractal materials, although the synthesis of such systems is notoriously difficult [19]. In 2014, a terpyridine-based architecture mimicking ST was synthesized in solution [20]. Subsequently, several research groups have successfully fabricated the fractal supramolecular materials featuring the ST pattern on the coinage metal surfaces: Ag(111) [21], Ag(100) [22], Au(111) [23–28], Au(100) [28,29], and Cu(111) [30], as well as on a graphite surface [31]. These fabricated fractal supramolecules can be organic, metal organic, CO compounds, etc. [16]. Theoretically, Monte Carlo simulations show that the formation of molecular STs in these systems is essentially related to directional intermolecular bonds [32,33].

As indicated above, previous fabrication of STs in experiments is by assembling small carbon-based nanocrystals into supramolecules. There has not yet been any report of the synthesis for STs comprised of single-element atoms. Obviously, experimental fabrication of such pure single-element STs is more challenging without the specifically shaped tectons providing directional intermolecular interactions [32,33]. In this work, by depositing Bi atoms on an InSb(111)B surface around 400 K, we have observed ST-like Bi films with a thickness of one to three monatomic layers (MLs) from our scanning tunneling microscope (STM) experiments. Our proposed theoretical model reveals that the formation of a Bi ST island requires an unusually large lattice mismatch between a monatomic Bi adlayer and substrate, relatively large adlayer-substrate and intra-adlayer elastic stiffnesses, and relatively weak intra-adlayer interatomic interactions. This formation mechanism essentially differs from that of the supramolecular STs synthesized previously.

In addition, it has been predicted theoretically that an ultrathin Bi film exhibits a stable nontrivial topological property [34–36], which makes the investigations of heteroepitaxial growth of ultrathin Bi films fundamentally interesting. Experiments have demonstrated the existence

（81）Controlling Cell Motion and Microscale Flow with Polarized Light Fields

PHYSICAL REVIEW LETTERS 126, 058001 (2021)

Controlling Cell Motion and Microscale Flow with Polarized Light Fields

Siyuan Yang,[1] Mingji Huang,[1] Yongfeng Zhao,[1] and H. P. Zhang[1,2,*]
[1]School of Physics and Astronomy and Institute of Natural Sciences, Shanghai Jiao Tong University, Shanghai 200240, China
[2]Collaborative Innovation Center of Advanced Microstructures, Nanjing 210093, China

(Received 14 September 2020; revised 26 November 2020; accepted 23 December 2020; published 4 February 2021)

We investigate how light polarization affects the motion of photosensory algae, *Euglena gracilis*. In a uniformly polarized field, cells move approximately perpendicular to the polarization direction and form a nematic state with zero mean velocity. When light polarization varies spatially, cell motion is coordinated by local polarization, and such light fields yield complex cell-number distribution and vortex patterns which are controlled by topological properties of the underlying fields. We further show that ordered cell swimming can generate effective flow. Experimental results are quantitatively reproduced by an active Brownian particle model in which particle swimming direction is dynamically coupled to local light polarization.

DOI: 10.1103/PhysRevLett.126.058001

Natural microswimmers, such as bacteria and algae, can achieve autonomous motion by converting locally stored energy into mechanical work [1–15]. Such cellular motility is not only an essential aspect of life but also an inspirational source to develop artificial microswimmers which propel themselves through self-generated fields of temperature, chemical concentration, or electric potential [1,3–7,12,13]. Both natural and artificial microswimmers have been used in a wide variety of applications [1]–[15].

To properly function in a fluctuating heterogeneous environment, microswimmers need to adjust their motility in response to external stimuli [16–23]. For example, intensity and direction of ambient light can induce a variety of motility responses in photosynthetic microorganisms [24–26] and artificial microswimmers [10–15]; these responses have been frequently used to control microswimmer motion [27,30,34–36,45–51]. Besides intensity and direction, light *polarization* can also affect microswimmer motility and lead to polarotaxis. *Euglena viridis* cells align their motion direction perpendicular to the light polarization, possibly to maximize the light absorption [44,53]; artificial microswimmers consisting of two dielectric nanowires move in the polarization direction [44]. These previous experiments have focused on uniform light fields [44,54,55]. The possibility to use complex polarization patterns to control prokaryotic microswimmers has not been explored.

In this Letter, we investigate *Euglena gracilis* cell motion in various polarized light fields in a quantitative and systematic fashion. Our experiments show that, while spatially uniform polarization aligns cells into a global nematic state with no net motion, spatially varying fields can induce both local nematic order and mean cell motion. Further, we show that ordered cell swimming can generate fluid flow that can transport passive tracers. Using the experimental data of individual cells, we construct a model to describe the influence of local light polarization on cell orientation dynamics and quantitatively reproduce all experimental observations.

Experiments.—*Euglena* cells are unicellular flagellated microorganisms with a rod-shaped body of a length $\sim 50\ \mu$m and a width $\sim 5\ \mu$m. As shown in Fig. 1(a) and Movie S1 in the Supplemental Material [56], cells swim at a mean speed $\sim 60\ \mu$m/s (with a standard deviation of $10\ \mu$m/s), while rolling around their long axis at a frequency of 1–2 Hz [57]. A photoreceptor on *Euglena* cell surface, marked as a red dot in Fig. 1(b), senses surrounding light and generates signals to modulate flagellar beating pattern [53,55].

In our experiments, *Euglena* culture is sealed in a disk-shaped chamber ($\sim 150\ \mu$m in thickness and 24 mm in diameter), which is placed on an illuminating light path, as shown in Fig. S1 [56]. A collimated blue light beam is used to excite cell photoresponse; the default light intensity is $100\ \mu$W/cm^2. Various polarized optical fields can be generated by using different birefringent liquid crystal plates and by changing relative angles between optical elements [56]. Cell motion is recorded by a camera mounted on a microscope. Default system cell density ($\rho_0 \approx 8$ cells/mm^2) is sufficiently low that we can use a standard particle tracking algorithm [58] to measure position, orientation, and velocity of cells. The current work mainly focuses on steady-state dynamics that is invariant over time.

Uniformly polarized light field.—*Euglena* photoreceptor contains dichroically oriented chromoproteins which lead to polarization-dependent photoresponses [53,59–61]. As shown in Fig. 1(a), cells in a uniformly polarized field tend to orient and swim perpendicularly to the polarization [53]; we denote such a targeted direction for cells as θ_T

（82）X-Ray Tomography Investigation of Cyclically Sheared Granular Materials

PHYSICAL REVIEW LETTERS 126, 048002 (2021)

X-Ray Tomography Investigation of Cyclically Sheared Granular Materials

Yi Xing,[1] Jie Zheng,[1] Jindong Li,[1] Yixin Cao,[2] Wei Pan,[1] Jie Zhang,[1,2] and Yujie Wang[1,*]
[1]School of Physics and Astronomy, Shanghai Jiao Tong University, 800 Dong Chuan Road, Shanghai 200240, China
[2]Institute of Natural Sciences, Shanghai Jiao Tong University, Shanghai 200240, China
[3]Materials Genome Initiative Center, Shanghai Jiao Tong University, 800 Dong Chuan Road, Shanghai 200240, China

(Received 4 July 2020; revised 26 October 2020; accepted 4 January 2021; published 27 January 2021)

We perform monochromatic x-ray tomography and shear force measurements on cyclically sheared granular systems with highly transient behaviors, and obtain the evolutions of macroscopic structure and macroscopic shear force during the shear cycle. We explain the macroscopic behaviors of the system based on microscopic processes, including particle level structural rearrangement and frictional contact evolution. Specifically, we show how contact friction can induce large structural fluctuations and cause significant shear dilatancy effect for granular materials, and we also construct an empirical constitutive relationship for the macroscopic shear force.

DOI: 10.1103/PhysRevLett.126.048002

Dense granular materials exhibit complex behaviors upon shear. Notable examples include significant dilatancy [1], formation of shear bands [2], emergence of anisotropic force networks [3], and critical state [4]. However, the theoretical understanding of sheared granular materials remains very challenging since conventional continuum mechanics are no longer applicable due to the disordered nature of granular materials, as well as the complex role friction plays [5,6]. In practice, empirical constitutive theories are normally employed, including the famous Mohr-Coulomb criterion [7] and more sophisticated viscoplastic models [8]. However, these models are mainly macroscopic ones with little microscopic basis despite the fact that it is well known experimentally that microscopic structure and dynamics can strongly influence the macroscopic response [9]. Granular materials belong in general to the family of disordered materials like metallic and colloidal glasses, foams, emulsions, etc., and physicists have tried to treat the flow of dense granular materials within the general framework of disordered materials [9]. For example, theories based on free volume [10], shear transformation zone [11], and soft glass rheology (SGR) rheology [12], which are built upon microscopic and mesoscopic information to predict the plastic behaviors of certain disordered materials, have been directly applied to the granular case [13,14]. However, granular materials possess some peculiar properties, e.g., force chains [15,16], significant volume and stress fluctuations [6,17,18], and complex microscopic dynamics [19], which are not shared among all disordered materials. These properties are mainly induced by the frictional interparticle contacts. Therefore, to construct the correct constitutive theory for the flow of dense granular materials, physics on particle and contact levels have to be considered [20].

In this Letter, we apply cyclic shear to a three-dimensional (3D) disordered granular system. The system displays highly transient dilational behavior and mechanical response since the system always has to reorganize upon sudden shear reversal [14,21]. By combining x-ray tomography and shear force measurements, we obtain both macroscopic structure evolution and macroscopic mechanical response of the system simultaneously. Based on these results, we can explain the macroscopic behaviors of sheared granular matter through the microscopic structural information including both particle level structural rearrangement and frictional contact evolution. We can then understand why granular materials demonstrate significant shear dilation as compared to other disordered materials, and also construct an empirical constitutive relationship to account for the macroscopic shear force behavior.

Our granular system consists of bidisperse smooth plastic beads ($\mu = 0.4$, diameters 5 and 6 mm; 7680 particles of each size). The bidisperse nature ensures no crystallization occurs in the system. The particles are placed in a shear cell mounted on a linear stage as shown in Fig. 1(a). The shear cell is in simple shear geometry and has an inner dimension of $24d \times 24d \times 34d$, where

FIG. 1. (a) Schematic of the experimental setup: granular packing is sheared by the motion of the three plates, and the macroscopic shear force τ measured by the force sensor. (b) Evolutions of the global volume fraction ϕ and shear force F within one cycle (ensemble averaged over 12 realizations).

（83）Connecting Packing Efficiency of Binary Hard Sphere Systems to Their Intermediate Range Structure

Connecting Packing Efficiency of Binary Hard Sphere Systems to Their Intermediate Range Structure

Houfei Yuan,[1] Zhen Zhang,[2] Walter Kob,[3,*] and Yujie Wang[1,†]
[1]School of Physics and Astronomy, Shanghai Jiao Tong University, Shanghai 200240, China
[2]Center for Alloy Innovation and Design, State Key Laboratory for Mechanical Behavior of Materials, Xi'an Jiaotong University, Xi'an 710049, China
[3]Laboratoire Charles Coulomb, University of Montpellier and CNRS, F-34095 Montpellier, France

(Received 31 August 2021; revised 9 November 2021; accepted 1 December 2021; published 23 December 2021)

Using computed x-ray tomography we determine the three-dimensional (3D) structure of binary hard sphere mixtures as a function of composition and size ratio of the particles q. Using a recently introduced two-point correlation function we reveal that this 3D structure has an intermediate and large length scale structurally regular order, the symmetry of which depends on q. The mutual structural correlation length has a maximum at the composition in which the packing fraction is highest. At the composition also the number of different local particle arrangements has a maximum, indicating that efficient packing of particles is associated with a structure that is locally maximally disordered.

DOI: 10.1103/PhysRevLett.127.278001

Hard sphere (HS) systems play a paramount role in statistical mechanics and material science since they are important models to study the behavior of many-particle systems like liquids, colloids, and metallic glasses [1–4]. Also in the domain of granular materials many experimental and theoretical studies have used HS-like systems since granular particles usually have a high modulus and the simplicity of the particle shape allows us to probe the influence of friction and roughness on the properties of granular assemblies [5,6]. Since for HS the interaction energy between the particles is trivial, the properties of such systems is encoded in their structure and hence many previous studies have aimed to characterize it on various length scales [1,4,6,7,8]. Many of these investigations focused on one-component systems since this choice facilitates the description of the packing structure [1,7]. However, in the context of the glass transition one also often uses weakly polydisperse samples or a slightly asymmetric binary mixture since this suppresses the crystallization of the liquid while keeping its structure close to the well understood one-component case [9,10]. These studies have shown that, depending on the composition and the packing fraction, the local structure, i.e., the first nearest neighbor shell, shows a surprisingly rich variety [10–13]. In contrast to these almost one-component systems, the case of mixtures in which the particles have a size ratio that differs significantly from unity has been studied much less [16–22]. Understanding this structure is, however, important since such highly asymmetric systems are relevant for describing the behavior of real granular materials, which are usually highly polydisperse as well as for the glass-forming ability of multicomponent systems like metallic glasses in which the atoms can have very different radii [23–29]. In addition it has recently been found that such strongly asymmetric mixtures can have local structures with unexpected symmetries which can, e.g., be used to create novel materials via self-assembly [30]. The main reason for our lack of understanding of these systems is that their theoretical description is significantly more complex and experiments on colloidal systems are hampered by the precise control of size ratio, while granular systems are prone to the phenomenon of phase separation [31,32]. A further problem that one faces with these systems is the difficulty to characterize their structure on intermediate length scales since the presence of two particle sizes gives rise to a highly complex distance dependency of the partial radial distribution functions, i.e., the standard quantities that are used to characterize the structure of many-body systems [19,33–35]. Because of these difficulties there is at present little insight on how the size ratio or the composition affects the packing density or the structure of asymmetric HS systems.

In this work we use the computed tomography (CT) technique to probe how composition and size ratio affect the packing fraction of a binary granular system. Using a recently developed method to characterize the structure of disordered systems at intermediate and large length scales we are able to show that a high packing fraction is intimately related to the presence of a short structural correlation length.

Our system is a binary mixture of particles (acrylonitrile butadiene styrene plastic), denoted in the following as "big" (b) and "small" (s) particles, with size ratio $q = d_b/d_s$, where d_s and $d_b = 7.0$ mm are the respective diameters. The number fraction of small particles will be denoted by c. We consider two size ratios: $q = 1.33$, which corresponds

（84）Dynamical Transitions and Critical Behavior between Discrete Time Crystal Phases

PHYSICAL REVIEW LETTERS 126, 020602 (2021)

Dynamical Transitions and Critical Behavior between Discrete Time Crystal Phases

Xiaojun Yang[1] and Zi Cai[1,2]
[1]Wilczek Quantum Center and Key Laboratory of Artificial Structures and Quantum Control, School of Physics and Astronomy, Shanghai Jiao Tong University, Shanghai 200240, China
[2]Shanghai Research Center for Quantum Sciences, Shanghai 201315, China

(Received 19 July 2020; revised 1 December 2020; accepted 21 December 2020; published 12 January 2021)

In equilibrium physics, spontaneous symmetry breaking and elementary excitations are two concepts closely related with each other: the symmetry and its spontaneous breaking not only control the dynamics and spectrum of elementary excitations, but also determine their underlying structures. In this Letter, based on an exactly solvable model, we propose a phase ramping protocol to study an excitationlike behavior of a nonequilibrium quantum matter, a discrete time crystal phase with spontaneous temporal translational symmetry breaking. It is shown that slow ramping could induce a dynamical transition between two Z_2 symmetry breaking time crystal phases in time domain, which can be considered as a temporal analog of the soliton excitation spatially sandwiched by two degenerate charge density wave states in polyacetylene. By tuning the ramping rate, we observe a critical value at which point the transition duration diverges, resembling the critical slowing down phenomenon in nonequilibrium quantum physics. We also discuss the effect of stochastic sequences of such phase ramping processes and its implication to the stability of the discrete time crystal phase against noisy perturbations.

DOI: 10.1103/PhysRevLett.126.020602

Usually the ground state energy of an equilibrium system does not have much to do with its observable behavior. What is physically important are the properties of low-lying excited states, which are likely to be excited owing to weak external fields or relatively low temperatures. For example, the thermal and elastic properties of a solid are determined by a few number of lattice wave excitations known as phonons [1]. Nonequilibrium quantum matter fundamentally differs from its equilibrium counterparts, and has received considerable interest in various fields ranging from ultracold atoms [2] to solid state physics [3] over the past decade. However, compared to equilibrium cases, much less is known about the "excitation" of nonequilibrium quantum matter, even its definition may be questionable, let alone its relationship with fundamental properties of nonequilibrium quantum matter, e.g., the symmetries and their spontaneous breaking.

As a prototypical example of nonequilibrium quantum matter, the time crystal (TC) phase has allowed new possibilities for the spontaneous symmetry breaking (SSB) paradigm [4], and have attracted considerable interest in its different forms [5–22]. Such a intriguing state, despite being proved to be forbidden in equilibrium [23,24], has been experimentally realized in nonequilibrium settings with periodic driving [25,26]. Its physical observables develop persistent oscillations whose periods are an integer multiple of the Hamiltonian period, thus spontaneously break the discrete temporal translational symmetry (DTTS). In equilibrium systems, the SSB is closely related to the elementary excitation: it does not only affect the dynamics and spectrum of an elementary excitation, but it also determines its structure. For example, for a one-dimensional (1D) system, a spontaneous discrete spatial translational (e.g., Z_2) symmetry breaking allows certain solitonlike excitation: a topological defect sandwiched by two Z_2 symmetry breaking phases [27]. A profound question is how to generalize such an idea into the nonequilibrium quantum matters with intriguing SSB absent in equilibrium physics (e.g., DTTS breaking).

In this Letter, we address this issue by studying a driven 1D interacting bosonic model that can manifest a subharmonic response for physical quantities, a signature of a discrete time crystal (DTC) phase. We impose a time-dependent perturbation on top of the periodical driving, which transiently breaks the original time translational symmetry, and we then monitor the response of the physical observable. It is shown that a slow perturbation may induce a dynamical transition between two Z_2 symmetry breaking DTC phases, as shown in Fig. 1. By tuning the ramping velocity, one can observe a critical point, at which the transition duration diverges, a reminiscence of the critical slowing down phenomenon [28,29]. Finally, we discuss the effect of multiple random phase ramping processes and its implication to the stability of the discrete time crystal phase against noisy perturbations.

Model and method.—We consider a 1D hardcore bosonic model with an infinite long-range interaction. The Hamiltonian reads as follows:

（85）Experimentally Detecting Quantized Zak Phases without Chiral Symmetry in Photonic Lattices

PHYSICAL REVIEW LETTERS 127, 147401 (2021)

Experimentally Detecting Quantized Zak Phases without Chiral Symmetry in Photonic Lattices

Zhi-Qiang Jiao,[1,2] Stefano Longhi,[3] Xiao-Wei Wang,[1,4] Jun Gao,[1,4] Wen-Hao Zhou,[1,4] Yao Wang,[1,4] Yu-Xuan Fu,[1] Li Wang,[1,4] Rao-Jing Ren,[1,2] Lu-Feng Qiao,[1,2] and Xian-Min Jin[1,2,5,*]

[1]Center for Integrated Quantum Information Technologies (IQIT), School of Physics and Astronomy and State Key Laboratory of Advanced Optical Communication Systems and Networks, Shanghai Jiao Tong University, Shanghai 200240, China

[2]CAS Center for Excellence and Synergetic Innovation Center in Quantum Information and Quantum Physics, University of Science and Technology of China, Hefei, Anhui 230026, China

[3]Dipartimento di Fisica, Politecnico di Milano, Piazza L. da Vinci 32, I-20133 Milano, Italy

[4]TIQC (IAIC-CNIC), Instituto de Física Interdisciplinar y Sistemas Complejos, IFISC (UIB-CSIC), Instituto de Física Interdisciplinar y Sistemas Complejos, E07122 Palma de Mallorca, Spain

[5]TuringQ Co., Ltd., Shanghai 200240, China

(Received 3 March 2021; accepted 27 August 2021; published 27 September 2021)

Symmetries play a major role in identifying topological phases of matter and in establishing a direct connection between protected edge states and topological bulk invariants via the bulk-boundary correspondence. One-dimensional lattices are deemed to be protected by chiral symmetry, exhibiting quantized Zak phases and protected edge states, but not for all cases. Here, we experimentally realize an extended Su-Schrieffer-Heeger model with broken chiral symmetry by engineering one-dimensional photonic lattices, where the long-range hopping breaks chiral symmetry but ensures the existence of inversion symmetry. By the averaged mean displacement method, we detect topological invariants directly in the bulk through the continuous-time quantum walk of photons. Our results demonstrate that inversion symmetry protects the quantized Zak phase and edge states can disappear in the topological nontrivial phase, thus breaking the conventional bulk-boundary correspondence. Our photonic lattice provides a useful platform to study the interplay among topological phases, symmetries, and the bulk-boundary correspondence.

DOI: 10.1103/PhysRevLett.127.147401

Topological phases of matter are fascinating states that escape from the standard description of Ginzburg-Landau theory, exhibiting protected edge states and quantized topological properties in the bulk [1–5]. A paradigm of topological phases in condensed-matter physics is the integer quantum Hall state in a two-dimensional electron gas [1]. Topological order is of major relevance in a variety of nonelectronic systems as well, including mechanical platforms, cold atoms, acoustics, trapped ions, and photonics [6–15]. A central result in the theory of topological matter is that bulk topological invariants are connected to the number of protected edge states (bulk-boundary correspondence) [4,5]. Hence, topological phases can be probed either in the bulk or at the edges, as demonstrated in several recent experiments for Hermitian and even some non-Hermitian systems [16–34]. However, the common belief that a nontrivial topological phase implies the presence of protected edge states is not a general result, and even in Hermitian systems it is known that there could exist nontrivial topological phases that do not exhibit edge states at all [4,35–37]. In such systems, edge dynamics alone cannot thus provide a safe diagnostic of a topological phase. A notable example is provided by one-dimensional (1D) and 2D lattices with broken chiral symmetry but with preserved inversion symmetry [4,36–41]. In the Altland-Zirnbauer (AZ) classification, nonstandard topological phases are identified by three main symmetries: time-reversal, chiral, and particle-hole symmetries [5,42]. In this scheme, a topologically nontrivial 1D system should possess chiral symmetry, and the bulk topological invariant is the winding number corresponding to a quantized Zak phase [43]. A paradigmatic example is provided by the famous Su-Schrieffer-Heeger (SSH) model of polyacetylene [7,44], where the bulk-boundary correspondence holds [4,44]. Experimental demonstrations of quantized Zak phases in the SSH model with chiral symmetry have been reported in recent works [29,45] using different platforms and methods to extract the Zak phase from bulk dynamics. Long-range hopping in the SSH model that breaks chiral symmetry makes the system topologically trivial. However, when inversion symmetry is preserved, the Zak phase remains quantized and one can introduce a Z_2 topological number that identifies two distinct topological phases, which are not caught by the AZ classification [36–38]. Interestingly, unlike the chiral SSH model, in the extended SSH model with inversion symmetry only, the quantized Zak phase can

0031-9007/21/127(14)/147401(6)

（86）Symmetry-Induced Error Filtering in a Photonic Lieb Lattice

Symmetry-Induced Error Filtering in a Photonic Lieb Lattice

Yi-Jun Chang, Yong-Heng Lu, Yao Wang, Xiao-Yun Xu, Wen-Hao Zhou, Wen-Hao Cui, Xiao-Wei Wang, Jun Gao, Lu-Feng Qiao, and Xian-Min Jin*

Center for Integrated Quantum Information Technologies (IQIT), School of Physics and Astronomy and State Key Laboratory of Advanced Optical Communication Systems and Networks, Shanghai Jiao Tong University, Shanghai 200240, China and

CAS Center for Excellence and Synergetic Innovation Center in Quantum Information and Quantum Physics, University of Science and Technology of China, Hefei, Anhui 230026, China

(Received 12 August 2020; accepted 20 January 2021; published 10 March 2021)

Quantum computation promises unmatchedly parallel information processing capacity by harnessing the superposition and entanglement of quantum states. However, it is still challenging to realize universal quantum computation due that the reliability and scalability are limited by unavoidable noises on qubits. Nontrivial topological properties like quantum Hall phases are found capable of offering protection, but require stringent conditions of topological band gaps and broken time-reversal symmetry. Here, we propose and experimentally demonstrate a symmetry-induced error filtering scheme, showing a more general role of geometry in protection mechanism and applications. We encode qubits in a superposition of two spatial modes on a photonic Lieb lattice. The geometric symmetry endows the system with topological properties featuring a flat band touching, leading to destructive interference of π-phase qubits and 0-phase qubits. The geometry exhibits a significant effect on filtering phase errors, which also qualifies it to monitor phase deviations in real time. The symmetry-induced error filtering can be a key element for encoding and protecting quantum states, suggesting an emerging field of symmetry-protected universal quantum computation and noisy intermediate-scale quantum technologies.

DOI: 10.1103/PhysRevLett.126.110501

Quantum systems have been considered as powerful platforms for processing massive information and solving classically intractable problems by encoding qubits [1,2]. Analog quantum computation has demonstrated the supremacy over classical computation [3,4], whereas the step to universal quantum computation is still blocked by noises [5]. Fault tolerance is crucial for realizing reliable quantum computation, which has been explored on various systems, such as trapped ions [6], spins in semiconductors [7], superconducting circuits [8], solid state [9] and quantum optics [10]. However, implementation of error correction usually needs ancillary qubits with extra hardware overhead [11], which limits the scalability of quantum computation. For example, a qubit encoded in a superposition of two photonic modes may undergo phase errors in logical operations, which can be corrected by cluster states [12,13] but put daunting constraints for quantum systems including sources and measurements.

Geometries play a key role widely in natural and artificial materials, and induce extraordinary particle behaviors featured by localization and regular distribution [14–21]. Compared with dispersionless localization [22–24], the self-stabilization of distributions modes protected by geometries is more attractive for quantum computation, such as quantum Hall and anomalous quantum Hall phases with topological band gaps and broken time-reversal symmetry [25,26]. Regardless of the band topology, many symmetric geometries can equally create self-stabilizing states. Two-dimensional materials with rotational and inversion symmetries can bring about Dirac points possessing extraordinary properties of topological charges [27–29]. A Lieb lattice builds a square-hollow geometry with fourfold rotational symmetry [30–32] and builds a topological system with a flat band touching at Dirac points, which enables stable states with special phase features and makes it possible to implement a filter capable of exciting and stabilizing specific quantum states [33–35]. Such a filter will be able to eliminate phase errors and improve the purity of quantum states.

Our work is based on the photonic Lieb lattice with three sites forming a right triangle in each unit cell. Waveguides consisting of periodic unit cells are fabricated by femtosecond laser direct writing and are arranged in a ribbon as shown in Fig. 1(a). The evolution of quantum states through the photonic lattice can be described by an equivalent Schrödinger equation $i\partial\Psi = H\Psi$, with evolution length z considered as time t. The Hamiltonian is expressed by the tight-binding form as [21],

$$H = \sum_{i,j} J a_i^\dagger a_j + \text{H.c.}, \tag{1}$$

（87）Microscopic structure and dynamics study of granular segregation mechanism by cyclic shear

SCIENCE ADVANCES | RESEARCH ARTICLE

CONDENSED MATTER PHYSICS

Microscopic structure and dynamics study of granular segregation mechanism by cyclic shear

Zhifeng Li[1], Zhikun Zeng[2], Yi Xing[1], Jindong Li[1], Jie Zheng[1], Qinghao Mao[1], Jie Zhang[1,2], Meiying Hou[2], Yujie Wang[1]*

Granular mixtures with size difference can segregate upon shaking or shear. However, the quantitative study of this process remains difficult because it can be influenced by many mechanisms. Conflicting results on similar experimental systems are frequently obtained when the experimental conditions are not well controlled, which is mainly due to the fact that many mechanisms can be at work simultaneously. Moreover, it is often that macroscopic empirical measures, which lack microscopic physical bases, are used to explain the experimental findings and therefore cannot provide an accurate and complete depiction of the overall process. Here, we carry out a detailed and systematic microscopic structure and dynamics study of a cyclically sheared granular system with rigorously controlled experimental conditions. We find that both convection and arching effect play important roles in the segregation process in our system, and we can quantitatively identify their respective contributions.

INTRODUCTION

RESULTS

Convection-induced global segregation

[1]School of Physics and Astronomy, Shanghai Jiao Tong University, 800 Dongchuan Road, Shanghai, 200240, China. [2]Beijing National Laboratory for Condensed Matter Physics, Institute of Physics, Chinese Academy of Sciences, Beijing, 100190, China.
*Corresponding author. Email: yujiewang@sjtu.edu.cn

（88）Anomalous Contribution to the Nematic Electronic States from the Structural Transition in FeSe Revealed by Time- and Angle-Resolved Photoemission Spectroscopy

Anomalous Contribution to the Nematic Electronic States from the Structural Transition in FeSe Revealed by Time- and Angle-Resolved Photoemission Spectroscopy

Yuanyuan Yang,[1] Qiye Wang,[1] Shaoxiong Duan,[1] Hongliang Wo,[1] Chaozhi Huang,[1,*] Shichong Wang,[1,*] Lingxiao Gu,[1] Qian Xiang,[1,2] Deng Qian,[1,2] Jun Zhao,[2,3] and Wentao Zhang[1,2,†]
[1]Key Laboratory of Artificial Structures and Quantum Control (Ministry of Education), Shenyang National Laboratory for Materials Science, School of Physics and Astronomy, Shanghai Jiao Tong University, Shanghai 200240, China
[2]State Key Laboratory of Surface Physics and Department of Physics, Fudan University, Shanghai 200433, China
[3]Key Laboratory for Laser Plasmas (Ministry of Education), School of Physics and Astronomy, Shanghai Jiao Tong University, Shanghai 200240, China
[4]Tsung-Dao Lee Institute, Shanghai Jiao Tong University, Shanghai 200240, China
[5]Collaborative Innovation Center of Advanced Microstructures, Nanjing University, Nanjing 210093, China
[6]Institute of Semiconductors and Quantum Computing, Fudan University, Shanghai 200433, China

(Received 19 October 2021; revised 16 January 2022; accepted 24 May 2022; published 15 June 2022)

High-resolution time- and angle-resolved photoemission measurements were made on FeSe superconductors. With ultrafast photon excitation, two critical evolution features that correspond to the ultrafast electronic phase transitions were found only in the d_{xz}-orbit-derived band near the Brillouin zone corner within our time and energy resolution. Upon comparison to the detailed temperature dependence measurements, we conclude that these are two equilibrium electronic phase transitions at approximately 90 and 120 K above the superconducting transition temperature, and an anomalous contribution on the order of 10 meV to the nematic states from the structural transition is experimentally determined. Our observations strongly suggest that the electronic phase transition at 120 K must be taken into account in the energy band developments of FeSe, and furthermore, the contribution of the structural transition plays an important role in the nematic phase of iron-based high-temperature superconductors.

DOI: 10.1103/PhysRevLett.128.246401

Nematic order in iron-based superconductors refers to an electronic phase with broken rotational symmetry but preserved translational symmetry and usually occurs at decreasing temperature combined with a lattice structure transition from tetragonal to orthorhombic phase. Such a nematic phase may play a pivotal role in high-temperature superconducting pairing, and its underlying physics is a predominant topic in the study of iron-based systems [1–6]. The electronic nematic phase can be a result of the tetragonal-to-orthorhombic structural phase transition, orbital correlation, or the set-in of magnetic order, and early theoretical and experimental work suggested that the structural orthorhombic lattice distortion may be too small to drive the nematic electronic properties, such as no phase transitivity [7–12]. However, there is still a lack of evidence of a purely electronic nematics phase transition, and how much the structural transition contributes to the band renormalization is still not clear experimentally.

FeSe with a superconducting transition at approximately 9 K, undergoes a tetragonal-to-orthorhombic lattice deformation and a breaking of rotational symmetry of electronic order (nematic phase) at the same temperature of approximately 90 K without the long-range magnetic order as discovered in many other iron-based materials, allowing us to study the pure nematic phase over a wide temperature range [7,13–18]. However, the extent of the individual contributions of the structural transition and the purely electrical order to the nematic electronic states is still unknown. As most characteristics of nematic order are measured at thermal equilibrium conditions [19–23], it is difficult to differentiate the nematic electronic order from that of the structural transition and determine the contribution to the nematic states from the structural transition. Taking advantage of ultrafast experiments by using strong ultrafast photon pulses to excite only the electronic states retaining the preserved orthorhombic lattice structure, it is possible to drive only the electronic phase transitions in an ultrafast manner without deforming the crystal lattice [27,28]. Thus, it is possible to isolate the electronic states from the lattice, and to clarify the origin of both the nematic and structural phase transitions and estimate the contributions of the structural transition to the nematicity.

In this Letter, we report two ultrafast purely electronic phase transitions and two equilibrium phase transitions above the superconducting transition temperature in FeSe revealed by time- and angle-resolved photoemission spectroscopy (TRARPES). In particular, with improved energy and pump fluence resolution [29], we demonstrate that the

（89）Nonlinear Thouless Pumping: Solitons and Transport Breakdown

Nonlinear Thouless Pumping: Solitons and Transport Breakdown

Qidong Fu,[1] Peng Wang,[1] Yaroslav V. Kartashov,[2,3] Vladimir V. Konotop,[4] and Fangwei Ye[1,*]
[1]School of Physics and Astronomy, Shanghai Jiao Tong University, Shanghai 200240, China
[2]Institute of Spectroscopy, Russian Academy of Sciences, Troitsk, Moscow Region, 108840, Russia
[3]Departamento de Física and Centro de Física Teórica e Computacional, Faculdade de Ciências, Universidade de Lisboa, Campo Grande, Edifício C8, Lisboa 1749-016, Portugal

(Received 3 June 2021, accepted 7 March 2022; published 15 April 2022)

One-dimensional superfluid pumping of matter waves by two overlaid optical lattices moving with respect to each other is considered in the presence of attractive nonlinearity. It is shown that there exists a threshold pumping level above which the matter transfer is completely arrested. Below this threshold, the transfer of both dispersive wave packets and solitons occurs in accordance with the predictions of the linear theory, i.e., it is quantized and determined by the local dynamical Chern numbers of the lowest bands. The breakdown of the transport is also explained by nontrivial topology of the bands. In that case, the nonlinearity induces Rabi oscillations of atoms between two (or more) lowest bands. If the sum of the dynamical Chern numbers of the populated bands is zero, the oscillatory dynamics of a matter soliton for quite extensive, which corresponds to the transport breakdown. Otherwise, the sum of the Chern numbers of the nonlinearly excited bands determines the direction and magnitude of the average velocity of matter solitons that remain quantized but admit fractional values. Thus, even in the strongly nonlinear regime the topology of the linear bands is responsible for the existence of solitons. The transition between different dynamical regimes is accurately described by the perturbation theory for solitons.

DOI: 10.1103/PhysRevLett.128.154101

Controlled unidirectional transfer of matter, light, or physical quantities like charge or spin in a medium is a fundamental problem. It was discovered by Thouless [1] that one-dimensional (1D) pumping of electrons by a slowly moving periodic potential over one pumping cycle is quantized with quanta being determined by the Chern numbers considered in the extended coordinate-time space. To date, Thouless pumping was experimentally observed in systems of cold bosonic [2–4] and fermionic [5] atoms, spin systems [6], optics [7–9], acoustics [10], and plasmonics [11].

Although topological pumping was originally introduced for essentially linear systems [1,12], physical realizations mentioned above provide opportunities for investigation of the phenomenon in nonlinear settings. For example, in the presence of optical Kerr nonlinearity or two-body interactions in Bose-Einstein condensates (BECs), interatomic interactions were intrinsically present in experiments with BECs in bipartite magnetic lattices where (nonquantized) transport was observed [13] and in the formation of the Mott insulator phase arresting tight binding of atoms upon pumping [3]. Nonlinear effects were explicitly included in the single-band tight-binding approximation for a gas of several spinor states of fermions in optical lattices [14] and in model of a nonlinear interferometer [15], where the obtained pump was fractional. Topological transport of interacting photons was described in [16]. Qualitatively new effects appear in the presence of sufficiently strong interactions. Using a Bose-Hubbard model, accounting for spin and the Hubbard interaction term, in [17] the authors reported the breakdown of the Thouless pumping, explained by closure of the gap computed using amplitude-dependent many-body ground states under twisted boundary conditions. Apparently, the effect may be dependent on the specific model, such as another realization of a spinful Bose-Hubbard model subject to both open and twisted boundary conditions, breakdown of pumping was not found [18].

All above results dealt with repulsive interatomic interactions and thus with stable nonlinear states of constant amplitudes. In this Letter, we address nonlinear Thouless pumping of matter waves in a BEC with a negative scattering length, loaded in an optical superlattice created by two lattices, overmoving with respect to the other. In this regime, a well-localized matter soliton is formed, and excitations from the upper bands of the lower lattice spectrum acquire special importance [19,20]. Our two main findings are as follows. First, there exists a threshold amplitude below which the pumping closely follows the prediction of the linear theory [1], even when solitons are formed. Above the threshold amplitude the transport either becomes fractional, acquires direction opposite to the moving substrate velocity, or is arrested, resulting in oscillatory motion of a soliton. Second, oscillations of a soliton relatively well described by the perturbation theory [21], have topological nature. They occur due to the

（5）专利授权情况佐证材料

序号	发明名称	类别	专利号	授权年份
1	一种用于二维材料薄膜厚度测量的高效光学测量方法	发明专利	ZL201811548329.6	2020
2	一种基于体全息存储技术的三维全息显示方法	发明专利	ZL201510874896.0	2018
3	电控连续渐变折射率电光晶体偏转器	发明专利	ZL201410338950.5	2017
4	采用基于短腔腔增强关联光谱技术测量气体浓度的装置测量气体浓度的方法	发明专利	ZL201310738166.9	2016
5	多通池内气体吸收光谱和吸收光程同步测量的装置和方法	发明专利	ZL201810503921.8	2021
6	一种基于光学捷变频的快速气体吸收光谱测量装置及方法	发明专利	ZL201910288076.1	2021
7	气体分子高分辨吸收光谱实验仪	实用新型	ZL202022671068.6	2021
8	一种采用气体放电驱动天线收发信号的装置	发明专利	ZL201811504774.2	2020
9	一种微波探测系统及方法	发明专利	ZL201610716125.3	2019
10	一种基于霍尔效应精确定位和测量转速的实验教学装置	实用新型	ZL201820959101.5	2019

11	反射式光学偏转器	发明专利	ZL202010929231.6	2022
12	基于聚合物透明电极的太赫兹波段电控液晶相移器的制备方法	发明专利	ZL201610251983.5	2018
13	一种非侵入红外复合吸收精测血糖变化的方法	发明专利	ZL201610614860.3	2019
14	基于波导与谐振腔耦合的微纳光学马达及其驱动方法	发明专利	ZL201810132603.5	2019
15	一种高效样品微粒汇集装置及光学汇集方法	发明专利	ZL202011155192.5	2021

（1）一种用于二维材料薄膜厚度测量的高效光学测量方法

证书号第3960093号

发明专利证书

发明名称：一种用于二维材料薄膜厚度测量的高效光学测量方法

发明人：高波;雷佳雨

专利号：ZL 2018 1 1548329.6

专利申请日：2018年12月18日

专利权人：哈尔滨工业大学

地址：150001 黑龙江省哈尔滨市南岗区西大直街92号

授权公告日：2020年08月28日　　授权公告号：CN 109373918 B

国家知识产权局依照中华人民共和国专利法进行审查，决定授予专利权，颁发发明专利证书并在专利登记簿上予以登记。专利权自授权公告之日起生效，专利权期限为二十年，自申请日起算。

专利证书记载专利权登记时的法律状况。专利权的转移、质押、无效、终止、恢复和专利权人的姓名或名称、国籍、地址变更等事项记载在专利登记簿上。

局长
申长雨

第1页(共2页)

其他事项参见续页

（2）一种基于体全息存储技术的三维全息显示方法

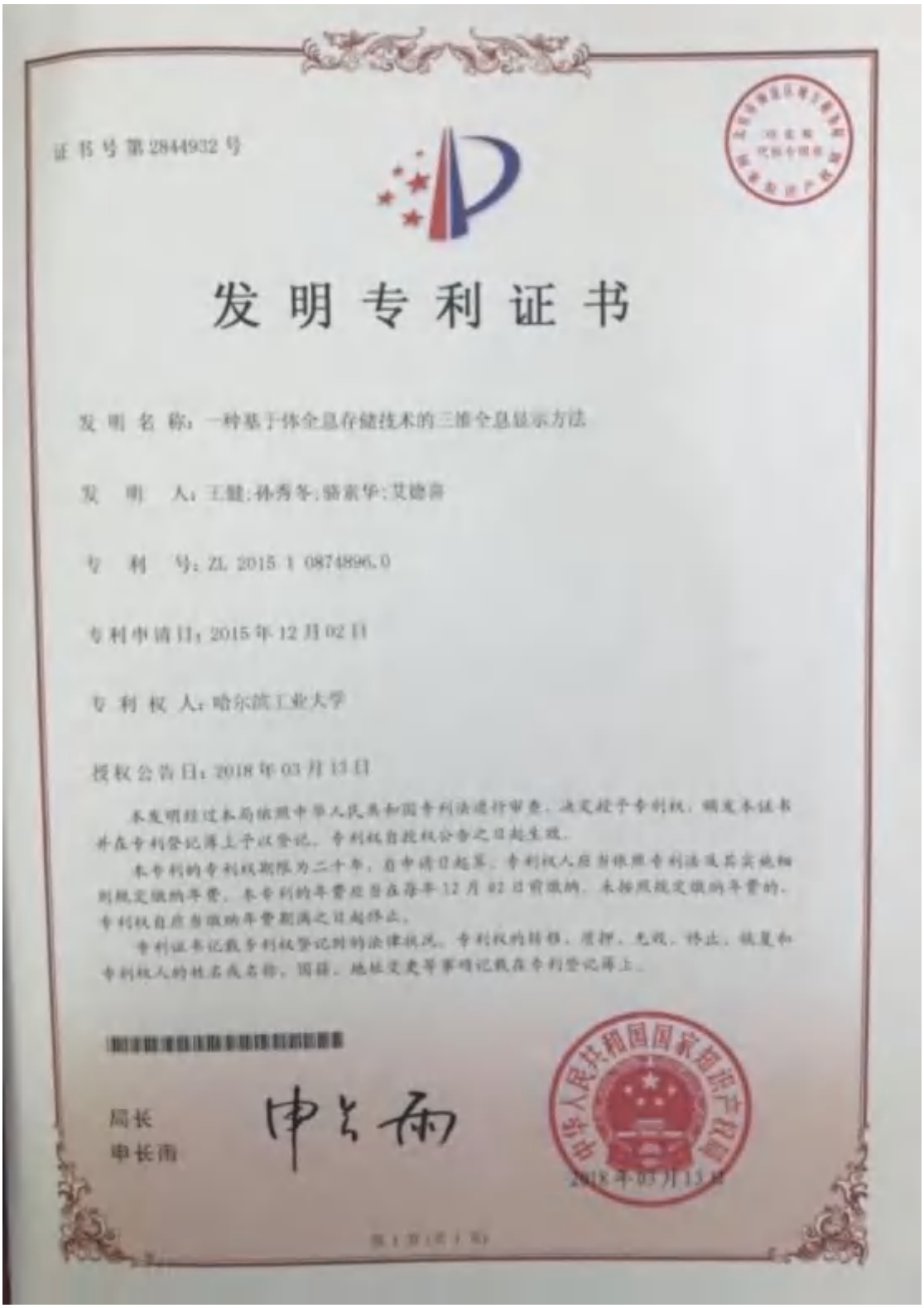

证书号第2844932号

发明专利证书

发明名称：一种基于体全息存储技术的三维全息显示方法

发明人：王健;孙秀冬;翁新华;艾德奇

专利号：ZL 2015 1 0874896.0

专利申请日：2015年12月02日

专利权人：哈尔滨工业大学

授权公告日：2018年03月13日

本发明经过本局依照中华人民共和国专利法进行审查，决定授予专利权，颁发本证书并在专利登记簿上予以登记。专利权自授权公告之日起生效。

本专利的专利权期限为二十年，自申请日起算。专利权人应当依照专利法及其实施细则规定缴纳年费。本专利的年费应当在每年12月02日前缴纳。未按照规定缴纳年费的，专利权自应当缴纳年费期满之日起终止。

专利证书记载专利权登记时的法律状况。专利权的转移、质押、无效、终止、恢复和专利权人的姓名或名称、国籍、地址变更等事项记载在专利登记簿上。

局长
申长雨

中华人民共和国国家知识产权局

2018年03月13日

（3）电控连续渐变折射率电光晶体偏转器

证书号第2365804号

发明专利证书

发明名称：电控连续渐变折射率电光晶体偏转器

发明人：田浩;周忠祥;姚博;谭鹏

专利号：ZL 2014 1 0338950.5

专利申请日：2014年07月16日

专利权人：哈尔滨工业大学

授权公告日：2017年02月01日

本发明经过本局依照中华人民共和国专利法进行审查，决定授予专利权，颁发本证书并在专利登记簿上予以登记。专利权自授权公告之日起生效。

本专利的专利权期限为二十年，自申请日起算。专利权人应当依照专利法及其实施细则规定缴纳年费。本专利的年费应当在每年07月16日前缴纳。未按规定缴纳年费的专利权自应当缴纳年费期满之日起终止。

专利证书记载专利权登记时的法律状况。专利权的转移、质押、无效、终止、恢复和专利权人的姓名或名称、国籍、地址变更等事项记载在专利登记簿上。

局长
申长雨

（4）采用基于短腔腔增强关联光谱技术测量气体浓度的装置测量气体浓度的方法

证书号第1931648号

发明专利证书

发明名称：采用基于短腔腔增强关联光谱技术测量气体浓度的装置测量气体浓度的方法

发明人：姜秀涛;董永康;武东城;哈斯乌力吉;吕志伟

专利号：ZL 2013 1 0738166.9

专利申请日：2013年12月29日

专利权人：哈尔滨工业大学

授权公告日：2016年01月20日

本发明经过本局依照中华人民共和国专利法进行审查，决定授予专利权，颁发本证书并在专利登记簿上予以登记，专利权自授权公告之日起生效。

本专利的专利权期限为二十年，自申请日起算。专利权人应当依照专利法及其实施细则规定缴纳年费，本专利的年费应当在每年12月29日前缴纳，未按照规定缴纳年费的，专利权自应当缴纳年费期满之日起终止。

专利证书记载专利权登记时的法律状况，专利权的转移、质押、无效、终止、恢复和专利权人的姓名或名称、国籍、地址变更等事项记载在专利登记簿上。

局长
申长雨

中华人民共和国国家知识产权局

2016年01月20日

第1页(共1页)

（5）多通池内气体吸收光谱和吸收光程同步测量的装置和方法

证书号第4664789号

发明专利证书

发明名称：多通池内气体吸收光谱和吸收光程同步测量的装置和方法

发明人：姜秀涛;陈晨;董永康;冯亚博

专利号：ZL 2018 1 0503921.8

专利申请日：2018年05月23日

专利权人：哈尔滨工业大学

地址：150001 黑龙江省哈尔滨市南岗区西大直街92号

授权公告日：2021年09月07日　　授权公告号：CN 108931498 B

国家知识产权局依照中华人民共和国专利法进行审查，决定授予专利权，颁发发明专利证书并在专利登记簿上予以登记。专利权自授权公告之日起生效。专利权期限为二十年，自申请日起算。

专利证书记载专利权登记时的法律状况。专利权的转移、质押、无效、终止、恢复和专利权人的姓名或名称、国籍、地址变更等事项记载在专利登记簿上。

局长
申长雨

国家知识产权局
2021年09月07日

第1页(共2页)

其他事项参见背面

（6）一种基于光学捷变频的快速气体吸收光谱测量装置及方法

证书号第4528054号

发明专利证书

发明名称：一种基于光学捷变频的快速气体吸收光谱测量装置及方法

发明人：娄秀涛;原子岳;董永康

专利号：ZL 2019 1 0288076.1

专利申请日：2019年04月10日

专利权人：哈尔滨工业大学

地址：150001 黑龙江省哈尔滨市南岗区西大直街92号

授权公告日：2021年07月06日　　授权公告号：CN 109959627 B

国家知识产权局依照中华人民共和国专利法进行审查，决定授予专利权，颁发发明专利证书并在专利登记簿上予以登记。专利权自授权公告之日起生效。专利权期限为二十年，自申请日起算。

专利证书记载专利权登记时的法律状况。专利权的转移、质押、无效、终止、恢复和专利权人的姓名或名称、国籍、地址变更等事项记载在专利登记簿上。

局长
申长雨

国家知识产权局

2021年07月06日

第1页(共2页)

其他事项参见背面

（7）气体分子高分辨吸收光谱实验仪

证书号第13450203号

实用新型专利证书

实用新型名称：气体分子高分辨吸收光谱实验仪

发　明　人：娄秀涛;赵海发

专　利　号：ZL 2020 2 2671068.6

专利申请日：2020年11月18日

专 利 权 人：哈尔滨工业大学

地　　址：150001 黑龙江省哈尔滨市南岗区西大直街92号

授权公告日：2021年06月18日　　授权公告号：CN 213482061 U

国家知识产权局依照中华人民共和国专利法经过初步审查，决定授予专利权，颁发实用新型专利证书并在专利登记簿上予以登记。专利权自授权公告之日起生效。专利权期限为十年，自申请日起算。

专利证书记载专利权登记时的法律状况。专利权的转移、质押、无效、终止、恢复和专利权人的姓名或名称、国籍、地址变更等事项记载在专利登记簿上。

局长
申长雨

国家知识产权局

2021年06月18日

第1页(共2页)

其他事项参见背面

（8）一种采用气体放电驱动天线收发信号的装置

证书号第3928004号

发明专利证书

发明名称：一种采用气体放电驱动天线收发信号的装置

发明人：袁承勋;李金明;阿斯塔菲耶夫·阿勒科山德库德利亚夫谢夫·安纳托利;周忠祥;王晓鸣

专利号：ZL 2018 1 1504774.2

专利申请日：2018年12月10日

专利权人：哈尔滨工业大学

地址：150001 黑龙江省哈尔滨市南岗区西大直街92号

授权公告日：2020年08月07日　　授权公告号：CN 109639310 B

国家知识产权局依照中华人民共和国专利法进行审查，决定授予专利权，颁发发明专利证书并在专利登记簿上予以登记。专利权自授权公告之日起生效。专利权期限为二十年，自申请日起算。

专利证书记载专利权登记时的法律状况。专利权的转移、质押、无效、终止、恢复和专利权人的姓名或名称、国籍、地址变更等事项记载在专利登记簿上。

局长
申长雨

国家知识产权局

2020年08月07日

第1页(共2页)

其他事项参见续页

（9）一种微波探测系统及方法

证书号第3275388号

发明专利证书

发明名称：一种微波探测系统及方法

发 明 人：周忠祥;吴忧;施扣忠;李均;袁承勋

专 利 号：ZL 2016 1 0716125.3

专利申请日：2016年08月24日

专 利 权 人：哈尔滨工业大学

地 址：150001 黑龙江省哈尔滨市南岗区西大直街92号

授权公告日：2019年03月01日　　授权公告号：CN 106323994 B

国家知识产权局依照中华人民共和国专利法进行审查，决定授予专利权，颁发发明专利证书并在专利登记簿上予以登记。专利权自授权公告之日起生效，专利权期限为二十年，自申请日起算。

专利证书记载专利权登记时的法律状况。专利权的转移、质押、无效、终止、恢复和专利权人的姓名或名称、国籍、地址变更等事项记载在专利登记簿上。

局长
申长雨

国家知识产权局

2019年03月01日

第1页(共2页)

其他事项参见背面

（10）一种基于霍尔效应精确定位和测量转速的实验教学装置

证书号第8926968号

实用新型专利证书

实用新型名称：一种基于霍尔效应精确定位和测量转速的实验教学装置

发 明 人：刘世刚;黄丽;赵海发

专 利 号：ZL 2018 2 0959101.5

专利申请日：2018年06月21日

专 利 权 人：哈尔滨工业大学

地 址：150001 黑龙江省哈尔滨市南岗区西大直街92号

授权公告日：2019年06月07日 授权公告号：CN 208954448 U

国家知识产权局依照中华人民共和国专利法经过初步审查，决定授予专利权，颁发实用新型专利证书并在专利登记簿上予以登记。专利权自授权公告之日起生效。专利权期限为十年，自申请日起算。

专利证书记载专利权登记时的法律状况。专利权的转移、质押、无效、终止、恢复和专利权人的姓名或名称、国籍、地址变更等事项记载在专利登记簿上。

局长
申长雨

国家知识产权局

2019年06月07日

第1页(共2页)

其他事项参见背面

（11）反射式光学偏转器

证书号第4966773号

发明专利证书

发明名称：反射式光学偏转器

发明人：田浩;王宇;谭鹏;孟祥达;周忠祥

专利号：ZL 2020 1 0929231.6

专利申请日：2020年09月07日

专利权人：哈尔滨工业大学

地址：150001 黑龙江省哈尔滨市南岗区西大直街92号

授权公告日：2022年03月01日　　授权公告号：CN 111999886 B

国家知识产权局依照中华人民共和国专利法进行审查，决定授予专利权，颁发发明专利证书并在专利登记簿上予以登记。专利权自授权公告之日起生效。专利权期限为二十年，自申请日起算。

专利证书记载专利权登记时的法律状况。专利权的转移、质押、无效、终止、恢复和专利权人的姓名或名称、国籍、地址变更等事项记载在专利登记簿上。

局长
申长雨

知识产权

第1页(共2页)

其他事项参见续页

（12）基于聚合物透明电极的太赫兹波段电控液晶相移器的制备方法

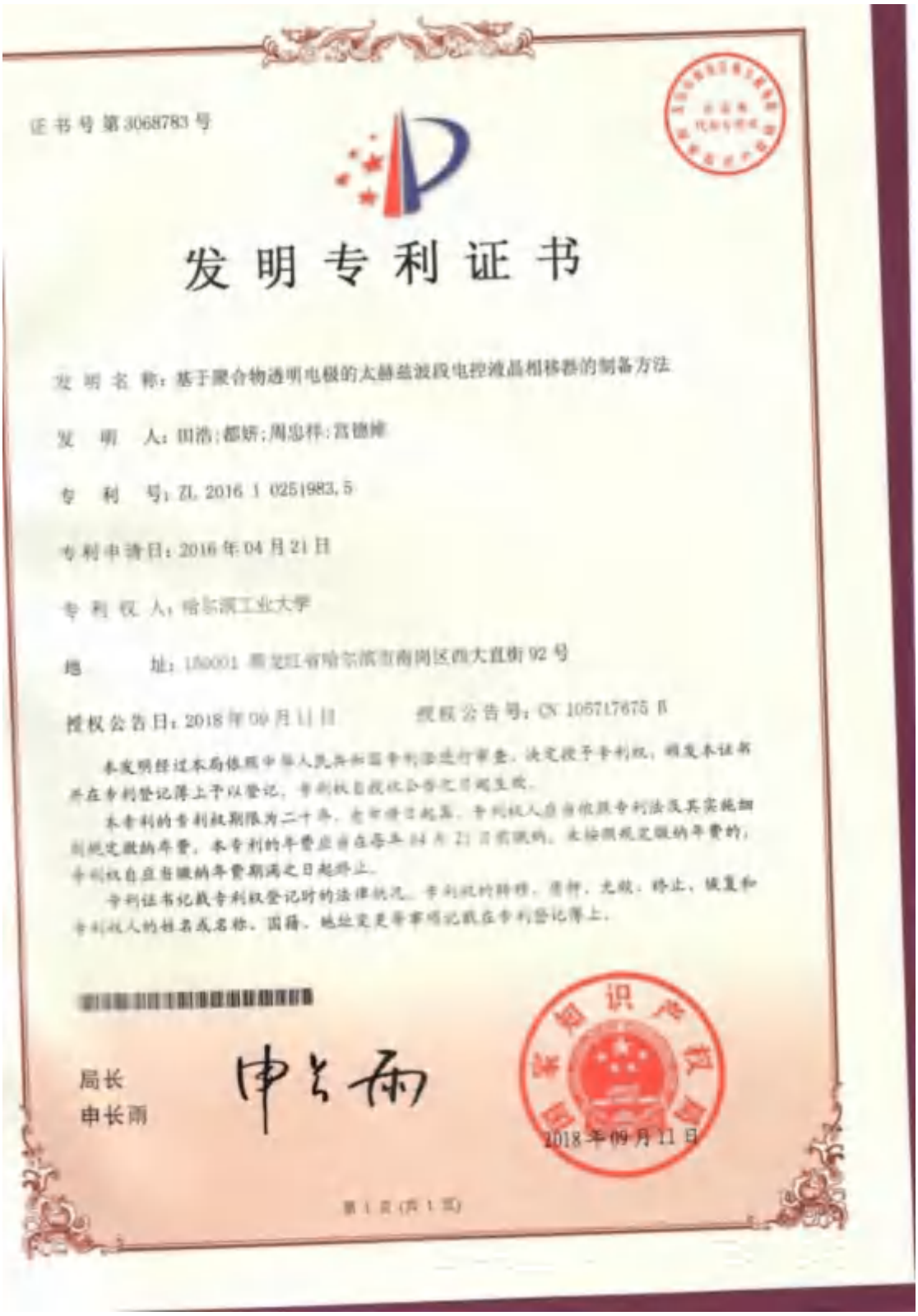

证书号第3068783号

发明专利证书

发明名称：基于聚合物透明电极的太赫兹波段电控液晶相移器的制备方法

发明人：田浩;都妍;周忠祥;宫德辉

专利号：ZL 2016 1 0251983.5

专利申请日：2016年04月21日

专利权人：哈尔滨工业大学

地址：150001 黑龙江省哈尔滨市南岗区西大直街92号

授权公告日：2018年09月11日　　授权公告号：CN 105717675 B

本发明经过本局依照中华人民共和国专利法进行审查，决定授予专利权，颁发本证书并在专利登记簿上予以登记，专利权自授权公告之日起生效。

本专利的专利权期限为二十年，自申请日起算，专利权人应当依照专利法及其实施细则规定缴纳年费，本专利的年费应当在每年04月21日前缴纳，未按照规定缴纳年费的，专利权自应当缴纳年费期满之日起终止。

专利证书记载专利权登记时的法律状况，专利权的转移、质押、无效、终止、恢复和专利权人的姓名或名称、国籍、地址变更等事项记载在专利登记簿上。

局长
申长雨

国家知识产权局
2018年09月11日

第1页(共1页)

（13）一种非侵入红外复合吸收精测血糖变化的方法

证书号第3300667号

发明专利证书

发明名称：一种非侵入红外复合吸收精测血糖变化的方法

发明人：孙芳魁;刘燕玲;丁卫强;李伟奇

专利号：ZL 2016 1 0614860.3

专利申请日：2016年07月30日

专利权人：哈尔滨工业大学

地址：150000 黑龙江省哈尔滨市南岗区西大直街92号

授权公告日：2019年03月19日　　授权公告号：CN 106137218 B

国家知识产权局依照中华人民共和国专利法进行审查，决定授予专利权，颁发发明专利证书并在专利登记簿上予以登记。专利权自授权公告之日起生效。专利权期限为二十年，自申请日起算。

专利证书记载专利权登记时的法律状况。专利权的转移、质押、无效、终止、恢复和专利权人的姓名或名称、国籍、地址变更等事项记载在专利登记簿上。

局长
申长雨

国家知识产权局
2019年03月19日

第1页(共2页)

其他事项参见背面

（14）基于波导与谐振腔耦合的微纳光学马达及其驱动方法

证书号第3630128号

发明专利证书

发明名称：基于波导与谐振腔耦合的微纳光学马达及其驱动方法

发明人：丁卫强;刘正君;耿勇;谭久彬

专利号：ZL 2018 1 0132603.5

专利申请日：2018年02月09日

专利权人：哈尔滨工业大学

地址：150001 黑龙江省哈尔滨市南岗区西大直街92号

授权公告日：2019年12月13日　　授权公告号：CN 108267815 B

国家知识产权局依照中华人民共和国专利法进行审查，决定授予专利权。颁发发明专利证书并在专利登记簿上予以登记。专利权自授权公告之日起生效，专利权期限为二十年，自申请日起算。

专利证书记载专利权登记时的法律状况。专利权的转移、质押、无效、终止、恢复和专利权人的姓名或名称、国籍、地址变更等事项记载在专利登记簿上。

局长
申长雨

国家知识产权局

2019年12月13日

第1页(共2页)

（15）一种高效样品微粒汇集装置及光学汇集方法

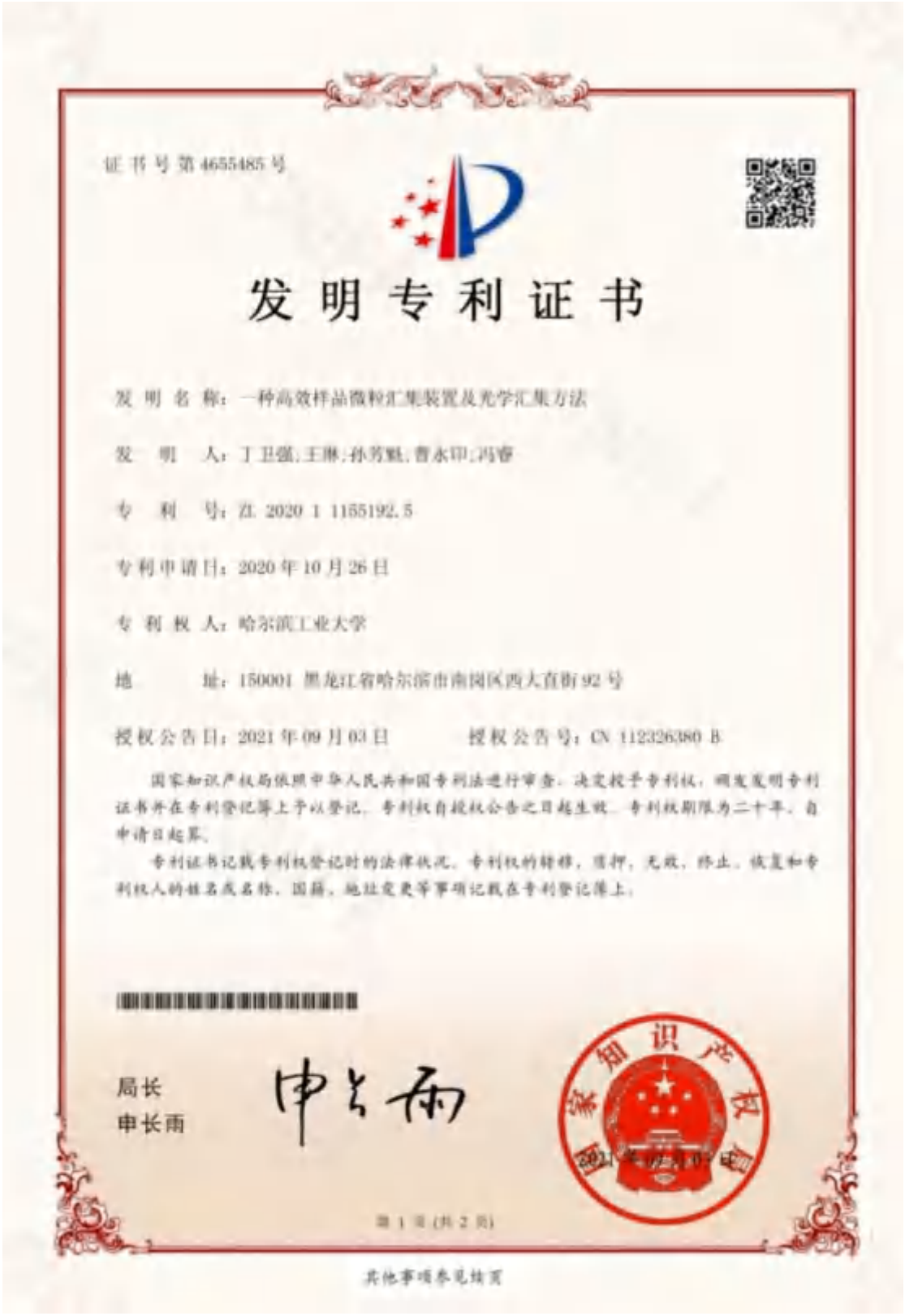

证书号第4655485号

发明专利证书

发明名称：一种高效样品微粒汇集装置及光学汇集方法

发明人：丁卫强;王琳;孙芳魁;曹永印;冯睿

专利号：ZL 2020 1 1155192.5

专利申请日：2020年10月26日

专利权人：哈尔滨工业大学

地址：150001 黑龙江省哈尔滨市南岗区西大直街92号

授权公告日：2021年09月03日　　授权公告号：CN 112326380 B

国家知识产权局依照中华人民共和国专利法进行审查，决定授予专利权，颁发发明专利证书并在专利登记簿上予以登记。专利权自授权公告之日起生效。专利权期限为二十年，自申请日起算。

专利证书记载专利权登记时的法律状况。专利权的转移，质押，无效，终止，恢复和专利权人的姓名或名称、国籍、地址变更等事项记载在专利登记簿上。

局长
申长雨

国家知识产权局

第1页(共2页)

其他事项参见续页

（6）学术竞赛等奖项佐证材料

序号	获奖名称	级别	获奖等级	学生姓名	年份
1	2019 年度中国光学学会光学优秀博士学位论文提名优秀论文	国家级	提名优秀论文	朱彤彤	2021
2	第十二届中国大学生物理学术竞赛	国家级	特等奖	骆全鑫、程湛博、厉彦榛、黄昕诺、岳琮沅	2021
3	第十一届中国大学生物理学术竞赛	国家级	特等奖	张晓、费汉露、杨承熹、孙思源、张灵昊	2020
4	大学生等离子体科技创新竞赛	国家级	特等奖	周晨、柴焱、李健飞、丁哲	2021
5	中国大学生物理学术竞赛东北赛区比赛	国家级	特等奖	杨昕昱、宋炳榕、徐皓培、李文宇、蒋知臻	2021
6	中国大学生物理学术竞赛东北赛区比赛	国家级	特等奖	赵博超、董璇琦、崔亚琦、周超、骆全鑫	2020
7	全国大学生光电设计竞赛	国家级	一等奖	刘辰翔、何雪铭、欧阳昊	2021
8	第七届全国大学生物理实验竞赛	国家级	一等奖	周宁	2021
9	第七届全国大学生物理实验竞赛	国家级	一等奖	李文宇、李思维、杨昕昱	2021
10	第七届全国大学生物理实验竞赛	国家级	一等奖	沈锐臻、罗艺卉、韩雨萌	2021
11	第七届全国大学生物理实验竞赛	国家级	一等奖	李磊、任睿溥、李俊杰	2021
12	第六届全国大学生物理实验竞赛	国家级	一等奖	张瑞祺、刘越莉、于翔、费汉露、李茵然	2020

13	第六届全国大学生物理实验竞赛	国家级	一等奖	唐爱国、周依凡、吴欢桐、刘辰翔、卢袁真子	2020
14	第三届“卓越杯”大学生物理实验竞赛	国家级	一等奖	张瑞祺、刘越莉、于翔	2020
15	第三届“卓越杯”大学生物理实验竞赛	国家级	一等奖	刘辰翔、唐爱国、周依凡	2020
16	第十二届大学生创新创业年会	国家级	优秀论文	尚鸣昊、王俞智、胡俊杰、张宇飞	2019
17	2018 年度工信创新奖学金	国家级	一等奖	谭鹏	2019
18	2017 年度工信创新奖学金	国家级	一等奖	冯冬冬	2018
19	2017 年度工信创新奖学金	国家级	一等奖	臧立新	2018
20	第十三届王大珩光学奖	国家级	高校学生光学奖	赵文宇	2017
21	第十一届国际天线传播和电磁理论学术研讨会	国家级	优秀论文	贾洁姝	2016
22	第六届等离子体物理和应用研讨会	国家级	优秀报告	姚静锋	2020
23	第十四届全国大学生节能减排社会实践与科技竞赛	国家级	一等奖	谢文棋、肖家豪、黄肖振、张博宇、刘嘉春	2021
24	第七届全国大学生物理实验竞赛（教学赛）	国家级	二等奖	周超、张晓	2021
25	第七届全国大学生物理实验竞赛	国家级	二等奖	马殿云、纪家清、杨志青	2021
26	第三届“卓越杯”大学生物理实验竞赛	国家级	二等奖	谢桂炎、骆全鑫	2020

27	第十四届全国大学生节能减排社会实践与科技竞赛	国家级	三等奖	李志鹏、郭启凡、邵俊超、邢瀚、薛健	2021
28	第五届全国大学生材料设计邀请赛	国家级	三等奖	孙思源、费汉露、乔琪、张晓、李茵然	2021
29	全国光学与光学工程博士生学术联赛	东北地区	二等奖 单场季军	王宇	2021
30	全国光学与光学工程博士生学术联赛	东北地区	二等奖	李航	2021
31	辽宁省优秀博士学位论文	省级		郭宇	2021
32	辽宁省优秀博士学位论文	省级		柳洪盛	2018
33	辽宁省优秀博士学位论文	省级		黄晓明	2016
34	辽宁省优秀博士学位论文	省级		蒋雪	2015
35	辽宁省优秀博士学位论文	省级		高峻峰	2015
36	黑龙江省高校科学技术奖	省级	二等奖	孟祥达	2020
37	第七届中国国际“互联网+”大学生创新创业大赛	省级	银奖	肖家豪、刘嘉春、谢文棋、黄肖振、张博宇	2021
38	第十二届工银融e联“挑战杯”黑龙江省大学生创业计划竞赛	省级	铜奖	邹明达、张显达、蒋昊、寇琦、张蕊	2020
39	研究生国家奖学金（博士42人次）	国家级		吴金雷等	2014-2021
40	研究生国家奖学金（硕士26人次）	国家级		王翰韬等	2014-2021

41	辽宁省优秀毕业生（6人次）	省级		王鹏等	2014-2022
42	第五届研究生十佳团队	校级		哈工大辐射与材料研究生团队	2017

（1）2019 年度中国光学学会光学优秀博士学位论文提名优秀论文证明

证 书

朱彤彤 同学：

您的论文《结构化背景中的光学牵引力和横向力》荣获 2019 年度中国光学学会光学优秀博士学位论文提名优秀奖。

特发此证，以资鼓励。

中国光学学会

2021 年 09 月 18 日

（2）第十一届中国大学生物理学术竞赛获奖证明

荣誉证书

HONORARY CREDENTIAL

哈尔滨工业大学代表队

队员：张 晓 费汉露 杨承鑫 孙思源 张灵昊

领队：张 宇 周 宁

在浙江大学举办的第十一届中国大学生物理学术竞赛中荣获

特等奖

特发此证，以资鼓励。

中国大学生物理学术竞赛组委会

2020年10月18日

（3）第十二届中国大学生物理学术竞赛获奖证明

荣誉证书

哈尔滨工业大学代表队

队 员：骆全鑫　程湛博　厉彦臻　黄昕诺　岳琮沅

领 队：张　宇　于东辉

在哈尔滨师范大学举办的第十二届中国大学生物理学术竞赛中荣获

特等奖

特发此证，以资鼓励。

中国大学生物理学术竞赛组委会

2021 年 8 月 24 日

（4）大学生等离子体科技创新竞赛获奖证明

证书编号：ICP2021-0-06

全国大学生等离子体科技创新竞赛

获奖证书

在2021年中国电工技术学会主办的“首届全国大学生等离子体科技创新竞赛”中，获得

特等奖

特发此证，以资鼓励。

作品名称：一种用于分析检测杂质气体的电离探测器及其运行方法

参赛高校：哈尔滨工业大学

参赛学生：周 晨、柴 焱、赵世鑫、李健飞、任博涵、王 晨

指导教师：袁承勋、王 玺

中国电工技术学会

二〇二一年十一月

（5）中国大学生物理学术竞赛东北赛区比赛特等奖获奖证明

（6）中国大学生物理学术竞赛东北赛区比赛特等奖获奖证明

（7）全国大学生光电设计竞赛获奖证明

获奖证书

学　　校：哈尔滨工业大学

学　　生：刘辰翔、何雪铭、欧阳昊

指导教师：李俊庆

在第九届全国大学生光电设计竞赛中荣获一等奖，

特发此证，以资鼓励。

第九届全国大学生光电设计竞赛组织委员会

（全国大学生光电设计竞赛委员会 代章）

二〇二一年八月三十一日

（8）第七届全国大学生物理实验竞赛获奖证明

获奖证书

Certificate of Award

哈尔滨工业大学 张宇 老师

所指导学生 周宁 同学在 2021 年第七届全国大学生物理实验竞赛（教学赛）—基础性实验题目中，荣获 一 等奖。

特发此证，以资鼓励。

高等学校国家级实验教学示范中心联席会

全国高等学校实验物理教学研究会

中国物理学会物理教学委员会

天津大学（代章）

南开大学

2021 年 7 月 20 日

（9）第七届全国大学生物理实验竞赛一等奖获奖证明

获奖证书

Certificate of Award

学　　校：哈尔滨工业大学
学　　生：李文宇 李思维 杨昕晃
指导教师：辛丽 王玉晓
参赛作品：霓与虹的再现

在 2021 年第七届全国大学生物理实验竞赛中荣获

一等奖

特发此奖，以资鼓励！

国家级实验教学示范中心联席会物理学科组
全国高等学校实验物理教学研究会
中国物理学会物理教学委员会

全国大学生物理实验竞赛组委会
南昌大学（代章）

证书编号：QGWLSYCX-1-0063

2021 年 12 月 5 日

（10）第七届全国大学生物理实验竞赛一等奖获奖证明

获奖证书

Certificate of Award

学　　校：哈尔滨工业大学
学　　生：沈锐臻 罗艺卉 韩雨萌
指导教师：刘伟龙 吕喆
参赛作品：一种基于泊肃叶定律的粘滞系数测量的改进装置

在 2021 年第七届全国大学生物理实验竞赛中荣获

一等奖

特发此奖，以资鼓励！

国家级实验教学示范中心联席会物理学科组
全国高等学校实验物理教学研究会
中国物理学会物理教学委员会

全国大学生物理实验竞赛组委会
南昌大学（代章）

证书编号：QGWLSYCX-1-0039

2021 年 12 月 5 日

（11）第七届全国大学生物理实验竞赛一等奖获奖证明

获奖证书

Certificate of Award

学　　校：哈尔滨工业大学
学　　生：李磊 任睿博 李俊杰
指导教师：魏波 王玉晓
参赛作品：一种形状记忆合金自驱动器

在 2021 年第七届全国大学生物理实验竞赛中荣获

一等奖

特发此奖，以资鼓励！

国家级实验教学示范中心联席会物理学科组
全国高等学校实验物理教学研究会
中国物理学会物理教学委员会

全国大学生物理实验竞赛组委会
南昌大学（代章）

证书编号：QGWLSYCX-1-0057

2021 年 12 月 5 日

（12）第六届全国大学生物理实验竞赛一等奖获奖证明

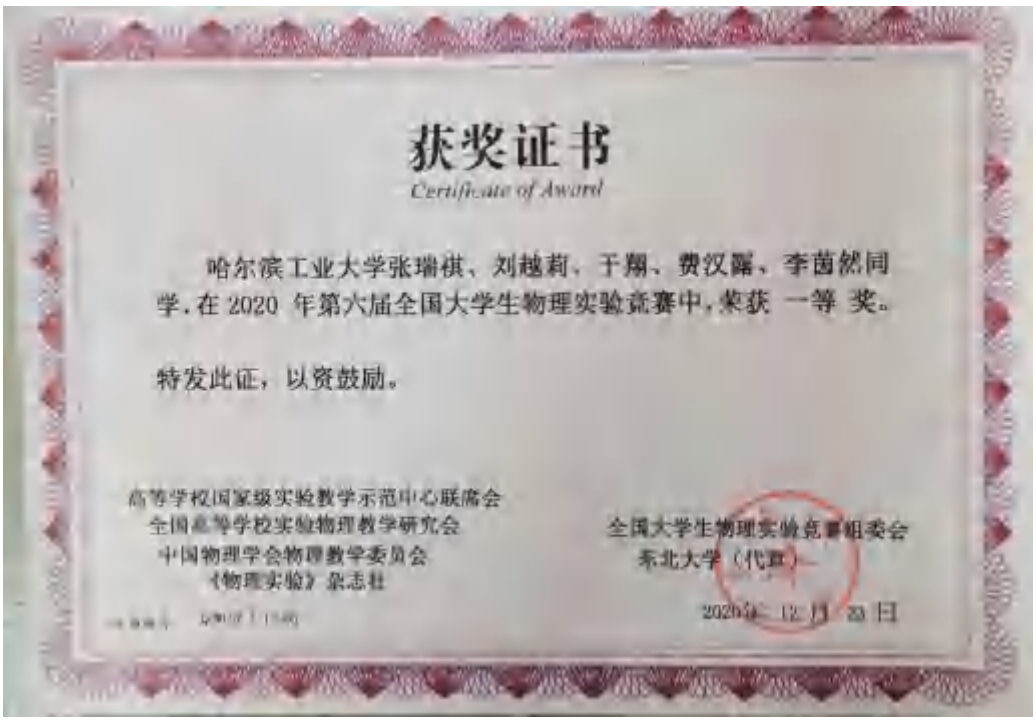

获奖证书

Certificate of Award

哈尔滨工业大学张瑞祺、刘越莉、于翔、费汉露、李茵然同学，在 2020 年第六届全国大学生物理实验竞赛中，荣获 一等 奖。

特发此证，以资鼓励。

高等学校国家级实验教学示范中心联席会
全国高等学校实验物理教学研究会
中国物理学会物理教学委员会
《物理实验》杂志社

全国大学生物理实验竞赛组委会
东北大学（代章）

2020年 12 月 20 日

（13）第六届全国大学生物理实验竞赛一等奖获奖证明

获奖证书

Certificate of Award

哈尔滨工业大学唐爱国、周依凡、吴欢桐、刘辰翔、卢袁真子同学，在 2020 年第六届全国大学生物理实验竞赛中，荣获 一等 奖。

特发此证，以资鼓励。

高等学校国家级实验教学示范中心联席会
全国高等学校实验物理教学研究会
中国物理学会物理教学委员会
《物理实验》杂志社

全国大学生物理实验竞赛组委会
东北大学（代章）

2020年 12 月 20 日

（14）第六届全国大学生物理实验竞赛一等奖获奖证明

荣誉证书

HONORARY CREDENTIAL

哈尔滨工业大学　　吕桔　张宇 老师

在第三届"卓越杯"大学生物理实验竞赛中，

指导参赛项目：无线电能传输

荣获 一等奖

参赛队：张瑞琪 刘越程 于翔

证书编号：2020ZYB-717

卓越联盟高校（同济大学代章）

2020 年 11 月 22 日

（15）第三届“卓越杯”大学生物理实验竞赛获奖证明

（16）第十二届大学生创新创业年会获奖证明

（17）2108 年度工信创新奖学金获奖证明

（18）2017 年度工信创新奖学金

（19）2017 年度工信创新奖学金

（20）第十三届王大珩光学奖获奖证明

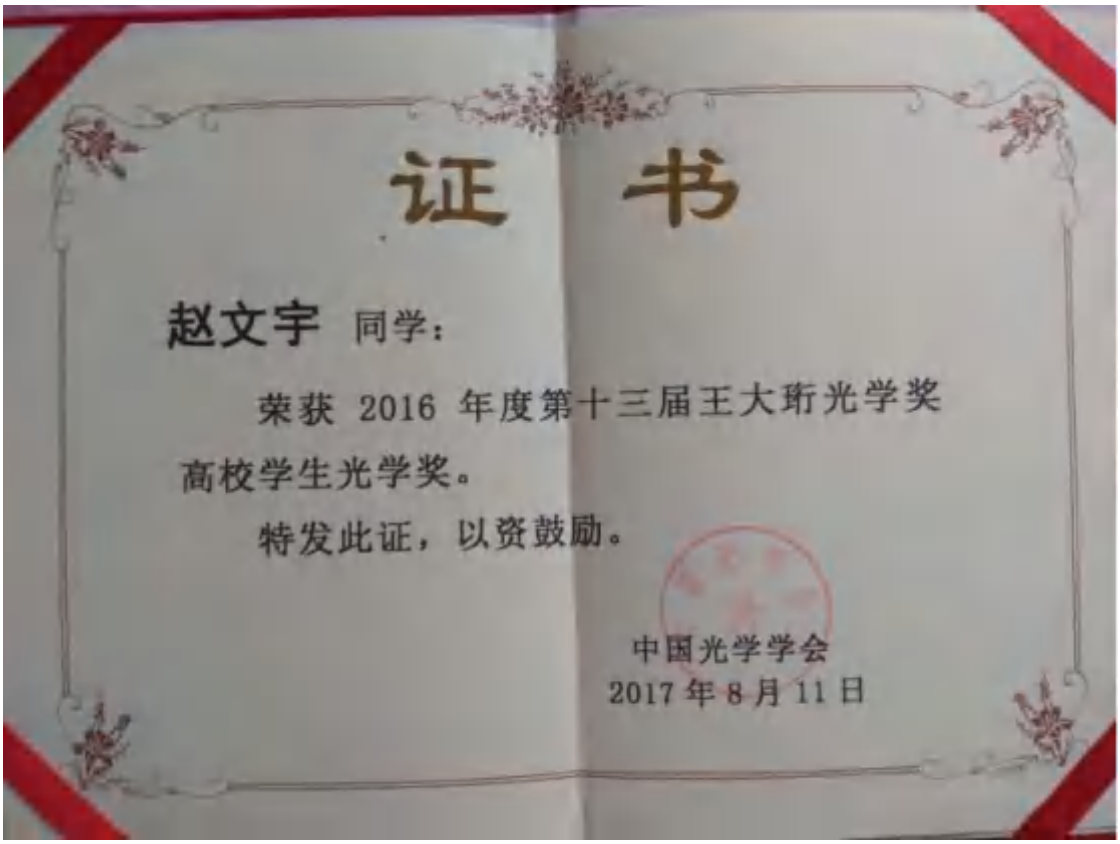

（21）第十一届国际天线传播和电磁理论学术研讨会优秀论文证明

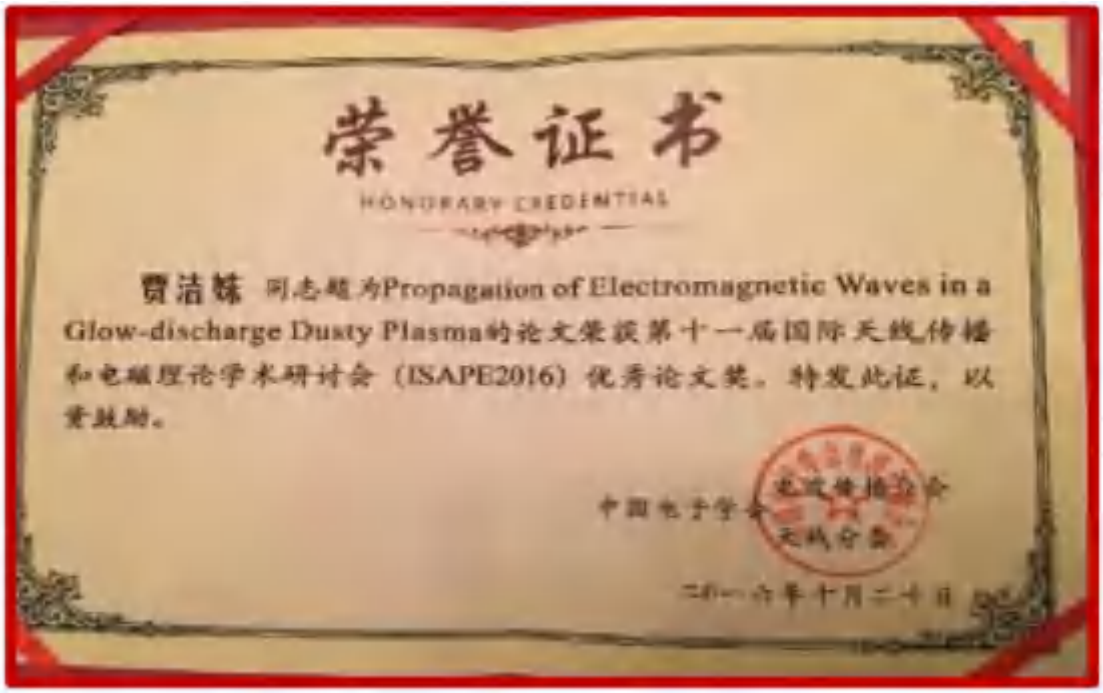

荣誉证书

HONORARY CREDENTIAL

贾洁婷 同志题为Propagation of Electromagnetic Waves in a Glow-discharge Dusty Plasma的论文荣获第十一届国际天线传播和电磁理论学术研讨会（ISAPE2016）优秀论文奖。特发此证，以资鼓励。

中国电子学会 天线分会

二〇一六年十月二十日

（22）第六届等离子体物理和应用研讨会优秀报告证明

哈爾濱工業大學

HARBIN INSTITUTE OF TECHNOLOGY

1920-2020

荣誉证书

姚静锋 同学题为的“Experimental and numerical investigation of the interaction of electromagnetic waves and plasma”报告荣获“第二届中俄等离子体物理暑期学校暨第六届等离子体物理和应用研讨会”（The 2nd Sino-Russia Summer School and 6th Workshop on Plasma Physics and Applications）优秀报告，特发此证，以资鼓励。

哈尔滨工业大学

物理学院

二零二零年七月[illegible]十八日

（23）第十四届全国大学生节能减排社会实践与科技竞赛获奖证明

证书编号：2021A-01-0027

“力诺瑞特杯”第十四届
全国大学生节能减排社会实践与科技竞赛

获奖证书

在2021年“力诺瑞特杯”第十四届全国大学生节能减排社会实践与科技竞赛中，经评审，获得全国 一等奖。

特发此证，以资鼓励。

作品名称：“行之灼灼”——一种基于力声光传感调光的智慧路灯系统

参赛高校：哈尔滨工业大学

作品类型：科技作品

参赛学生：谢文棋 肖家豪 黄肖振 张博宇 刘嘉春

指导教师：李德友 宫汝志

大学生节能减排

全国大学生节能减排社会实践与科技竞赛委员会

2021年8月

（24）第七届全国大学生物理实验竞赛（教学赛）二等奖获奖证明

获奖证书

Certificate of Award

哈尔滨工业大学　张宇　老师

所指导学生 周超、张晓 同学在 2021 年第七届全国大学生物理实验竞赛（教学赛）—综合性实验题目中，荣获 二 等奖。

特发此证，以资鼓励。

高等学校国家级实验教学示范中心联席会
全国高等学校实验物理教学研究会
中国物理学会物理教学委员会

天津大学（代章）
南开大学
2021 年 7 月 20 日

（25）第七届全国大学生物理实验竞赛二等奖获奖证明

获奖证书

Certificate of Award

学　　校：哈尔滨工业大学
学　　生：马殷云　纪家清　杨志青
指导教师：吕喆　张宇
参赛作品：多功能气体声速测量系统

在 2021 年第七届全国大学生物理实验竞赛中荣获

二等奖

特发此奖，以资鼓励！

国家级实验教学示范中心联席会物理学科组
全国高等学校实验物理教学研究会
中国物理学会物理教学委员会

全国大学生物理实验竞赛组委会
南昌大学（代章）
2021 年 12 月 5 日

证书编号：QGWLSYCX-2-0170

（26）第三届“卓越杯”大学生物理实验竞赛二等奖获奖证明

荣誉证书

HONORARY CREDENTIAL

哈尔滨工业大学　　吕喆　王玉晓 老师

在第三届“卓越杯”大学生物理实验竞赛中，

指导参赛项目：超声声镊

荣获 二等奖

参 赛 队：谢桂奕 骆全鑫

证书编号：2020ZYB-□14

卓越联盟高校（同济大学代章）

2020 年 11 月 22 日

（27）第十四届全国大学生节能减排社会实践与科技竞赛证明

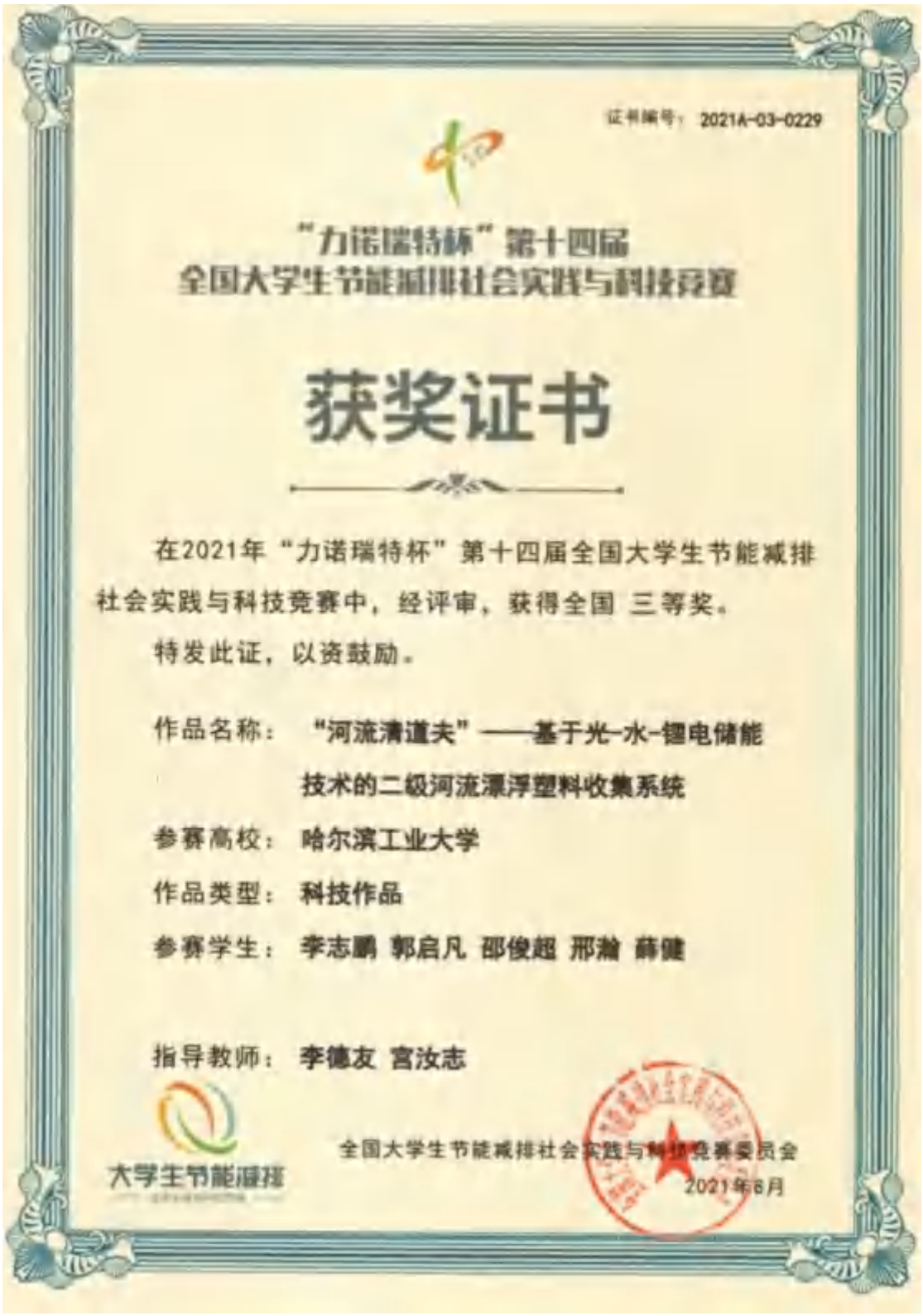

证书编号：2021A-03-0229

“力诺瑞特杯”第十四届
全国大学生节能减排社会实践与科技竞赛

获奖证书

在2021年“力诺瑞特杯”第十四届全国大学生节能减排社会实践与科技竞赛中，经评审，获得全国 三等奖。

特发此证，以资鼓励。

作品名称：“河流清道夫”——基于光-水-锂电储能技术的二级河流漂浮塑料收集系统

参赛高校：哈尔滨工业大学

作品类型：科技作品

参赛学生：李志鹏 郭启凡 邵俊超 邢瀚 薛健

指导教师：李德友 宫汝志

大学生节能减排

全国大学生节能减排社会实践与科技竞赛委员会

2021年8月

（28）第五届全国大学生材料设计邀请赛三等奖

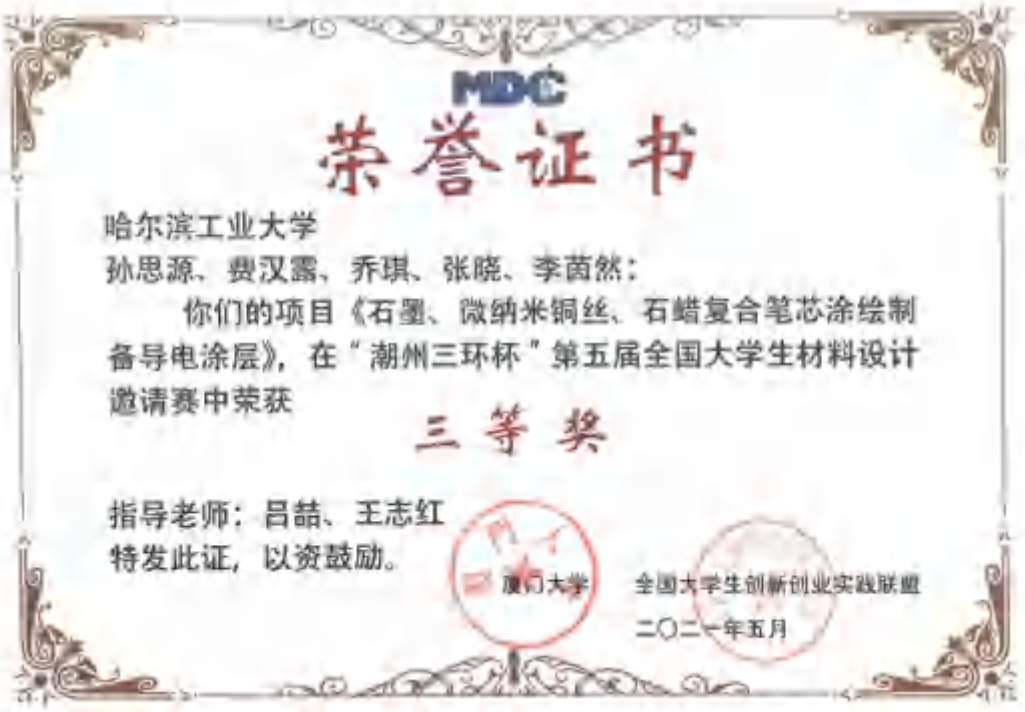

MDC

荣誉证书

哈尔滨工业大学

孙思源、费汉露、乔琪、张晓、李茵然：

你们的项目《石墨、微纳米铜丝、石蜡复合笔芯涂绘制备导电涂层》，在“潮州三环杯”第五届全国大学生材料设计邀请赛中荣获

三等奖

指导老师：吕喆、王志红

特发此证，以资鼓励。

厦门大学　全国大学生创新创业实践联盟

二〇二一年五月

（29）全国光学与光学工程博士生学术联赛获奖证明

2021年·全国光学与光学工程博士生学术联赛

获奖证书

CERTIFICATE OF AWARD

王宇 同学：

你在2021年全国光学与光学工程博士生学术联赛中，成绩优异，荣获 东北 赛区 二 等奖。

特发此证，以示表彰。

全国光学与光学工程博士生学术联赛组委会

时间：2021年3月

（30）全国光学与光学工程博士生学术联赛获奖证明

（31）辽宁省优秀博士学位论文证明


荣誉证书

HONORARY CREDENTIAL

郭宇

您的《二维硫属化物的电子性质和氧化行为的第一性原理研究》被评为 2020 年辽宁省优秀博士学位论文。

编号：LNYB2020002

二〇二一年五月九日

（32）辽宁省优秀博士学位论文证明

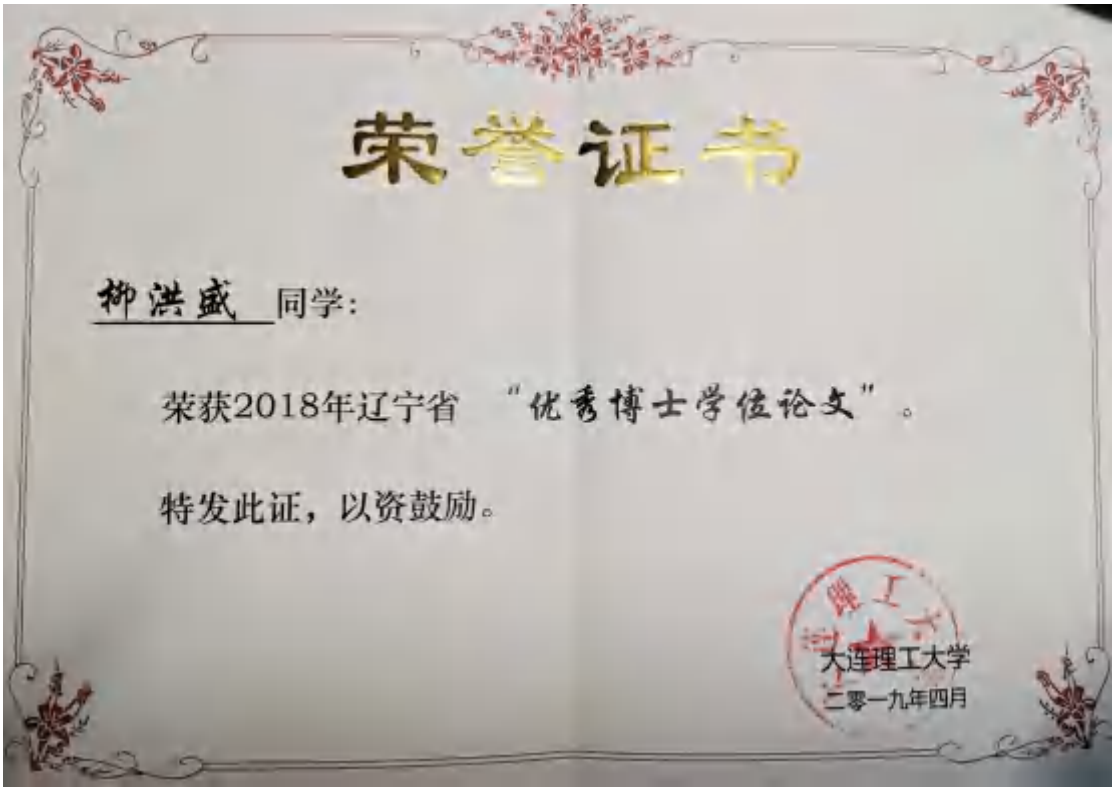
荣誉证书

柳洪盛 同学：

荣获2018年辽宁省 “优秀博士学位论文”。

特发此证，以资鼓励。

大连理工大学

二零一九年四月

（33）辽宁省优秀博士学位论文证明


证 书

CREDENTIAL

黄晓明

您的《合金团簇结构和磁性的第一性原理研究》被评为2016年辽宁省优秀博士学位论文。

编号:2016008

二〇一七年四月十二日

（34）辽宁省优秀博士学位论文证明

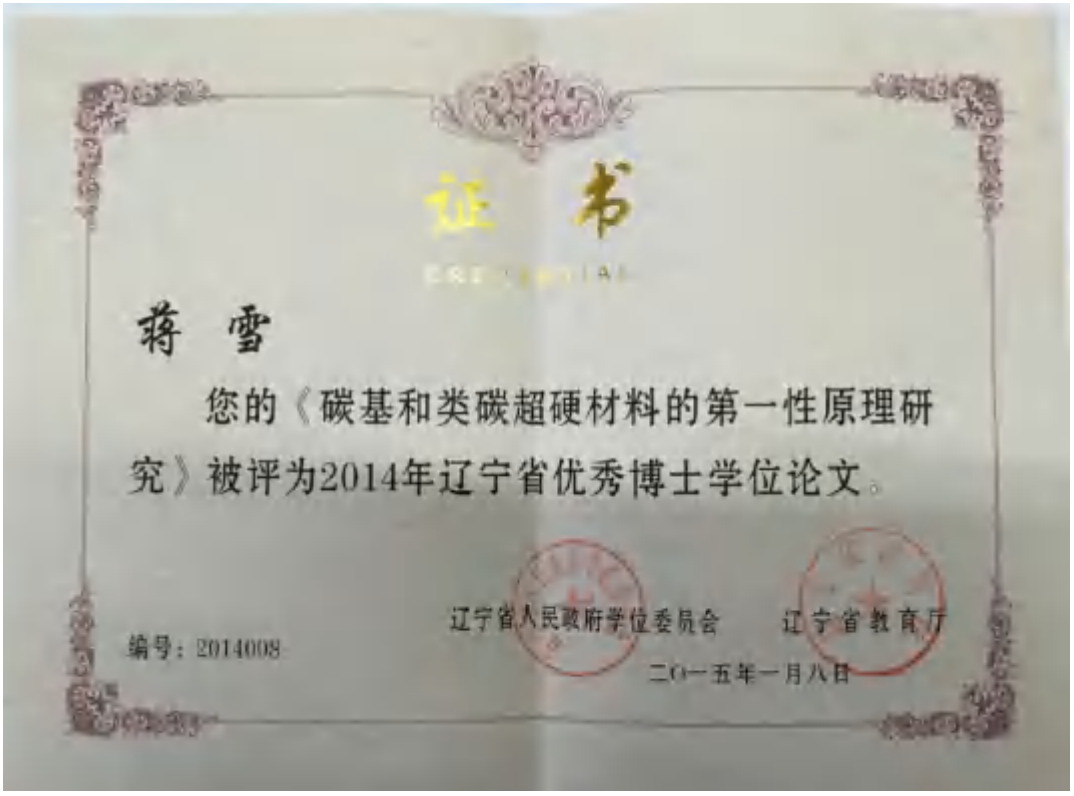
证 书

蒋 雪

您的《碳基和类碳超硬材料的第一性原理研究》被评为2014年辽宁省优秀博士学位论文。

辽宁省人民政府学位委员会　　辽宁省教育厅

编号：2014008

二〇一五年一月八日

（35）辽宁省优秀博士学位论文证明


荣誉证书

HONORARY CREDENTIAL

高峻峰 同学：

您的论文《过渡金属表面石墨烯和硅烯的成核生长机理与相互作用》被评为2014年辽宁省优秀博士学位论文。

特发此证，以资鼓励。

大连理工大学（代章）

二零一五年四月三十日

（36）黑龙江省高校科学技术奖

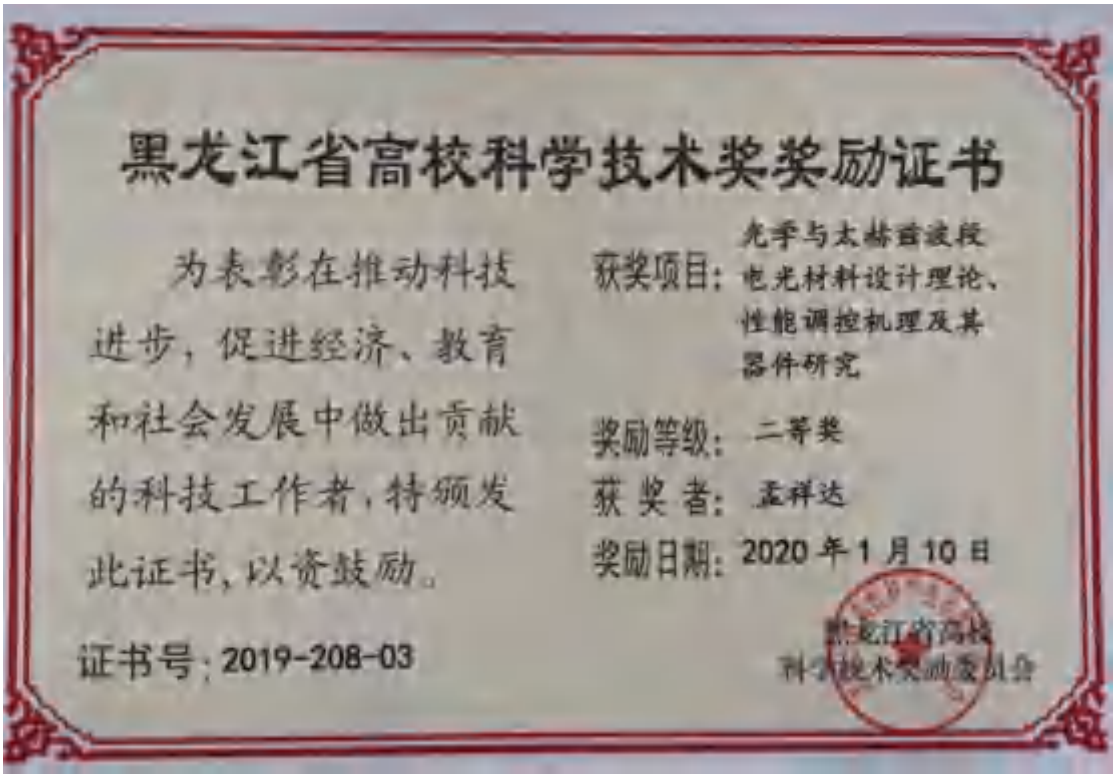
黑龙江省高校科学技术奖奖励证书

为表彰在推动科技进步，促进经济、教育和社会发展中做出贡献的科技工作者，特颁发此证书，以资鼓励。

获奖项目：光学与太赫兹波段电光材料设计理论、性能调控机理及其器件研究

奖励等级：二等奖

获 奖 者：孟祥达

奖励日期：2020年1月10日

证书号：2019-208-03

黑龙江省高校科学技术奖励委员会

（37）第七届中国国际“互联网+”大学生创新创业大赛获奖证明

获奖证书

肖家豪、刘嘉乔、谢文祺、黄肖振、张博宇：

你们的作品《“行之灼灼”——一种基于力声光传感调光的智慧路灯系统》荣获“建行杯”第七届黑龙江“互联网+”大学生创新创业大赛

银奖

指导教师：李德友、宫治杰

黑龙江省教育厅

2021年8月6日

（38）第十二届工银融 e 联“挑战杯”黑龙江省大学生创业计划竞赛

挑战杯

获奖证书

郁明达、张昱达、蒋 昊、范 琦、张 鑫 同学：

你（们）的项目《利用环保溶剂回收废旧材料制备再生纤维素材料的新方法》

在第十二届工银融 e联“挑战杯”黑龙江省大学生创业计划竞赛中荣获：

铜奖

指导教师：李德友

特颁此证，以资鼓励。

共青团黑龙江省委员会　黑龙江省教育厅　黑龙江省科学技术协会　黑龙江省学生联合会

二〇二〇年九月

（39）研究生国家奖学金（博士 42 人次）

（40）研究生国家奖学金（硕士 26 人次）证明

（41）辽宁省优秀毕业生证明

（42）第五届研究生十佳团队证明

（7）教学项目佐证材料

序号	项目名称	项目来源	负责人	年份
1	物理学科研究生教学与科研融合研究与实践	中国学位与研究生教育学会	田浩	2020
2	“一带一路”背景下哈工大对俄罗斯高校基础学科前沿科学研究提升计划	2021 年度教育部“一带一路”教育合作项目	李均	2019
3	依托国家级研究生联合培养实践基地高质量培养体系及方法研究	中国学位与研究生教育学会面上项目	李德友	2021
4	理论力学“一流课程”课程思政建设的探索与实践	教育部高等学校教学指导委员会	任延宇	2021
5	现代光电信息专业实验教学中心建设	教育部产学合作协同育人项目	王健	2020
6	数学物理方法教学内容完善及教学体系优化设计	教育部高等学校物理学类专业教学指导委员会	姜向前	2016
7	创建以学生为主体的力学课程教学规范	教育部高等学校教学指导委员会	任延宇	2016
8	应用物理专业“科教融合”人才培养模式研究与实践	省高等教育教学改革一般研究项目	吕喆	2018
9	光电信息科学与工程专业资源共享课程建设—《光电信息功能材料》的教材建设	黑龙江省高等教育学会“十三五”高等教育科研课题	周忠祥	2016
10	基于人才个性化培养的基础物理分层次教学研究	黑龙江省高等教育学会“十三五”高等教育科研课题	孟庆鑫	2016
11	物理学科拔尖研究生的原始创新能力培养路径与培养实践	黑龙江省教育厅	丁卫强	2021
12	基于对俄合作提升研究生培养国际化水平	黑龙江省教育厅	袁承勋	2021
13	辽宁省一流线下课程：光波导技术	辽宁省教育厅	李淑凤	2022
14	国家本科教学工程项目：普通物理	中华人民共和国教育部	李淑凤	2021
15	以研究性实验为依托的物理拔尖人才创新能力培养研究与实验	辽宁省教育厅	赵纪军	2021
16	国家本科教学质量工程项目“基础拔尖人才”：王大珩班物理拔尖学生培养	中华人民共和国教育部	赵纪军	2020
17	国家本科教学质量工程项目强基计划：应用物理学	中华人民共和国教育部	赵纪军	2020
18	辽宁省线下一流课程：现代固	辽宁省教育厅	赵纪军	2020

	体物理学			
19	国家一流线上课程：大学物理	中华人民共和国教育部	李淑凤	2020
20	国家一流专业建设：应用物理学	中华人民共和国教育部	赵纪军	2019
21	中央高校教育教学改革专项，《固体物理学》特色课程群建设	中华人民共和国教育部	赵纪军	2019
22	大学物理 Mooc 练习活动资源建设及与传统教学融合模式的研究与实践	教育部高等学校教学指导委员会	李淑凤	2016
23	国家综合改革重点建设专业	辽宁省教育厅	赵纪军	2014
24	辽宁省教改项目“王大珩物理科学班”科研创新体系的全面建设	辽宁省教育厅	赵纪军	2016
25	辽宁省精品资源共享课：固体物理学	辽宁省教育厅	赵纪军	2015
26	辽宁省普通高等教育本科教学改革研究项目，“王大珩物理科学班”科研创新体系的全面建设	辽宁省教育厅	赵纪军	2015
27	辽宁省质量工程项目“应用物理学-优势特色专业”	辽宁省教育厅	赵纪军	2014
28	辽宁省教改项目,《大学物理》跨校修读课程资源与教学模式优化共享的实践研究	辽宁省教育厅	李淑凤	2021
29	大学物理跨校修读课程教学模式的研究与实践	辽宁省教育厅	李淑凤	2018
30	校研究生教改重点项目“物理学研究生课程思政体系建设”	大连理工大学	蒋雪	2021
31	校教改重点项目：中白“同窗友情”模式下深化“融合创新”合作办学的实践	大连理工大学	赵纪军	2022
32	校课程思政示范课：学术规范与科技英语写作	大连理工大学	赵纪军	2019
33	《计算凝聚态物理》课程教学与多元化育人模式探索	大连理工大学	蒋雪	2020

（1）物理学科研究生教学与科研融合研究与实践

中国学位与研究生教育学会

学会 2020 年面上课题立项通知

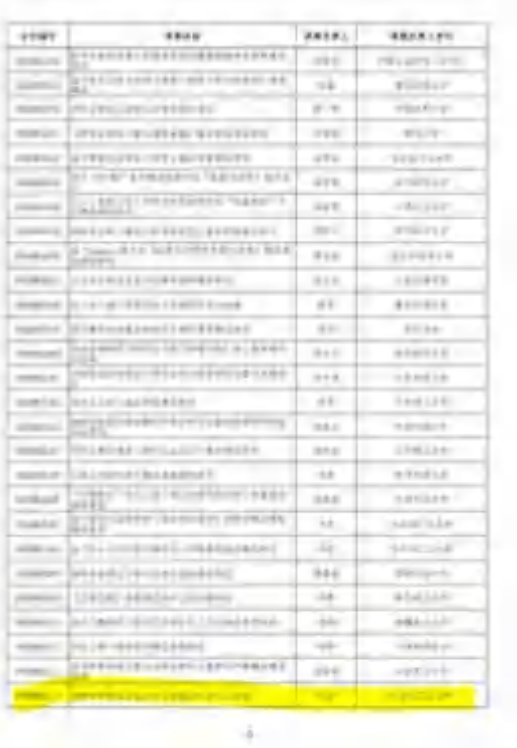

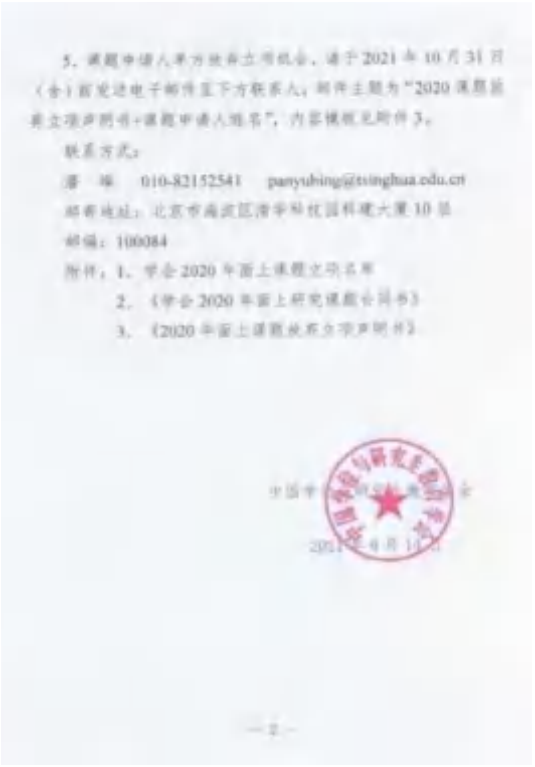

5. 课题申请人单方获得立项机会，请于 2021 年 10 月 31 日（含）前发送电子邮件至下方联系人，邮件主题为“2020 课题名称+课题申请人姓名”，内容模板见附件 3。

联系方式：

潘 瑜 010-82152541 panyuhing@tsinghua.edu.cn

邮寄地址：北京市海淀区清华科技园科建大厦 10 层

邮编：100084

附件：1. 学会 2020 年面上课题立项名单

2. 《学会 2020 年面上研究课题合同书》

3. 《2020 年面上课题获批立项声明书》

（2）“一带一路”背景下哈工大对俄罗斯高校基础学科前沿科学研究提升计划

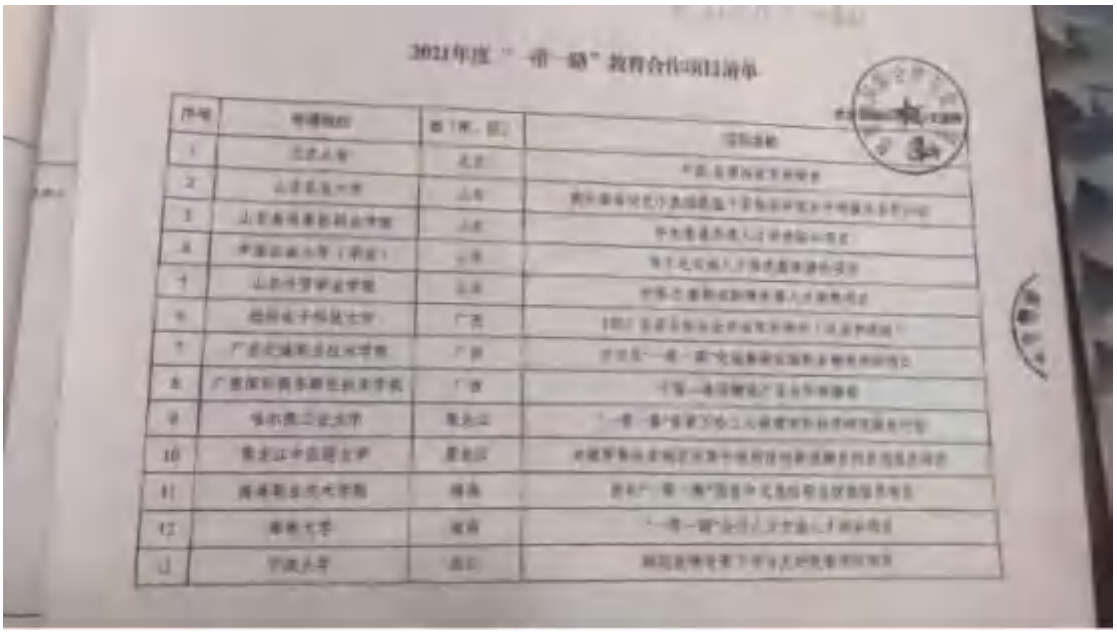

（3）依托国家级研究生联合培养实践基地高质量培养体系及方法研究


学位与研究生教育研究课题

合同书

中国学位与研究生教育学会

二〇二一年九月

七、合同签署

（4）理论力学“一流课程”课程思政建设的探索与实践

教育部高等学校物理学类专业教学指导委员会

2021 年度高等学校理论力学课程教学研究项目

立项通知

任延宇老师，您好：

您 2021 年申报的理论力学课程教学研究项目《理论力学“一流课程”课程思政建设的探索与实践》，经过答辩及专家讨论后已经立项，项目编号为 JZW-21-LL-06，请按照项目申报书和理论力学课程研究会要求认真执行，并及时提交中期报告和结题报告。

课程研究会感谢您的支持！

理事长：

教育部高等学校物理学类专业教学指导委员会

高等学校理论力学课程研究会

南开大学物理学院（挂靠单位（代章））

2021 年 8 月 30 日

（5）现代光电信息专业实验教学中心建设

教育部高等教育司关于公布2019年第二批产学合作协同育人项目立项名单的通知

教高司函〔2020〕6号

各省、自治区、直辖市教育厅（教委），新疆生产建设兵团教育局，有关高等学校、有关企业：

为深入贯彻《国务院办公厅关于深化产教融合的若干意见》（国办发〔2017〕95号）精神，落实《教育部 工业和信息化部 中国工程院关于加快建设发展新工科 实施卓越工程师教育培养计划2.0的意见》（教高〔2018〕3号）要求，深化产教融合，校企协作，我司组织有关企业和高校深入实施产学合作协同育人项目。

《教育部高等教育司关于公布有关企业支持的产学合作协同育人项目申报指南（2019年第二批）的通知》发布后，有关高校积极组织师生向企业提交项目申请，有关企业组织专家开展项目论证工作，并自愿企业双方达成合作意向的项目向社会公示。经教育部产学合作协同育人项目专家组审定，现将立项项目名单予以公布（见附件）。

根据《教育部办公厅关于印发〈教育部产学合作协同育人项目管理办法〉的通知》（教高厅〔2020〕1号）要求，有关高校要加强对项目的指导和管理，项目负责人要与相关企业加强联系，按照要求高质高效推进项目实施。有关企业要保证资金及软硬件投入按计划到位，规范项目管理，保证项目顺利实施。通过政府搭台、企业支持、高校对接、共建共享、深化产教融合，促进教育链、人才链与产业链、创新链有机衔接，以产业和技术发展的迫切需求驱动高校人才培养改革，培养支撑引领经济社会发展需要的高素质专门人才。

附件：1.2019年第二批产学合作协同育人项目立项名单（按企业排序）

2.2019年第二批产学合作协同育人项目立项名单（按高校排序）

教育部高等教育司

2020年6月3日

附件1

2019年第二批产学合作协同育人项目立项名单（按企业排序）

项目编号	公司名称	项目类型	承担学校	项目名称	项目负责人
[redacted]					
[redacted]					

项目编号	公司名称	项目类型	承担学校	项目名称	项目负责人
[redacted]					
[redacted]					
[redacted]					
[redacted]					
[redacted]					

（6）数学物理方法教学内容完善及教学体系优化设计

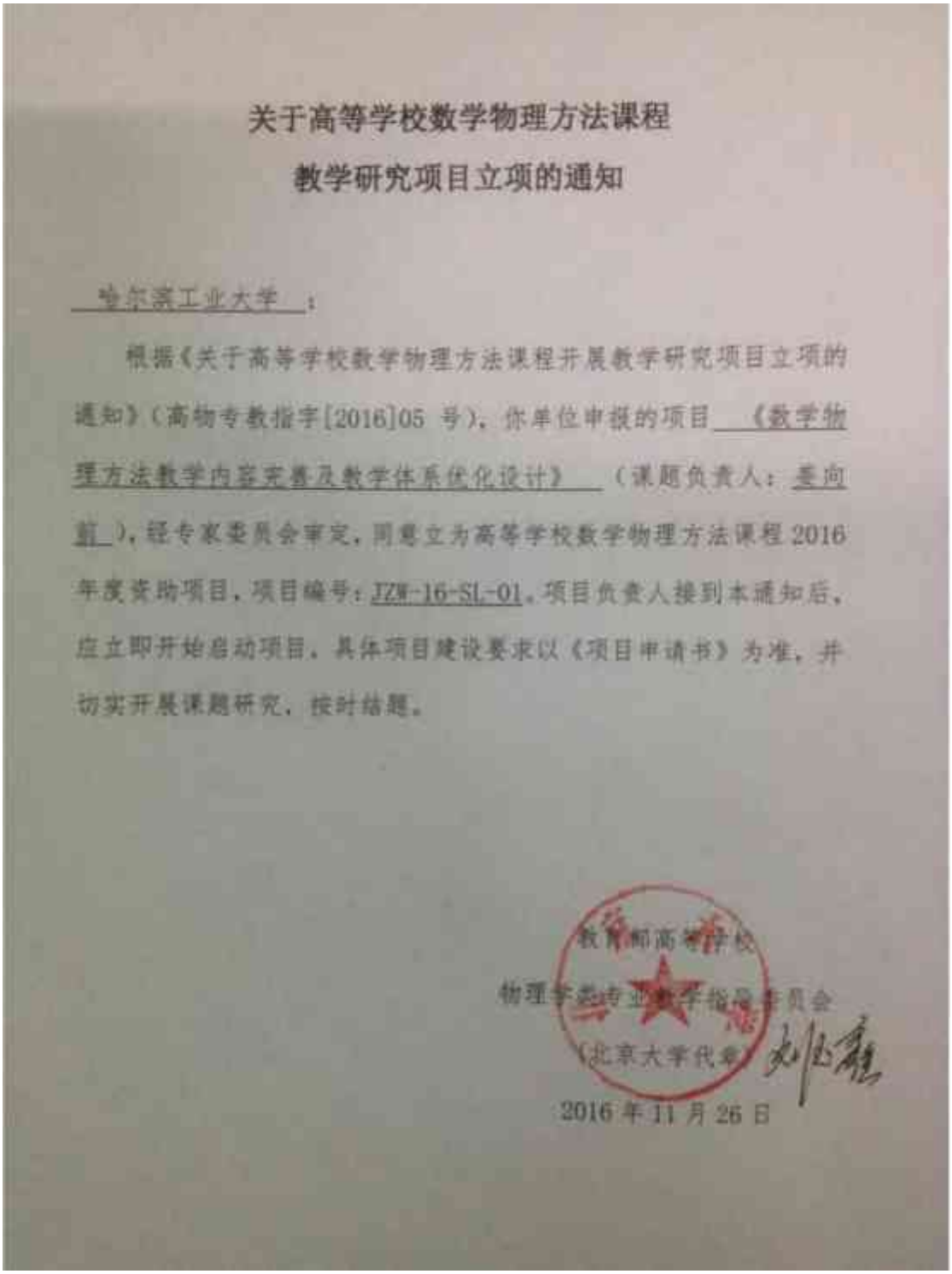

关于高等学校数学物理方法课程
教学研究项目立项的通知

哈尔滨工业大学：

根据《关于高等学校数学物理方法课程开展教学研究项目立项的通知》（高物专教指字[2016]05 号），你单位申报的项目《数学物理方法教学内容完善及教学体系优化设计》（课题负责人：姜向前），经专家委员会审定，同意立为高等学校数学物理方法课程 2016 年度资助项目，项目编号：JZW-16-SL-01。项目负责人接到本通知后，应立即开始启动项目，具体项目建设要求以《项目申请书》为准，并切实开展课题研究，按时结题。

教育部高等学校
物理学类专业教学指导委员会
（北京大学代章）

2016 年 11 月 26 日

（7）创建以学生为主体的力学课程教学规范

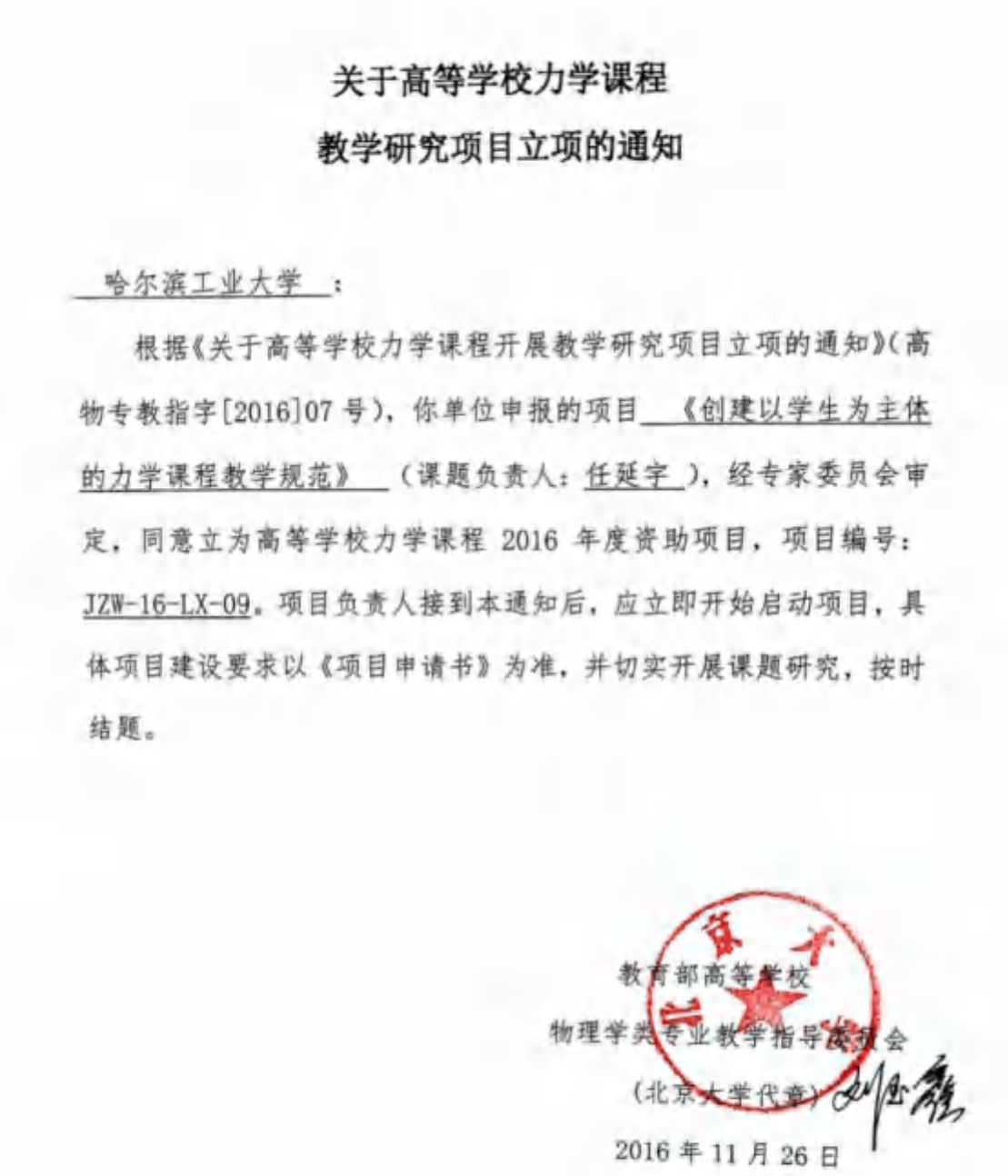

关于高等学校力学课程
教学研究项目立项的通知

哈尔滨工业大学：

根据《关于高等学校力学课程开展教学研究项目立项的通知》（高物专教指字[2016]07号），你单位申报的项目《创建以学生为主体的力学课程教学规范》（课题负责人：任延宇），经专家委员会审定，同意立为高等学校力学课程2016年度资助项目，项目编号：JZW-16-LX-09。项目负责人接到本通知后，应立即开始启动项目，具体项目建设要求以《项目申请书》为准，并切实开展课题研究，按时结题。

教育部高等学校
物理学类专业教学指导委员会
（北京大学代章）
2016年11月26日

（8）应用物理专业“科教融合”人才培养模式模式研究与实践

黑龙江省教育厅

黑教高函〔2018〕608号

省教育厅关于公布2018年度高等教育教学改革研究项目立项结果的通知

各普通本科高校：

按照《省教育厅关于开展2018年度高等教育教学改革研究项目申报与结题的通知》（黑教高函〔2018〕281号）要求，我厅组织开展了2018年度高等教育教学改革研究项目立项工作，现将结果予以公布。其中，重点委托项目立项73项，一般研究项目备案586项。

请各高校认真按照《关于印发省教育厅关于进一步加强普通高等学校教育教学改革与研究的指导意见的通知》（黑教发〔2017〕9号）要求，加强对立项项目的支持和管理，对立项项目按照不低于1:1的标准足额落实配套经费，并指导项目主持人按期完成研究工作，培育更多优质教学成果。我厅将根据高校项目整体完成和推广情况，本着激励原则，动态调整下一年度立项指标。

180									
181									
182									
183									
184									
185									
186									
187									

（9）光电信息科学与工程专业资源共享课程建设—《光电信息功能材料》的教材建设

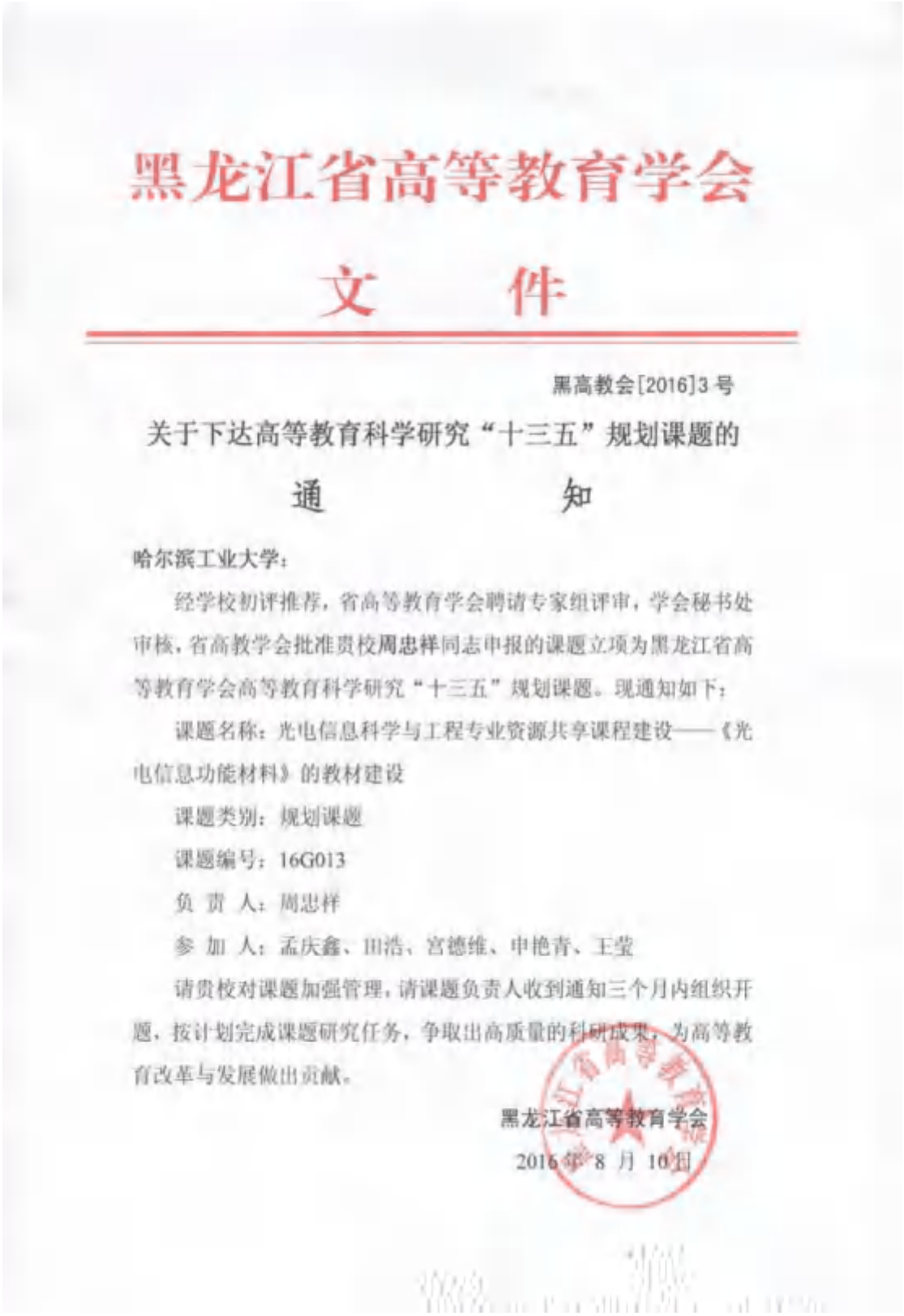

黑龙江省高等教育学会

文　　件

黑高教会[2016]3号

关于下达高等教育科学研究“十三五”规划课题的

通　　知

哈尔滨工业大学：

经学校初评推荐，省高等教育学会聘请专家组评审，学会秘书处审核，省高教学会批准贵校周忠祥同志申报的课题立项为黑龙江省高等教育学会高等教育科学研究“十三五”规划课题。现通知如下：

课题名称：光电信息科学与工程专业资源共享课程建设——《光电信息功能材料》的教材建设

课题类别：规划课题

课题编号：16G013

负 责 人：周忠祥

参 加 人：孟庆鑫、田浩、宫德维、申艳青、王莹

请贵校对课题加强管理，请课题负责人收到通知三个月内组织开题，按计划完成课题研究任务，争取出高质量的科研成果，为高等教育改革与发展做出贡献。

黑龙江省高等教育学会

2016年8月10日

（10）基于人才个性化培养的基础物理分层次教学研究

黑龙江省高等教育学会

文　　件

黑高教会[2016]3号

关于下达高等教育科学研究“十三五”规划课题的

通　　知

哈尔滨工业大学：

经学校初评推荐，省高等教育学会聘请专家组评审，学会秘书处审核，省高教学会批准贵校孟庆鑫同志申报的课题立项为黑龙江省高等教育学会高等教育科学研究“十三五”规划课题。现通知如下：

课题名称：基于人才个性化培养的基础物理分层次教学研究

课题类别：规划课题

课题编号：16G014

负 责 人：孟庆鑫

参 加 人：张宇、李均、骆素华、张伶莉、袁承勋、吴琦、韩权

请贵校对课题加强管理，请课题负责人收到通知三个月内组织开题，按计划完成课题研究任务，争取出高质量的科研成果，为高等教育改革与发展做出贡献。

黑龙江省高等教育学会

2016年 8 月 10日

（11）物理学科拔尖研究生的原始创新能力培养路径与培养实践

哈尔滨工业大学推荐申报2021年度黑龙江省高等教育教学改革研究项目立项名单

序号	学院名称	项目名称	项目负责人	项目参与人（共4人，按照排序填）				备注
				1	2	3	4	
1								
2								
3								
4								
5								
6								
7								
8								
9								
10								
11								

（12）基于对俄合作提升研究生培养国际化水平

哈尔滨工业大学推荐申报2021年度黑龙江省高等教育教学改革研究项目立项名单

序号	学院名称	项目名称	项目负责人	项目参与人（共4人，按照排序填）				备注
				1	2	3	4	
1								
2								
3								
4								
5								
6								
7								
8								
9								
10								
11								

（13）剩余部分教改项目证明材料

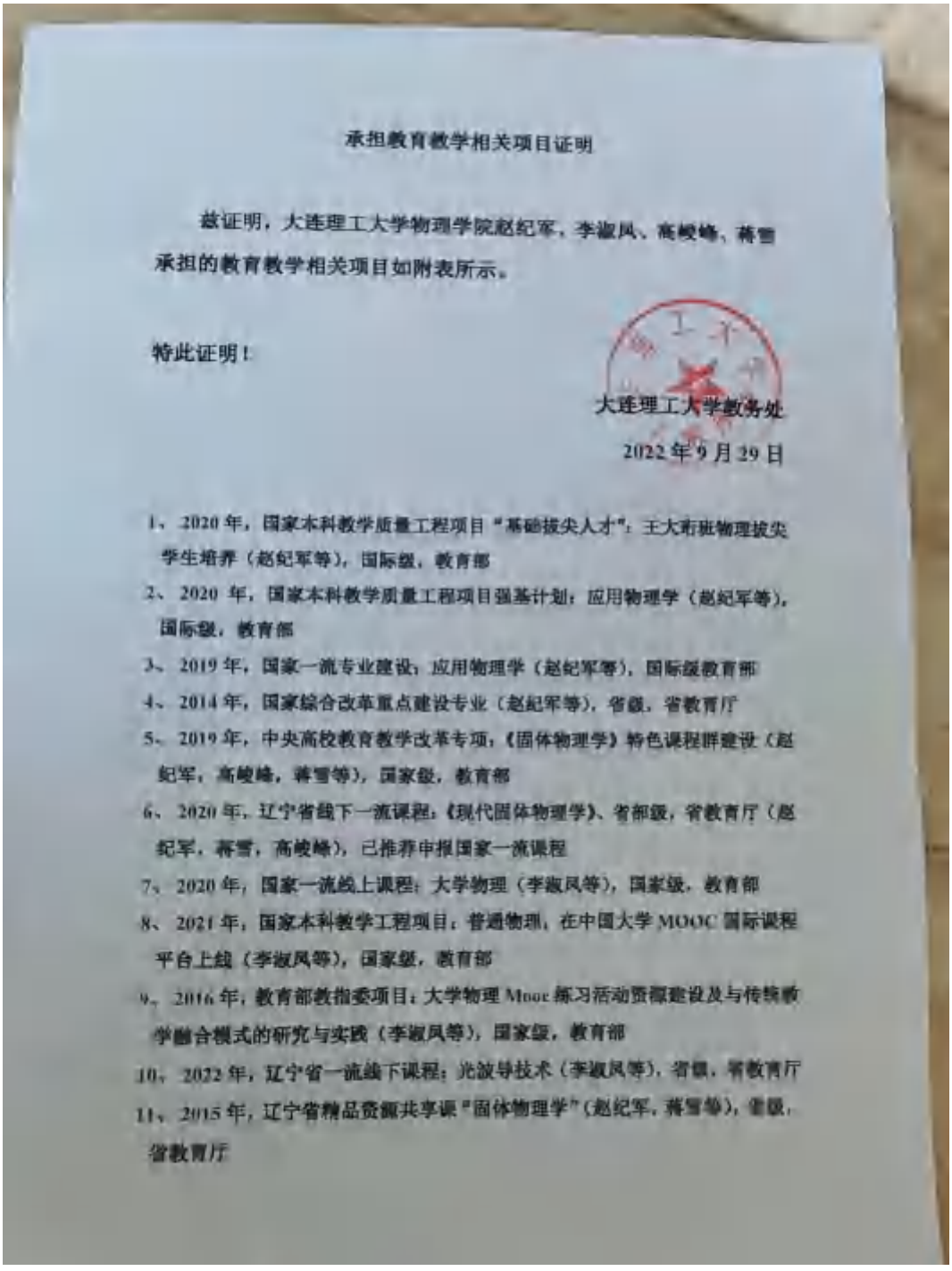

承担教育教学相关项目证明

兹证明，大连理工大学物理学院赵纪军、李淑凤、高峻峰、蒋雪承担的教育教学相关项目如附表所示。

特此证明！

大连理工大学教务处

2022年9月29日

1、2020年，国家本科教学质量工程项目“基础拔尖人才”：王大珩班物理拔尖学生培养（赵纪军等），国际级，教育部

2、2020年，国家本科教学质量工程项目强基计划：应用物理学（赵纪军等），国际级，教育部

3、2019年，国家一流专业建设：应用物理学（赵纪军等），国际级教育部

4、2014年，国家综合改革重点建设专业（赵纪军等），省级，省教育厅

5、2019年，中央高校教育教学改革专项：《固体物理学》特色课程群建设（赵纪军，高峻峰，蒋雪等），国家级，教育部

6、2020年，辽宁省线下一流课程：《现代固体物理学》、省部级，省教育厅（赵纪军，蒋雪，高峻峰），已推荐申报国家一流课程

7、2020年，国家一流线上课程：大学物理（李淑凤等），国家级，教育部

8、2021年，国家本科教学工程项目：普通物理，在中国大学MOOC国际课程平台上线（李淑凤等），国家级，教育部

9、2016年，教育部教指委项目：大学物理Mooc练习活动资源建设及与传统教学融合模式的研究与实践（李淑凤等），国家级，教育部

10、2022年，辽宁省一流线下课程：光波导技术（李淑凤等），省级，省教育厅

11、2015年，辽宁省精品资源共享课“固体物理学”（赵纪军，蒋雪等），省级，省教育厅

12、2016年，辽宁省教改项目"王大珩物理科学班"科研创新体系的全面建设（赵纪军等），省级，省教育厅

13、2015年，辽宁省普通高等教育本科教学改革研究项目："王大珩物理科学班"科研创新体系的全面建设（赵纪军等），省级，省教育厅

14、2014年，辽宁省质量工程项目："应用物理学"优势特色专业"（赵纪军等），省级，省教育厅

15、2021年，省教改项目："《大学物理》跨校修读课程资源与教学模式优化共享的实践研究"（李淑凤等），省级，省教育厅

16、2018年，省教改项目：大学物理跨校修读课程教学模式的研究与实践（李淑凤等），省级，省教育厅

17、2021年，省教改项目：以研究性实验为依托的物理拔尖人才创新能力培养研究与实践，省级，省教育厅

18、2019年，校课程思政示范课：学术规范与科技英语写作（赵纪军，蒋雪等），校级，大连理工大学

19、2022年，校教改重点项目：中白"同窗友情"模式下深化"融合创新"合作办学的实践（高峻峰等），校级，大连理工大学

20、2021年，校教改重点项目：物理学研究生课程思政体系建设（赵纪军，蒋雪），校级，大连理工大学

21、2020年，校课程思政先导课：《计算凝聚态物理》课程教学与多元化育人模式探索（蒋雪，赵纪军），校级，大连理工大学

（8）教学论文发表佐证材料

序号	文章名称	刊物名称及级别 /会议名称	第一作者	出版年份
1	Geometric explanation of conic-section interference fringes in a Michelson interferometer.	American Journal of Physics (SCI 期刊)	方光宇	2013
2	Naked-eye observation of visible spectra using a transmission-grating-based spectrometer.	European Journal of Physics (SCI 期刊)	林珊	2021
3	工程类专业学位研究生培养的治理改革——基于政策供需协调视角的多案例比较研究	中国高教研究 （北大核心期刊）	王健	2022
4	麦克斯韦－玻尔兹曼分布在易辛模型中的应用	大学物理 （北大核心期刊）	应涛	2021
5	半无界空间上函数的傅里叶－贝塞尔积分展开	大学物理 （北大核心期刊）	姜向前	2020
6	熵概念的延拓——从热熵到信息熵	大学物理 （北大核心期刊）	李均	2020
7	砷化镓、硅单晶太阳能电池特性研究实验教学设计	实验技术与管理 （北大核心期刊）	王一	2020
8	在课堂演示实验中引入光学异常透射现象	大学物理 （北大核心期刊）	裴延波	2020
9	用低功率可见二极管激光器开展倍频实验	实验技术与管理 （北大核心期刊）	娄秀涛	2019
10	迈克尔逊干涉在电场-应变效应测量中的应用	大学物理 （北大核心期刊）	宫德维	2019
11	浅谈利用薛定谔方程计算量子态的时间演化	大学物理 （北大核心期刊）	宋杰	2019
12	建立自主探究性实验教学模式提升实验教学的人才培养水平	物理实验 （北大核心期刊）	赵海发	2018

13	基于光致瞬态光栅测量液体内的声速	物理实验 （北大核心期刊）	刘伟龙	2018
14	用外腔半导体激光获取强荧光物质的拉曼特征峰值	物理实验 （北大核心期刊）	娄秀涛	2017
15	波尔共振实验中基于旋转矢量的相位差分析	大学物理 （北大核心期刊）	姜向前	2017
16	工科院校物理演示实验体系的实践与探索	实验室研究与探索 （北大核心期刊）	靳辰飞	2016
17	核物理多功能教学实验仪教学应用与功能开发	物理实验 （北大核心期刊）	任延宇	2016
18	等厚干涉实验中缺陷检测的数值模拟	物理实验 （北大核心期刊）	刘建龙	2015
19	物理学拓展课程提升学生综合素质	物理与工程 （其他）	王晓鸥	2015
20	气体分子高分辨吸收光谱测量的实验设计与教学实践	中国现代教育装备 （其他）	娄秀涛	2021
21	关于“光的偏振”教学的一些尝试	物理与工程 （其他）	刘志国	2020
22	关于“光的干涉”部分教学模式的探讨	物理通报 （其他）	曹永印	2019
23	光学干涉在二次电光系数测量中的应用与分析	物理与工程 （其他）	田浩	2015
24	“工作室物理”教学中的演示实验	物理与工程 （其他）	王晓鸥	2017
25	刚体定点转动代数讲法的教学实践	物理与工程 （其他）	任延宇	2017
26	工作室物理教学中的互动反馈教学设计	物理通报 （其他）	张伶莉	2016

27	利用通识课程《物理学史》来传递物理文化和培养物理思维——通识课程《物理学史》建设及改革初探	物理通报（其他）	孟庆鑫	2016
28	分离变量法教学内容优化及本征值问题引入方式研究	物理通报（其他）	姜向前	2018
29	压缩传感在物理演示实验中的应用	物理与工程（其他）	靳辰飞	2016
30	学科思维导图与物理知识网络的构建	物理与工程（其他）	李淑凤	2018
31	《大学物理》MOOC 练习资源建设及其与传统教学模式的融合	物理与工程（其他）	李淑凤	2017
32	静电场中的相关能量	物理与工程（其他）	李淑凤	2016
33	基于教学的洛伦兹变换推导的探讨	物理与工程（其他）	李淑凤	2014

（1） Geometric explanation of conic-section interference fringes in a Michelson interferometer., 2013 American Journal of Physics

Geometric explanation of conic-section interference fringes in a Michelson interferometer

Guangyu Feng,[a] Li Huang, Li Xin, Haila Zhao, and Lin Hua
Department of Physics, Harbin Institute of Technology, Harbin 150001, P.R.China

Lei Wu[b]
Center for Engineering Training and Basic Experimentation, Northeastern University, Shenyang 110819, P.R.China

(Received 4 January 2013; accepted 6 June 2013)

A simple geometric method based on wave-front analysis is developed to provide a concise explanation for the various interference fringes in a Michelson interferometer without the compensator plate. In view of the fact that a homocentric pencil of rays from a point light source becomes astigmatic as it passes obliquely through a glass plate, the wave-front deviation from a spherical one is obtained by calculating the astigmatic focal distance of the central ray. If the compensator plate is removed, the two central rays along the interfering paths have different astigmatic focal distances (AFDs); therefore, the optical path length difference can always be compensated with the movement of the reflective mirrors. The wave-front difference or the optical path difference is determined to the accuracy of second order by computing the two pairs of principal curvature radii and the trivial point-by-point calculation of the optical path length difference (OPD) is avoided. Numerical results support the theoretical analysis well. [DOI: 10.1119/1.4811780]

I. INTRODUCTION

The Michelson interferometer (MI) is a standard topic in undergraduate physics courses and laboratories. It is also a versatile device which can readily be modified to measure such quantities as refractive index and linkage.[1–3]

The most commonly observed interference fringes in the MI are circular bands and parallel straight lines, either localized or nonlocalized, the formation of which is analyzed in most textbooks.[4] These fringes are viewed in a standard MI setup with the compensator plate (CP) in place, the role of which is also well explained in texts.[5] However, it is not an uncommon misconception among students that for the MI without the CP illuminated by a monochromatic light source, the optical path length difference could be compensated by the movement of either one of the two reflective mirrors. Therefore, students do not expect to see interference fringes with shapes of conic sections such as ellipses, hyperbolas, or parallel straight lines rather than circles when the compensator plate is removed, although this is a well-known phenomenon among professionals.[6]

The formation of these conic section fringes differs in principle from hyperbolic fringes produced with tilted reflective mirrors. Numerical calculations based on geometric optics can simulate the phenomena, which can also be visualized with the help of commercial software such as OPTICS.[7] Theoretical equations describing conditions for the appearance of different fringe shapes have also been derived in Ref. 8. Although the equations are correct and applicable, they are complicated and lack clear physical significance and consequently do not appeal to undergraduate students.

In this paper, we present a concise explanation of conic-section fringes by comparing the wave-fronts of the interfering waves and calculating their difference. The calculation is simplified by representing each of the wave-fronts locally with an elliptic paraboloidal surface, whose principal centers of curvature coincide with the primary and secondary foci of the central ray. Because the parameters of the foci have simple analytical expressions, which are already introduced in high-school geometric optics, this method is easier for students to understand. In addition to its educational purpose, this geometric method can also be adapted for applications in areas such as imaging, thickness and refractive index measurement, wave-front sensing and optical tomography.

II. THEORETICAL ANALYSIS

In a standard Michelson interferometer, as shown in Fig. 1, the compensator plate CP is a duplicate of the beam-splitter BS, which guarantees that the beam reflected from the movable mirror M_1 and the beam from the stationary mirror M_2 pass through the same thickness of glass.

To be specific, without losing generality, we assume the light is emitted by a monochromatic point source. Other types of light sources and the corresponding interference fringes, such as an extended light source and localized fringes of equal inclination or equal thickness, can be analyzed in the same way.

The point light source S_0 emits a spherical wave, which is divided in amplitude into two parts by the BS. The two waves are then reflected by the mirrors and recombined by the BS, and interference fringes appear on the screen. If we remove the CP, the wave reflected by the BS passes through the BS three times, while the transmitted wave passes through the BS only once. The two different optical paths are depicted in Fig. 2. The virtual point sources in the two arms are denoted by S_{01} and $S_{02}}$, respectively.

In a homogeneous isotropic medium, each ray—a straight line and normal to the wave-front. The properties of the wave-front can be studied by observing the behavior of the rays normal to it.[9] We now analyze how the spherical wave-front from S_0 is affected by its passage through the glass

（2）Naked-eye observation of visible spectra using a transmission-grating-based spectrometer. 2021 European Journal of Physics

IOP Publishing
European Journal of Physics
Eur. J. Phys. 42 (2021) 055302 (10pp)
https://doi.org/10.1088/1361-6404/ac087a

Naked-eye observations of visible spectra using a transmission-grating-based spectrometer

Shan Lin, Qingxin Yang, Weilong Liu, Xiaoou Wang, Junqing Li and Haifa Zhao

School of Physics, Harbin Institute of Technology, Harbin, People's Republic of China

E-mail: qxyang@hit.edu.cn

Received 26 January 2021, revised 26 May 2021
Accepted for publication 4 June 2021
Published 24 June 2021

Abstract

Naked-eye observations of visible spectra using a transmission-grating-based spectrometer, with the spectral resolution of 0.2 nm @ 550 nm, are reported in this article. The resultant accuracy of the wavelength readout with the naked-eye is better than 1 nm. The diffraction angles are precisely confirmed when the virtual diffraction image of the entrance slit (line spectrum) are collinear with two collimating slits. Furthermore, a converging lens is used to magnify the tiny light source (or narrow slit), and receive more radiant flux, with no effect on the accuracy of the spectral measurement. The spectrometer provides a good training aid for college students because (1) it is a low cost and handy demo experiment; (2) it has no optoelectronic sensor, it is completely naked-eye observation; (3) it helps students intuitively understand the diffracting and imaging processes; (4) the resolving power meets the requirements for teaching purposes.

Keywords: naked-eye observation, transmission-grating-based spectrometer, diffraction image, demonstrations experiment

(Some figures may appear in colour only in the online journal)

1. Introduction

The operating principle of widely used blazed reflection grating based spectrometer (Czerny–Turner design) is as follows [1]: the target light rays, after the entrance slit, are reflected and collimated by a concave mirror, and then decomposed by the grating. The deflected parallel

Author to whom any correspondence should be addressed.

（3）工程类专业学位研究生培养的治理改革——基于政策供需协调视角的多案例比较研究

2022年第3期 中国高教研究

DOI:10.16298/j.cnki.1004-3667.2022.03.13

工程类专业学位研究生培养的治理改革*

——基于政策供需协调视角的多案例比较研究

王健 孟繁辉 李钰 刘泽静

摘 要：大国竞争时代的科技人才需求催化了工程类专业学位研究生教育的蓬勃发展，但培养制度与社会需求的协调性仍然不足。如何实现供需协调是值得思考的"机理式"命题。首先基于实践侧"教学-科研-实践"三元角模式和供给侧"管理点、要素和技术"三个维度构建供给侧治理模型；然后通过多案例比较从制度设计和制度执行两个层面解构宏观模式；最后进行理论模型与实证模式总配，运用"点-面"和"理论-实践"二维检验解释政策供需的内在逻辑。研究表明，工程类专业学位研究生培养的治理改革可以围绕管理结构、资源配置、实时基础、治理机制和培养主体五个方面进行突破，形成产教融合新格局，完善研究生教育学位治理的治理基础。

关键词：研究生教育；工程类专业学位；培养体系改革；供需协调；多案例研究

一、问题的提出

2020年以来美国陆续发布的《国防授权法案》均旨在通过美国国家科学技术基金会推动技术转化、增加研发经费、支持重点领域的研究生科研活动、创新实践平台建设和技术商业化。中美战略竞争愈发激烈，科技创新、技术产业化成为大国竞争的主要方式[1]，是实现关键科学技术全球领先的基本前提。注重工程类专业学位研究生培养，推动产学研融合，是科技创新与成果转化和人才供需协调的重要方式[2]；将研究生培养与市场联系起来是创新竞争的关键层面[3]，是推动高水平科技自立自强的人才供给保障[4]。

中国经济实力的突破需要优化科技创新需求和人力资本投入的协调性[5]。从供给侧视角来看，中国科学技术已经逐渐走向前沿，模仿创新已经难以满足发展需求，市场中工程技术人才的需求结构更加复杂[6]。为服务国家重大战略和重大社会挑战，增加专业学位研究生培养规模和提升培养质量是一种必然趋势。中国专业学位研究生的招生和毕业规模处于逐年增加的趋势，原有培养体系不能适应招生规模扩张后的培养压力，难以满足市场对人才质量的要求，倒逼研究生教育教学治理改革的有效性。因此进行工程类专业学位研究生培养体系的改革已经成为一个重要议题。

（一）设计点：工程类专业学位研究生的培养缺陷

宏观视角下，国家发展阶段和市场需求驱动要素变化的，需求重心可能会随领域热点的变化而发生转移[7]。微观视角下，不同专业、岗位和企业对研究生的职业素养需求也存在差异，因此培养制度的供给需要具有动态匹配特性[8]。然而，供给要素的动态匹配需要有明确的需求定位作为方向引导。在工程教育领域中，由"教学-科研-实践"构成的三角模式能够概括工程类专业学位研究生的培养导向[9]，每个具体的培养目标都可以依据"教学-科研-实践"三个方面进行调整，以适应不同的培养需求。

但随着研究生规模扩大和工程技术人才素质要求的提高，培养制度供给出现了无效供给、供给质量低、供需结构失调等问题[10]。具体问题可从三角模式的三个方面展开。

其一，基础教学方面存在组织管理不独立、教育治理专业性不强、培养目标模糊的问题。工程专业

*本文是2020年中国学位与研究生教育学会重大课题"'双一流'建设研究生教育高质量发展研究"（2020XJ17）的研究成果

（4）麦克斯韦－玻尔兹曼分布在易辛模型中的应用. 大学物理

麦克斯韦-玻尔兹曼分布在易辛模型中的应用

（5）半无界空间上函数的傅里叶－贝塞尔积分展开. 大学物理

半无界空间上函数的傅里叶-贝塞尔积分展开

姜向前，侯晋川，孟庆鑫，张　宇

（6）熵概念的延拓——从热熵到信息熵. 大学物理

第39卷第10期
2020年10月
大学物理
COLLEGE PHYSICS
Vol.39 No.10
Oct. 2020

熵概念的延拓——从热熵到信息熵

李　均，王志诚，吴雨轩，袁　志，袁承勋，王　莹，孟庆鑫，霍　雷

在物理学科中的热力学中，熵(Entropy)是描述热力学系统状态的物理量，这也是熵最初被创造时的目的. 借鉴于物理学中熵的概念，香农为了定量描述一条信息的信息量而在通信领域引入信息熵. 本文将探讨热力学第二定律的成果能否应用到信息领域，即热力学熵与信息熵的相关性.

1　热力学中的熵

1.1　热力学中重要的定律及定理——熵概念的伏笔

人们最初研究热力学的目的是为了应用热力学的原理制造某种机器代替人力对外做功，所以便有了人们对热机的研究[1]. 说到热机便不得不提1824年法国工程师卡诺在他的论文《关于热力学的几点设想》中提出的一种理想热机——卡诺热机[2]，这种热机的工作循环由两个准静态等温过程和两个准静态绝热过程组成. 卡诺同时也证明了这种热机的效率最大，为提高热机效率指明了方向. 由此引出的卡诺定理也为后来的熵概念的提出埋下了伏笔.

自然界中发生的所有热力学过程必须遵循能量转化和守恒定律，卡诺循环在不违背热力学第一定律的情况下出现了可逆与不可逆这两个关键词，这个问题研究的便是热力学过程发生的方向性问题了. 解决这个问题的是热力学第二定律.

在卡诺定理的基础上，1850年克劳修斯在其论文《关于热动力》，1851年开尔文在其论文《热动力理论》中分别提出了热力学第二定律[3].

克劳修斯表述：不可能使热量从低温物体传向高温物体而不引起其他变化；

开尔文表述：不可能从单一热源吸取热量，使之完全变为有用的功而不引起其他变化.

1.2　克劳修斯熵

随着对热力学第二定律的深入研究，人们发现一切与热现象有关的实际过程都是不可逆的，一切自然过程都有其方向性问题，这表明热力学系统所进行的不可逆过程的初态和终态之间存在巨大的差异性[1]. 这种差异决定了热力学过程的方向性. 为了研究这种差异性，我们应该要对热力学系统的状态进行定性或定量的描述.

克劳修斯首先达成了这个成就. 在对卡诺定理及热力学第二定律的研究中，克劳修斯提出了克劳修斯等式[4]. 在可逆循环中，从一个状态到另一个状态的过程中，$\oint \frac{\delta Q}{T}=0$ ($\oint \frac{\delta Q}{T}$ 称为热温比)，$\int \frac{\delta Q}{T}$ 的积分与过程无关，只与始末状态有关，这在物理意义上说明系统中存在一个状态函数，1865年克劳修斯在其论文《力学的热理论的主要方程之便于应用的形式》命名这种状态函数为熵[5]，可逆循环中就有 $\int \frac{\delta Q}{T}=S_2-S_1$

这是熵在历史舞台上的首次露面，而且熵是系统状态函数这一基本点为后来所有的熵理论的[illegible]

（7）砷化镓、硅单晶太阳能电池特性研究实验教学设计. 实验技术与管理

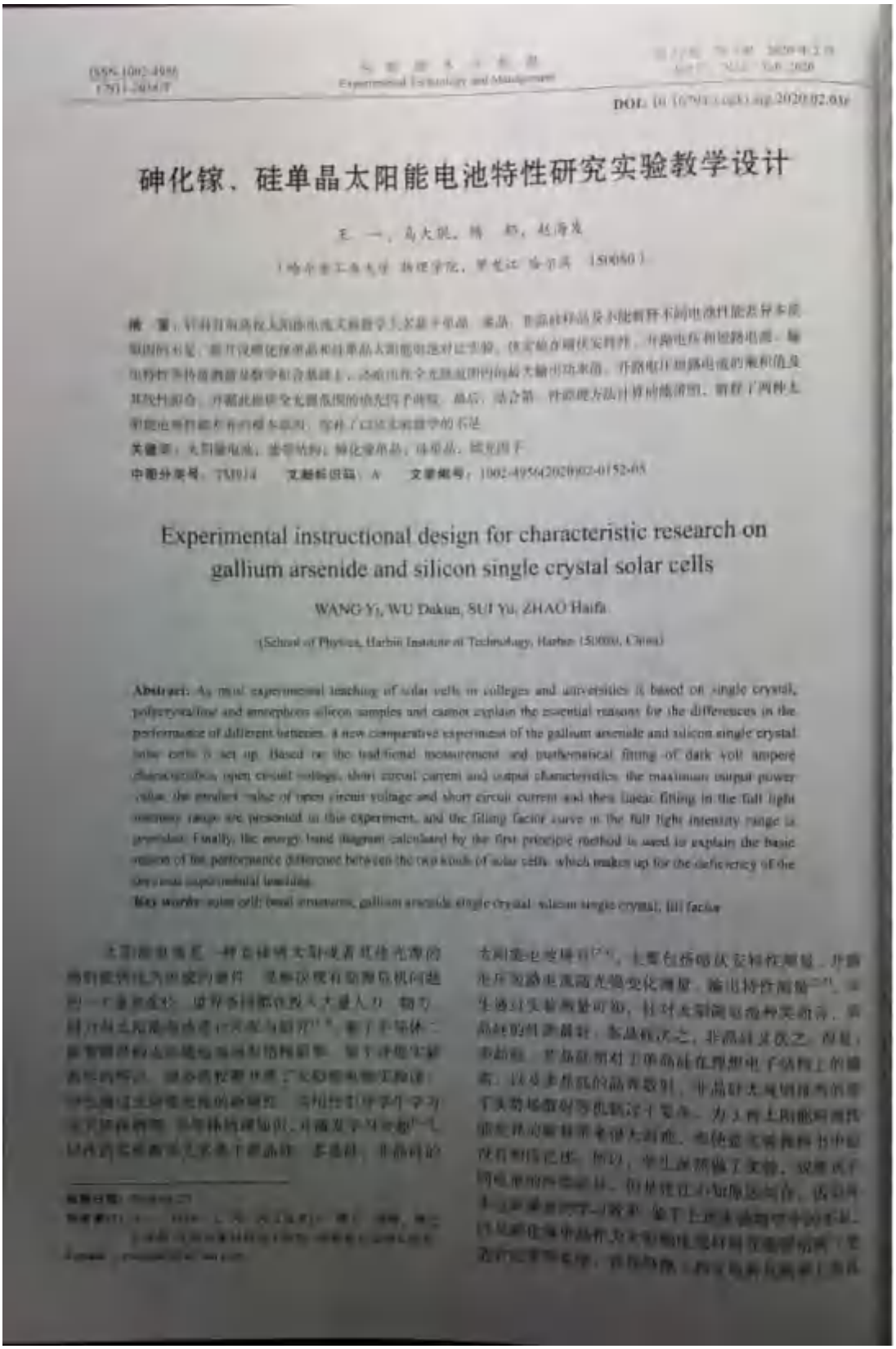

砷化镓、硅单晶太阳能电池特性研究实验教学设计

王一，乌大昆，隋 郁，赵海发

（哈尔滨工业大学 物理学院，黑龙江 哈尔滨 150080）

Experimental instructional design for characteristic research on gallium arsenide and silicon single crystal solar cells

WANG Yi, WU Dakun, SUI Yu, ZHAO Haifa

(School of Physics, Harbin Institute of Technology, Harbin 150080, China)

（8）在课堂演示实验中引入光学异常透射现象. 大学物理

在课堂演示实验中引入光学异常透射现象

[redacted]

[redacted]

[redacted]

单缝衍射是大学物理光学部分的重要内容[1-2]，该内容的讲授通常会使用课堂演示实验，使学生能够更容易地实现理解衍射的物理图像. 另一方面，纳米光子学在最近20年成为光学的前沿研究领域之一. 不透明金属薄膜上的纳米缝或纳米孔[3]及其结构阵列[4]的异常光学透射现象的物理机制品研究是纳米光子学研究领域的重要课题. 该课题的研究对于纳米尺度光探测的实现具有基础研究意义和重要应用价值[5-6]. 本文拟探索在单缝衍射课堂演示实验中引入纳米单缝的光学异常透射现象，使学生能够接触和了解当前光学研究的前沿问题.

1 银膜上纳米单缝的异常光学透射

当不透明金属薄膜上的缝或孔的尺寸相比入射光的波长甚大时，它们的衍射可以用基于惠更斯-菲涅尔原理的半波带法和振幅矢量法来分析. 根据这两种光波近似为标量波，其结果是：入射的透射光的能量近似等于入射到缝或孔上的光的能量. 定义透射总能量与入射到孔或缝面积上的能量的比值为它们的透射率，在这种条件下孔和缝的透射率近似等于1. 这是大学物理光学部分讨论的内容. 当缝或孔的尺寸接近或小于光的波长时，考虑光波的衍射效应不能简单地近似为标量场，而必须考虑矢量的麦克斯韦方程. 基于矢量的波方程，Bethe考虑了小于波长的单个圆孔的衍射，发现其透射率与孔的半径的四次方成正比. 对于亚波长尺度的圆孔，其透射率在千分之一或更小的量级上[7].

1998年，Ebbesen研究组首次报道了不透明金属薄膜上纳米孔周期性结构的异常光学透射现象[3]. 该现象表现为在特定波长平面光波的照射下，金属纳米孔二维阵列的零级透射率（与入射光共线的透射光的总能量与入射光能量的比值）高于所有的孔在薄膜表面占有面积的总和与薄膜表面的总面积的比值. 也就是说此时该孔阵列的透射率大于1. 这要比Bethe给出的近似于或小于波长的孔的透射率大若干个数量级. 目前该现象的解释主要有基于激发表面波（包括表面等离激元、复合衍射隧道效应和准位波等）模式和基于空间布洛赫（Bloch）模式两个物理模型[8]. 本文以银膜上的纳米单缝为例，说明异常透射产生的机理.

对于银膜表面纳米尺度单缝的光学透射，平面光波垂直入射到薄膜表面并与缝中自由电子耦合而为表面等离激元. 表面等离激元是电磁波沿导体与介质界面传播的电磁激发，是束缚在界面上并沿界面传播的表面波. 它由电磁场与导体中自由电荷（在这里指金中的自由电子）集体振荡耦合而产生，并随着传播的电子疏密波[9]. 这种模式的电磁波能束缚在金属表面附近，其波矢比激发表面波的入射

[redacted]

[redacted]

（9）用低功率可见二极管激光器进行倍频实验. 实验技术与管理

实 验 技 术 与 管 理

虚拟仿真技术

用低功率可见二极管激光器进行倍频实验

娄秀涛，徐连杰，赵海发

（哈尔滨工业大学 应用物理专业国家级实验教学示范中心，黑龙江 哈尔滨）

摘 要：针对用高功率近红外固体激光器进行激光倍频实验存在光路调节难度大、安全防护要求高的问题，提出一种基于低功率连续可见二极管激光的倍频实验方案：使用功率小于 10 mW、中心波长 [illegible] nm 的二极管激光作为基频光，利用偏硼酸钡晶体生成了 nW 级光功率的倍频紫外激光，并由高放光电倍增管探测。实验结果显示倍频光功率与基频光功率为二次函数关系，倍频效率与基频光功率为一次函数关系，实验结果与理论值高度吻合。该实验方案具有光路校准难度小和安全防护要求低的优点。

关键词：二极管激光；倍频实验；实验教学

中图分类号：[illegible]　　**文献标识码**：A　　**文章编号**：[illegible]

Experiment of frequency doubling with low power visible diode laser

LOU Xiutao, XU Lianjie, ZHAO Haifa

(National Experimental Teaching Demonstration Center for Applied Physics Major, Harbin Institute of Technology, Harbin [illegible], China)

Abstract: In view of the difficulty of adjusting the optical path and the high requirement of safety and protection in the laser frequency doubling experiment of high power near-infrared solid-state laser, a scheme of the frequency doubling experiment based on the low power continuous visible diode laser is proposed. By using a diode laser with a power of less than 10 mW and a central wavelength of [illegible] nm as the fundamental frequency light, a frequency-doubled ultraviolet laser with a power of nW is generated by BBO crystal, and is detected by an efficient photomultiplier tube. The experimental results show that the power of doubled frequency light is the quadratic function with the power of fundamental frequency light, and the efficiency of doubled frequency light is the linear function with the power of fundamental frequency light. The experimental results are in good agreement with the theoretical results. This proposed experimental scheme has the advantages of low difficulty in optical calibration and safety requirement for safety protection.

Key words: diode laser; frequency doubling experiment; experimental teaching

非线性光学是现代光学的一个重要分支，利用非线性效应获取短波激光已成为激光技术研究的一个热点方向[1-2]。在大学物理实验和近代物理实验等课程中开设的激光倍频实验[3-4]，多采用波长 1 064 nm 的高功率近红外固体激光器[5-6]作为光源。然而，高功率不可见光源在实验中存在光路调节难度大和安全防护要求高的问题。

本文提出一种采用低功率、连续可见二极管激光（LD）为光源的倍频实验方案：采用功率小于 10 mW 的 [illegible] nm 绿色 LD 光源作为基频光[7]，使用偏硼酸钡（BBO）晶体生成 nW 级倍频紫外激光，并由光电倍增管（PMT）探测。基频光为低功率可见光，大大降低了倍频实验的光路校准难度和安全防护要求。同时，nW 级光探测实验可进一步丰富学生关于微弱光信号检测方面的知识。

[illegible]

基金项目：国家自然科学基金项目（[illegible]）；黑龙江省高等学校教改工程项目（[illegible]）

作者简介：娄秀涛（[illegible]），男，山东东阿，博士，副教授，博士生导师，主要研究方向为原子分子物理与激光光谱学

E-mail: [illegible]

（10）迈克尔逊干涉在电场-应变效应测量中的应用. 大学物理

第38卷第8期 大 学 物 理 Vol.38 No.8
2019年8月 COLLEGE PHYSICS Aug. 2019

迈克耳孙干涉在电场-应变效应测量中的应用

宫德维，王晓明，赵 [illegible]
（哈尔滨工业大学 物理学院，黑龙江 哈尔滨 150001）

摘要：本文将大学物理光学教学中的迈克耳孙干涉应用于电场-应变效应的测量，给出了利用迈克耳孙干涉仪测量电场-应变效应的实验装置，对铌酸锂($LiNbO_3$)晶体电场-应变效应进行了实验测试，并对影响测量精度的因素进行了分析. 结果表明可以利用迈克耳孙干涉的方法对电场-应变效应进行测量.

关键词：迈克耳孙干涉；电场-应变效应；压电效应；电致伸缩效应
中图分类号：O 431 文献标识码：A 文章编号：1000-0712(2019)08-0046-04
【DOI】10.16854/j.cnki.1000-0712.180607

迈克耳孙干涉仪是美国物理学家迈克耳孙和莫雷合作于1881年发明的光学仪器，当时的主要目的是为研究"以太"漂移而设计制造. 它利用了光学中的分振幅法产生双光束以实现干涉，是大学物理光学部分的重要教学内容之一[1-3]. 通过调整迈克耳孙干涉仪中的反射镜位置，可以产生等倾干涉条纹，也可以产生等厚干涉条纹. 当某一干涉臂改变λ/2光程差时，就可以观察到干涉条纹移动一条. 因此，在近代物理和近代计量技术中，如在光谱精细结构的研究和用光波标定标准米尺等实验中都有着重要的应用[4].

电场-应变效应是一种在外电场作用下，电介质发生应变的现象，其应用十分广泛. 一般情况下，电场-应变效应主要包含以下两种效应：1）逆压电效应，这时应变与所加电场强度成线性关系；2）电致伸缩效应，这时应变与所加电场强度成平方关系. 压电效应和电致伸缩效应都是交叉效应，又称为机电耦合效应. 一般情况下所观察到的效应常常是综合效应，即是两种效应的综合，至于何种为主要的效应，则要看这两者何者强了. 具有电场-应变效应的材料是制作换能器、驱动器、传感器、变压器等电子产品的核心材料，广泛应用于航空航天、智能电网、家用电器、汽车制造、地质探测等技术领域. 对于电场-应变材料来说，外电场作用下产生的应变响应大小是衡量其性能指标的一个重要指标. 因此，给出电场-应变材料的电场-应变响应大小是科研人员很关心的问题之一. 本文首先分析了迈克耳孙干涉仪测量电场-应变效应的工作原理，并利用迈克耳孙干涉仪对电介质材料 $LiNbO_3$ 晶体进行了实验测量，最后对影响测量精度的因素进行了分析.

1 迈克耳孙干涉仪测量电场-应变效应原理

利用迈克耳孙干涉仪测量材料的电场-应变效应的原理如图1所示，该装置主要元件包括激光器、半透半反镜、反射镜、待测样品（电介质材料）、显微镜. 从激光器发出的光，经过半透半反镜分成两路，其中，一路照射到反射镜上，被反射镜反射，进入显微镜中，另一路照射到待测样品上，这里待测样品上表面已经镀制上一层反射膜，其表面相当于反射镜，这样入射光也被反射到显微镜中，两路光相遇产生干涉条纹.

当作用在待测样品上的外电场不是很强时，在外电场作用下，电介质内部分子原来处于平衡状态的正负电荷中心，在外电场作用下，会发生相对位移，偏离原来的位置，最终在电介质内部弹性力的作用下达到新的平衡状态. 由于正负电荷中心的重新分布，电介质内部分子排列也会变化，这样导致电介质的形状发生相应变化，即发生了应变. 一般情况下，材料的应变与电场是线性关系，这就是逆压电效应，这时，应变与电场的关系可以写为

收稿日期：2018-12-05；修回日期：2019-02-27
基金项目：哈尔滨工业大学教学改革项目"[illegible]"，黑龙江省高等教育教学改革"十三五"规划课题([illegible])资助

作者简介：宫德维（1975—），男，[illegible]
通讯作者：[illegible] E-mail: [illegible]

（11）浅谈利用薛定谔方程计算量子态的时间演化. 大学物理

第38卷第12期 大学物理 Vol.38 No.12
2019年12月 COLLEGE PHYSICS Dec. 2019

浅谈利用薛定谔方程计算量子态的时间演化

宋 杰，王晓鹏，霍 雷，张 宇，赵 远
（哈尔滨工业大学 物理学院，哈尔滨 黑龙江 150001）

摘要：量子力学教学中，薛定谔方程是描述一个量子系统变化的核心部分。学生对薛定谔方程的学习，可以理解量子物理和经典物理的不同之处。在量子物理教学中，薛定谔方程的讲解是一个非常重要的内容。然而在教学中学生对于薛定谔方程的理解，通常局限在定态薛定谔方程，而对于量子态随着时间的变化部分并不清楚。因此我们引入耦合腔模型：一个单光子在一个耦合的腔系统中，研究光子在不同腔中的概率随着时间变化关系。在薛定谔绘景中利用量子态的演化描述光子在耦合腔中的跳跃过程，给出几率随着时间变化的解析表达式，从而更加直观的理解微观粒子在一个量子系统中的规律。

关键词：量子系统；单光子；耦合腔
中图分类号：O 413.1 文献标识码：A 文章编号：1000-0712(2019)12-0015-03
【DOI】10.16854/j.cnki.1000-0712.190??

传统力学主要研究宏观尺度的问题，在经典物理中存在许多尚未解决的科学问题，许多科研人员仍在研究基本的力学现象[1,2]，然而对于微观世界的规律，需要利用量子力学来描述[3,4]。量子力学和相对论是现代物理的重要组成部分，从教学的角度而言，学习量子力学的部分学生觉得量子力学是一个不重要的学科，甚至在未来的工程应用或科学研究中都试图回避带有量子的概念。随着科学技术的发展，更多的学科需要考虑量子效应，而且通过引入量子效应，能取得非常大的进展。例如，利用量子系统实现的量子计算机[5]，能够解决经典计算机不能解决的问题；基于量子态的通信任务，能够实现完全安全的通信方案[6]。此外基于量子态，对目标进行探测，也可能极大的提高探测的精度[7]。由此可见，量子物理会在未来的科学研究中占有越来越重要的地位[8-10]。

在大学物理的教学过程中，应将该技术与教育教学深度融合。本文主要针对薛定谔方程去描述一个量子系统的演化问题。微观粒子的定态薛定谔方程已经有很经典的例子，例如势阱中的微观粒子的计算。而学生对薛定谔方程中的时间演化部分，学习效果较差。因此，我们引入一个耦合腔模型，该模型是量子技术中的一个重要的模型[11]。然而该模型涉及到量子光学相应的知识点，而本文回避复杂的推导和表示，从简单的物理过程描述，建立量子态随着时间变化的方程，从而让学生体会薛定谔方程主导的量子系统随着时间变化有什么特征。由于该系统是一个真实的实验系统，从而一个侧面让学生了解到已经有大量的实验从不同角度证实了薛定谔方程正确性。讲解过程中对于量子态的性质进行了详细的解释，让学生加深对于量子态性质的理解。通过对该模型的量子态的性质讨论，引导学生考虑量子纠缠态的特征。

哈尔滨工业大学在2018年下半年开展了"新时代新工科大学物理教学体系"的改革，在原有的大学物理教学中增加了部分量子物理的比重，让学生看到所学习的量子力学部分知识点，在以后的工作和学习中都能够学以致用，激发学生参与当前的前沿内容的动力，从而认识到量子力学中的方程和假设是被实验所证实的，进一步提升学生的科研能力。

1 增加内容特点与学生学习成效的分析

薛定谔方程时间演化教学内容特点：薛定谔方程是量子物理中最核心的内容之一，其所描述的物理系统和经典系统具有完全不同的性质，因此有必要建立物理模型，并进行方程的求解，进一步理解量子态的叠加性质，以及量子物理和经典物理之间的

收稿日期：[illegible]；修回日期：[illegible]
基金项目：新时代新工科大学物理教学体系建设项目资助[illegible]
作者简介：宋杰[illegible]

（12）建立自主探究性实验教学模式提升实验教学的人才培养水平，物理实验

物 理 实 验
PHYSICS EXPERIMENTATION

建立自主探究性实验教学模式 提升实验教学的人才培养水平

赵海发·刘世刚·黄 丽·刘建龙
（哈尔滨工业大学 物理实验中心，黑龙江 哈尔滨）

摘 要：为了实现从"重视知识传授"向"重视能力培养"转变，实现"以教为主"向"以学为主"转变，在大学物理实验课堂教学中建立了自主探究性实验教学新模式，开设了与之配套的系列自主探究型实验项目。教学实践表明，该方法在培养学生的实验能力和知识的应用能力方面取得了较好的效果。

关键词：自主探究；实验教学；DIY

作为基础性实验课程，大学物理实验在高校理工科各专业人才培养体系中占有重要的基础地位。但是传统的物理实验教学模式，注重知识的学习和技能的培训，在对学生能力的培养和创新意识的培养方面存在不足。针对该问题，我们近年在教学模式上做了有针对性的改革，从[时]年起建立了自主探究性的实验教学新模式。自主探究式的实验教学模式，其主要着眼点是通过教学设计让学生深度参与实验探究的全过程，学生通过自主设计、自主搭建、自主调试、自主探索的方式，建立实验系统并进行项目研究。在教师的指导下学生自主深度参与包括实验系统关键部件的设计和搭建的实验全过程，对学生深入学习促进自身能力的提高产生了很大的推动力。实践表明，这种实验教学模式激发了学生学习的主动性和勇于接受挑战的积极性，改变了以往学生实验主要是利用现成仪器进行测量的实验学习模式，在课堂教学中，形成了科学探索和研究的氛围，实验的过程使学生在知识、能力和素质[方]面得到了协调发展。

1 自主探究性实验教学的要点和内容

为了实现从"重视知识传授"为"重视能力培养"转变，实现"以教为主"向"以学为主"转变，我们在大学物理实验课堂教学中建立了自主探究性（Do it yourself，DIY）实验教学新模式，并研发出了与之配套的系列自主探究性 DIY 实验新项目。

DIY 自主探究性实验教学是基于问题导向教学法（Problem based learning，PBL），通过学生"自主设计、自主搭建、自主调试、自主探索"的实验教学过程，实现教与学的良性互动，把科学研究的理念和方法贯穿在整个课堂教学过程中的一种教学模式。图 1 是 DIY 探究性实验的教学过程框图。

图 1 DIY 自主探究性实验的教学过程框图

在 DIY 探究性实验项目选择上，注重选择兼具新颖性、技术性、挑战性的实验课题，并注重和已经学过的物理实验内容相衔接。先后开发了[3]种 DIY 探究性实验项目：DIY 电磁混合磁悬浮实验，DIY 磁耦合共振式无线电力传输实验，DIY 自组光学显微镜，摆振耦实验。

以"DIY 电磁混合磁悬浮实验"的课堂教学为例，指导教师首先组织学生研讨实现电磁混合磁悬浮的物理机理和技术途径，明确实验任务和

收稿日期：
作者简介：赵海发（1962—），男，黑龙江友谊人，哈尔滨工业大学物理实验中心教授，硕士，从事大学基础实验教学方向的研究工作。

（13）基于光致瞬态光栅测量液体内的声速，物理实验

基于光致瞬态光栅测量液体内的声速

刘伟龙，黄　丽，杨庆鑫，杨延强，赵海发
（哈尔滨工业大学 物理系，黑龙江 哈尔滨）

[摘　要] 光束通过调制与检偏光栅，其检测光的强度发生周期性变化，变化频率即为介质密度振荡的频率，由此可以测量介质中的声速．利用光致瞬态光栅测量了常温、常压条件下蒸馏水和乙醇中的声速，介质为 [illegible] 和 [illegible]，与文献报道结果相符．光学非接触式的声速测量方法，便于与其他装置联合使用，可用于研究高温、高压等极端条件下液体中的声速．

[关键词] 光致瞬态光栅；声速；非接触式测量；液体

声速是物理学、生物学、天文学以及海洋学等许多研究领域都需要的重要参量，都等为探索介质内部微观结构，分子运动和分子间相互作用等提供重要信息．因此对气态、液态及固态介质中声速的测量都具有重要意义．在大学物理实验中通常开设空气中声速测量[1]和声光衍射方法测量液体中的声速[2]等综合性实验，这些实验普遍采用超声换能器在介质中产生固定频率的超声波，再利用压电效应或光栅衍射原理对超声波的波长进行探测．通常需要将介质与超声换能器直接接触，属于接触式测量．本文介绍基于光致瞬态光栅测量介质中声速的方法．该方法具有非接触测量的优点，可用于研究高温、高压等极端条件下材料中的声速．

1　光致瞬态光栅测量介质中声速的原理

利用光致瞬态光栅技术测量介质中声速的原理如图1所示[3]．来自同一光源波长为 λ 的二个垂直线偏振光脉冲以夹角 θ 入射到介质中，当二个光脉冲实现时间、空间重合时，在介质中产生干涉，设其形成的干涉条纹间距为 d．如果介质在激发光的波长处有吸收，则会跃迁至激发态，形成激发态分子布居数光栅．介质分子通过无辐射弛豫从激发态跃迁回基态的过程中释放出的热能将会使干涉条纹的亮纹区域被瞬时加热，从而在介质中产生瞬态的热光栅．此后，热扩散作用将会驱动高温区域（即干涉条纹的亮纹区域）的分子向低温区域（即干涉条纹的暗纹区域）移动，导致介质中某一确定位置处的密度发生周期性振荡，密度的周期性变化对应介质中对向传播的超声波．超声波的波长即为干涉条纹间距 d，频率即为介质密度振荡的频率 f，与声速 v 的关系为

$$v = f\lambda \qquad (1)$$

图1　光致瞬态光栅技术测量声速的原理图

密度的周期性变化会在介质中形成周期性变化的折射率分布，即瞬态布拉格光栅．让另一束光

*第十一届全国高等学校物理实验教学研讨会（论文编号：[illegible]）

作者简介：刘伟龙（1987—），男，吉林白山人，哈尔滨工业大学物理系讲师，博士，从事物理实验教学及超快光谱学研究工作．

（14）用外腔半导体激光获取强荧光物质的拉曼特征峰值. 物理实验

第37卷 第3期 物 理 实 验
2017年3月 PHYSICS EXPERIMENTATION

用外腔半导体激光获取强荧光物质的拉曼特征峰位

娄秀涛，徐连杰
（哈尔滨工业大学 物理系，黑龙江 哈尔滨）

摘 要：利用外腔半导体激光器为激发光源，采用移频激发法测量了强荧光物质三环唑的拉曼特征峰位. 实验结果显示，在 [illegible] nm 和 [illegible] nm 激发波长下采集的三环唑样品拉曼光谱信号严重重合，[illegible]，拉曼差分光谱 [illegible] 有明显的拉曼特征峰，与文献报道一致.

关键词：拉曼光谱；外腔半导体激光；荧光物质；移频激发
中图分类号：[illegible] 文献标识码：A 文章编号：[illegible]

光学类实验不仅是在普通物理实验教学中占有一定的比重，而且也是近代物理实验课程的主要内容. 激光拉曼光谱是分子光谱学的重要分支，是一种重要的物质结构和物质成分分析手段，也是普通物理实验中吸收光谱实验内容的扩展，因而有很多高校将其纳入了近代物理实验教学内容. 目前大多数高校所开设的拉曼光谱实验采用的样品都是四氯化碳，它具有丰富的振动模式，因而具有典型的拉曼特征峰. 为了拓展实验内容，可以增加实验系统和实验参量的优化环节，或者引入新的测量样品. 在实际的生产生活应用中，很多物质的拉曼特征峰并不十分明显，甚至会被淹没在强烈的荧光背景中. 开展对强荧光物质拉曼特征峰的测量可以进一步丰富学生对于激光拉曼光谱的认识. 本文以水稻种植中广泛使用的农药三环唑为测量样品，采用自制的可调谐外腔半导体激光器（External cavity diode laser, ECDL）为激发光源，应用移频激发法获取三环唑的拉曼特征峰位. 将可调谐外腔半导体激光器引入物理实验教学已见诸报道，可进一步丰富和拓展近代物理实验中激光特性和参量测量实验的有关内容.

1 实验原理

1.1 移频激发拉曼光谱

在拉曼光谱检测中，测量的拉曼信号往往是叠加在大的荧光背景之上，后者常常比前者大几个数量级，给拉曼光谱分析带来很大困难. 对于分子的某一振动模式其拉曼位移是一定的，因此拉曼散射光的频率会随着入射激光的频率变化而等量变化. 但是荧光的发射频率却对入射激光频率的变化不敏感，因此可利用拉曼散射光和荧光的这一特性差异，通过改变激发光的波长来抑制荧光背景. 图1展示了移频激发法的主要过程和原理. 从图中可以看出，将2个不同波长激光激发产生的拉曼光谱相减，可以有效抑制荧光，从而获得较为"纯粹"的拉曼差分光谱.

图1 移频激发拉曼光谱原理示意图

1.2 外腔半导体激光器

一般来说，ECDL是通过外部的光栅将部分激光能量反馈给LD芯片使特定频率的模式在竞争中胜出，从而达到选模的目的. 光外腔的构理

"第X届全国高等学校物理实验教学研讨会"论文
收稿日期：[illegible]；修改日期：[illegible]
基金项目：黑龙江省高等学校教改工程项目（[illegible]）
作者简介：娄秀涛（[illegible]），男，山东郓城人，哈尔滨工业大学物理系副教授，博士，主要从事大学物理和大学物理实验的教学工作，研究方向为激光光谱学.

（15）波尔共振实验中基于旋转矢量的相位差分析，大学物理

大 学 物 理

波尔共振实验中基于旋转矢量的相位差分析

1 受迫振动与强迫力的旋转矢量表示

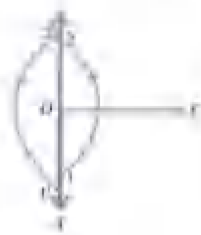

图1 受迫振动的旋转矢量表示

（16）工科院校物理演示实验体系的实践与探索. 实验研究与探索

工科院校物理演示实验体系的实践与探索

靳辰飞， 张思琦， 韩 权， 张伶莉， 王晓鹏， 赵 远
（哈尔滨工业大学 物理系，黑龙江 哈尔滨 150001）

摘 要: [illegible]

关键词：演示实验；大学物理；教学方法改革；工科院校
中图分类号：[illegible] 文献标志码：[illegible]
文章编号：[illegible]

Practice and Explore on Physics Demonstration Experiment System of Engineering Colleges

[illegible]
(Department of Physics, Harbin Institute of Technology, Harbin [illegible], China)

Abstract: [illegible]

Key words: demonstration experiment; university physics; teaching methods reform; engineering colleges

0 引 言

[illegible]

（17）核物理多功能教学实验仪教学应用与功能开发. 物理实验

物 理 实 验
PHYSICS EXPERIMENTATION

近代与综合实验

核物理多功能教学实验仪的教学应用与功能开发

任延宇，马永和，霍　雷，冯启春，唐圭新
（哈尔滨工业大学 物理系，黑龙江 哈尔滨 150001）

摘　要：根据教学要求自主设计了核物理多功能教学实验仪，该仪器集高压、低压、放大、单道脉冲幅度分析器、IVC、VFC、定时、定标、控制与显示于一体，有充足的公共资源，通过总线不同种类的探测器，选配不同种类、不同能量的放射源和不同几何配置的被探测样品，实现多功能的实验教学任务。

关键词：核物理；放射源；探测器
中图分类号：O571.1　　文献标识码：A　　文章编号：1005-4642(2015)05-0001-04

核物理实验是核物理专业的中心教学环节，随着科学技术的进步和实验手段的提高，近年来出现了一些新的高性能实验仪器设备[1-3]，特别是计算机在核物理实验中的应用，为核物理实验增添了无限的生机，推动了核科学技术的变革，开创了核技术应用的新时代。核仪器的小型化、微机化、智能化，都促进了原子核物理不断开拓新的研究和应用领域。核物理实验是理论与实践密切结合的基础课程，体现了多种学科实验技术的综合应用。核物理实验教学可以培养学生理论联系实际，善于发现问题、分析问题和解决实际问题的能力，使学生初步掌握核物理的研究方法、核物理实验的特点、一般流程和规律，培养严谨的科学态度、实事求是和坚韧不拔的工作作风。

基础性的核物理实验主要是强度测量，其次是能量测量，测量系统往往由高压电源、低压电源、线性脉冲放大器[4-5]、单道脉冲幅度分析器、定标器等仪器组成。测量系统连接繁琐且所占空间很大。随着 NIM 系统的出现，组合插件构成的测量系统可使仪器结构紧凑，连接方便，但 NIM 系统成本较高，功能也较为单一。

为满足核物理专业的教学需求，哈尔滨工业大学物理系自主设计了核物理多功能教学实验仪器，如图 1 所示。自制的核物理多功能教学实验仪器是集高压、低压、放大、单道脉冲幅度分析器、IVC、VFC、定时、定标、控制与显示于一体，在充分利用主机公共资源的基础上，通过后面板上的接插件切换不同类型的探测器、选配不同种类、不同能量的放射源和被探测器及不同几何参量的被探测样品，可实现多样性配置，从而实现多样性的功能。

图 1　核物理多功能教学实验仪实物图

1　核物理多功能教学仪的结构概述

图 2 为核物理多功能教学实验仪的电气组成原理框图。低压电源采用组件电源，固定在机壳地板上，±15 V 为线性脉冲放大器、甄别及分析供电，±12 V 为 I/V 和 V/F 变换及高压电源供电，+5 V 为定时、定标、控制和显示供电，+24 V

作者简介：任延宇（1980—），男，辽宁沈阳人，哈尔滨工业大学物理系讲师，博士，从事高能重离子核物理领域的研究。

（18）等厚干涉实验中缺陷检测的数值模拟，物理实验

物 理 实 验
PHYSICS EXPERIMENTATION

生 词

等厚干涉实验中缺陷检测的数值模拟

刘建龙[1]，高 扬[2]
[1] 哈尔滨工业大学 物理系，黑龙江 哈尔滨
[2] 黑龙江大学 电子工程学院，黑龙江 哈尔滨

摘 要：利用数值方法研究了等厚干涉实验中不规则缺陷时的干涉条纹，给出了不同缺陷尺寸、高度或曲率情况下的条纹变化情况，讨论了利用干涉图像进行缺陷检测的方法。该研究给出等厚干涉实验中的典型问题的数值求解方法，结果和表现，便于理解。

关键词：等厚干涉；数值仿真；缺陷检测
中图分类号：O436.1　　文献标识码：A　　文章编号：

1 引 言

等厚干涉实验是物理实验课程中的经典实验项目，其中牛顿环和劈尖干涉实验最为典型，在大学物理实验课堂上也最为常见[1]。学生可以通过实验来观察干涉现象，同时也学习了利用等厚干涉进行曲面曲率和薄膜厚度测量的方法。实际上，等厚干涉实验除了用来做曲率和厚度测量外[2]，另外一个典型的应用就是玻璃表面缺陷的检测[3]。然而，带有特定尺寸和形状的缺陷的平面玻璃不易加工，这也影响了这类实验的开设。目前，多数物理实验教材只把这个问题作为讨论题供学生思考，然而，仅靠理论分析，无法验证分析的准确性，也不能得到直观的认识。

事实上，当牛顿环或劈尖干涉装置的玻璃表面存在的凸起或凹陷形状比较规则，且变化比较平缓时，可以利用计算机程序来模拟其产生的干涉现象，并给出干涉条纹的形状和分布，进而研究干涉条纹随结构参量变化的规律。在本次研究中，选择劈尖干涉装置，研究玻璃存在球面凸起或凹陷时，不同缺陷尺寸、高度和曲率对干涉条纹的影响。

2 原理与公式

图1为劈尖装置示意图，1块平板玻璃水平放置，另一块玻璃与水平玻璃存在一定夹角。下侧玻璃上表面存在1个球面凸起缺陷，2块玻璃之间形成一定角度的空气间膜。当一单色平面波从上向下垂直照射到劈尖装置上时，其中一部分光在AB表面反射并与从CD面反射的光发生干涉。假设干涉的2束光的强度均为I_0，则距离C点水平距离为x处的干涉条纹的强度可以写为[4]：

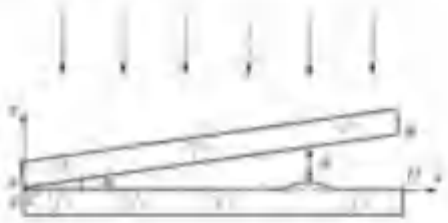

图1 存在缺陷的楔形结构图

$$I(x)=4I_0\cos^2[\varphi(x)/2] \quad (1)$$

其中λ为入射光在真空中的波长，$\varphi(x)$为x位置处2个玻璃表面的距离，如图1所示。在无缺陷的位置，空气间膜的厚度为线性变化，即：

$$d(x)=x\tan\alpha \quad (2)$$

其中α为劈尖的夹角。在缺陷位置，空气间膜的厚度不再是线性变化，考虑到缺陷的形状为球形

*第十届全国高等学校物理实验教学研讨会*论文
收稿日期：2014-03-26；修改日期：2014-04-08
基金项目：黑龙江省高等教育教学改革项目资助(JG2012010001)；哈尔滨工业大学"本科生教学建设项目"资助(No.HITJX2012005)
作者简介：刘建龙(1977-)，男，湖南常德人，哈尔滨工业大学物理系高级工程师，博士，主要从事大学物理实验教学和创新元件等研究。

（19）物理学拓展课程提升学生综合素质，物理与工程

物理与工程

物理学拓展课程提升学生综合素质

王晓晗 孟庆鑫 张伶莉 张春风 宋 杰 吉德荣 霍 雷 张 宇 赵 远
（哈尔滨工业大学物理系，黑龙江 哈尔滨）

摘 要 在大学物理课程教学中，受到学时及自身体系的限制，教师很难将物理学的前沿问题、最新发展以及对其他学科的影响更多地传授给学生，这在一定程度上影响了学生综合素质的提升。本文通过"改变世界的物理学"课程的教学实践介绍物理学拓展课程在创新人才培养以及在提升学生综合素质中的作用。

关键词 物理学拓展；综合素质；物理学思维方法

PHYSICS CURRICULUM DEVELOPMENT PROMOTES STUDENT'S COMPREHENSIVE QUALITY

Wang Xiaoan Meng Qingxin Zhang Lingli Hou Chunfeng
Sun Jie Gong Dewei Hao Lei Zhang Yu Zhao Yuan

Abstract Restricted by the teaching hours and system, in the teaching of university physics courses, teachers can hardly instruct frontier physics problems, the newest development and its influence on other subjects to students, which affects the improvement of students' comprehensive quality to some extent. This paper introduces the role of physics curriculum development in the cultivation of innovative talents and improving students' comprehensive quality through the teaching practice of the course "physics changes the world".

Key words physics development; comprehensive quality; thinking methods of physics

学生综合素质的提升有赖于知识面是否广泛，思维方法是否正确。物理学对提升学生的综合素质起到不可替代的作用，这是因为在物理学发展过程中的每一次重大突破不仅带来物理学新领域、新方向以及交叉学科和新技术学科的崛起，而且改变了人们的思维方式。"物理学为科学进步和发明的利用，提供所需训练有素的人才；物理学在培养化学家、工程师、计算机科学家，以及其他物理科学和生物医学科学工作者的教育中，是一个重要的组成部分"[1]，物理学的思维方法在现代信息化战争中也发挥着重要作用[2]。

但受到大学物理课程学时及自身体系的限制，教师很难将物理学的前沿问题、物理学的最新发展以及对其他学科的影响更多地传授给学生，这在一定程度上影响了学生对物理学重要性的认识，也影响了学生学习物理的兴趣。所以有必要开设物理学拓展课程，将大学物理课程中涉及不到的前沿问题、与其他专业融合、渗透以及物理学思维方法对高新技术发展的推动作用介绍给学生。

我校于 [illegible] 年秋季学期率先以"改变世界的物理学"为题为本科生开设了全校任选的物理学拓展课程。自开课以来，一直受到学生们的喜爱，平均每年的选课人数在 [illegible] 人左右，选课人数位于全校公共选修课前列。"改变世界的物理学"课程获得了 [illegible] 年哈尔滨工业大学优秀课程称号。本文基于"改变世界物理学"课程的教学理念和教学实践介绍物理学拓展课程在创新人才培养以及在提升学生综合素质中的作用。

[illegible]

作者简介：王晓晗，女，博士，教授，主要从事大学物理和研究生物理课程的教学工作。[illegible]

（20）气体分子高分辨吸收光谱测量的实验设计与教学实践，中国现代教育装备

2021年2月
总第355期

中国现代教育装备

ISSN1672-1438
CN11-4994/T

自制教学仪器设备

气体分子高分辨吸收光谱测量的实验设计与教学实践

哈尔滨工业大学应用物理专业国家级实验教学示范中心 黑龙江哈尔滨 150001

摘 要：

关键词：

1 研究背景

2 实验原理

2.1 LD波长调谐原理

$$\lambda = 2nL/m \qquad (1)$$

作者简介：

基金项目：

（21）关于“光的偏振”教学的一些尝试. 物理与工程

物理与工程 Vol.30 No.3 2020

关于"光的偏振"教学的一些尝试

刘志国 黄湘强 张伶莉 曹永印 王庆东 王晓晖 张 宇 赵 远
（哈尔滨工业大学物理学院，黑龙江 哈尔滨 150001）

摘 要 在大学物理教学中，让学生更好地掌握知识，是每一名教师的职责。根据实验是物理科学的特点，课堂教学应更多地强调演示实验和实际应用。按照这一想法，笔者在2018年秋季学期对"光的偏振"部分做了新的教学尝试。课堂教学以演示实验开始，结合实验现象来介绍物理知识，分析实验条件对实验现象的影响，并通过实际应用来加深对物理知识的理解。实践表明，教学效果良好，大部分学生对这种教学模式持肯定态度。本文介绍新教学模式的指导思想、实施方案和学生反馈。

关键词 大学物理教学；光的偏振；演示实验

AN ATTEMPT ON TEACHING "POLARIZATION OF LIGHT"

LIU Zhiguo HUANG Xiqiang ZHANG Lingli CAO Yongyin WANG Qingdong WANG Xiaoou ZHANG Yu ZHAO Yuan
(College of Physics, Harbin Institute of Technology, Harbin, Heilongjiang 150001)

Abstract In college physics teaching, students' better acquisition of knowledge has been the responsibility of every teacher. According to the characteristic of experimental science, college physics teaching should focus more on demonstration experiments and practical application. Based on the idea, a new teaching method on "polarization of light" was tried in fall semester of 2018. The class begins with demonstration experiments, and relative knowledge is conveyed accompanying experimental phenomena. Then the influence of experimental conditions on phenomena is discussed, and applications are given for better understanding of physical knowledge. Practice shows that the teaching effect is pretty good, and the majority of students have positive attitude towards this teaching method. This paper introduces the guiding ideology, implementation plan and student feedback of the new teaching method.

Key words college physics teaching; polarization of light; demonstration experiment

教育的目标是"授之以渔"，而非"授之以鱼"，也就是说，育人是教育的根性目的。在教育过程中，学生是学习的主体，教育目标的达成，离不开学生的主动学习。因此，调动学生的学习积极性，让学生能够主动地学习，在课堂教学中至关重要，在高等教育中更是如此。

我校的大学物理课程是在本科一年级的春季学期和二年级的秋季学期讲授的。经过高考前的紧张复习和磨练，加上高考后漫长的暑假，一部分学生在学习上比较懒散，甚至出现厌学情绪，在课

收稿日期：2019-12-02；修回日期：2019-04-07
基金项目：哈尔滨工业大学2018年教改项目"新时代新工科大学物理教学体系"（无编号）；黑龙江省教育科学规划课题"新时代新工科大学物理专业新型学体系建设与实践"（GJB1340251）；黑龙江省高等教育科学"十三五"规划课题"1+4"新高考制度下大学物理教学应对策略研究"（黑龙江省重点课题，GJB1318030）；黑龙江省高等教育教学改革项目"以创建学术资源平台优化创新人才培养"（SJGY20170048）。
作者简介：刘志国，男，教授，主要从事超导物理方面的研究和大学物理教学工作，liuzhiguo@hit.edu.cn；
通讯作者：赵远，男，教授，主要从事光电信号检测和大学物理教学工作，zhaoyuan@hit.edu.cn。
引文格式：刘志国，黄湘强，张伶莉，等. 关于"光的偏振"教学的一些尝试[J]. 物理与工程，2020，30(3)：84-88.

（22）关于“光的干涉”部分教学模式的探讨. 物理通报

关于"光的干涉"部分教学模式的探讨*

曹永印　张伶莉　张　宇　王晓鸥　赵　远
（哈尔滨工业大学物理学院　黑龙江 哈尔滨　[illegible]）

（收稿日期：[illegible]）

摘　要：对大学物理"光的干涉"部分教学模式进行探讨，通过物理过程引领教学的展开，理论与实验相结合，建立"双光束干涉模型"，以此作为贯穿"光的干涉"部分的主线，引入物理规律相对应的工程技术应用，提高学生的兴趣，让课堂变得生动有趣，提高课堂上学生的抬头率.

关键词：大学物理　光的干涉　教学模式

1　引言

高等教育应以人才培养为根本，大力提升本科生教学质量；以改革创新为引领，不断增强科技核心竞争力. 大学物理作为理工科大学的一门公共基础课，在人才培养方面发挥着重要作用. 但是，随着社会的发展，大学物理教学面临的问题越来越多，互联网的发展导致学生学习知识多元化，但是掌握知识的方法简单化，碎片化问题也越发严重. 大学物理传统的教学模式是老师讲，学生被动地听，学生兴趣缺失，课堂参与度不够，最终导致的结果是学生学习大学物理，只是为了应付考试，能力并未得到真正的提高[1]. 要想改变这些问题，大学物理教师应在课堂上吸引住学生的注意力，提高学生的兴趣. 如何做到这一点，就需要正确处理"教"与"学"的问题；需要大学物理教师在教学理念、教学方法、教学内容、教学模式等多方面下功夫[2]. 本文主要针对"光的干涉"部分的教学模式展开探讨. 学生在高中时对光学部分的知识掌握主要在于几何光学，如光的直线传播原理、折射定律、反射定律等，而对于杨氏双缝干涉、薄膜干涉及等厚干涉等"光的干涉"内容还很陌生[3]，光的相干叠加，理论性太强，不利于学生理解和掌握. 为了让学生真正掌握"光的干涉"部分的知识，本文将从以下教学过程安排探讨新的教学模式.

2　教学过程

本文提出的新的教学模式需要引入物理过程，每节课对应一个物理过程，具体教学过程如图1所示.

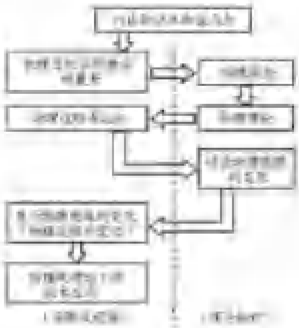

图1　基于物理过程的教学过程

（1）首先介绍本节课的知识点和能力培养. 大学物理教学应始终以学生为中心[4]，每一节课程都应让学生在开始本节课之前就了解到本节课的知识点，以及本节课主要培养自己哪些方面的能力. 例如：杨氏双缝干涉的主要知识点为杨氏双缝干涉的光程差、条纹位置和条纹间距等. 主要培养的能力有近似处理问题的能力以及多角度思考问题的能力.

---

* 黑龙江省教育科学"十三五"规划课题"新时代理工科大学物理创新教学体系建设与实践"（项目编号：[illegible]）；哈尔滨工业大学教学发展基金"新时代理工科大学物理教学体系".
作者简介：曹永印（[illegible]），男，博士，副教授，硕士生导师，主要从事[illegible]方面的研究.
通讯作者：赵远（[illegible]），男，博士，教授，博士生导师，主要从事[illegible]方面的研究.

（23）光学干涉在二次电光系数测量中的应用与分析，物理与工程

物理与工程 Vol.[illegible] No.[illegible] [illegible]

光学干涉在二次电光系数测量中的应用与分析

田 浩 周志祥 王晓鹏 宫德维 董 蔚 张 宇
（哈尔滨工业大学物理系，黑龙江 哈尔滨 [illegible]）

摘 要 为了更加深入地掌握光学干涉原理以及晶体材料的电光效应，我们搭建了利用干涉原理的典型光学系统——马赫-曾德尔电光系数干涉测量系统。首先，结合光学干涉原理和晶体材料的二次电光效应，进行了详细的理论推导，证明了测量方法的正确性和可行性。之后，以铌酸钾钠（KNTN）晶体作为研究对象，在实验中测量得到了其二次电光系数 s_1 为 [illegible] $m^2 \cdot V^{-2}$。在此过程中，通过对马赫-曾德尔光学干涉测量系统的理论剖析与实际应用，相信可以帮助同学们更深入地理解和掌握光学干涉、晶体折射率及其电光效应的本质与原理。

关键词 电光效应；电光系数；干涉

APPLICATION AND ANALYSIS OF THE OPTICAL INTERFERENCE IN THE QUADRATIC ELECTRO-OPTIC COEFFICIENT MEASUREMENT

Tian Hao Zhou Zhongxiang Wang Xiaopeng Gong Dewei Dong Wei Zhang Yu
([illegible])

Abstract In order to further understand the interference and the electro-optic effect, we set up a typical optical system based on the theory of the interference, which is the Mach-Zehnder interferometer measurement system of the electro-optic coefficients. Finally, the detailed theoretical derivation has been carried out based on the combination of optical interference principle and the quadratic electro-optic effect of crystalline materials. The derivations prove the validity and the feasibility of the measurement. Then, the quadratic electro-optic coefficient was determined in the experiment with measuring the potassium sodium niobate (KNTN) crystal as the research object, and the [illegible] $m^2 \cdot V^{-2}$. During this process, by the help of students further understand and grasp the nature and the principle of theoretical interference, the refractive index of crystals, and the electro-optic effect, through the analysis and realization of the Mach-Zehnder optical interferometer system.

key words electro-optic effect; the electro-optic coefficient; interference

光学干涉是指两列或两列以上的光波在空间中重叠时发生叠加从而形成新波形的现象，这不仅是物理学中最重要的物理概念之一，在大学物理教学中也有着至关重要的地位，而且还具有着重要的理论和应用价值[1]，例如迈克耳孙干涉、是齐物理学领域中常见的光学干涉现象，利用其干涉原理，可以研究光温度、压强、电场、磁场等物理量

[illegible]
基金项目：[illegible]

（24）“工作室物理”教学中的演示实验. 物理与工程

“工作室物理”中的演示实验

王晓鸥 张竹君 [illegible] 李 均 [illegible] 赵 亮
（哈尔滨工业大学理学院物理系，黑龙江 哈尔滨 150001）

摘 要 “工作室物理”教学生的探索研究进入到课堂教学中，通过演示实验和教学软件激发学生主动学习，也叫作 TEAL (Technology Enabled Active Learning)。TEAL 充分体现了“以学生为中心”的教学理念，充分发挥学生自主学习的积极性。而课堂演示实验直观，真实，可信度高，学生可直接参与其中，起到了教与学的互动。由学生自己做演示实验，分析实验现象，总结实验规律，使学生从被动获取知识到主动获取知识，从而锻炼了思维能力，是培养学生创新思维，创造能力以及提升学生实践能力的最好的手段和途径。

关键词 工作室物理；演示实验；互动式教学

在传统的“灌输式”教学模式中，学生是被动的倾听者，按受者，他们的注意力主要是放在对知识要点的掌握上。这在一定程度上剥夺了学生自主学习，主动获取知识的行为，限制了学生的创新与创造性思维的发展，同时也违背了“以学生为中心”的教学理念。

“工作室物理”（Studio Physics）教学模式[1]是指导教师引导，学生主动获取知识，主动探索物理规律，学生之间，师生之间互动，互助式的教学模式，是充分发挥学生自主学习，实现“以学生为中心”的教学理念的最佳教学模式。这种教学模式需要在专有教室中进行，主要是营造一个以学生为中心的主动学习环境(Student-Centered Active Learning Environment for Undergraduate Programs，简写：SCALE-UP)。这种教学模式通过演示实验和教学软件激发学生主动学习，所以通常也叫作 TEAL (Technology Enabled Active Learning)。这种教学模式培养学生从三维角度思考问题。由于学生们通常接触的多为平面的屋角和平面的书页，因此思维方式被限定在二维的范围内，而对于物理现象的理解常需要从三维的角度思考问题，尤其在力学、电磁场和光学领域。

目前，世界上已有亚古所高校针对其不同需求，采用了“工作室物理”教学模式。如美国的麻省理工学院（MIT），斯坦大学，莱鲁大学，台湾的中正大学，等等[2-5]。并且，美国一些大学已经开始在化学，工程类等[6-8]课程中实施这种教学模式。我校（哈尔滨工业大学）从 2014 年开始试行这种教学模式[9]，取得了一定的成果。今年春季学期学校建成了 4 个“工作室物理”教室，营造了 SCALE-UP 学习环境，如图 1 所示，从最初的一个试点班增加到 4 个班。但由于条件所限，我们只是基于课堂随机实验引导学生自己动手做演示实验，仔细观察、总结实验规律，从而分析，归纳出物理规律，激发学生自主学习的兴趣，同时也培养了学生的科研能力，创造能力，提升了学生的科学素养。

收稿日期：2017-04-19
基金项目：[illegible]
作者简介：[illegible]
引文格式：[illegible]

（25）刚体定点转动代数讲法的教学实践. 物理与工程

教学经验交流

刚体定点转动代数讲法的教学实践

任延宇 霍 雷 冯启春 唐国新
（哈尔滨工业大学物理系，黑龙江 哈尔滨 150001）

摘 要 代数是人们描述自然规律的一个极为重要的数学工具，但它自身的抽象性又使得初学者很难掌握这一数学工具。理论力学是物理系本科生的第一门理论课程，其运用数学工具处理物理问题的训练明显较普通物理加强。我们尝试在理论力学课的刚体力学一章采用代数讲法，从而使抽象的数学理论与具体的物理图像有了直接的对应，并为后续专业类课程学习打下了良好的基础。

关键词 理论力学；刚体定点转动；线性代数

USING THE ALGEBRAIC METHOD TO TEACH THE FIXED POINT ROTATION OF RIGID BODY

REN Yanyu HUO Lei FENG Qichun TANG Guoxin
(Department of Physics, Harbin Institute of Technology, Harbin Heilongjiang 150001)

Abstract Algebra is a very important mathematical tool in physics research and applications. But it is also very difficult for beginners to learn due to its abstractness. Theoretical mechanics is the first theoretical course of physics undergraduates, and its training of using mathematical tools to deal with physical problems is more important than that of general physics. We try to use algebraic method to teach the fixed point rotation of rigid body in theoretical mechanics course. It can make a connection between the abstract mathematical theory and specific physical images and lay a solid foundation for the follow-up courses.

Key words theoretical mechanics; the fixed point rotation of rigid body; algebraic method

代数无论在物理学研究还是在应用领域都是一个极为重要的数学工具。初学者由于缺乏实际应用方面的训练很难掌握这一数学工具。这很大程度上是由于线性代数通常在大一上学年学习，而大量应用代数知识的专业类课程一般都安排在大三下学年或者大四上学年。鉴于这样的情况，我们尝试在大二上学年理论力学课的刚体一章就引入代数讲法。这样做的原因在于：刚体的定点转动可以用固定在刚体上的刚体坐标系（刚体系）来描述，这样对刚体的描述就转化为对两个坐标系间相互关系的描述，从而可以用代数理论严格表示出来。此外，刚体转动是同学们在日常生活中常见的现象，通过将转动与代数理论的结合可以帮助同学们更好地复习和理解大一刚刚学过的线性代数的很多抽象公式。经过我们多年的教学尝试，这一教学思路已经取得了较好的教学效果。现在给出这一讲法的主要步骤[1]。

令 [illegible] 是转动前的刚体系 [illegible] 是转

收稿日期：[illegible]；修回日期：[illegible]
基金项目：高等学校力学课程 [illegible] 年度资助项目（项目编号：[illegible]）
作者简介：任延宇，男，副教授，主要从事 [illegible]
引文格式：任延宇，霍雷，冯启春，等. 刚体定点转动代数讲法的教学实践[J]. 物理与工程，[illegible]

（26）工作室物理教学中的互动反馈教学设计. 物理通报

工作室物理教学中的互动反馈教学设计*

张伶莉 王晓鸥 孟庆鑫 韩 权 靳辰飞 俞素华 张 杰
哈尔滨工业大学物理系 黑龙江 哈尔滨 150001

（收稿日期：2015-11-25）

摘 要：[illegible]提高了学生学习的主动性，[illegible]
[illegible]

关键词：工作室物理教学 互动反馈 大学物理

“工作室物理”(Studio Physics)教学模式是由美国伦斯勒工学院创立的一种集成了理论和实验的教学方式。这种新的教学模式的教学理念是引导学生主动获取知识，探索物理规律，其最大优势是将实验和理论课教学有机结合。目前，这种工作室物理教学模式已在美国、中国台湾地区以及一些欧洲国家的大学推行了将近20年的时间[1~3]，并取得了良好的教学成效。哈尔滨工业大学从2014年也开始在大学物理课中进行工作室物理试点班(97人)教学尝试，深受学生们欢迎，取得良好的教学效果[4]。在实践的探索中，我们发现在进行工作室物理教学过程中，教师对学生课堂活动的引导是提高这种教学模式教学效果的关键。我们下一步将会在正常的教学班级(一般人数在150人左右)中推行这种教学模式，希望有更多的学生受益。在考虑如何将工作室物理教学模式应用于正常教学班级(一般为150人左右的教学班)时，我们面临的首要问题是，如何能够帮助教师充分掌控课堂，在学生分组进行实验探索时引导学生，督促引导学生的学习活动。经过多方面的调研和尝试，我们认为将互动反馈教学系统运用到工作室物理教学课堂中，是一种非常行之有效的方法。

提高教学质量，促进学生发展是学校永恒的主题。为了保证教学质量，一个核心的问题就是了解学生对知识的掌握程度，合理安排教学内容并调整教学进度，在教学中加强和促进教学过程中师生之间的沟通、交流与互动是很必要的。然而，在现实的教学环境下，由于班级规模、上课学时等现实因素的限制，要想在教学过程中充分体现师生之间的交流与互动并非易事。而“互动反馈教学系统”正好弥补了这个问题。互动反馈教学系统是一种提高课堂互动、鼓励学生参与到教学活动中的管理工具。它是基于互动式学习理论设计的一种允许学生在课堂上通过手持设备以选择或数字来回答问题的学生互动反馈系统[5]。教师上课时根据教学的内容提出标准化的问题(例如选择题或者数字化的问题)，学生利用手持设备选择答案，系统后台具备数据记录、统计、分析等管理功能，可以将学生的回答答案实时形成统计报表显示在屏幕上，教师可以随时查看，并根据报表掌握学生的掌握程度，即时调整进度。除了以上出题，系统还支持抢答测试、投票游戏、淘汰比赛、抢权发言、问卷调查、点名考勤等多种形式的互动方式，活跃了课堂，激发了学生参与到课堂中的积极性，高效地促进了教师的课堂教学活动[6]。在大班工作室教学模式中，借助于互动反馈教学系统，可以开展多种形式的师生互动，能够有效地掌控课堂，促进师生互动，解决了课堂反馈教学实践过程中存在的问题。

1 实践成效以及发现的问题

从2014年，我校开始每学期都从英才学院抽出一个班级进行工作室物理教学尝试，已经进行了3

* [illegible]

（27）利用通识课程《物理学史》来传递物理文化和培养物理思维——通识课程《物理学史》建设及改革初探， 物理通报

课程改革探索与讨论

利用通识课程《物理学史》来传递物理文化和培养物理思维

——通识课程《物理学史》建设及改革初探

孟庆鑫 侯春风 李助鹏 张 宇 韩 权

（哈尔滨工业大学物理系 黑龙江 哈尔滨 [illegible]）

（收稿日期：[illegible]）

摘 要：通过问卷调查深入了解学生对《物理学史》课程的需求，分析了将《物理学史》建设为本科生通识课程的可行性，根据学生对该课程的需求，对物理学史课程的教学理念、教学内容和考核手段等方面都做了改革。实践结果表明，物理学史课程的教学可以实现传递物理文化、培养物理思维能力的教学目标。

关键词：通识课程 物理学史 教学内容 教学目标

1 引言

物理学史是人类对自然界各种物理现象的认识史，主要研究物理学发生和发展的基本规律，包括物理学概念、思想的发展和变革，物理学发展与社会背景关系，各个分支学科间联系以及与其他学科的联系。近年来，人们对物理学史的素质教育功能及其在大学物理、大学物理实验教学中的作用进行了深入的探讨和教学实践研究。很多高校的物理专业，都将物理学史设为通识性的基础必修课或选修课程。可以说物理学史的教育地位已经被广大物理教师和教育学家认可。但是，作为通识课程的物理学史应该具有怎样的教学理念？究竟应该讲什么怎么讲？这些内容是否对学生有吸引力？如何能让这门既有科学性又有文化性的课程担负起素质教育的责任？这些都是需要我们进行深入探讨的。

2 问卷调查

为了解决这些问题，我们面向哈尔滨工业大学[illegible]年入学的本科生发放了调查问卷，共发放[illegible]份问卷，收回有效问卷[illegible]份。问卷内容涉及本课程的选修意愿、课程内容和学习方式等几个方面，目的是为了了解学生对物理学史的需求情况。问卷涉及的问题以及调查结果如表1所示。

表1 调查问卷

问题	选择	所占比例
1.是否愿意选修《物理学史》通识课程	A.愿意	[illegible]
	B.不愿意	[illegible]
	C.无所谓	[illegible]
2.能否自学完成《物理学史》课程	A.能	[illegible]
	B.不能或不想自学	[illegible]
	C.可以自学一部分	[illegible]
	D.希望通过Wiki进行学习	[illegible]
	E.能自学，但需要老师帮助和指导	[illegible]
3.你希望通过《物理学史》了解哪些内容（多选）	A.物理发展史中的逸闻趣事	[illegible]
	B.激发对物理的学习兴趣	[illegible]
	C.物理学家的思维习惯、物理思想	[illegible]
	D.了解物理学的前沿	[illegible]
	E.物理学的研究方法	[illegible]

调查结果表明，多数同学对《物理学史》这门通识课程有兴趣，会选择选修。还有一部分同学没有明确的反对。这就是说，针对全校开设这样一门通识选修课程具有可行性。在对该课程教学手段的调查（问题2）结果表明，认为学习过程不需要老师参与的同学（选择A的）约为[illegible]，而[illegible]的学生（选择

[illegible]

作者简介：孟庆鑫（[illegible]），[illegible]

（28）分离变量法教学内容优化及本征值问题引入方式研究. 物理通报

分离变量法教学内容优化及本征值问题引入方式研究

姜雨辰　孟凡鑫　学　宇
（哈尔滨工业大学物理系　黑龙江 哈尔滨　150001）

[收稿日期:2017-05-04]

摘　要:现有数学物理方法教学体系中,分离变量法在前,本征值问题在后.而分离变量过程中,又涉及到本征值问题,这样的安排导致学生在学习分离变量法过程中,不能很好地理解本征值问题是分离变量法的基础,不利于学生严密逻辑思维能力的培养.针对这个问题我们开展了分离变量法教学内容优化的研究,提出一种更有利于学生严密逻辑思维能力培养的分离变量法教学方案:将本征值问题提前,将其置于定解问题之后,分离变量法之前,进而,为避免直接引入 Sturm-Liouville 方程的导致的突兀性问题,给出了分离变量法教学顺序调整后的 Sturm-Liouville 方程的引出方案.

关键词:分离变量法　本征值问题　教学内容优化

数学物理方法是物理系的主干课程之一,是一门利用数学语言描述并解决自然科学及工程技术中所遇到的一些问题,建立定解问题,求解定解问题的专业基础课.课程的教学目的是通过课程的学习进一步提高学生的数学素养和应用数学知识解决复杂物理问题的能力;为理论物理课程的学习打下牢固的基础.但现有的教材内容体系存在一些问题,不利于学生严密思维能力的培养.我们知道,求解定解问

Rethinking on the Adiabatic Process of Ideal Gas from Microcosmic Perspective

Qin Tian　Yang Tianyi　Yang Chenglin　Li JingYi　He LanXin　Huang Min
(Mingshang Institution of Xindu No.1 High School, Chengdu, Sichuan　610500)
Zhao Yunhe
(Department of Physics, Beijing Normal University, Beijing　100875)

Abstract: The paper "Deducing adiabatic equation of ideal gas via kinetic theory of gas" (College Physics(March 2017) mentioned a microcosmic way to calculate the ideal gas adiabatic formula: the physical nature of this derivation is the collective effect of the gas molecules on the piston wall, that is, the microscopic interpretation of the gas pressure. Based on this point, this paper gives the corresponding derivation from the perspective of the external work of gas molecules, and finds a more intuitive solution in its given model and correspond more directly to the first law of thermodynamics. This more directly links itself to the micro-process and microscopic ideal gas state equation.

Key words: ideal gas; adiabatic process; microscopic work

（29）压缩传感在物理演示实验中的应用．物理与工程

物理实验

压缩传感在物理演示实验中的应用

靳辰飞　张思琦　韩　权　赵　远
（哈尔滨工业大学物理系，黑龙江 哈尔滨 150001）

摘　要　将科研前沿技术融入到物理演示实验中有助于大学生科研兴趣和创新能力的提高。我们将近几年兴起的科研热点问题——压缩传感技术融入到物理演示实验中，研制了一套值得推广的单像素成像演示实验设备。该设备符合物理演示实验要求的易操作性和便携性，还兼有现象明显和原理深刻的特点。可演示的内容不仅涉及光学、统计物理、光电器件等相关知识，同时还涵盖了信息技术、通信技术、计算机科学等多个交叉领域的基本知识。本实验对开发并通过物理演示实验来提高大学生创新能力和科研兴趣方面具有参考价值。

关键词　演示实验；科技前沿；压缩传感；单像素成像

AN APPLICATION OF COMPRESSIVE SENSING TECHNOLOGY IN PHYSICS DEMONSTATION EXPERIMENT

Jin Chenfei　Zhang Siqi　Han Quan　Zhao Yuan
(Department of Physics, Harbin Institute of Technology, Harbin, Heilongjiang 150001)

Abstract　Merging the cutting edge science and technology into physical demonstration experiment will help students improve research interests and creative ability. By integrating the compressive sensing technology, which is a hot topic rising in recent years, into demonstration experiments, we developed a set of single pixel imaging demonstration equipment which is worthy to be popularized. The device meets the requirement of physical demonstration experiment for its ease and portability. It also has some characteristics of evidencing visible phenomenon and revealing profound principle. The contents of our device are not only related to physics knowledge including optics, statistical physics and optoelectronic devices, but also cover the basics of a plurality of cross-cutting areas of information technology, communications technology and computer science. This article will be very valuable for enhancing students' creativity and research interests through physics demonstration experiments.

Key words　demonstration experiment; technological frontiers; compressive sensing; single pixel imaging

物理学是实验的科学，这决定了物理演示实验在大学物理的教学中占有十分重要的地位。然而，现有的演示实验目前多数侧重于通过简单直观的实验来帮助学生理解大学物理的课堂教学内容，而不能引起学生对科学问题的深入思考和有效地激发学生的科研兴趣[1]。演示实验内容严重与现代科技前沿脱钩，忽视了尖端科研技术在提高大学生科研兴趣和创新能力方面起到的重要作用。本文以工科大学的物理演示实验设计为背景，通过将近几年兴起的科研热点之一——压缩传感融入到演示实验中，研制了一套值得推广的单像

收稿日期：[illegible]
基金项目：[illegible]
作者简介：靳辰飞，男，副教授，[illegible]

（30）学科思维导图与物理知识网络的构建

学科思维导图与物理知识网络的构建

李淑凤 李雪春 杨 琳 许佳琳[1] 卢春林[1] 张 赫[1]
（大连理工大学物理学院，基础物理国家级实验教学示范中心，辽宁 大连 116024）

摘 要 大学物理是面向理工科学生的一门基础课程，在高校教学中的重要性毋庸置疑。学习大学物理，不仅要掌握自然界的客观规律、分析和研究方法，更重要的是从整体上认识和掌握物理学并应用于实际。物理学中很多物理量有着内在的必然的联系，通过绘制学科思维导图或概念图，来探究这些相关联的物理量的关系和本质、物理规律的适用范围，可以更透彻地理解和掌握物理知识。本文将思维导图工具引入大学物理的教学中，利用思维导图帮助学生通过物理量间的关联，构建知识网络，激发学生的学习热情，提高学习效率和教学效果。

关键词 大学物理；思维导图；学科思维导图；概念图

0 引言

作为基础学科的大学物理课程，是高校为理工科学生提供的全面系统地掌握物理学基础的重要课程。大学物理涉及力学（质点运动学、质点动力学、刚体、振动、波动、相对论基础）、热学（气体动理论、热力学）、电磁学（静电、稳恒磁场、电磁感应）、光学（干涉、衍射、偏振）、量子力学（波粒二象性、薛定谔方程等）等五个主要部分，包含了物质的基本结构、物质运动、物质的相互作用与转化的普遍规律，其基本概念、基本定理、定律被广泛应用于所有的学科领域。因为涵盖内容广，概念、物理量、公式、定理定律繁多，学生在大学物理课程的学习中，不仅要掌握自然界的客观规律、研究方法和解题技能，还要从整体上认识和掌握物理学，因此有相当大的难度，也让很多学生感到畏惧和排斥。

思维导图，是一种发散性的、图像式思维的工具，是英国著名心理学家、教育学家 Tony Buzan 发明的一种有效的思维模式[1]。思维导图运用图文并重的技巧，把各级主题的关系用相互隶属与相关的层级图表现出来，把主题关键词与图像、颜色等建立记忆链接，充分运用左右脑的机能，在科学、逻辑，判断与艺术、图像、感觉等之间平衡发展。思维导图既可以优化人们的思维和记忆，提高工作和学习效率，又能激发人的创造力。

多年来，思维导图这一功能强大的思维工具，已经被越来越多的人掌握和使用，广泛地应用于商业、学习以及日常生活中，特别是随着众多的思维导图制作软件的推出和不断更新，如 Mindmanager、XMIND、mindmap、FreeMind、NovaMin、Mind Vector 等，更多的人喜欢上这一工具。哈佛大学、剑桥大学、伦敦经济学院等知名学府正在使用和教授思维导图，华中科技大学 2013 年在国内率先推出了思维导图公开课，得到学生热烈欢迎。把学科思维导图的图、文、色、关联引入大学物理教学，特别是后学习阶段，对学生整合物理知识，提高学习兴趣和学习效率大有帮助。已有老师在进行这方

收稿日期：[illegible]
基金项目：[illegible]
作者简介：[illegible]
引文格式：[illegible]

（31）《大学物理》MOOC 练习资源建设及其与传统教学模式的融合


《大学物理》MOOC 练习资源建设及其与传统教学模式的融合

1 大学物理 MOOC 练习活动资源建设

（32）静电场中的相关能量

静电场中的相关能量

李淑凤　王艳辉　马春利　李雪春　邓　琳
（大连理工大学物理与光电工程学院，辽宁 大连　116024）

摘　要　从点电荷到带电体，对静电场中引入的几个相关能量，即电势能、电场能、电相互作用能、自能、固有能、互能等做了剖析和探究。电势能是带电体间或带电体与电场间的相互作用能，具有相对性和共有性。在指定电荷相距无限远电势能为零的条件下，解析法给出的电场能本质上就是电势能，自能即固有能和互能分别是对单一带电体的电场能和多带电体间的相互作用能的另一种表述。论文还进一步对点电荷电场能发散问题做了讨论，指出了球形带电体场能公式的适用极限。

关键词　电场能；电势能；自能；互能；点电荷自能

静电场中，根据电场力对电荷做功与路径无关，引入了电势能的概念。电势能是电荷与场源电荷或与其所激发的电场之间的相互作用能，因此为系统所共有，但其具有相对性的属性。另一方面，在静电场中移动电荷，电场力能够做功又说明静电场蕴含一定的能量，这就是静电能。电容器放电有发光、发热等现象产生，就是电容器储存的静电能转换为其他形式能量的结果。对于静电场中这两个能量-电势能和静电能，一般教材中少有对其关系做进一步的说明，容易让学生产生疑惑。那么电场能与电势能是否是两种不同性质的能量，有什么区别和联系呢？关于这方面的教学研讨成果也时有发表[1-3]。本论文从静电学中电势能和电场能两个概念的引入出发，探究它们的实质和内在关联，指出电场能的本质就是电势能。文中也对自能和互能做了讨论，并从点电荷的电场能积分公式发散，说明点电荷作为一个理想化的模型，在非理想情况下其自能公式的适用极限。

1　点电荷系的电势能

最简单的带电体就是点电荷。当两个点电荷 q_1 和 q_2 从相距无限远移至相距 r_{12} 时，电场力做功 $A=-\frac{q_1q_2}{4\pi\varepsilon_0 r_{12}}$，设两点电荷相距无限远时系统电势能为零，由保守力做功等于势能的减少量，则两电荷相距 r_{12} 时系统的电势能就是

$$W_{12}=\frac{q_1q_2}{4\pi\varepsilon_0 r_{12}} \tag{1}$$

这一势能也是移动电荷过程中外界克服电荷间相互作用的库仑力所做的功，因此也称为电荷间的相互作用能。式（1）写成另一种形式为

$$W_{12}=\frac{1}{2}(U_1q_1+U_2q_2) \tag{2}$$

其中，U_1 是点电荷 q_2 产生的电场在 q_1 所在位置的电势；U_2 是点电荷 q_1 产生的场在 q_2 所在位置的电势。后面的讨论如无特别说明均设定无限远点为电势零点。如果继续往系统内移入第三个点电荷 q_3，

收稿日期：2016-04-23
基金项目：教育部高等学校大学物理课程教学指导委员会教学研究项目(DWJZW201404dx)；大连理工大学教育教学改革基金(YB2016067)。
作者简介：李淑凤，女，副教授，主要从事物理教学及普通光学的教学研究。lsf@dlut.edu.cn
引文格式：李淑凤，王艳辉，马春利，等. 静电场中的相关能量[J]. 物理与工程，2016，26(Z1)：49-52.

（33）基于教学的洛伦兹变换推导的探讨

基于教学的洛伦兹变换推导的探讨

李凯成 刘 圣 郑 旭 李宏春
（大连理工大学物理与光电工程学院，辽宁 大连 116024）

摘 要 介绍了国内外大学物理教材中的几种洛伦兹变换的推导方法，从教学出发，对相对论中洛伦兹变换推导给出处理和讨论。

关键词 相对论教学；洛伦兹变换；推导

狭义相对论是大学物理教学中的难点，教师在讲授过程中，能够提供的实例有限，而对于经典时空观已经根深蒂固的学生，在学习的过程中更是有许多难以理解，感觉不可思议的问题，让学生欣然接受相对论理论并学懂学透，对教师也是一个挑战。

众所周知，爱因斯坦的两条假设是狭义相对论的根本，由此得到的洛伦兹变换又是新时空理论、描述物理量的变换以及所有物理理律的协变性的基础。关于洛伦兹变换，各类普通院校使用的各类教材[1-7]及一些文章[8-9]中，有多种推导方法。但部分推导或者因后果没有文代清楚，或者推导过程中关系式的给出不令人信服，或者又引入许多新假设，这样的推导不但教师不自信，学生也会有抵触心理。因此让学生一开始就能接受洛伦兹变换，无疑在后面的教学中会收到明理成章，事半功倍的效果。

1 基于物理教学的几种推导方法

在下面的推导中涉及的两个惯性参考系 S（时空坐标用 (x,y,z,t) 表示）和 S'（时空坐标用 (x',y',z',t') 表示）均按常规的约定，即 x 轴和 x' 轴重合、y、z 轴和 y'、z' 轴相互平行，并且在 $t=t'=0$ 时，原点 O 和 O' 重合，S' 相对 S 以速度 u 沿 $x'(x)$ 轴作匀速直线运动。在这样的约定下，绝大多数的推导都直接给出洛伦兹变换中的两个关系式即 $y=y'$，$z=z'$，其余两个关系式的推导大致可总结为如下3种。

推导1：考虑到运动的相对性，S' 相对 S 以速度 u 沿 $x(x')$ 轴作匀速直线运动，则有 S 相对 S' 以速度 $-u$ 沿 x 轴作匀速直线运动，文献[10]将其称为爱因斯坦条件。

质量 O 点的坐标，在 S 系总有 $x=0$，在 S' 系则总有 $x'=-ut'$，即 $x'+ut'=0$。对此特殊点二者同时为零，可认为在任意时刻，对任意点，二者有比例关系

$$x=k(x'+ut') \tag{1}$$

同理质量 O' 点的坐标时，可得

$$x'=k'(x-ut) \tag{2}$$

根据狭义相对论的相对性原理，两惯性系等价，有 $k=k'$，两假设零时刻在原点发出一个光信号，利用光速不变原理，$x=ct$，$x'=ct'$，结合式（1）和式（2）可确定出系数 $k=1/\sqrt{1-u^2/c^2}$，不再赘述。

推导2：首先说明要推导的变换常是线性的，于是将变换直接写成如下形式

$$x'=\alpha x+\beta t \tag{3}$$

$$t'=\gamma x+\delta t \tag{4}$$

并据此计算出 O' 在 S 系中的速度 $\mathrm{d}x/\mathrm{d}t=u$ 和 O 在 S' 系中的速度 $\mathrm{d}x'/\mathrm{d}t'=-u$，其次是根据空间的

（9）教师获奖佐证材料

序号	成果名称/获奖名称	级别	获奖等级	负责人/教师姓名	年份
1.	中国政府友谊奖	国家级		A. A. Kudryavtesv	2021
2.	国家技术发明奖	国家级	一等奖	马晶	2014
3.	国防技术发明奖	国家级	特等奖	马晶	2013
4.	国防科技进步奖	国家级	一等奖	马晶	2018
5.	教育部长江学者特聘教授	国家级		赵纪军	2017
6.	国家自然科学二等奖	国家级	二等奖	赵纪军	2010
7.	国家技术发明奖	国家级	二等奖	马晶	2009
8.	国防科技进步奖	国家级	二等奖	马晶	2010
9.	国防科技进步奖	国家级	二等奖	马晶	2008
10.	国防技术发明奖	国家级	二等奖	马晶	2008
11.	国防科学技术奖	国家级	二等奖	马晶	2006
12.	国防科技进步奖	国家级	三等奖	马晶	2002
13.	2017年度国防科技工业十大创新人物	国家级		马晶	2017

14.	CCTV 科技盛典“2017 年度科技创新人物”	国家级		马晶	2017
15.	全国“最美教师”荣誉称号	国家级		马晶	2016
16.	全国模范教师	国家级		马晶	2014
17.	国防科技创新团队奖	国家级		马晶	2015
18.	国家万人计划领军人才	国家级		赵纪军	2017
19.	国家千人青年项目	国家级		高峻峰	2018
20.	国家自然科学基金优秀青年基金	国家级		周思	2022
21.	全国高等学校教师自制实验设备创新大赛	国家级	一等奖	王健	2021
22.	第一届“高等教育杯”全国高等学校物理基础课程青年教师讲课比赛	国家级	一等奖（冠军）	孟庆鑫	2014
23.	2018 年全国高校教师教学创新大赛——第五届全国高等学校教师自制实验教学仪器设备创新大赛	国家级	银奖	刘世刚	2018
24.	第六届“高等教育杯”全国高等学校物理基础课程青年教师讲课比赛	国家级	二等奖	张伶莉	2021
25.	全国高等学校教师自制实验设备创新大赛	国家级	三等奖	娄秀涛	2021
26.	全国大学生创新创业实践联盟年会优秀论文	国家级	三等奖	高波	2018
27.	国务院特殊津贴	国家级		赵纪军	2016

28.	国务院特殊津贴	国家级		马晶	2015
29.	全国光学与光学工程博士生学术联赛	国家级	百强导师奖	田浩	2021
30.	全国光学与光学工程博士生学术联赛	国家级	百强导师奖	丁卫强	2021
31.	黑龙江省发明奖	省级	特等奖	马晶	2016
32.	黑龙江省课程思政教学竞赛	省级	特等奖	任延宇	2021
33.	中国高等学校十大科技进展	省部级		谭立英	2017
34.	中国高等学校十大科技进展	省部级		马晶	2013
35.	自然科学奖	省部级	二等奖	赵纪军	2017
36.	辽宁省五一劳动奖章	省部级		赵纪军	2021
37.	第六届“高等教育杯”全国高等学校物理基础课程青年教师讲课比赛	东北地区	一等奖	张伶莉	2021
38.	龙江学者支持计划-特聘教授	省级		田浩	2019
39.	黑龙江省五一劳动奖章	省级		马晶	2017
40.	黑龙江省青年教学名师			李均	2021
41.	“龙江楷模”	省级		谭立英	2018
42.	先进技术应用转化大赛	省部级	金奖	马晶	2019

43.	黑龙江省青年教师教学竞赛	省级	理科组一等奖	任延宇	2020
44.	黑龙江省高校微课教学竞赛	省级	一等奖	任延宇	2018
45.	卓越大学联盟青年教师教学创新大赛	省级	一等奖	任延宇	2018
46.	第三届“高等教育杯”全国高等学校物理基础课程青年教师讲课比赛	省级	一等奖	黄丽	2017
47.	第二届“高等教育杯”全国高等学校物理基础课程青年教师讲课比赛	省级	一等奖	韩权	2016
48.	黑龙江省高等学校课程思政示范课程	省级		任延宇	2020
49.	黑龙江省高等学校物理基础课程青年教师讲课比赛	省级	二等奖	李均	2018
50.	教育部自然科学奖	省部级	二等奖	赵纪军	2016
51.	河北省自然科学奖	省部级	二等奖	赵纪军	2018
52.	辽宁省自然科学奖	省部级	二等奖	赵纪军	2019
53.	山西省自然科学奖	省部级	二等奖	赵纪军	2021
54.	哈尔滨工业大学第二届课程思政教学竞赛	校级	一等奖	周可雅	2021
55.	哈尔滨工业大学优秀教育教学管理奖	校级		张宇	2021
56.	哈尔滨工业大学 2020 年教学贡献奖励	校级	一等奖	时红艳	2020
57.	基于分类人才培养的物理分层次教学模式研究	校级	一等奖	孟庆鑫	2019

58.	固体光学课程研究型教学理论与实践	校级	二等奖	田浩	2017
59.	首届哈尔滨工业大学“育人新星”青年导师	校级		田浩	2021
60.	哈尔滨工业大学 2021 年教学贡献奖励	校级	教学优秀奖一等奖	李均	2021
61.	哈尔滨工业大学首届课程思政教学竞赛	校级	特等奖	任延宇	2019
62.	第七届校青年教师教学基本功竞赛	校级	一等奖	李均	2018
63.	在线教学“我最喜爱的课程”奖	校级		李均	2020

（1）中国政府友谊奖获奖报道

（2）国家技术发明一等奖获奖证明

国家技术发明奖

证　书

为表彰国家技术发明奖获得者，特颁发此证书。

项目名称：星地激光链路系统技术

奖励等级：一等

获 奖 者：马晶（哈尔滨工业大学）

中华人民共和国国务院

2014年12月12日

证书号：2014-F-24201-1-01-R01

（3）国防技术发明特等奖获奖证明

（4）国防科技进步一等奖获奖证明

（5）教育部长江学者特聘教授证明

長江學者獎勵計劃

CHANG JIANG SCHOLARS PROGRAM

特 聘 教 授

Chang Jiang Scholars

兹批准 大连理工大学

聘任 赵纪军 为教育部 2017 年度“长江学者奖励计划”特聘教授，聘期 5 年。

中华人民共和国教育部

MINISTRY OF EDUCATION, PEOPLE'S REPUBLIC OF CHINA

编号：T2017032 2018 年 5 月

（6）国家自然科学二等奖获奖证明

国家自然科学奖

证 书

为表彰国家自然科学奖获得者，特颁发此证书。

项目名称：原子团簇和团簇组装的尺寸效应和奇特物性

奖励等级：二等

获 奖 者：赵纪军(南京大学)

中华人民共和国国务院

2010年11月29日

证书号：2010-Z-102-2-02-R03

（7）国家技术发明二等奖获奖证明

国家技术发明奖

证　书

为表彰国家技术发明奖获得者，特颁发此证书。

项目名称：卫星激光通信关键技术及应用

奖励等级：二等奖

获 奖 者：马　晶（哈尔滨工业大学）

中华人民共和国国务院

2009 年 12 月 23 日

证书号：2009-F-24201-2-03-R01

（8）国防科技进步二等奖获奖证明

（9）国防科技进步二等奖获奖证明

（10）国防技术发明奖二等奖获奖证明


国防技术发明奖

荣誉证书

为鼓励自主创新，表彰国防技术发明奖获得者，特颁此证

获奖项目：激光星间链路关键技术及高速轻型激光链路终端工程样机研制

获 奖 者：马 晶

获奖等级：二等奖

获奖日期：二〇〇六年十二月

No. 2008GFFMJ2006-002

（11）国防科学技术奖二等奖获奖证明


国防科学技术奖

荣誉证书

为表彰在推动国防科学技术进步、对国防现代化建设作出突出贡献者，特颁此证，以资鼓励

获奖项目：空间激光数字通信技术研究

获 奖 者：马晶

获奖等级：二等奖

获奖日期：二〇〇六年十二月

No. 2006GFJ2226-1

（12）国防科技进步三等奖获奖证明


国防科学技术奖

荣誉证书

为表彰在推动国防科学技术进步、对国防现代化建设作出突出贡献者，特颁此证，以资鼓励。

获奖项目：中继卫星间链路技术

获 奖 者：马晶

获奖等级：三等奖

获奖日期：二〇〇一年十一月

No. 2002GFJ3405-1

（13）2017 年度国防科技工业十大创新人物

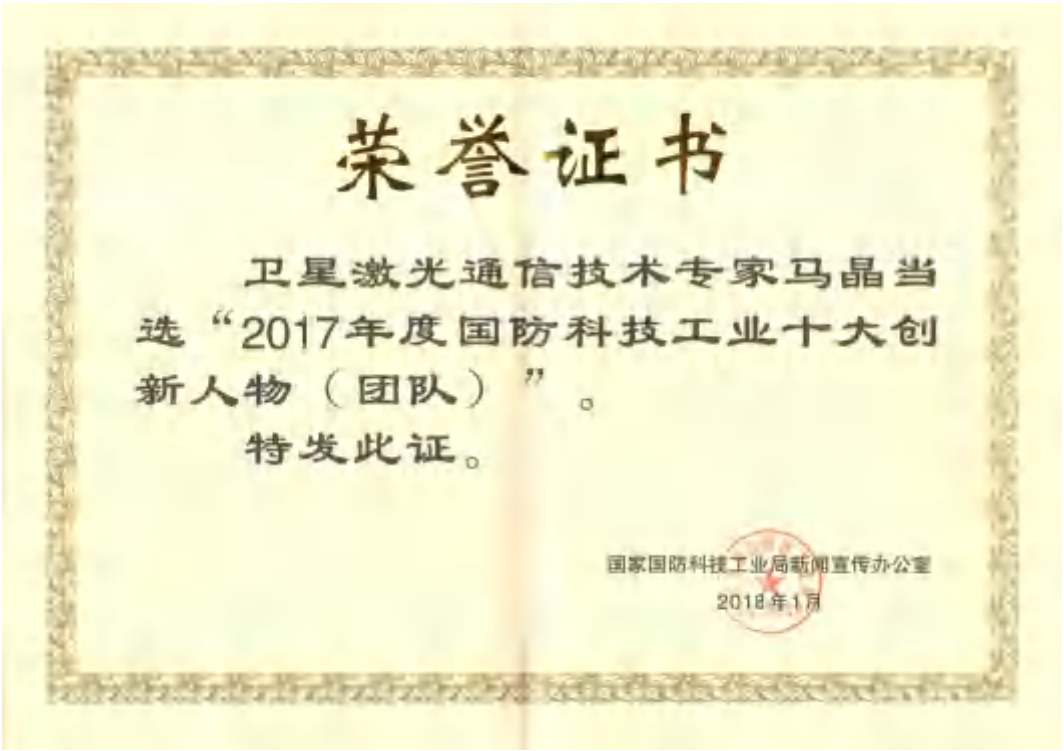
荣誉证书

卫星激光通信技术专家马晶当选“2017年度国防科技工业十大创新人物（团队）”。

特发此证。

国家国防科技工业局新闻宣传办公室

2018年1月

（14）CCTV 科技盛典“2017 年度科技创新人物”

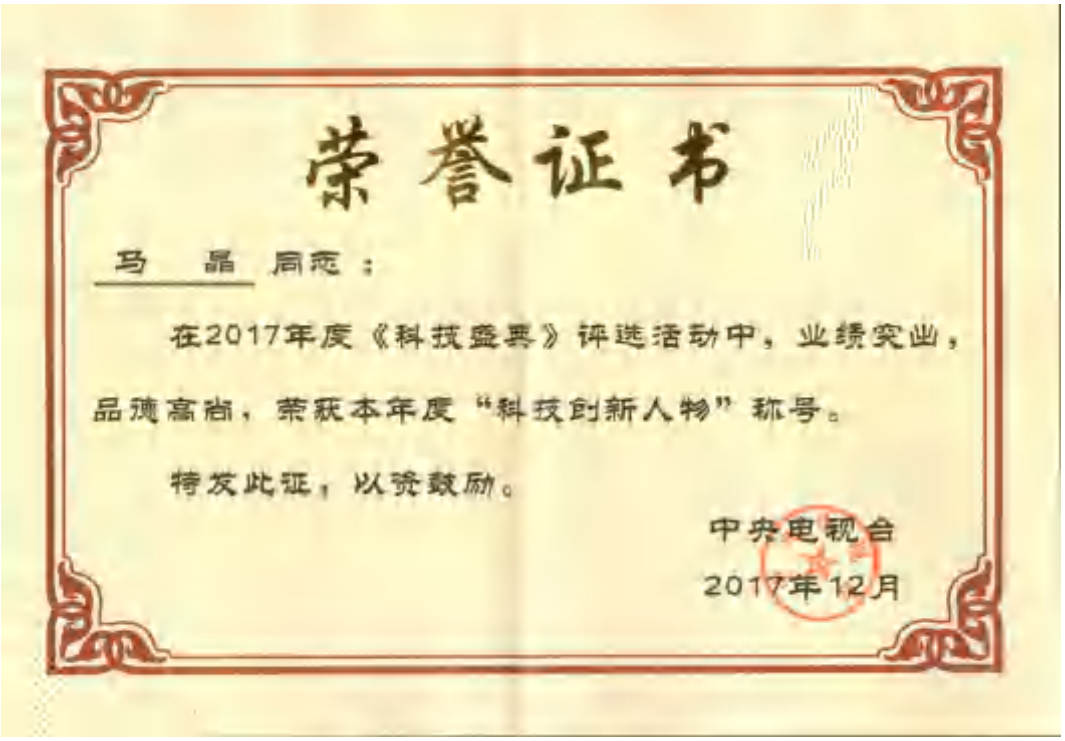

荣誉证书

马　晶 同志：

在2017年度《科技盛典》评选活动中，业绩突出，品德高尚，荣获本年度“科技创新人物”称号。

特发此证，以资鼓励。

中央电视台

2017年12月

（15）全国最美教师荣誉称号

（16）全国模范教师

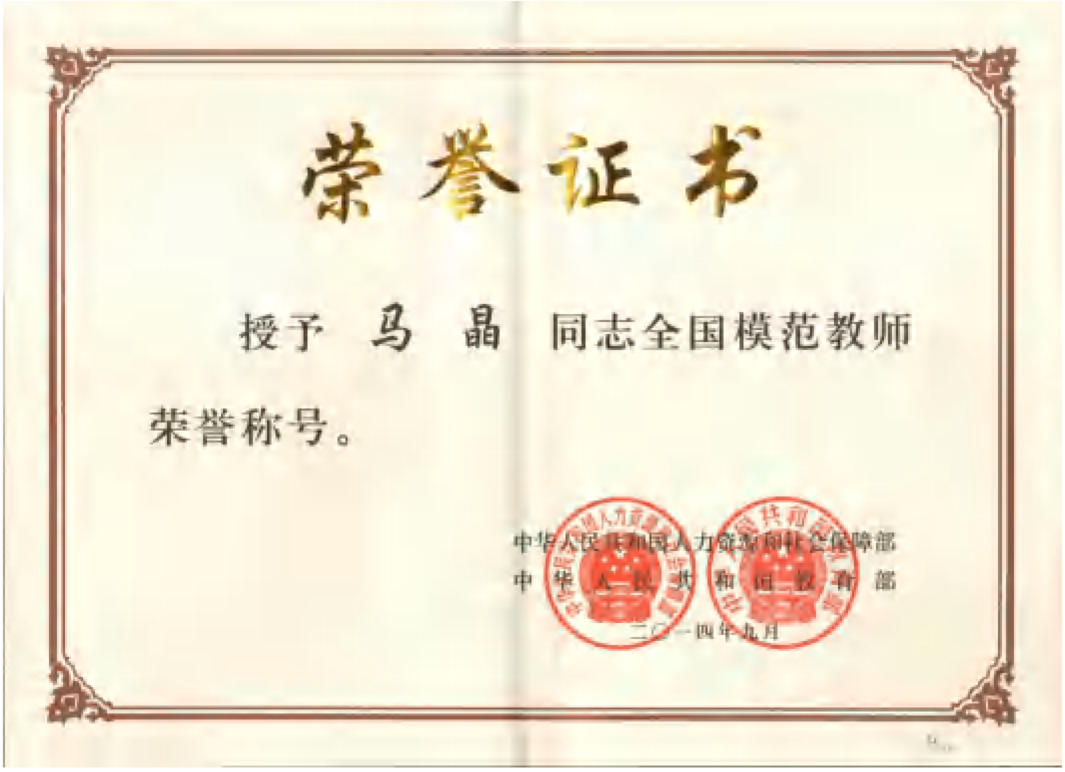

（17）国防科技创新团队奖获奖证明

（18）国家万人计划领军人才证明


证书编号：W03020226

万人计划

Wanren Jihua

国家高层次人才
特殊支持计划入选证书

赵纪军 同志

入选国家高层次人才特殊
支持计划领军人才

中共中央组织部
人力资源和社会保障部

（19）国家千人青年项目证明

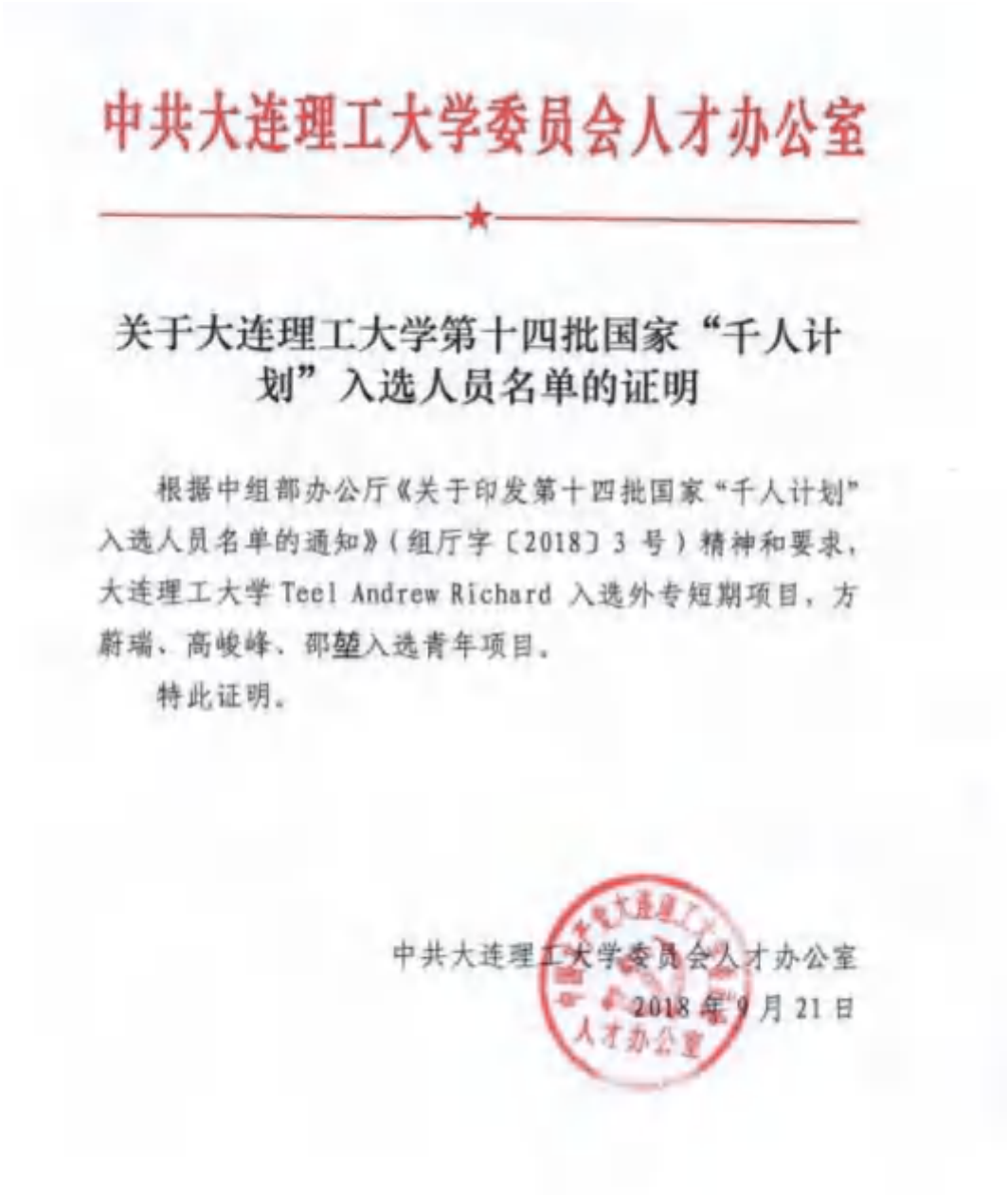

中共大连理工大学委员会人才办公室

关于大连理工大学第十四批国家“千人计划”入选人员名单的证明

根据中组部办公厅《关于印发第十四批国家“千人计划”入选人员名单的通知》（组厅字〔2018〕3号）精神和要求，大连理工大学Teel Andrew Richard入选外专短期项目，方蔚瑞、高峻峰、邵堃入选青年项目。

特此证明。

中共大连理工大学委员会人才办公室

2018年9月21日

（20）国家自然科学基金优秀青年基金证明

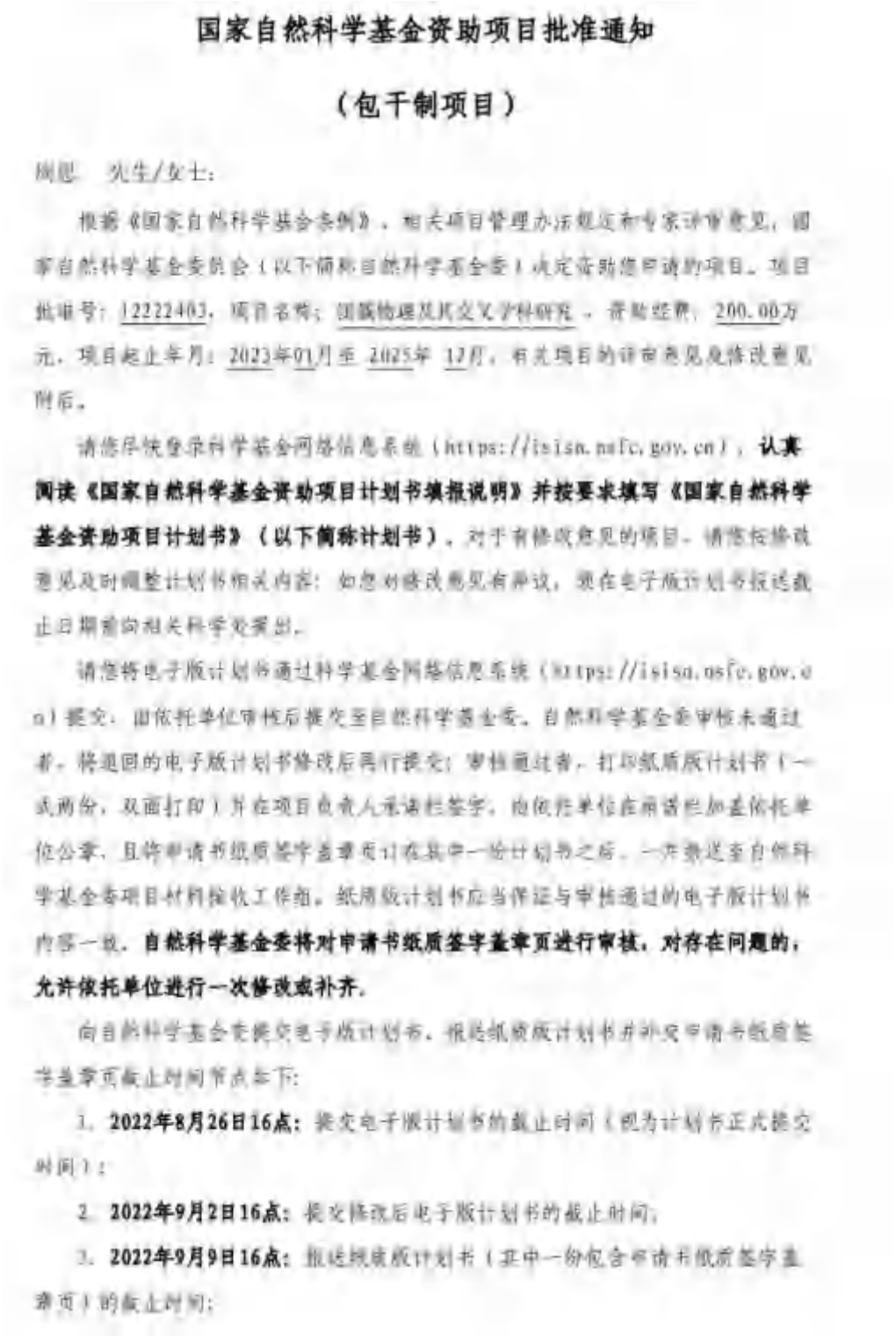

国家自然科学基金资助项目批准通知

（包干制项目）

刘思　先生/女士：

根据《国家自然科学基金条例》，相关项目管理办法规定和专家评审意见，国家自然科学基金委员会（以下简称自然科学基金委）决定资助您申请的项目。项目批准号：12222403，项目名称：团簇物理及其交叉学科研究，资助经费：200.00万元，项目起止年月：2023年01月至2025年12月，相关项目的评审意见及修改意见附后。

请您尽快登录科学基金网络信息系统（https://isisn.nsfc.gov.cn），**认真阅读《国家自然科学基金资助项目计划书填报说明》并按要求填写《国家自然科学基金资助项目计划书》（以下简称计划书）**。对于有修改意见的项目，请您按修改意见及时调整计划书相关内容；如您对修改意见有异议，须在电子版计划书报送截止日期前向相关科学处室提出。

请您将电子版计划书通过科学基金网络信息系统（https://isisn.nsfc.gov.cn）提交，由依托单位审核后提交至自然科学基金委。自然科学基金委审核未通过者，将退回电子版计划书修改后再行提交；审核通过者，打印纸质版计划书（一式两份，双面打印）并在项目负责人承诺栏签字，由依托单位在相应栏加盖依托单位公章，且将申请书纸质签字盖章页打在其中一份计划书之后，一并报送至自然科学基金委项目材料接收工作组。纸质版计划书应当保证与审核通过的电子版计划书内容一致。**自然科学基金委将对申请书纸质签字盖章页进行审核，对存在问题的，允许依托单位进行一次修改或补齐。**

向自然科学基金委提交电子版计划书、报送纸质版计划书并补充申请书纸质签字盖章页截止时间节点如下：

1. **2022年8月26日16点：**提交电子版计划书的截止时间（视为计划书正式提交时间）；

2. **2022年9月2日16点：**提交修改后电子版计划书的截止时间；

3. **2022年9月9日16点：**报送纸质版计划书（其中一份包含申请书纸质签字盖章页）的截止时间；

（21）全国高等学校教师自制实验设备创新大赛一等奖获奖证明

获奖证书

王健、骆素华、黄丽、孙芳魁、杨昆老师：

您的作品“盘式光学体全息存储与再现实验教学系统”荣获全国高校教师教学创新大赛——第六届全国高等学校教师自制实验教学仪器设备创新大赛自由设计类

一等奖

特发此证，以资鼓励。

证书编号：ZZJY202106809

中国高等教育学会
2021年6月

（22）第一届“高等教育杯”全国高等学校物理基础课程青年教师讲课比赛国家级一等奖（冠军）证明

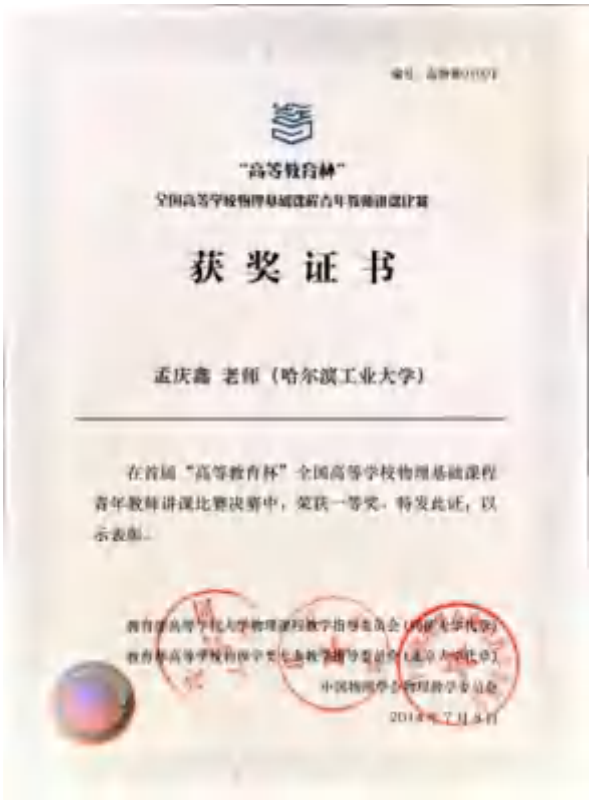

“高等教育杯”

全国高等学校物理基础课程青年教师讲课比赛

获 奖 证 书

孟庆鑫 老师（哈尔滨工业大学）

在首届“高等教育杯”全国高等学校物理基础课程青年教师讲课比赛决赛中，荣获一等奖，特发此证，以示表彰。

（23）2018 年全国高校教师教学创新大赛——第五届全国高等学校教师自制实验教学仪器设备创新大赛证明

（24）第六届“高等教育杯”全国高等学校物理基础课程青年教师讲课比赛国家级二等奖证明

（25）全国高等学校教师自制实验设备创新大赛三等奖获奖证明

获奖证书

娄秀涛、赵海发老师：

您的作品“气体分子高分辨吸收光谱实验仪”荣获全国高校教师教学创新大赛——第六届全国高等学校教师自制实验教学仪器设备创新大赛自由设计类

三等奖

特发此证，以资鼓励。

证书编号：ZZJY202106068

中国高等教育学会
2021年6月

（26）全国大学生创新创业实践联盟年会优秀论文获奖证明

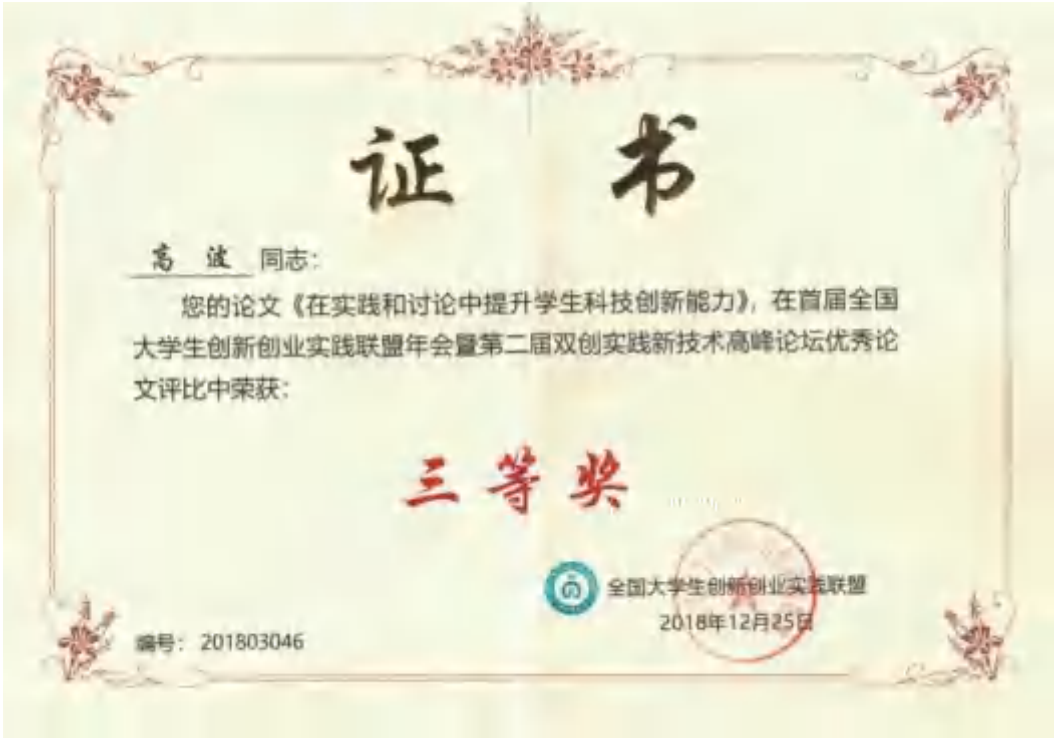

证 书

高 波 同志：

您的论文《在实践和讨论中提升学生科技创新能力》，在首届全国大学生创新创业实践联盟年会暨第二届双创实践新技术高峰论坛优秀论文评比中荣获：

三等奖

全国大学生创新创业实践联盟
2018年12月25日

编号：201803046

（27）国务院特殊津贴证明

证书

赵纪军同志：

为了表彰您为发展我国自然科学研究事业做出的突出贡献，特决定发给政府特殊津贴并颁发证书。

政府特殊津贴第2016[illegible]号

2016 年 [illegible] 月 [illegible] 日

（28）国务院特殊津贴证明

证书

马晶同志：

为了表彰您为发展我国工程技术事业做出的突出贡献，特决定发给政府特殊津贴并颁发证书。

政府特殊津贴第2014[illegible]号

[illegible] 年 [illegible] 月 [illegible] 日

（29）全国光学与光学工程博士生学术联赛百强导师奖证明

（30）全国光学与光学工程博士生学术联赛百强导师奖证明

（31）黑龙江省科学技术奖二等奖获奖证书

（32）黑龙江省课程思政教学竞赛特等奖证明


获奖证书

—— 哈尔滨工业大学 ——

任延宇 老师：

荣获黑龙江省首届高等学校

课程思政教学竞赛：

特等奖

黑龙江省教育厅

2021年10月26日

（33）2017 年度中国高等学校十大科技进展获奖证明

荣誉证书

哈尔滨工业大学：

你校 谭立英 主持完成的“高轨同步轨道卫星星地双向高速激光通信”入选 2017 年度“中国高等学校十大科技进展”，特发此证。

教育部科学技术委员会

二〇一七年十二月二十七日

（34）2013 年度中国高等学校十大科技进展获奖证明

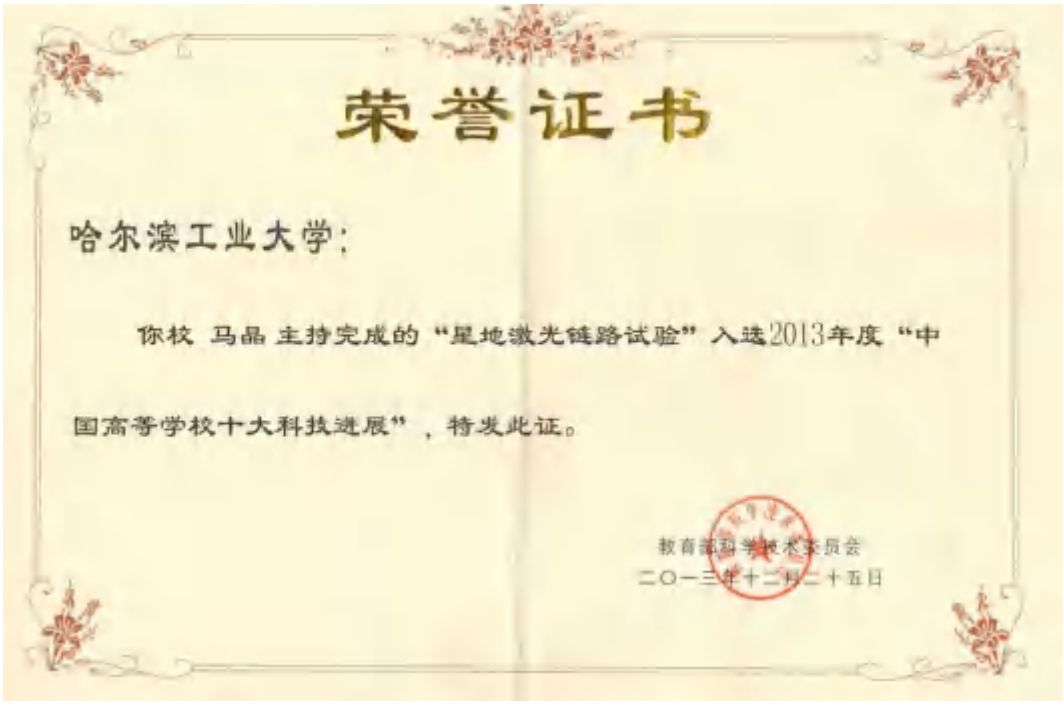

荣誉证书

哈尔滨工业大学：

你校 马晶 主持完成的“星地激光链路试验”入选2013年度“中国高等学校十大科技进展”，特发此证。

教育部科学技术委员会

二〇一三年十二月二十五日

（35）自然科学奖二等奖获奖证明

获奖项目：二维原子晶体及其衍生物的基础物性、储氢特性和衬底调控的研究

获 奖 者：赵纪军(第1完成人)

奖励等级：自然科学奖二等奖

奖励日期：2017年2月

证 书 号：2016-061

为表彰在促进科学技术进步工作中做出重大贡献，特颁发此证书。

中华人民共和国教育部

二〇一七年二月二十二日

（36）辽宁省五一劳动奖章证明

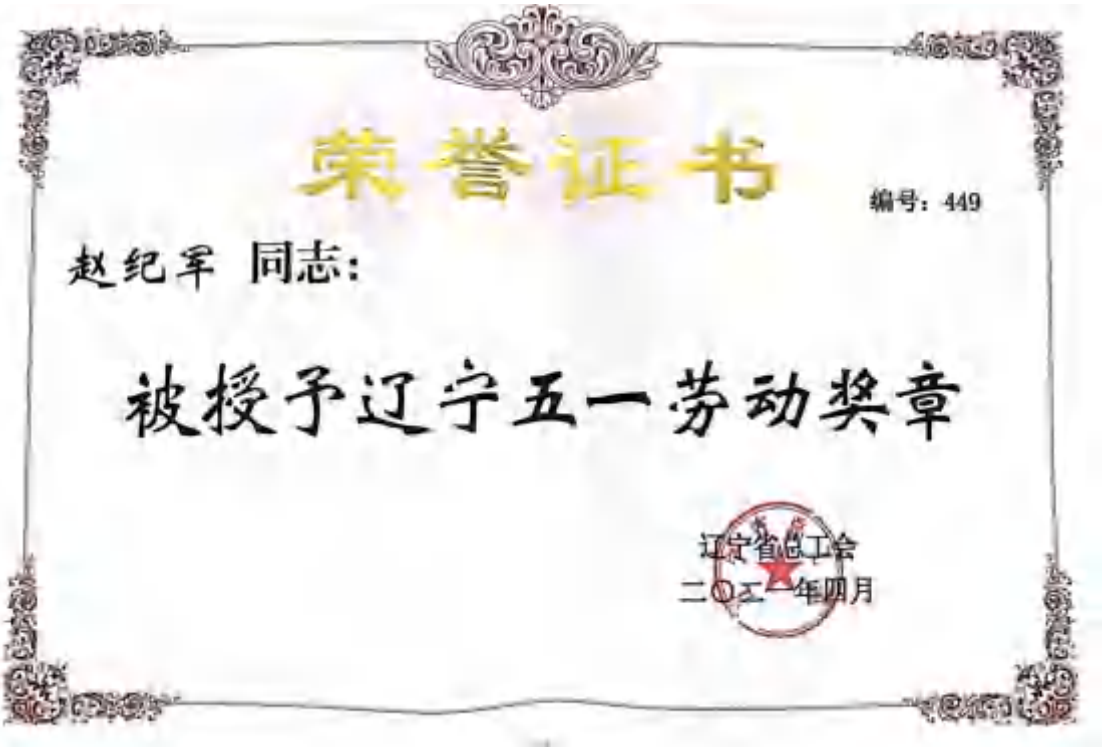

荣誉证书

编号：449

赵纪军 同志：

被授予辽宁五一劳动奖章

辽宁省总工会

二〇二一年四月

（37）第六届“高等教育杯”全国高等学校物理基础课程青年教师讲课比赛东北赛区一等奖证明

编号：东北06002

“高等教育杯”

全国高等学校物理基础课程青年教师讲课比赛

获 奖 证 书

张伶莉 老师（哈尔滨工业大学）

在第六届“高等教育杯”全国高等学校物理基础课程青年教师讲课比赛东北赛区中，荣获一等奖。特发此证，以示表彰。

教育部高等学校大学物理课程教学指导委员会 清华大学代章

中国物理学会物理教学委员会

2024年6月28日

（38）龙江学者支持计划-特聘教授证明

（39）黑龙江省五一劳动奖章

（40）黑龙江省青年教学名师证明

2021年黑龙江省教学名师候选人名单

序号	申报人姓名	学校名称	备注
普通高等学校（113名）			
1	[illegible]	[illegible]	[illegible]
2	[illegible]	[illegible]	[illegible]
3	[illegible]	[illegible]	[illegible]
4	[illegible]	[illegible]	[illegible]
5	[illegible]	[illegible]	[illegible]
6	[illegible]	[illegible]	[illegible]
7	[illegible]	[illegible]	[illegible]
8	[illegible]	[illegible]	[illegible]
9	[illegible]	[illegible]	[illegible]
10	[illegible]	[illegible]	[illegible]
11	[illegible]	[illegible]	[illegible]
12	[illegible]	[illegible]	[illegible]
13	[illegible]	[illegible]	[illegible]
14	[illegible]	[illegible]	[illegible]

（41）“龙江楷模”荣誉称号

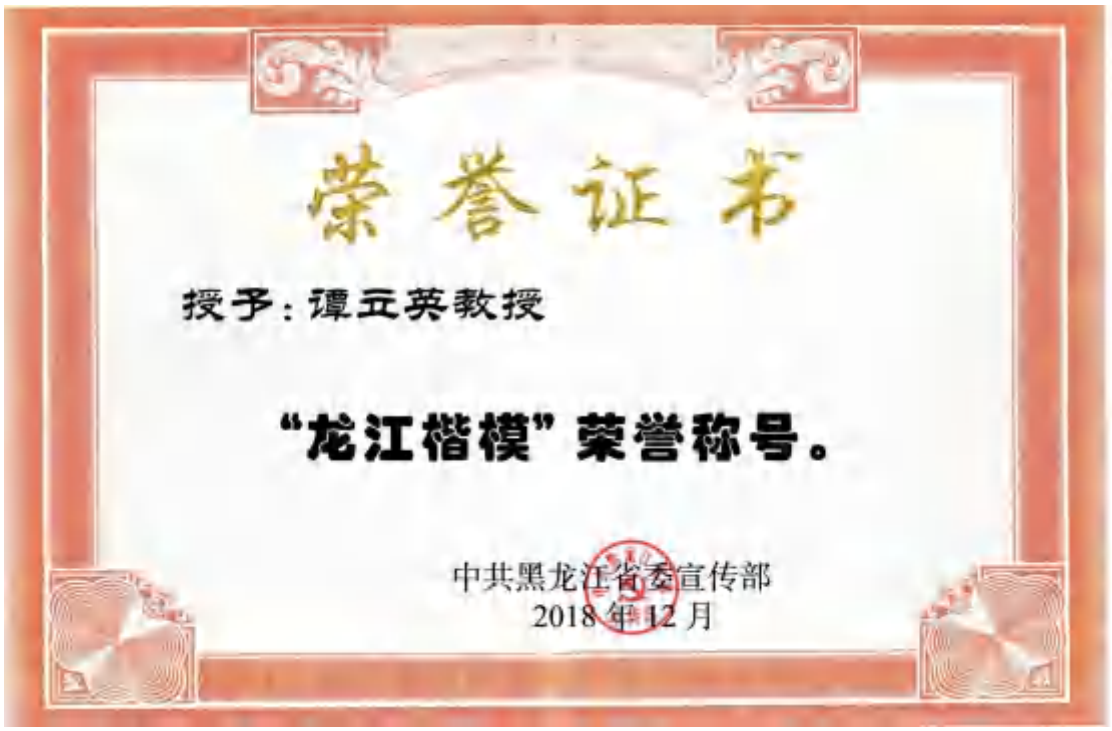

（42）2019 年先进技术应用转化大赛金奖

（43）黑龙江省青年教师教学理科组一等奖获奖证明

荣誉证书

任延宇 老师：

您在第五届黑龙江省青年教师教学竞赛中荣获

理科组一等奖

特发此证，以资鼓励。

黑龙江省教育厅

黑龙江省教科文卫体工会委员会

2020年8月

（44）黑龙江省高校微课教学竞赛一等奖证明

荣誉证书

CERTIFICATE OF HONOR

将此证书颁发给

任延宇

在参加黑龙江省高校师资培训中心举办的第五届黑龙江省高校微课教学比赛活动中

获得 一 等奖

特发此证，以资鼓励

黑龙江省高校师资培训中心

黑龙江省分中心

教育部全国高校教师网络培训黑龙江省中心

二〇一八年十一月十四日

（45）卓越大学联盟青年教师教学创新大赛一等奖证明

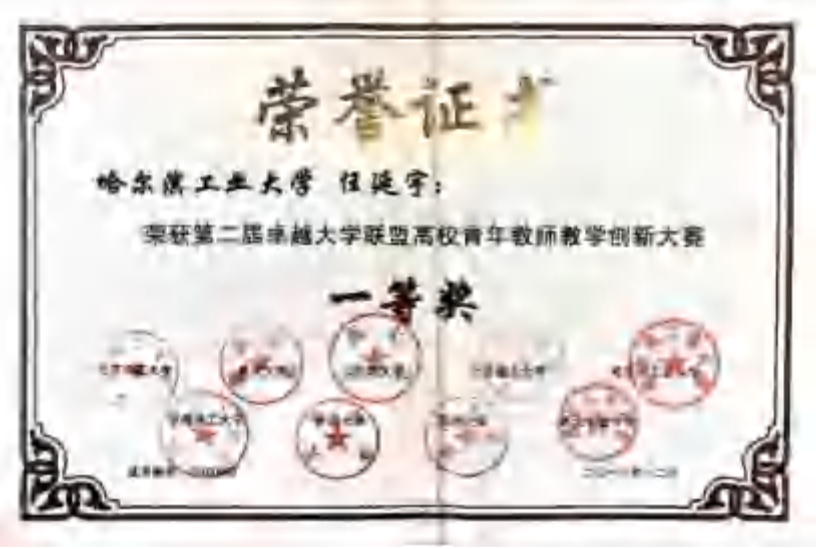
荣誉证书

哈尔滨工业大学 任课字：

荣获第二届卓越大学联盟高校青年教师教学创新大赛

一等奖

（46）第三届“高等教育杯”全国高等学校物理基础课程青年教师讲课比赛省级一等奖证明


“高等教育杯”

全国高等学校物理基础课程青年教师讲课比赛

获奖证书

黄丽 老师（哈尔滨工业大学）

在第三届“高等教育杯”全国高等学校物理基础课程青年教师讲课比赛东北赛区复赛中，荣获一等奖。特发此证，以示表彰。

中国物理学会物理教学委员会

2017年7月31日

（47）第二届“高等教育杯”全国高等学校物理基础课程青年教师讲课比赛省级一等奖证明

编号：黑02002

“高等教育杯”

全国高等学校物理基础课程青年教师讲课比赛

获 奖 证 书

韩 权 老师（哈尔滨工业大学）

在第二届“高等教育杯”全国高等学校物理基础课程青年教师讲课比赛黑龙江赛区荣获一等奖。特发此证，以示表彰。

黑龙江省物理学会

2016 年 7 月 27 日

（48）黑龙江省高等学校课程思政示范课程获奖证明

荣誉证书

HONORARY CREDENTIAL

哈尔滨工业大学：理论力学

被认定为2020年黑龙江省高等学校课程思政建设示范课程。

黑龙江省教育厅

2020年12月

（49）黑龙江省高等学校物理基础课程青年教师讲课比赛二等奖证明

编号：第04004

"高等教育杯"

全国高等学校物理基础课程青年教师讲课比赛

获奖证书

李均 老师（哈尔滨工业大学）

在第四届"高等教育杯"全国高等学校物理基础课程青年教师讲课比赛黑龙江赛区比赛中，荣获二等奖。特发此证，以示表彰。

黑龙江省物理学会

2019年7月10日

（50）教育部自然科学奖二等奖获奖证明

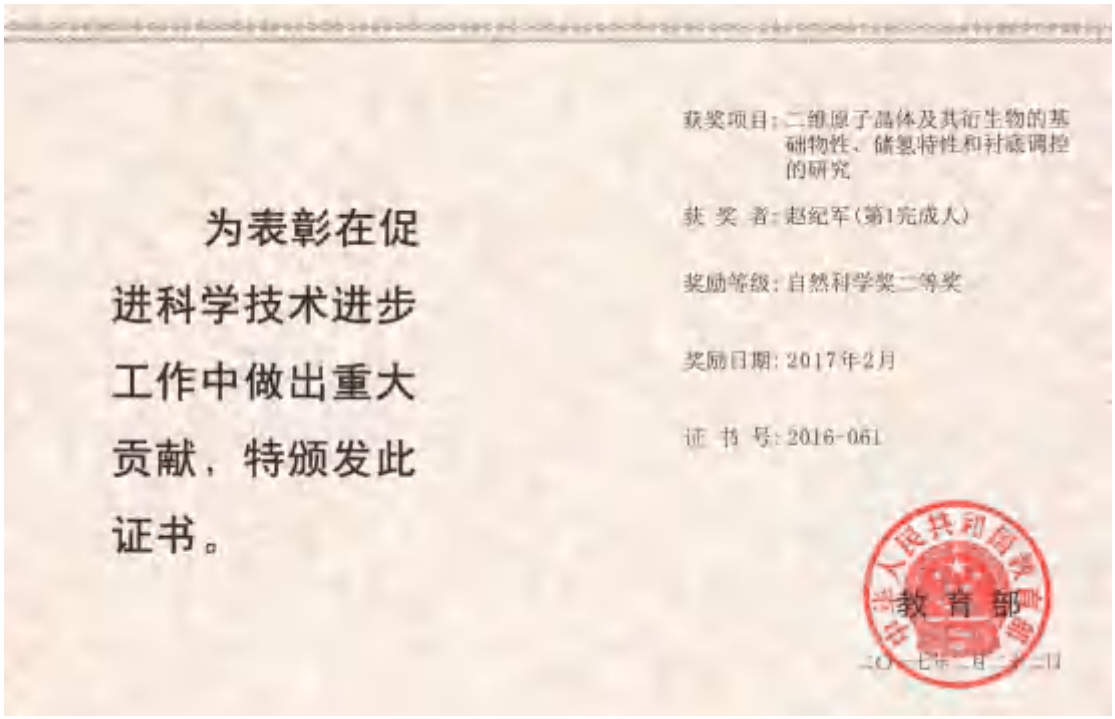

为表彰在促进科学技术进步工作中做出重大贡献，特颁发此证书。

获奖项目：二维原子晶体及其衍生物的基础物性、储氢特性和衬底调控的研究

获 奖 者：赵纪军（第1完成人）

奖励等级：自然科学奖二等奖

奖励日期：2017年2月

证 书 号：2016-061

中华人民共和国教育部

（51）河北省自然科学奖二等奖获奖证明

河北省科学技术奖

证 书

为表彰河北省科学技术奖获得者，特颁发此证书。

项目名称：共价键材料和金属间化合物力学性质的理论计算方法与应用

奖种类别：自然科学奖

奖励等级：二等

获 奖 者：赵纪军

2018年度·证书号：2018ZR2001-3

（52）辽宁省自然科学奖二等奖获奖证明

辽宁省科学技术奖励

证 书

为表彰辽宁省科学技术奖获得者，

特颁发此证书。

奖励种类：自然科学奖

项目名称：二维原子晶体的生长机理和缺陷调控

奖励等级：二等

获 奖 者：[illegible]大连理工大学）

2019年12月26日

证书号：2019-2-2-03-R02

（53）山西省自然科学奖二等奖获奖证明

山西省科学技术奖

证　书

为表彰山西省科学技术奖获得者，

特颁发此证书。

项目名称：二维材料的晶界、界面和缺陷效应的理论探索

获奖类别：自然科学奖

获奖等级：二等

获 奖 者：张均锋（山西师范大学）赵纪军（大连理工大学）
高峻峰（大连理工大学）韩梅娟（大连理工大学）
苏 艳（大连理工大学）

二〇二一年三月

证书号：2019-Z-2-007

（54）哈尔滨工业大学第二届课程思政教学竞赛一等奖获奖证明


获奖证书

物理学院 周可雅 老师：

荣获“哈尔滨工业大学第二届课程思政教学竞赛”

一等奖

特发此证，以资鼓励。

哈尔滨工业大学

2021年10月5日

（55）哈尔滨工业大学优秀教育教学管理奖获奖证明


荣誉证书

张宇 老师：

荣获2021年度“优秀教育教学管理奖”。

特发此证，以资鼓励。

哈尔滨工业大学教学管理中心

二〇二一年五月二十八日

（56）哈尔滨工业大学 2020 年教学贡献奖励一等奖获奖证明


荣誉证书

时红艳 老师：

荣获哈尔滨工业大学2020年教学贡献奖励（教学优秀奖 一等奖）。

特发此证，以资鼓励。

哈尔滨工业大学

二〇二〇年七月三十一日

（57）基于分类人才培养的物理分层次教学模式研究校级一等奖证明


哈尔滨工业大学 HARBIN INSTITUTE OF TECHNOLOGY

教学成果奖获奖证书

获奖成果：基于分类人才培养的物理分层次教学模式研究

获 奖 人：

获奖等级：一等奖

（58）固体光学课程研究型教学理论与实践或研究生教育成果奖证明

2017年度研究生教育成果奖评审结果

序号	成果名称	院（系）	评审结果
1	[illegible]	研究生院	一等奖
2	[illegible]	航天学院	一等奖
3	[illegible]	化工与化学学院	一等奖
4	[illegible]	外国语学院	一等奖
5	研究生国际化高水平课程建设的探索与实践	研究生院	一等奖
6	基于OBE的"EDA/SOPC 三同实践"课程改革与实践	电气学院	一等奖
7	"互联网+" [illegible]	交通学院	一等奖
8	[illegible]	外国语学院	一等奖
9	[illegible]	电气学院	二等奖
10	固体光学课程研究型教学理论与实践	理学院物理系	二等奖
11	[illegible]	[illegible]	二等奖
12	[illegible]	建筑学院	二等奖
13	《最优化方法》研究生精品课程建设	理学院数学系	二等奖
14	[illegible]	外国语学院	二等奖
15	[illegible]	外国语学院	二等奖
16	[illegible]	经管学院	二等奖
17	[illegible]	外国语学院	二等奖
18	[illegible]	能源学院	二等奖
19	[illegible]	建筑学院	二等奖
20	[illegible]	航天学院	二等奖

（59）首届哈尔滨工业大学“育人新星”青年导师证明

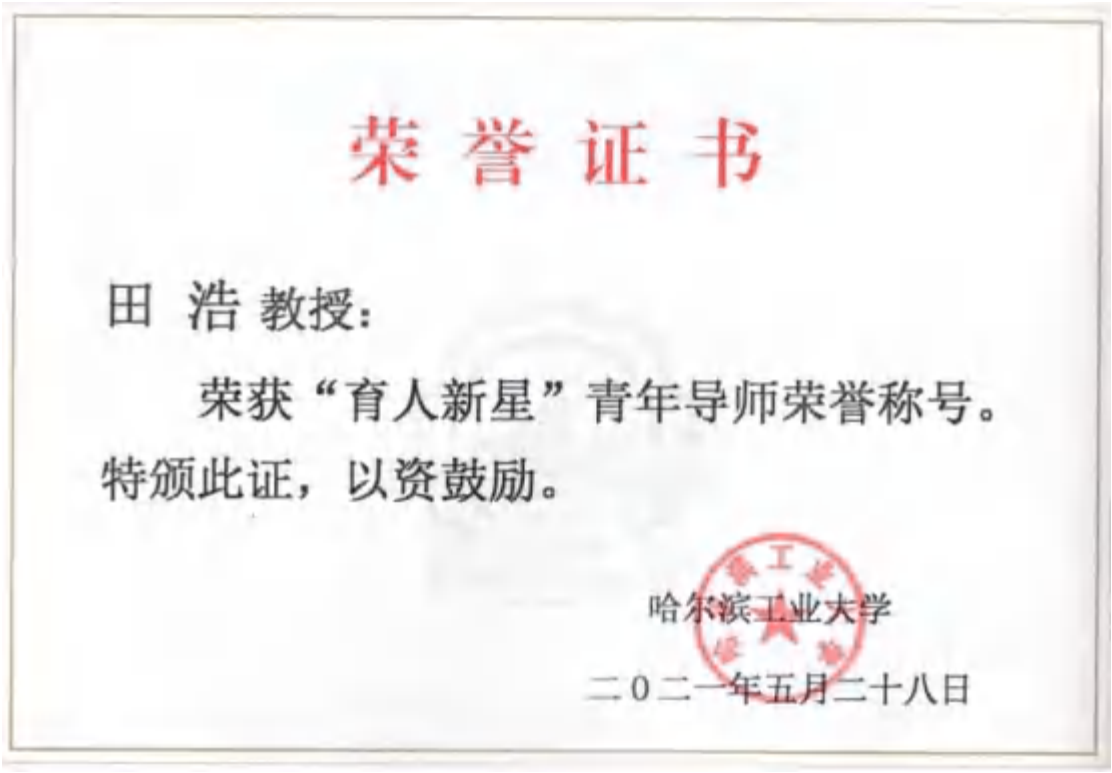

荣誉证书

田 浩 教授：

荣获“育人新星”青年导师荣誉称号。

特颁此证，以资鼓励。

哈尔滨工业大学

二〇二一年五月二十八日

（60）哈尔滨工业大学 2021 年教学贡献奖获奖证明

荣誉证书

李 纳 老师：

荣获哈尔滨工业大学2021年教学贡献奖励

（教学优秀奖 一等奖）。

特发此证，以资鼓励。

哈尔滨工业大学

二〇二一年十一月十日

（61）哈尔滨工业大学首届课程思政教学竞赛校级特等奖获奖证明


荣誉证书

物理学院 任延宇 老师：

荣获“哈尔滨工业大学首届课程思政教学竞赛”

特等奖

特发此证，以资鼓励。

哈尔滨工业大学

二〇一九年十二月

（62）第七届校青年教师教学基本功竞赛一等奖证明

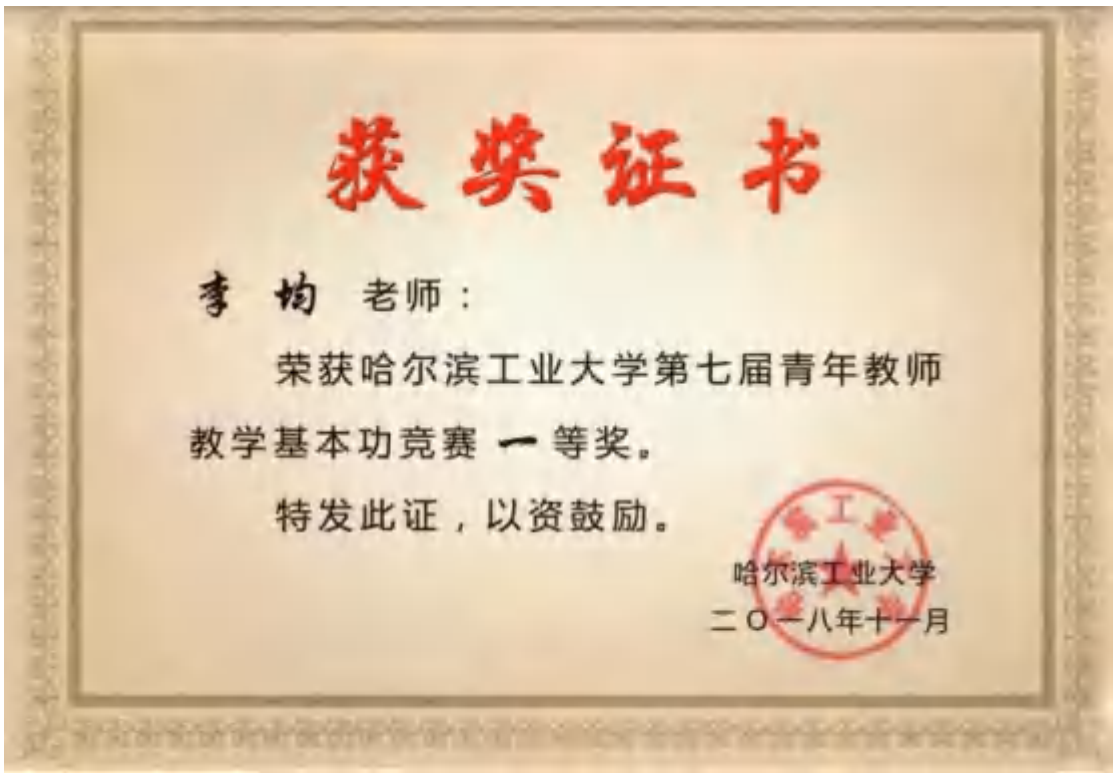
获奖证书

李 均 老师：

荣获哈尔滨工业大学第七届青年教师教学基本功竞赛 一 等奖。

特发此证，以资鼓励。

哈尔滨工业大学

二〇一八年十一月

（63）在线教学“我最喜爱的课程”奖证明

荣誉证书

HONORARY CREDENTIAL

李均老师:

荣获“在线教学‘我最喜爱的课程’奖”荣誉称号。特发此证，以资鼓励。

哈尔滨工业大学本科生院

二〇二〇年五月二十二日